Characterization and Analysis of Boral® from the Zion Nuclear Power Plant Spent Fuel Pool

March 2019

SRNL-TR-2018-00244, Revision 0

Characterization and Analysis of Boral® from the Zion Nuclear Power Plant Spent Fuel Pool

March 2019

APPROVALS

AUTHORS:

_____

Roderick E. Fuentes   Date

_____

Luke C. Olson   Date

_____

Ronald L. Kesterson   Date

CO-AUTHORS/CONTRIBUTORS:

_____

John I. Mickalonis   Date

_____

Christopher G. Verst   Date

_____

Poh-Sang Lam   Date

_____

Charles J. Coleman   Date

_____

Brenda L. Garcia-Diaz   Date

TECHNICAL REVIEW:

_____

Bruce J. Wiersma   Date

APPROVAL:

_____

Kristine E. Zeigler   Date

_____

Robert L. Sindelar   Date

SUMMARY

The Savannah River National Laboratory was contracted by the U.S. Nuclear Regulatory Commission, Office of Regulatory Research to conduct a research project that entailed detailed corrosion performance evaluation of Boral® neutron absorber material (NAM) panels taken from the Zion Spent Fuel Pool (SFP), a Pressurized Water Reactor (PWR) SFP, following service experience of 22+ years prior to its retrieval as part of pool decommissioning. Characterization of the physical condition of the as-received, retrieved materials was performed to assess the corrosion attack of the aluminum due to this service. The results of the as-received characterization showed that the panels experienced very little degradation. Minor pitting was observed along with discoloration, but no service-induced blistering was observed.

The corrosion performance of BORAL® materials to broad water chemistry and temperature conditions was evaluated using specimens cut from the cladding and the exposed (de-clad) core of the Boral® NAM panels. The corrosion performance was measured using standard electrochemistry (EC) testing methods with water chemistry and temperature conditions that included nominal SFP conditions and off-normal pool conditions of both PWR and Boiling Water Reactor (BWR) pools. Semi-empirical modeling was performed to allow corrosion rates to be estimated at conditions within the range of the test conditions. The results of the corrosion testing showed that the corrosion rate measured for the cladding under normal operating conditions was about 2.54 µm/year (0.10 mils/year), which is consistent with the results obtained during the BORAL® materials qualification testing. The corrosion rates increased under off-normal conditions (i.e. exposed core, increased temperature and increased chloride levels), but the corrosion rates were such that during anticipated off-normal excursions, the NAM would continue to perform its safety function.

A test protocol using a chemical analysis method to evaluate the ^{10}B areal density (AD) of the service-experienced, radiologically-contaminated materials was also developed. Measurements using the protocol were performed on several of the Zion panels at specific locations, and the results were compared to those using neutron-attenuation methods. The mean values of the ^{10}B areal density measurements obtained by chemical analysis compared well with the neutron attenuation results.

This project final report describes the materials, the test conditions, and the results of the corrosion testing and AD measurements.

The information generated in this research can be applied to evaluate the potential performance of the Boral NAM to periods of extended operation and to off-normal upset events in an SFP.

SPECIAL ACKNOWLEDGEMENT

TABLE OF CONTENTS

LIST OF TABLES

LIST OF FIGURES

LIST OF ABBREVIATIONS

AD   Areal Density

BWR   Boiling Water Reactor

CPP   Cyclic Potentiodynamic Polarization

CR   Corrosion Rate

EC   Electrochemical

EDS   Energy Dispersive X-ray Spectroscopy

EIS   Electrochemical Impedance Spectroscopy

EPRI   Electric Power Research Institute

ICP   Inductive Coupled Plasma

LCM   Laser Confocal Microscopy

LPR   Linear Polarization Resistance

NAM   Neutron Absorber Material

NRC   U.S. Nuclear Regulatory Commission

OCP   Open circuit potential

PPB   Parts Per Billion by Weight

PPM   Parts Per Million by Weight

PSU   Pennsylvania State University

PWR   Pressurized Water Reactor

SCE   Saturated Calomel Electrode

SEM   Scanning Electron Microscopy

SFP   Spent Fuel Pool
SNF   Spent Nuclear Fuel

SRNL   Savannah River National Laboratory

TIMS   Technical Information Management System

VCI   Vapor Corrosion Inhibitor

XRD   X-ray Diffraction

1.0 Introduction

1.1 SRNL Project for NRC-RES

The Zion Nuclear Power Plant (Zion) in Zion, Illinois is being decommissioned using the DECON strategy including the Spent Fuel Pool (SFP) where Boral® panels had been used as a neutron absorber material (NAM). The U.S. Nuclear Regulatory Commission (NRC), Office of Regulatory Research (RES) contracted the Savannah River National Laboratory (SRNL) to perform activities to characterize the Boral® panels following their service-experience in the Zion SFP, and their corrosion response to service conditions, including off-normal water chemistry and temperature conditions. Degradation leading to the physical loss of NAM may affect the safety function of the panels.

1.2 Boral® Panel Design and Application in the Zion SFP

A NAM in wide use in SFPs is Boral®. Boral® contains the strong neutron absorber ^{10}B present in natural boron (19.9% ^{10}B in natural B). The Boral® panels are comprised of a core of B_4C particles in an aluminum (Al 1100) matrix and this cermet core is sandwiched between two aluminum (Al 1100) sheets or the cladding (Figure 1). These panels are attached axially along the sides of the SFP rack cells.
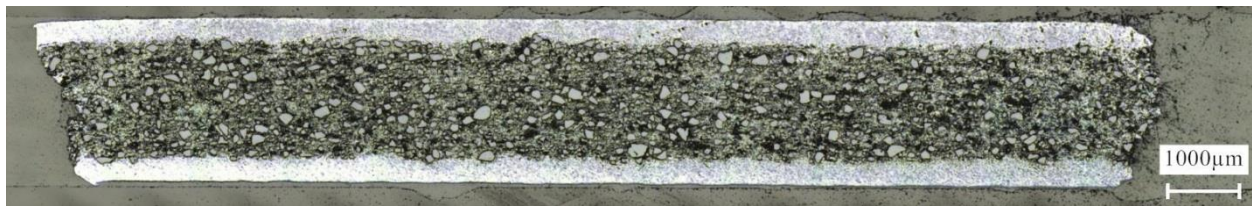
Figure 1. Laser Confocal Microscope montage image of Boral® panel 5M7E-2 specimen
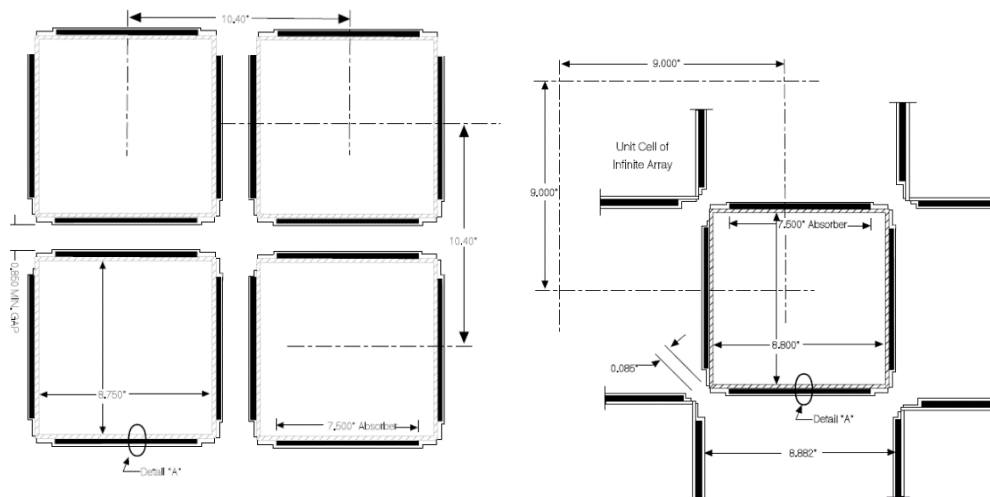
Figure 2. Region 1 (left) and Region 2 (right) (courtesy of EPRI)

The Boral® panels obtained from Zion were from two regions of the SFP. Both the panel design (thickness) and the attachment of the panels differ between the regions. The "Region 1 attachment" has bare Boral®

panels held in place by a small capture tab at the top and bottom and at axial locations by stainless steel straps to each of the four sides of a storage cell as shown in Figure 2. The other attachment configuration, noted as Region 2, has Boral® panels encased in a vented stainless-steel sheath and attached to the sides of a cell. In addition, the cell-to-cell pitch in Region 1 is larger, and Region 1 grid contains neutron flux traps.

As shown in Figure 2, the Region 2 storage rack was formed by attaching individual cells together diagonally at the corners. A major difference between the two designs is that for the bare plates in Region 1 there are two panels between adjacent stored fuel assemblies but for the encased panels in Region 2 there is only one Boral® panel between adjacent assemblies. Also, as shown in the following section, there are some Region 1 exterior cells with encased panels.

2.0 Material Source

2.1 <u>Service History</u>

The source Boral® NAM was taken from panels of two Zion SFP module sections (Module B (Region 1 storage cell) and Module P (Region 2 storage cell)). The racks used in these modules were fabricated by U. S. Tool & Die and installed in the Zion SFP in 1992.

During the service of the Boral® panels in the fuel pool, the water quality was monitored and recorded. The results from January 1995 through January 2015 were reviewed, and a summary of the water chemistry at the inlet and outlet to the filter/deionizer system is shown in Table 1 and Table 2, respectively. The boron levels represent daily readings and the other elements were measured once per week. In general, the water quality is considered very good and there were no flags regarding prolonged conditions for accelerated aluminum corrosion.

Table 1. Filter/deionizer Inlet Water Chemistry

Data from 1/24/1995 to 1/9/2015

	High	Low	Average
pH	5.64	4	4.63
Boron (ppm)	2721	1834	2204.0
Fluoride (ppb)	4	0.06	0.65
Chloride (ppb)	284	0.35	11.84
Silica (ppb)	355.5	6.1	170.7
Spec. Cond. (μS/cm)	40.5	3.4	6.8
Sodium (ppb)	451.2	0.83	36.7
Sulfate (ppb)	215.4	0.71	5.89
Calcium (ppb)	153	0.3	6.26
Magnesium (ppb)	71.2	0.52	8.54

Table 2. Filter/deionizer Outlet Water Chemistry

Data from 12/8/2010 to 1/6/2015

	High	Low	Average
pH	5.27	4.23	4.56
Boron (ppm)	2228	367	1967.0
Fluoride (ppb)	2.88	0.2	0.73
Chloride (ppb)	1.78	0.5	0.8
Silica (ppb)	355.5	6.1	220
Spec. Cond. (μS/cm)	8.7	2.29	7.37
Sodium (ppb)	101	0.21	14.54
Sulfate (ppb)	5.9	1.01	2.28
Calcium (ppb)	20.5	0.5	5.63
Magnesium (ppb)	1.85	0.5	1.68

2.2 Panel Removal and Handling

This investigation of service-experienced Boral® is under an NRC-EPRI Memorandum of Understanding. Under contract to EPRI, Curtiss-Wright (NETCO) oversaw the removal of the modules from the Zion SFP, the initial cutting of module sections, and shipment to the Veolia North America's Alaron Nuclear Services (or Alaron) facility in Wampum, PA where the panels were removed from the storage rack modules. Details of these activities are recorded in references 1 and 2. A summary of the panel handling and retrieval is provided in the following figures and notes.

Figure 3 shows the relative positions in the fuel pool of the modules from which the panels were removed for evaluations.

Figure 4 shows the specific cell faces from which the Region 2 panels were retrieved. After the chosen modules were removed from the pool they were sectioned using a rope saw and a reciprocating saw. The final cell group was "encapsulated" by an epoxy type spray coating to mitigate radioactive material contamination.

These module sections are smaller arrays of cells cut from the intact modules. Figure 5 shows a section of Region 1 before cutting. A single full-sized cell is a ~9-in square stainless-steel storage tube that is about 15 ft long. The Module B section is a 4 x 3 array of spent nuclear fuel (SNF) storage cells measuring 2.7

ft x 3.5 ft x 14.6 ft. A similar 4 x 9 array of cells was cut from Module P with cells measuring 6.8 ft x 3.1 ft x 15 ft.

The Module P and B sections were shipped to Alaron for further cutting and sectioning. For the materials shipped to SRNL, Alaron removed 14 panels (eight from Module B and six from Module P) by cutting the capture tabs or wrapper plates. Each of the panels was sectioned into 12 separate one-foot long panel specimens for a total of 168 panel specimens. Each panel specimen was identified by:

a. the cell number; example 5M12 (row and column as shown in Figure 6)
b. the relative axial position (1 through 12; 1 being the bottom and 12 the top plate)
c. the cell face direction from which the panel was removed (N- North, E- East, W-West, S-South). For example; a plate designated 5M12S5 is from the south face panel of cell 5M / 12 and is the 5th section up (about 1.524m (5 feet)) from the bottom.

The panel specimens were individually wrapped in paper with Vapor Corrosion Inhibitor (VCI). Six panel specimens from each entire panel length were shipped to SRNL and the remaining six panel specimens were sent to PSU for evaluations by EPRI.

It is noted that two of the Region 1 panels, 2J19N and 2L19N, were encased in wrappers whereas the remaining Region 1 panels were held to the storage racks with stainless steel straps.

A list of the panel specimens sent to SRNL is included in Table 3.

Table 3. List of Panel Sections received at SRNL

Region/Module	Panel ID	Sections
1 / B	2J19N	2,4,6,8,10,12
1 / B	2K19W	1,3,5,7,9.11
1 / B	2K20S	2,4,6,8,10,12
1 / B	2K21N	1,3,5,7,9.11
1 / B	2L19E	2,4,6,8,10,12
1 / B	2L19N	1,3,5,7,9.11
1 / B	2L19S	2,4,6,8,10,12
1 / B	2L20N	1,3,5,7,9.11
2 / P	5L9E	2,4,6,8,10,12
2 / P	5L9S	2,4,6,8,10,12
2 / P	5M7E	2,4,6,8,10,12
2 / P	5M7S	1,3,5,7,9.11
2 / P	5M12E	1,3,5,7,9.11
2 / P	5M12S	1,3,5,7,9.11
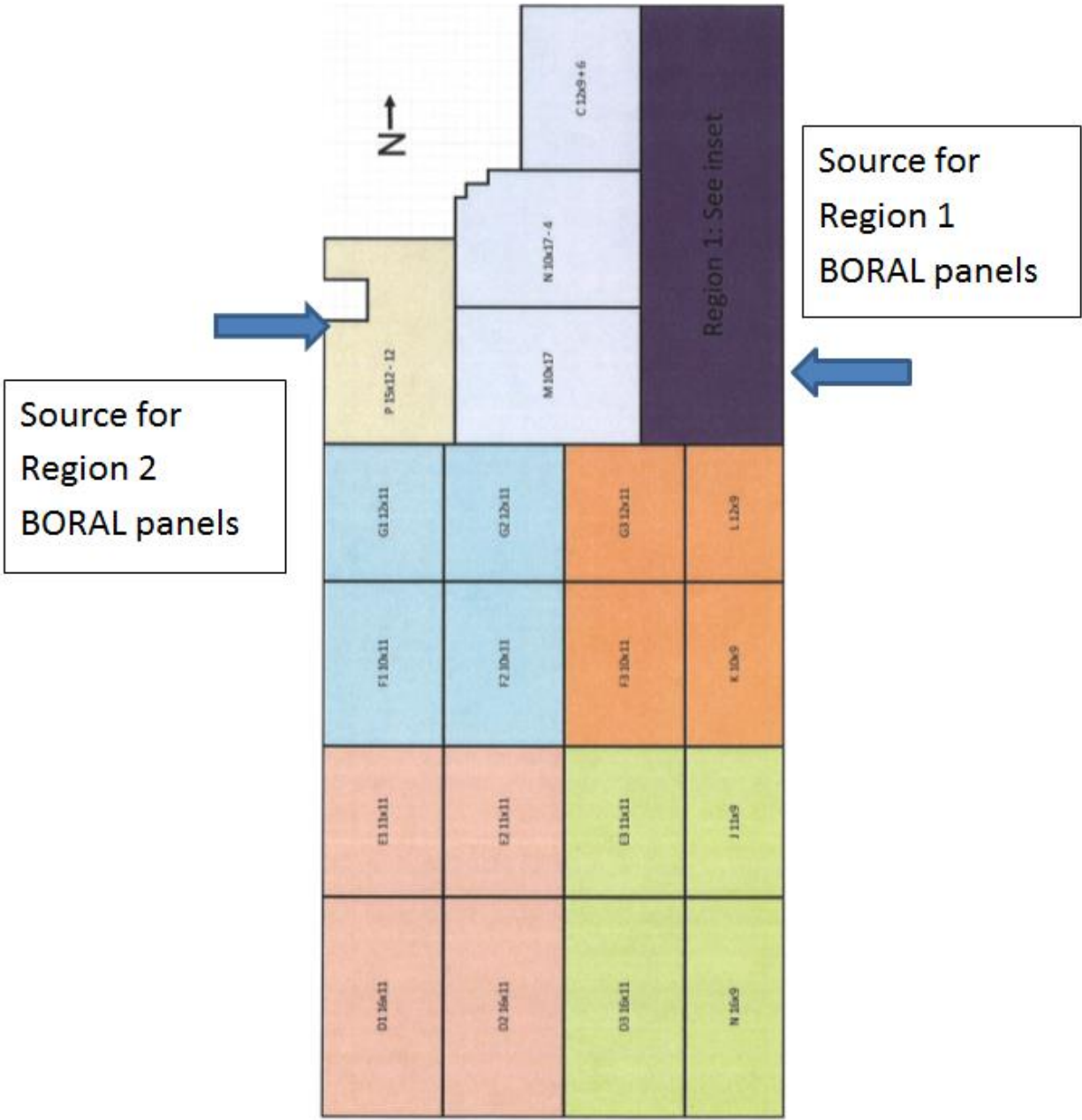
Figure 3. Storage layout of modules in fuel pool (courtesy of EPRI) l
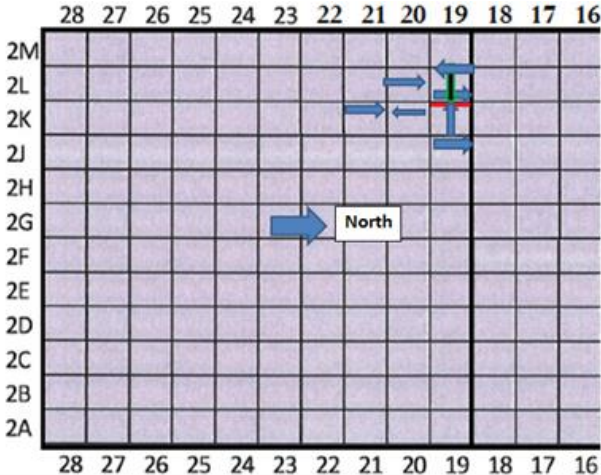
Figure 4. Cell faces from which panels sent to SRNL originated (courtesy of EPRI)

Figure 5. Module B (Region 1) section from Zion SFP during initial cutting of module for removal of Boral® panels at Alaron (photo courtesy of M. Harris, NETCO [1]
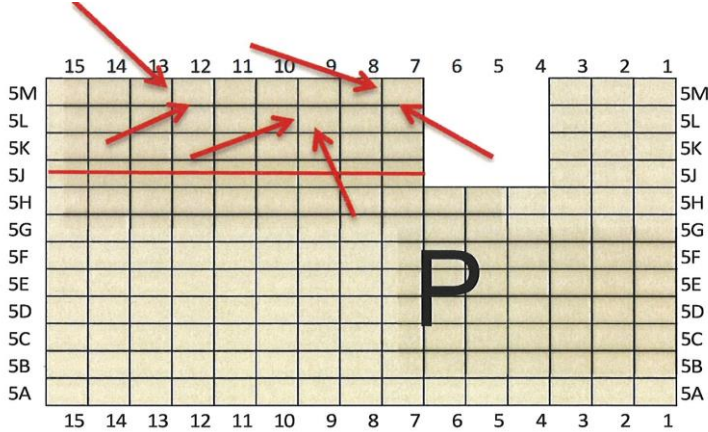
Figure 6. Layout showing specific cells and faces from where the Region 2 panels were removed (courtesy of EPRI)

3.0 Test Program Objectives

The high-level objectives of the research project were to evaluate the performance of Boral® as a NAM to:

(1)   Identify the degradation mechanisms affecting the Boral® panels removed from the Zion SFP,

(2)   Evaluate the performance of the Boral® panels under normal operating and off-normal conditions,

(3)   Assess the ability of the Boral panels to perform their safety function following exposure to off-normal conditions, and

(4)   Develop long-term predictions of the progression of Boral® corrosion degradation in the SFP environment.

The following tasks were identified to help achieve the project objectives:

Microstructural Evaluation: Included visual examination of the as-received panels, dimensional characterizations and metallurgical evaluations of the surface and cross-section microstructure.

Blister Evaluation: Included characterization of blisters and blister formation and matrix delamination effects, if any, in received panels in addition to generation and evaluation of fresh blisters.

Cermet Core Corrosion: Evaluate cermet core material (Al-B_4C) corrosion rates.

Cladding Corrosion: Estimate the corrosion rates for the aluminum cladding exposed to simulated spent fuel pool environments. The testing consisted of corrosion potential, potentiodynamic polarization resistance and anodic polarization measurements.

Boron Areal Density Measurements: Quantify the ^{10}B areal density of selected samples via a Boral® sample chemical digestion and followed by ^{10}B isotopic measurements.

4.0 Test and Evaluation Methods

This chapter provides a description of the methods to characterize the physical condition of the as-service-experienced Boral® NAM panels. This chapter also provides a description of the corrosion test methods used to evaluate the corrosion performance of the materials to broad water chemistry and temperature conditions using specimens cut from the cladding and from the exposed (de-clad) core of the Boral® NAM panels. This chapter also provides a description of the chemical method developed and implemented to measure the ^{10}B areal density.

The results of the characterization and testing are given in chapter 5.

4.1 As-received condition assessment.

4.1.1 Visual
Physical condition characterization of the panel specimens was done at SRNL. The surface conditions of the entire set of 84 panel specimens were smear tested for radiation contamination levels and photos were taken to document the panel surface conditions. A compendium of the receipt characterization radiation and photographs was prepared (Appendix F).

From the visual examinations, some areas of specific interest on the sections were noted. The as-received surfaces of some samples were examined for surface pitting using a laser confocal microscope (LCM) that provided quantitative surface contour depth measurements. Other samples were mounted and polished for cross-sectional views to characterize microstructures and obtain dimensional measurements (component thicknesses).

4.1.2 Microstructure

The visual inspection results identified areas for more detailed evaluations. Sections from these areas were taken and mounted for LCM and optical evaluations using standard metallographic techniques.

For accurate measurements of surface layer thicknesses, one sample from 2K20S-10 was Ni plated using an electro-less Ni bath. The electro-less Ni plating preserved the surface condition from further disturbances and allowed for a more nuanced measurement and characterization of the oxide coated surface. The Ni-plated coupon was then sandwiched between two glass plates for edge retention and the "sandwich" was held together using standard steel metallography clips and mounted using EpoFix epoxy. The sample was then polished to a mirror polish and analyzed initially using a back-scatter electron microscope and LCM.

4.1.3 Dimensional Characterization

Two panels from Region 1 and three from Region 2 were selected for detailed dimensional measurements. The panel identifications are listed in Table 4. They are in sets of three sections from each of the five full length panels. The sections were chosen to represent the top, middle and bottom areas of each panel. Section #1 is the bottom section and #12 is the top. Plate thicknesses (using a micrometer) and widths (using a caliper) were measured at specific positions to determine relative dimensional changes between and along the different panels. The measurements were taken at equivalent locations on the selected panels per the template shown in Figure 7. Section length measurements were not taken since they varied with the cutting procedure and thus have no direct reference to the panel characteristics. In addition to the standard dimensional measurements, for the Region 1 sections that had artifacts from the hold down straps, a set of thickness measurements were taken at the locations of the strap in contact with the Boral® panel as shown in Figure 7. Supplemental cross-sectional cladding thickness measurements at one of the strap locations were also made on panel section 2K20S-10.

Table 4. List of Dimension Samples

Panel	Sections
2L19S	**2, 8, 12**
2K20S	**2,6, 12**
519E	**2, 8, 12**
5M7E	**2, 6, 12**
5M12E	**1, 7, 11**
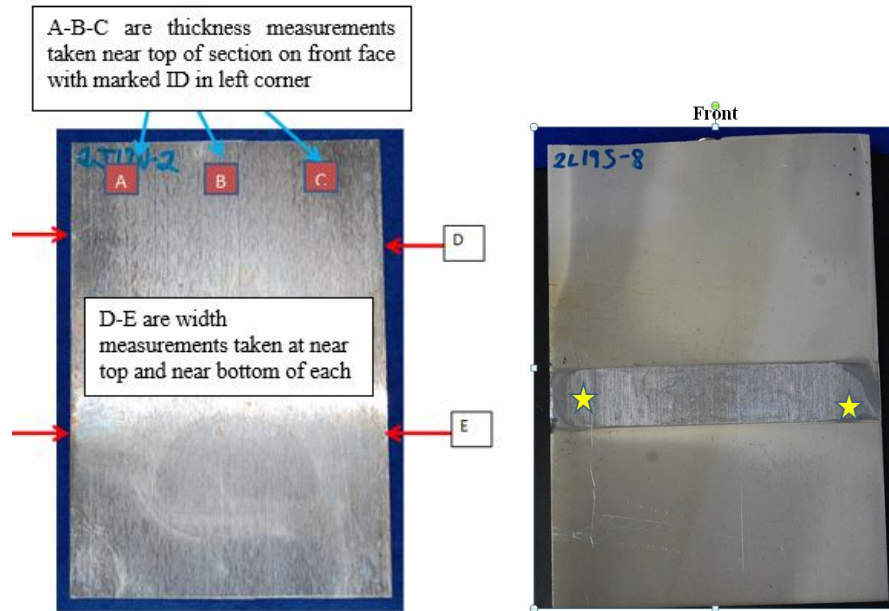
Figure 7. Thickness and Width Measurement Template and Example of Thickness Measurement Location at Strap Contact Location

4.2 Blister Evaluation

Boral® NAM panels are prone to blistering while in service in SFPs. This task was initially designed to evaluate service-induced or "in-pool" blisters that might be present on the panels from the Zion SFP to gain insights into the blistering mechanism and to assess the impact blistering might have on the configuration of the cermet core. Upon examination of all the panels removed from the Zion SFP, including the panels provided to EPRI, no service-induced blisters were observed. Two of the panels blistered during the torch cutting removal process, but these were not considered relevant. However, these two panels are discussed below for completeness.

Since no service-induced blisters were observed, steam-induced or "lab-formed" blisters were created and evaluated. The lab-formed blisters provide: i) an assessment of the mechanical strength at the cermet core -clad interface; and ii) an assessment of typical temperatures required to induce blister generation for a condition with unquantified trapped gas and water vapor.

The postulated mechanism [3] for the cause of in-pool blister formation observed on some Boral® panels in general service has been attributed to the ingress of water into the Boral® core and a subsequent oxidation reaction with the aluminum matrix forming an aluminum oxide. This oxide formation releases hydrogen which is retained in the matrix because the oxide formation also effectively seals the ingress/egress matrix pathways. Along with the hydrogen there is also some moisture retention as hydroxides and perhaps free water depending on the exposure timing. With continued corrosion and hydrogen build-up, a blister can form.

For creating lab-formed blisters, heating the panel with trapped hydrogen and/or water can cause increased pressure leading to blistering at the clad/core interface. That is, hydrogen and/or water vapor (steam) may

migrate to local voids at the clad/core interface, presumed to be a location susceptible to mechanical failure. Sufficient pressure in the interconnected pores would cause an interface failure and a subsequent blister in the clad at the location. However, steam-induced blistering is not expected under normal or off-normal conditions at temperatures below the saturation temperature of the SPF water.

The lab-formed blisters were used to obtain exposed cores for corrosion testing by peeling off the clad, starting at the blister dome.

The weights of the samples exposed to the blister conditions were measured and the incremental weight loss at the different temperature exposures provided an indication of the moisture levels in the Boral® samples.

4.2.1 Blisters Formed During Panel Removal

Three sections (1, 9 and 11) from panel 2K21N had blisters that were generated by excess heating from a torch during panel removal from the cell. An example from panel 1 is shown in Figure 8.
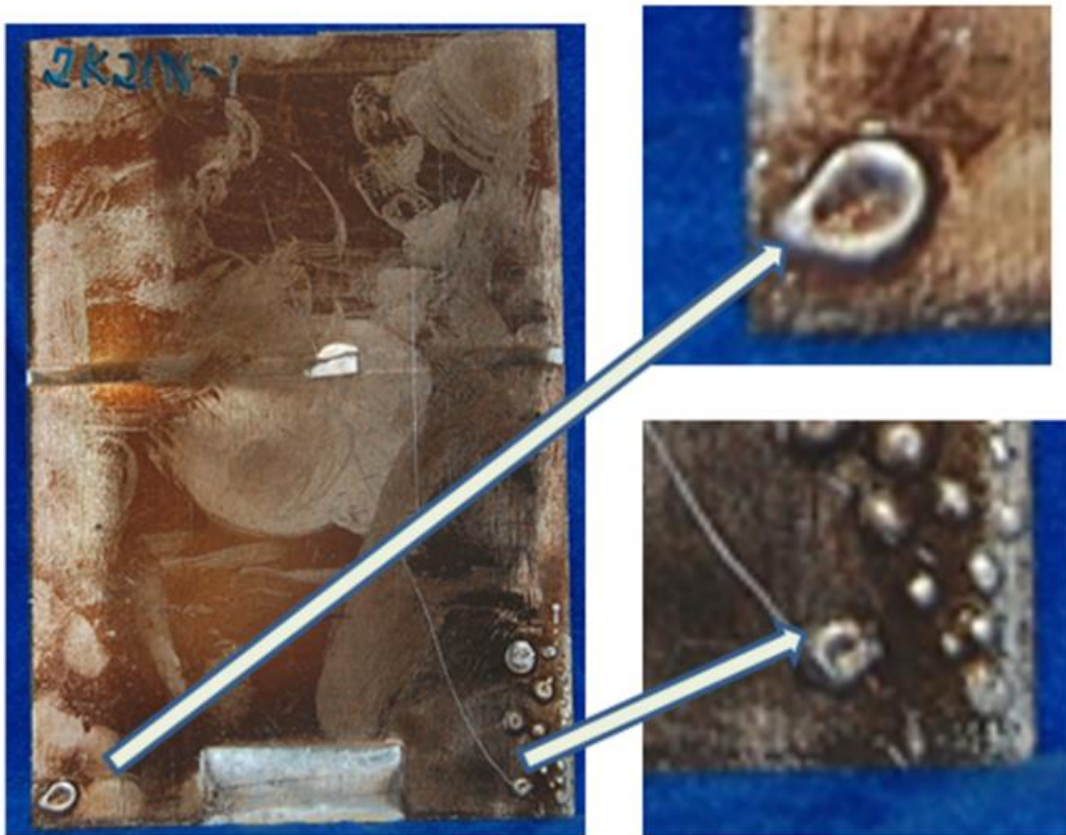
Figure 8. Blisters Formed on Section 2K21N-1 Due to Excessive Heating (Inadvertent Torch Contact) During Panel Removal

4.2.2 Lab Generated Blisters

Since there were no naturally formed blisters to evaluate, a procedure was implemented to artificially generate blisters on panel samples. The initial procedure was to heat a panel sample in an oven to 515°F (268°C) for ten minutes. This procedure was not successful in generating a blister on the panel surface of a sample from 2L19N-9. Two additional panels were selected for the blister formation procedure, 5M7S-9 and 5L9S-12. Lab induced blisters were generated in these panels.

4.3 <u>Areal Density (AD) Measurements</u>

EPRI performed ^{10}B areal density measurements on several Boral® panels in the Zion SFP using the Boron-10 Areal Density Gage for Evaluating Racks (BADGER) system as part of a cooperative research project with the NRC. BADGER is a neutron attenuation testing system that is used to evaluate *in situ* NAMs installed in the SFP racks. In addition to the AD measurements performed using BADGER, EPRI measured the AD of all the panels sections it received (i.e. half the total number of sections) via neutron attenuation measurements performed at The Pennsylvania State University (or PSU) and reported the results in EPRI report #3002008196 titled, "Evaluation of Boral® Panels from Zion Spent Fuel Pool and Comparison to Zion Coupons." [3]

The purpose of this task is to measure the AD of Boral® panels using chemical analysis methods as an independent verification of the AD measurements performed via BADGER and PSU neutron attenuation methods. EPRI provided two panels for which AD measurement values were obtained by both neutron attenuations methods: one panel section from Region 1 and one panel section from Region 2. Chemical analysis of both panel sections was performed to measure the total boron, isotopic ^{10}B and ^{11}B to estimate the ^{10}B areal density. The process used to perform the chemical analysis is described below.

The methods described in ASTM C791 [4] were followed to measure total boron, ^{10}B, and ^{11}B to estimate the ^{10}B areal density. ASTM C791 is a standard for the analysis of boron carbide powder and pellets; it does not address the ^{10}B areal density measurement for Boral® with the aluminum component that is present in Boral®. Thus, calculations exterior to the scope of ASTM C791 were made to address the Boral® compound. The SRNL protocol for the characterization involved a multi-step process for Boral® specimen digestion for chemical analysis: 1) dissolve the Al-clad and matrix Al using hot NaOH, then evaporate the solution, 2) dissolve the carbides in a hot Na_2O_2 caustic solution, followed by 3) nitric acid addition and dilution for ICP analysis. Inductively Coupled Plasma Optical Emission Spectrometry/Mass Spectrometry (ICP-OES/MS) methods were used to measure total boron and Thermal Ionization Mass Spectrometry (TIMS) were used to measure ^{10}B masses in the samples. With the mass of ^{10}B and the Boral® sample surface area known, the Boron Areal Density (AD) can be calculated as gm ^{10}B per cm^2.

Prior to receiving the two test panels from EPRI, a set of five samples were cut from panel 2K20S-10 to help establish the testing protocol. Five adjacent samples were removed from the panel, measured and weighed. The samples were nominally 1 cm. x 1 cm. in length and width. The specific steps in the sample preparation included:

- Weigh and measure the sample into a Zr crucible. Sample should not be larger than 1.27 cm by 1.27 cm (1/2 inch by 1/2 inch) to minimize potential for hydrogen generation.
- Dissolve the Al in the sample with hot NaOH.

- Evaporate the water introduced with NaOH solution by placing the Zr crucible in a drying oven set at 115 °C.
- Add Na_2O_2 to the dry residue and heat at 675 °C in a muffle furnace until the boron carbide particles dissolve and the flux appears smooth.
- Remove the crucible from the muffle furnace and cool to room temperature.
- Dissolve the flux residue with deionized water, transferring the caustic solution and flux residue to a volumetric flask, and then add nitric acid.
- Dilute to desired volume in a plastic volumetric flask and run through mass spectrometer to measure isotopes.

With the testing protocol established, a set of seven samples were cut from panels 2K21N-2 (one sample) and 5M7S-6 (six samples), Region 1 and Region 2 panels respectively. As will be discussed further in the section on the testing results, decontamination of the Region 1 panel section was not fully achieved. As a result, only one sample from panel section 2K21N-2 was available for testing.

4.4 Electrochemical (EC) Testing

4.4.1 Material preparation – cladding material

Panels 5L9S-4, 5L9S-12 (Region 2) and 2K20S-10 (Region 1) were selected for this study. Panels from Region 1 were decontaminated, as needed for clean laboratory work, by immersing them in a dilute solution of nitric acid and cutting parts that have active fixed contamination. Region 2 panels had low radioactive contamination and did not need to go through the process of nitric acid decontamination. Nitric acid cleaning was not used on specimens tested in the as-received condition with attendant oxide.

Using a shear, pieces were cut into 2 cm x 2 cm sections yielding a surface area of 4 cm^2. The pieces were cleaned with distilled water and degreased with acetone. Silver epoxy was mixed and used to electrically connect one side of the panel with a coated purple wire. The coupons were mounted using a two-part acrylic solution (VariDur from Buehler). Figure 9 shows a picture of the sample after being mounted. For experiments with a fresh ground cladding surface, the specimen was ground/re-ground to 600 grit immediately prior to immersion in the test solutions. For every experiment with attendant oxide, a new sample mounted in acrylic was used.

Figure 9. Picture of Region 2 sample connected with purple coated wire and mounted in acrylic

4.4.2 Simulant–Water Chemistry Test Conditions

Boiling water reactor (BWR) and pressurized water reactor (PWR) SFP water chemistry simulants were prepared to evaluate the effects of various levels of potentially aggressive species. The potentially aggressive species identified for evaluation included chloride, sulfate and fluoride based on historical Zion SFP chemistry records, EPRI guidelines for SFP water chemistry control limits and operating experience [5, 6]. Three categories of SFP water chemistry simulants were evaluated and designated as "nominal", "base" and "off-normal" for PWR and BWR SFPs resulting in a total of six simulants. The difference between the BWR and PWR simulants was that the PWR simulants contained boron as boric acid. The "nominal" simulant was based on an average historical concentration profile from the Zion SFP, the "base" simulant was based on the maximum limits of the SFP water chemistry guidelines, and the "off-normal" solution represents contaminant concentrations 100 times higher than the water chemistry guidelines for the aggressive species.

Table 5 shows the six simulants created for study. They are in ascending order from lower to higher concentration of aggressive constituents.

Table 5. Water Chemistries

Solution	Boron Concentration (mg/L)	Concentration of aggressive species (mg/L)			pH
		Chloride	**Sulfate**	**Fluoride**	
1-PWR nominal	2500	0.012	0.006	0	4-5
2-BWR nominal	0	0.012	0.006	0	5-7
3-PWR base	2500	0.15	0.15	0.01	4-5
4-BWR base	0	0.15	0.15	0.01	5-7
5-PWR off-normal	2500	15	15	1	4-5
6-BWR off-normal	0	15	15	1	5-7

4.4.3 EC Testing Apparatus

The electrochemical cells staged in the radiological hood are shown in Figure 10. Each cell contains a glass vessel on top of a hot plate for heat control. Each glass cell contained approximately 500 mL of simulant. Two carbon graphite rods connected by a cable served as the counter electrode. A saturated calomel electrode (SCE) was used as the reference electrode. Prior to each test, the electrode was checked against a standard before testing (a SCE in 1 M KCl solution not used for testing). The SCE was placed in a salt bridge to provide connection and be apart from the hot plate to minimize disturbances in reference potential.

A VSP potentiostat (Bio-Logic Science Instruments) was used with two channels for parallel electrochemical testing. The ASTM standards for linear polarization resistance (LPR) [7], electrochemical impedance spectroscopy (EIS) [8], and cyclic potentiodynamic polarization (CPP) [9, 10] were used. The ASTM G5 [9] test method check was followed before and after testing using the standard sulfuric acid solution.

An electrochemical routine was prepared to perform LPR, EIS and CPP experiments. Open circuit potential (OCP) was measured until the potential of the sample equilibrated in the solution. This time can vary from

2 to 7 hours. After the OCP was equilibrated to at least +/- 10 mV in 1 hour, LPR was performed over a potential range of +/- 25 mV around the OCP at a rate of 0.167 mV/s.

Figure 10. Two separate electrochemical tests in progress in the radiological hood. The cells are connected to a potentiostat and computer. Nitrogen gas was adapted for running ASTM G5 experiments.

4.4.4 Sample preparation for EC testing

EC corrosion rates were measured for simulant bath temperatures ranging from room temperature to 98 °C. Sample test conditions included as-received surfaces, ground (fresh) surfaces, aged oxide surfaces and exposed core surfaces.

(a) The data for a freshly ground surface provides a base line set of information for the Boral® Al clad without a pre-established oxide film and possibly an upper bound for the corrosion rate. The fresh surface was generated by grinding the surface with 600 grit SiC immediately prior to immersion into the solution for EC testing.
(b) The as-received condition represents the clad surface with the oxide film developed during pool exposure, but, in this as-received condition, the surface also has been exposed to decontamination procedures and subjected to drying conditions which can potentially change the surface oxide structure. An evaluation of the as-received surface oxide and EC testing indicated that the structure of the oxide was indeed likely altered from what is expected for oxides formed under SFP water conditions. Thus, this condition is considered less relevant due to the surface changes that occurred and is not discussed in the body of this report but is included in Appendix A.
(c) The aged oxide or in-service oxide condition consists of a fresh surface that is exposed to the test environment (without electrical stimulation) for a controlled time interval lasting up to 5 weeks for some samples.
(d) The exposed core surface was generated by peeling clad from the core substrate using blisters generated on select panel surfaces by furnace exposure, as discussed previously.

4.4.5 Electrochemical Test Procedure

The EC testing procedure is very detailed and encompasses a number of different second level procedures. The scope of the procedure development is extensive and has been included as Appendix A to this report.

4.5 Immersion Testing

The EC testing conducted has shown low corrosion rates for the materials even in very aggressive water solutions (solutions 3 and 4) at high temperatures (up to the 98 °C). These findings have influenced the project decision to test at two more aggressive conditions; 98 °C and 125 °C to evaluate the potential for loss of B$_4$C from an exposed core specimen. The 98 °C immersion testing condition was selected to substantiate the EC testing results.

Tests at Atmospheric Pressure

Test solution #5, off-normal PWR water chemistry, was chosen for this test. The solution was contained in a 2-liter vessel, heated to 98 °C and mildly stirred. The test duration was 432 hours (12 days) with the potential to extend the duration if notable B$_4$C loss was observed. The exposed core surface was obtained from panel 5L9E-6 by peeling off the clad after blisters were induced by heating.

Four specimens were removed from the panel; three were exposed in the test and one was kept as a control. The weights of the samples were measured prior to the immersion in the solution. The samples were washed with nitric acid after the test. The acid will remove the oxide but not significantly attack the core material. Then the samples were cleaned, dried and weighed on the high-precision balance.

Figure 11. Setup for Immersion Test

Pressure Vessel Tests

The saturation temperature of the water in the SFP at the base of the fuel bundle is estimated to be 123 °C (254 °F) based on standard steam tables and is the maximum expected temperature. Thus, corrosion testing at 125 °C (257 °F) in a Parr vessel filled with the off-normal PWR solution (solution #5) was performed to simulate off-normal conditions. A Parr vessel is a small autoclave vessel that can be loaded with a coupon and test fluid, closed and heated to a set temperature.

For the core exposure tests, the coupons removed from panel 5L9S-4 were ground with 600 grit SiC paper to remove the cladding on both sides of the sample and expose the core. (These tests were performed prior to the development of the technique of removing the cladding by pre-blistering and peeling.) The total surface area of each sample was very close to 1 in ^{2} (6.78 cm^2). Samples were combined with about 10 grams of off-normal PWR solution (solution #5). During the test at 125 °C, the internal pressure was about 19 psig (saturation pressure for steam at 125 °C). For sample/coupon #4 in the pressure vessel test, the solution was refreshed after 3 hours, then after 24 hours, and the test was terminated after 3 days. The volume of the Parr vessel is relatively small and chemical reactions that occur during the test cycle release compounds into the test solution that is not removed will affect the test conditions, albeit the initial test condition was within the ASTM G31 standard [add reference: *ASTM G31 - 72(2004) Standard Practice for Laboratory Immersion Corrosion Testing of Metals*] for specimen surface area to water volume. Nevertheless, the solution is periodically refreshed /replaced to maintain a controlled test environment. For the other 3 coupons, the solutions were replaced every 3 days. For 9 and 12-day exposure runs, solution samples were taken from the last 3 days of each run. One solution sample was analyzed for pH and conductivity then saved. The other sample solution was passed through a filter with filtrate imaged under bifocal light microscope and SEM to detect any particulate in the solution.

The samples were weighed after each pre-determined exposure interval. The weights were compared to the starting weights to determine the trends of weight gain/loss during exposures. Depending on scheduled exposure duration, weights were measured after 3 hours, 24 hours (1 day), 48 hours (2 days), 72 hours (3 days), 144 hours (6 days) and 216 hours (9 days) on various samples.

5.0 Results and Discussion

5.1 <u>As-Received Condition</u>

5.1.1 Surface Radiological Condition

Upon receipt of the panel sections at SRNL, they were measured to determine their radiological conditions. Both probe and smear techniques were used. The results are summarized in Table 6. A general observation is that Region 2 sections have significantly less surface radiological activity than Region 1. This is attributed to Region 1 panels being strapped to the rack and directly exposed to the fuel pool environment in contrast to the Region 2 panels which were encased in the stainless steel sheath. Variations in Region 1 panel radiological conditions may be attributed to differing degrees of the epoxy sealant coverage.

Table 6. Summary of Radiological Measurements of the Boral® Sections

Panel	MR/HR Dose	ALPHA CPM/100 CM² Probe	BETA/GAMMA CPM/100 CM² Probe	ALPHA CPM /100 CM² Smear	BETA/GAMMA CPM/100 CM² Smear	Section #
2J19N	1	ND	7000	ND	5000	12
2K19W	1	400	220000	ND	40000	1
2K20S	1.5	200	180000	ND	10000	10
2K21N	1.5	1000	300000	ND	40000	11
2L19E	1	200	200000	ND	30000	12
2L19N	1	ND	4000	ND	2000	1
2L19S	1	250	150000	ND	40000	10
2L20N	1.5	250	100000	ND	12000	11
5L9E	1	ND	5000	ND	ND	6
5L9S	1	ND	ND	ND	ND	2
5M17E	1	ND	7000	ND	ND	12
5M7S	1	ND	ND	ND	ND	7
5M12E	1	ND	10000	ND	ND	1
5M12S	1	ND	6000	ND	1000	11

5.1.2 General Visual Observations

The following observations were made based on the visual inspections of the as-received specimens:

Paint - The surfaces of some panels appear to be masked by the encapsulation paint to varying degrees. The exposed Region 1 surfaces are most affected. An example of the paint condition is shown in Figure 12. Note that the overspray stopped running when the hold down strip was encountered. Region 1 has more general paint coverage than Region 2 which would be expected since Region 2 panels were in a steel sheath when the paint was applied.

Figure 12. Front of Panel 2L19E-6, an example of a worst-case condition of encapsulation paint coverage

Figure 13. Example of Flow Hole Indications on Panels 2J19L and 5L19 E

Flow holes - For Region 2 - module P panels the Boral® core was sheathed in stainless steel which was attached to the cell wall. The holes were assumed to have been drilled post fabrication through the sheath outer wall at the top of the panel. The holes are termed "flow holes" by the authors. The authors' understanding is that the holes were drilled post-fabrication to reduce hydrogen gas buildup in response to sheath seal weld failures allowing water ingress with corrosion and concomitant hydrogen generation.

Some of the Region 1 cells also had sheathes and flow holes. Panel sections 2J19N and 2L19N do not have surface indications of strap contact and 2J19N has a flow hole indication. Panel 12 from 2L19N was not included in the shipment so the verification of a flow hole cannot be made for that panel. An example of the flow hole indication is shown in Figure 13. The visual observation is that there is clad penetration at the flow hole. Options for this condition include that the clad penetration occurred during the machining of the flow hole (if drilled post-fabrication) and/or that there is some electrochemical assisted corrosion that occurred in service.
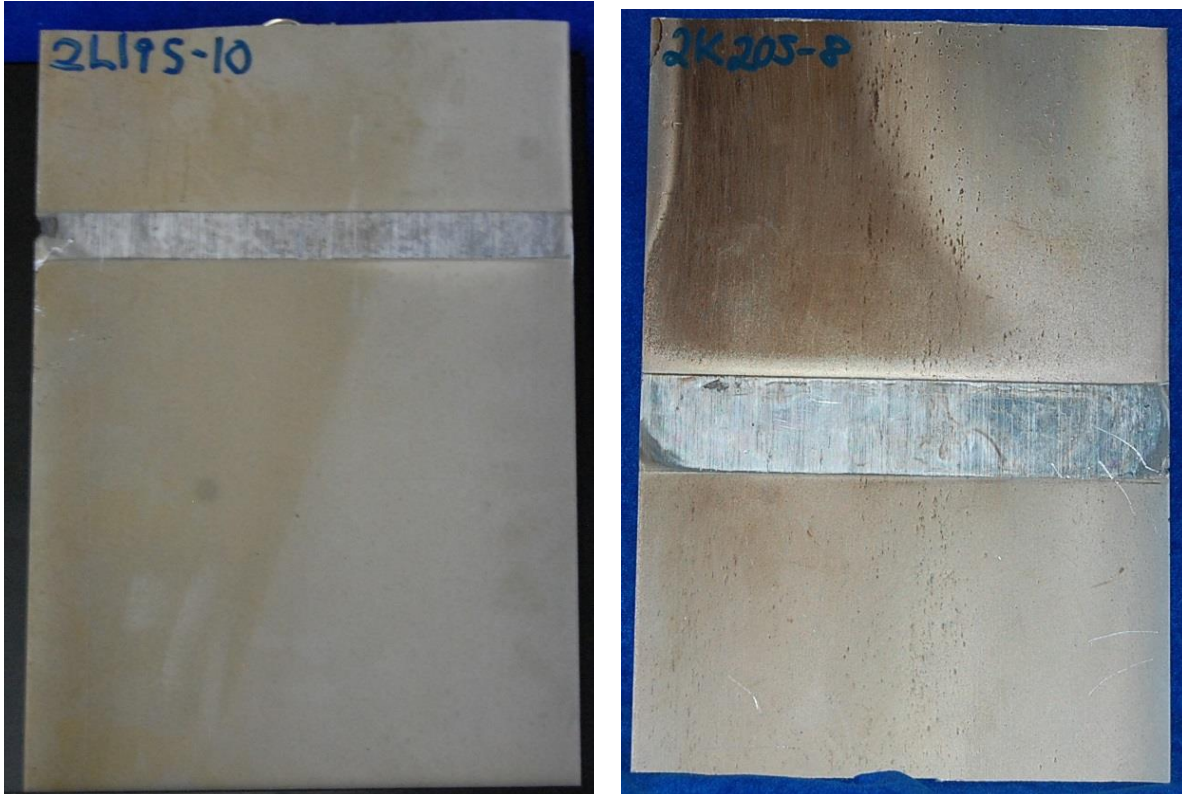
Figure 14. Example of Residual Indications from Straps

Metal Retaining Straps Indications - On Region 1 /module B panels, the exposed Boral® was attached to the cell walls by metal bands and end tabs, refer to Figure 14. The area under the straps visually appears to have less corrosion than the adjacent areas. This condition will be addressed further in Section 5.1.3. Examples of the strap indications are found in Figure 14.

Surface pitting was observed but for most of the panels it was not very severe. For a few panels, the pitting appeared to have penetrated the clad. The surface condition with the paint and some other residual materials did not support a quantitative pitting characterization. Figure 15 shows an example of a potentially severe pitting condition.
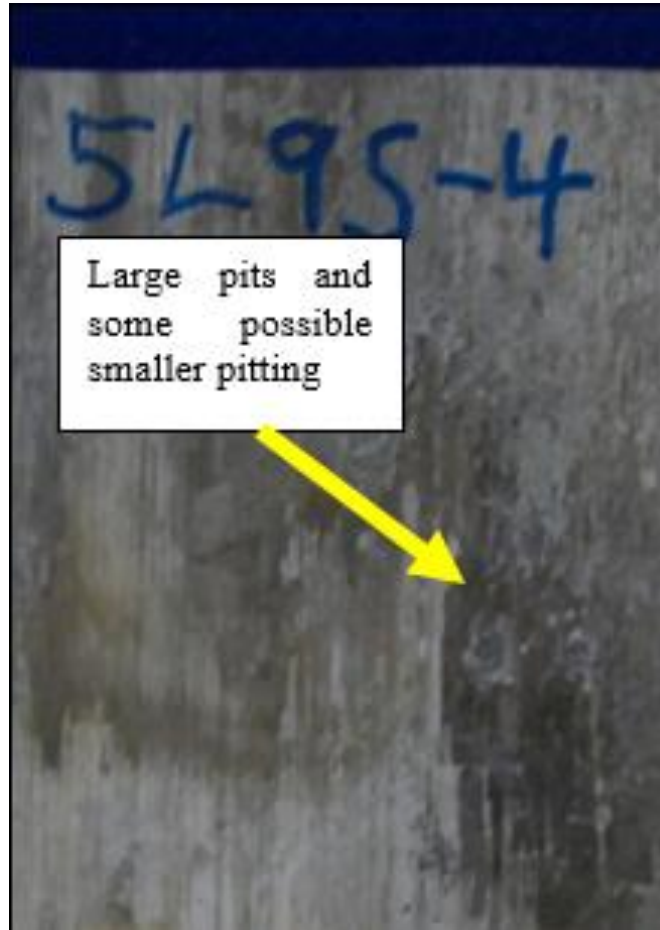
Figure 15. Possible Worst-Case Pitting Condition

Blisters - The panel sections were inspected for any surface blistering. There were four sections that had blisters that are attributed to excessive heat during panel removal and are not suspected of formation during normal operation. The panels were 2K21N-1, -3, -9 and -11. Examples of the condition are shown in Figure 16. There were no observed blisters on any of the panel sections except for the heat related handling blisters noted on 2K21N.
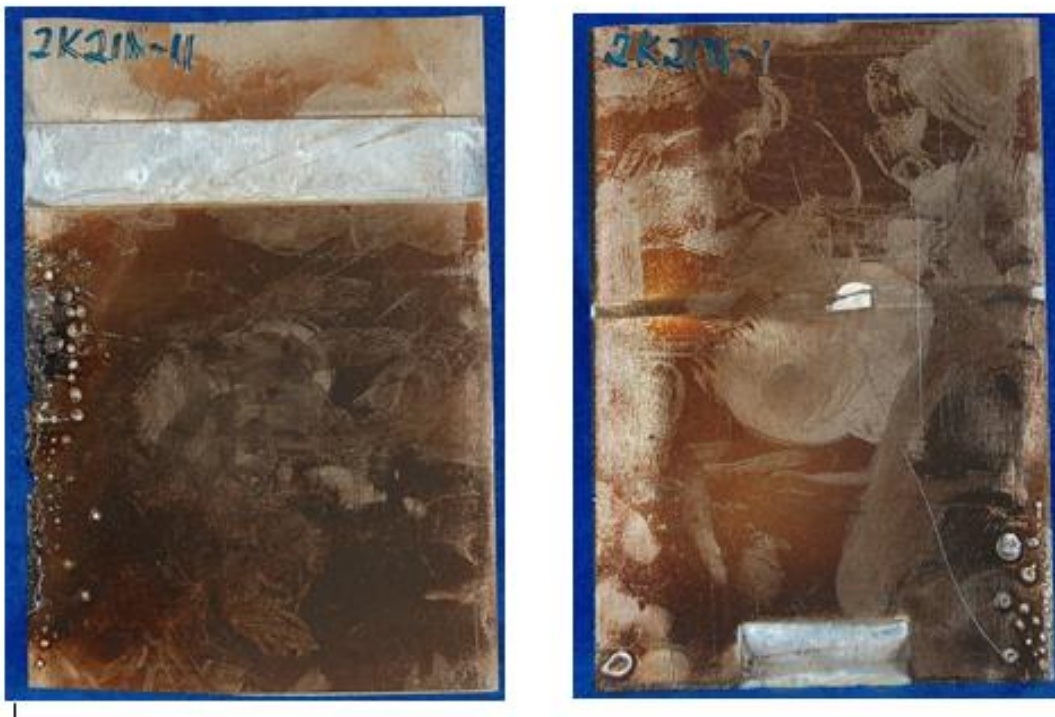
Figure 16. Observed Blisters Due to Excessive Heat During Panel Removal

General Corrosion and Flow Patterns - There are no obvious areas of heavy localized corrosion on the panels. The surface depression relative to the area under the steel straps in Region 1 (Figure 14) suggests that there has been measurable surface corrosion and that most of the resultant oxide is no longer adherent to the plate surface.

Taking into account the more direct application of the sealant to the exposed Region 1 panels relative to the Region 2 panels, the Region 1 panels still have a more uniform surface with less mottling and less irregular surface depths compared to Region 2. Refer to Figure 17 and Figure 18 for comparison examples. While not easily observed, there does appear to be a series of flow patterns on the plates. These flow patterns are best seen on the back of the plates and show an axial (bottom to top) flow. Region 2 has more prominent axial flow indications compared to Region 1. This may be a result of a mild convection flow within the sheath associated with axial temperature gradients and the "open" sides of the panel in Region 1. Figure 19 has examples of flow patterns.
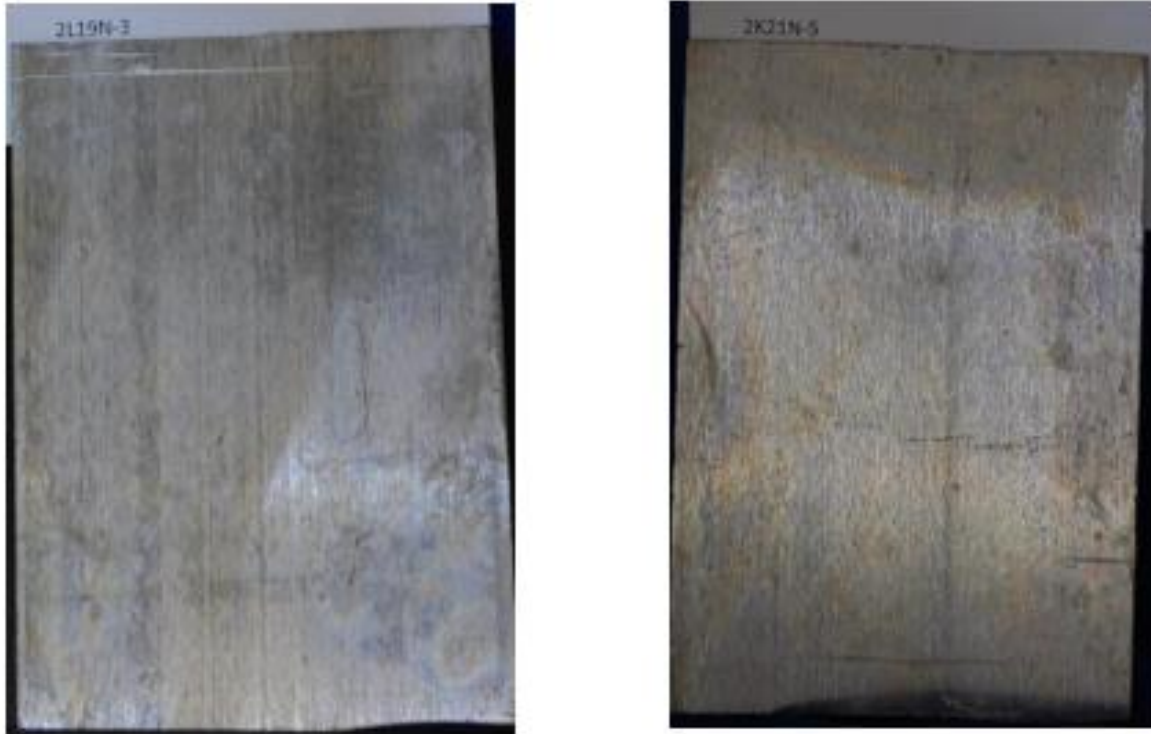
Figure 17. Typical Surfaces from Region 1 Panels – Back sides with no heavy sealant present.

Figure 18. Back Surfaces of Region 2 Panels with Mottled and Irregular Surface Conditions

Back Side

Front Side

Back Side

Back Side

Figure 19. Examples of Flow Patterns on Panels; Panel 5L9E-8 is front and back views and is from Region 2. Panels 2K21N-7 and 2K20S-10 are back side views of panels from Region 1.

Surface pitting, surface contour and surface corrosion results are summarized below, and the detailed evaluations are presented in Appendix B.

- Surface Pitting
  Two sections from section 5L9S-4 were chosen to characterize a representative worst-case pitting condition. A magnified view of the pitted area and the depth profile from the LCM indicates that the pit surface morphology is oval with dimensions of 1.5 mm x 0.8 mm (0.059 in x 0.031 in). The depth of the pit is measured to range from 250-300 microns (9.8 – 11.8 mils) deep relative to the current surface plane. Subsequent evaluations of cross-section views indicate that this is the thickness range of the cladding in Region 2 from which this sample originates.

- Surface Contour
  A sample from section 5L9S-4 was examined to obtain a representative measure of the surface contour profiles observed on some of the sections. The surfaces of Region 1 were "smoother" with less irregularities than those observed from Region 2. A magnified view of the surface shows a range in surface peaks and valleys of from 25 to 60 microns (0.98 to 2.3 mils) in relative height differences. There is a distinct axial flow orientation to the surface contour patterns.

- Hold Down Strap and Tab Indications on Region 1 Panels
  Most of Region 1 panels were not enclosed in a sheath but were directly exposed to the pool water and were held to the cell walls by stainless steel straps at intervals along the length of the panel. The surface texture at the locations where the straps were in direct and sustained contact with the Boral® panels was different than the texture observed on the adjacent surfaces which were continuously exposed to the SFP environment. The surface texture under the straps appeared to be the as-manufactured surface texture and showed minimal evidence of corrosion. A cross-section sample indicates a "plateau" height of about 80 microns or 3.15 mils and represents a conservative (low) estimate of the clad surface removal by corrosion during operation.

- Surface Corrosion
  A representative sample from Region 1, panel 2K20S-10 and Region 2, panel 5M7S-7 were obtained and Ni plated for edge retention prior to mounting for surface interface and oxide layer characterization. The oxide films on 2K20S-10, the 5M7S-7 varies locally with a thickness of 1 to 3 microns which is typical of PWR SFPs [11].

5.1.3 Dimensional Measurements
Dimensional measurements were made on 15 panel sections to characterize the current condition and to determine if any dimensional changes occurred due to service in the fuel pool. The measurements provided data to estimate the corrosions rates experienced by the Boral® panels in the SFP. The detailed results of the dimensional inspections are contained in Appendix C and are summarized below:

- The thickness and width measurements are listed in Table 7. The average thickness for the six Region 1 sections is 2.5273 mm (0.0995 inches) with values ranging from 2.446 to 2.593 mm (0.0963 to 0.1021

inches). The nine measurements from the Region 2 sections had an average thickness of 2.253 mm (0.0887 inches) with values ranging from 2.164 to 2.383 mm (0.0852 to 0.0938 inches). On average, Region 1 is thicker than Region 2 panels by 2.794 mm (0.11 inches). Some of the range in values may be attributed to the presence of the epoxy sealant and manufacturing tolerances, but, as discussed later, there is a component related to the axial position also present. The widths are relatively consistent with no significant variation within a region. On average, Region 1 panels are wider than Region 2 panels by 18.796 mm (0.74 inches).

Table 7. Summary of With and Thickness Measurements

Panel #		THICKNESS-inches			Avg Thickness	WIDTH-inches		AVG WIDTH
		A	B	C		D	E	
2L19S-2		0.0992	0.0978	0.0972	0.09807	8.269	8.275	8.272
2L19S-8		0.101	0.0979	0.1	0.09963	8.267	8.27	8.269
2L19S-12		0.1019	0.1018	0.1012	0.10163	8.275	8.275	8.275
	avg	0.1007	0.0992	0.0995	0.09978	8.2703	8.2733	8.272
2K20S-2		0.1021	0.0963	0.0948	0.09773	8.275	8.267	8.271
2K20S-6		0.1021	0.0993	0.0968	0.0994	8.264	8.266	8.265
2K20S-12			0.101	0.0982	0.0996	8.271	8.276	8.274
	avg	0.1021	0.0989	0.0966	0.09919	8.27	8.2697	8.270
5L9E-2		0.089	0.0871	0.0858	0.0873	7.531	7.525	7.528
5L9E-8		0.0929	0.0868	0.0852	0.0883	7.54	7.532	7.536
5L9E-12		0.0871	0.0883	0.0854	0.08693	7.537	7.536	7.537
	avg	0.0897	0.0874	0.0855	0.08751	7.536	7.531	7.534
5M7E-2		0.0895	0.0894	0.0895	0.08947	7.523	7.526	7.525
5M7E-6		0.0902	0.0908	0.089	0.09	7.528	7.525	7.527
5M7E-12		0.0938	0.0895	0.0909	0.0914	7.535	7.54	7.538
	avg	0.0912	0.0899	0.0898	0.09029	7.5287	7.5303	7.530
5M12E-1		0.0888	0.0882	0.0861	0.0877	7.549	7.551	7.550
5M12E-7		0.0892	0.0882	0.0871	0.08817	7.53	7.534	7.532
5M12E-11		0.0895	0.0891	0.0881	0.0889	7.538	7.528	7.533
	avg	0.0892	0.0885	0.0871	0.08826	7.539	7.5377	7.538

- Axial thickness variations
  The average panel thicknesses for the samples measured are 2.527 mm (0.0995 inches) for Region 1 and 2.253 mm (0.0887 inches) for Region 2 in the areas where the panel has been directly exposed to the fuel pool water. There were additional thickness measurements taken in specific areas on Region 1 panels which had thicker values. The thickness measurements are documented in Figure 20 and show a trend for thicker measurements near the top axial position. If the difference in panel thickness is not due to manufacturing processes or the epoxy paint, the results suggest that there may be differing surface corrosion rates depending on axial location with the highest near the panel bottom. The "-1" location is the bottom axial section and "-12" is the top section from the panels.
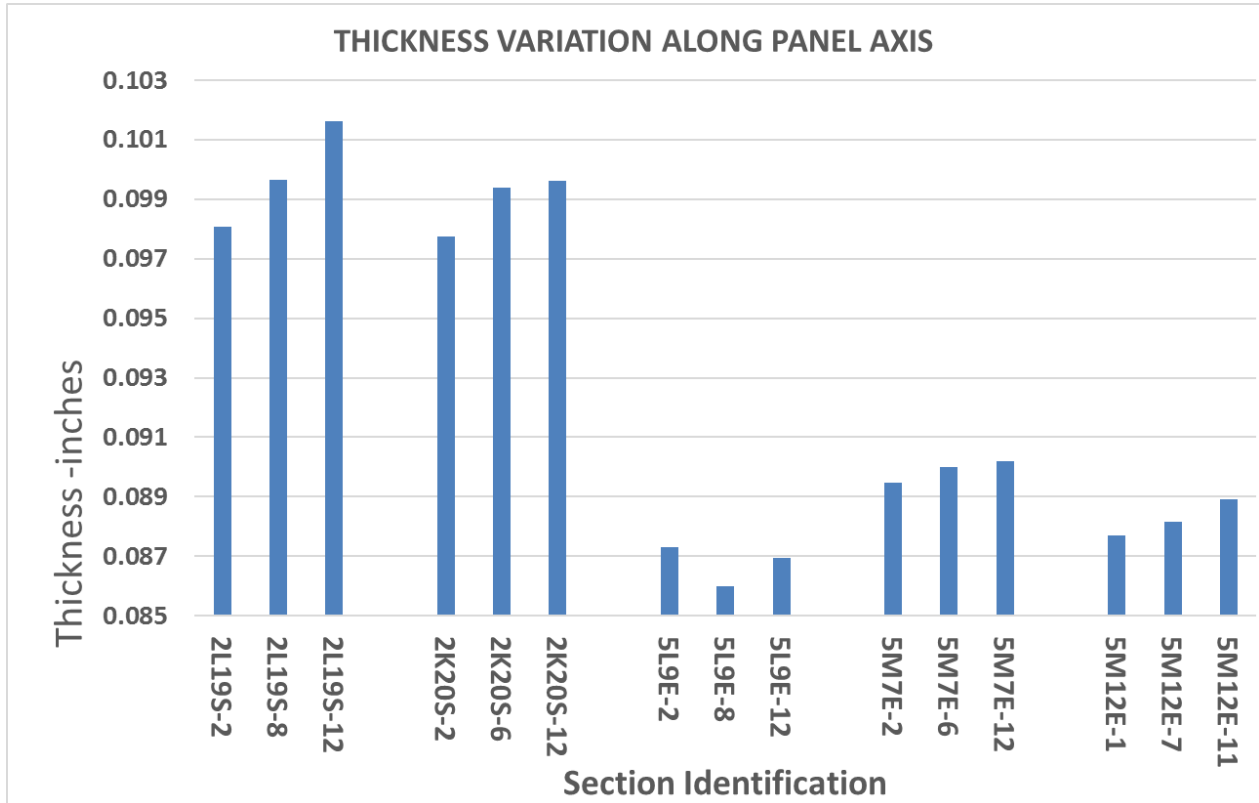
Figure 20. Showing the trend for Increasing Thickness (lower corrosion) at the Higher Axial Locations

- Region 1 Strap effects

  Upon the initial visual inspection of the segments it was observed that the Region 1 sections that were in contact with the stainless-steel hold down straps had a raised surface at the locations under the strap. Specific thickness measurements were taken at these strap locations for comparison with adjacent non-strap locations. The panel surfaces at the strap location look similar to what would be expected as the as-fabricated surface condition. It is postulated that the stainless-steel straps protected the clad area from water contact. The only galvanic attack region was observed immediately adjacent to the strap/clad interface and is minor, as seen in Figure 22.

  The difference in thickness between these two locations is assumed to be a function of the surface corrosion occurring on one side of the panel section. The measurements are shown graphically in Figure 21.
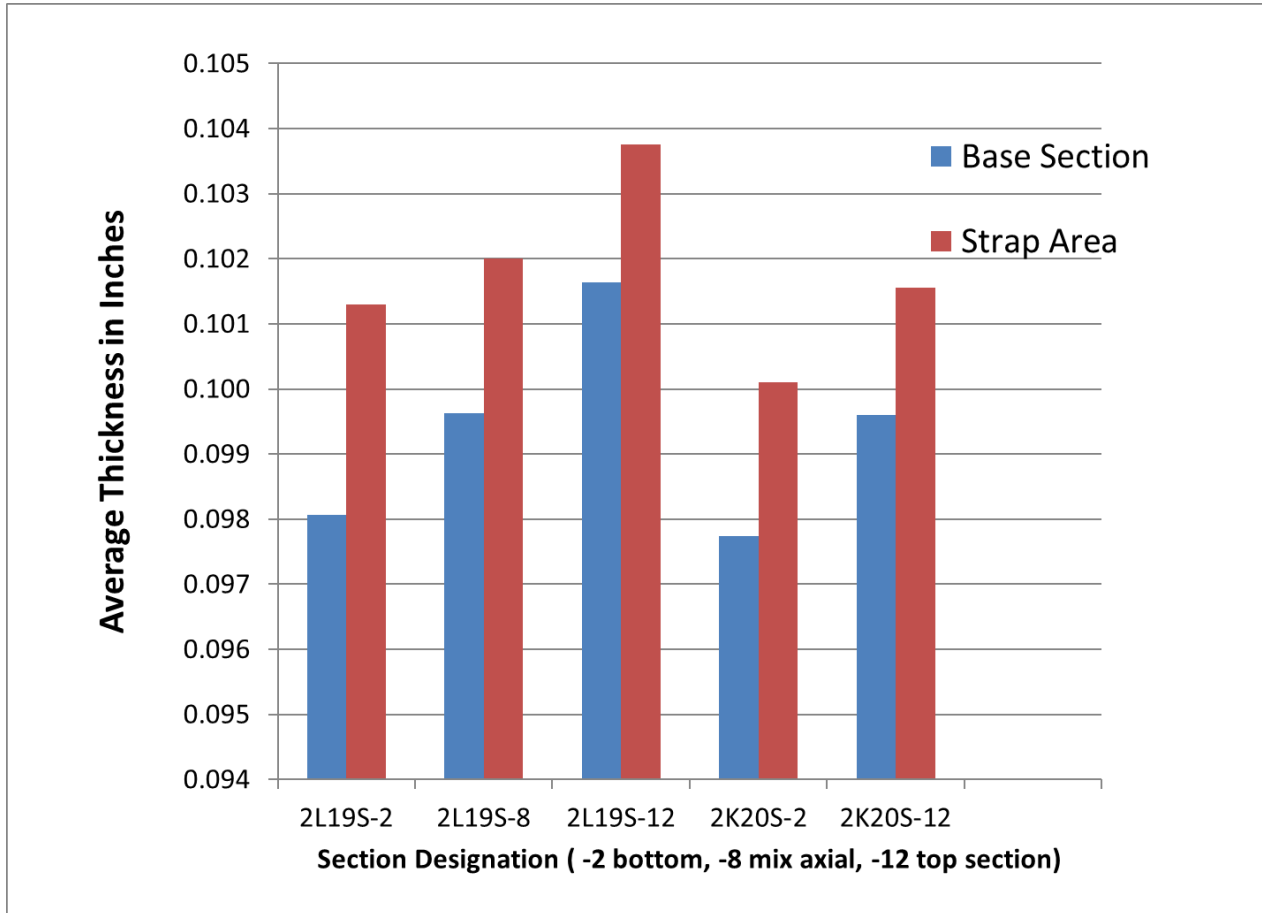
Figure 21. Comparison of Thickness at Strap and Non-Strap Areas

Comparing the strap area thicknesses to the non-strap area thicknesses, and using the step-height change between the protected clad (strap) and the non-protected clad (non-strap) thicknesses, it is estimated that:

- There is a difference in thickness of approximately 0.05 mm (0.002 inch) for both 2L19S-12 and 2K20S-12 sections between strap and non-strap area. It is assumed that no corrosion occurs directly under the strap. That is, the strap is 100% protective to the original clad underneath it.
- There are slight differences in the step height (thickness) of the strap to adjacent non-strap region going from top to bottom. This suggests a difference in corrosion of about 0.05 to 0.08 mm (2 to 3 mils) with the bottom being greater. Specifically, the difference in thickness between the strap and non-strap regions from bottom to top are as follows:
  - Panel section 2L19S-2: 0.081 mm (0.0032 inch) (bottom), 0.058 mm (0.0023 inch) (mid-panel) and 0.053 mm (0.0021 inch) (top)
    Panel section 2K20S: 0.061 mm (0.0024 inch) (bottom) and 0.048 (0.0019 inch) (top)
- The 24.9 mm (0.098 inch) thicknesses in the non-strap area compared to the starting thickness estimates indicate single sided corrosion in the range of 0.05 to 0.08 mm (2 to 3 mils) in the bottom locations for Region 1 or about 0.0025 to 0.004 mm/yr (0.1 to 0.15 mils/year) for a 20-year life.

The cross-section measurement of sample 2K20S-10 is shown in Figure 22 below. The epoxy paint was not observed on the specimen. The image shows: i) the cladding thickness immediately under the strap to

be 0.08 mm (3 mils) greater than the cladding thickness remote from the strap; and ii) apparent galvanic attack immediately at the strap/clad interface. The average cladding thickness for the two strap locations is 0.315 mm (12 mils). The average cladding thickness of the 5 non-strap locations is 0.235 mm (9 mils). The difference is 0.080 mm (3 mils) and is conservatively assumed to be due to corrosion and corresponds to a corrosion rate over 22 years of approximately 0.0035 mm/year (0.14 mils/year). The data from the cross-section measurements match well with the macro measurement comparisons.
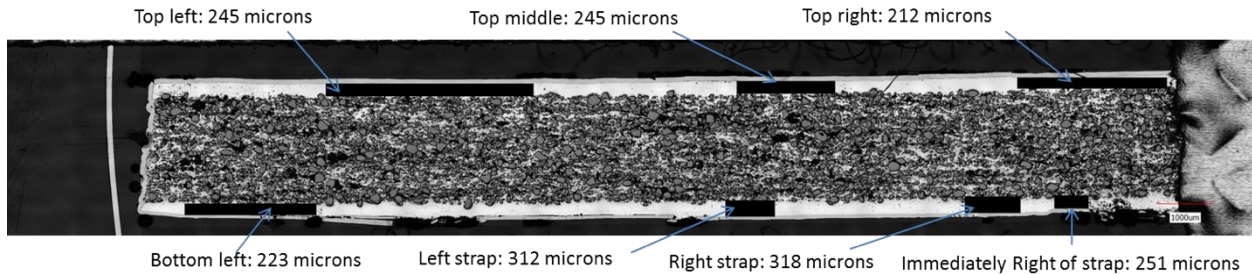
Figure 22. Cross-sectional view of panel section 2K20S-10 at the location of a strap showing the local cladding thickness

As mentioned, the cross-section view of a sample from 2K20S-10 (Region 1 panel) indicate the clad thickness away from the raised strap contact area to be on average 0.235 mm (0.0092 inch). The view (Figure 22) also shows a "band" above the cladding. This band is the nickel plating that was applied to this metallurgical specimen to aid in polishing for microscopy examination.

The micrographs of Region 1 and Region 2 specimens is shown in Figure 23 below. The micrographs are at the same magnification and show that the Region 1 specimen had a core region thickness of approximately 80 mils and the Region 2 specimen had a core region thickness of approximately 60 mils. The claddings were both approximately 10 to 13 mils, depending on local variation.
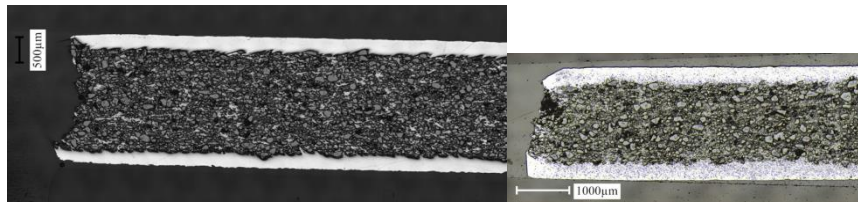
Figure 23. Region 1 specimen 2L19N-9 with a total thickness of ~2580 μm on left and Region 2 specimen 5L9E-6 with a total thickness of ~2160 μm on right

5.2 Blister Evaluation

5L9S-12 Blisters

Blisters were produced in panel specimen 5L9S-12 as shown in Figure 24. The panel was placed in air in an oven at 268 °C (515 °F) for a total time of one hour. A sound was heard and blisters were observed after the few minutes of exposure; no significant growth occurred with the remaining exposure. The blistered panel sample had a measured weight loss of 2.33 grams from the initial weight of 215.39 grams which is assumed to be moisture loss. There were seven blisters observed on the front face with diameters of 6.5, 3,

4, 2.3, 6.4, 5.7 and 1.8 cm. There were 3 blisters on the back with diameters of 8.5, 2.3 and 1.5 cm. One mid-sized (about 2.5 cm diameter) blistered area was sectioned and mounted for viewing as shown in Figure 25. Some of the B$_4$C particles are retained/embedded in the aluminum cladding. It is estimated from the visual exam that $\leq$ 5% of the B$_4$C is embedded in the aluminum cladding. The blister lift-off gap at the peak distance is equal to or greater than the core thickness. Figure 26 is a confocal view of the blister prior to sectioning and shows the relative height to be 1709 microns or 67 mils.
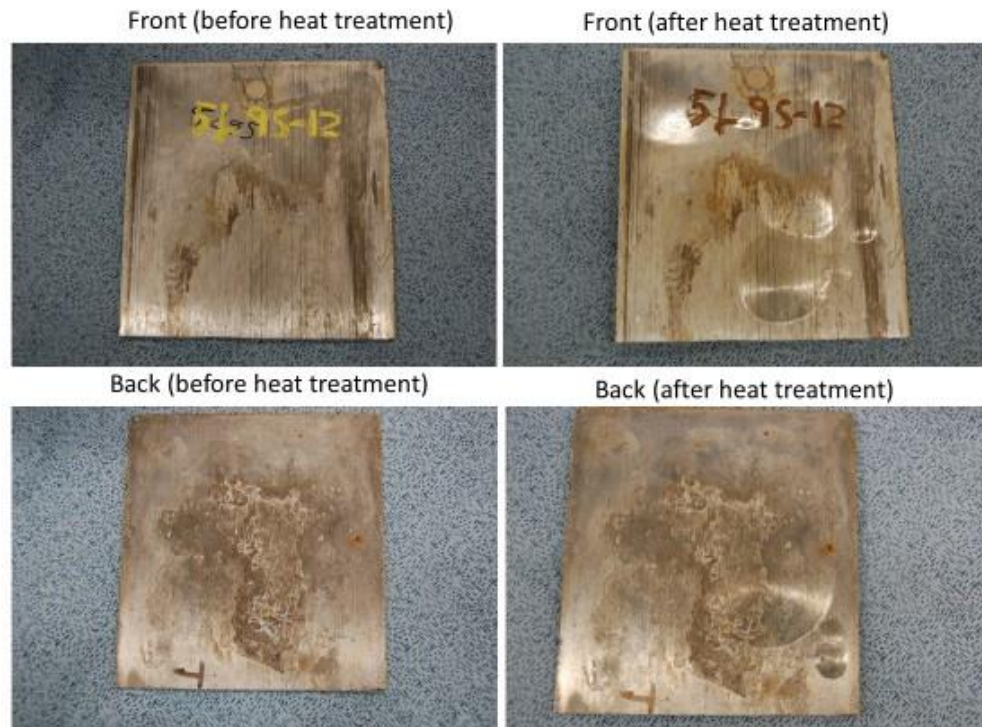
Figure 24. Blister formation on Sample from 5L9S-12
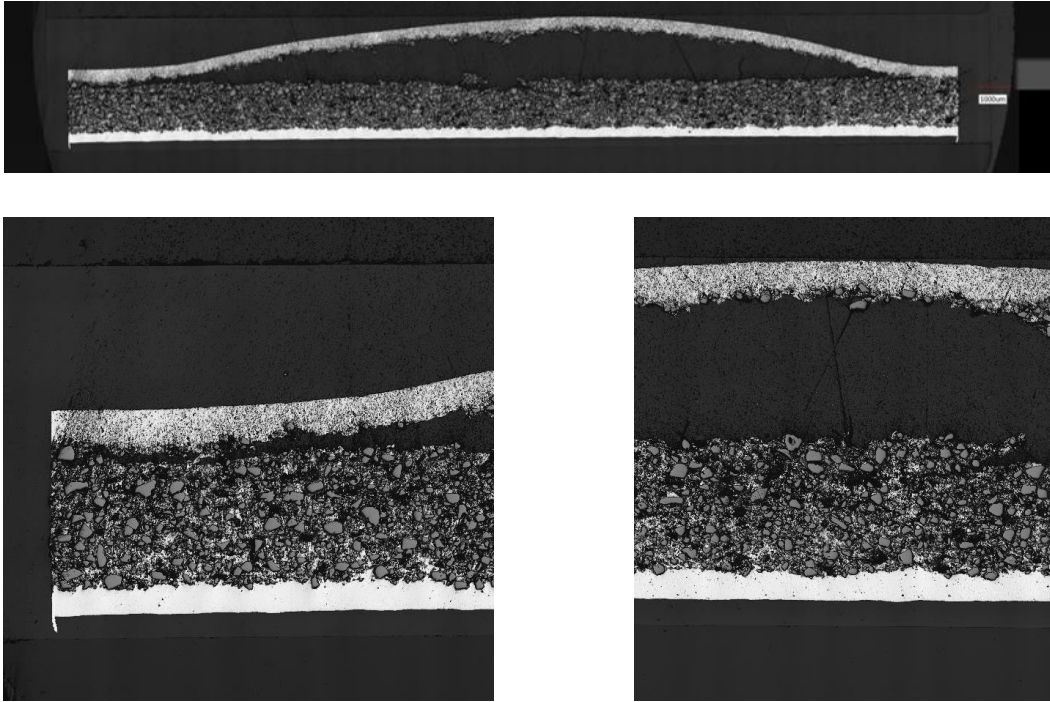
Figure 25. Sample 5L9S-12 Blister Morphology
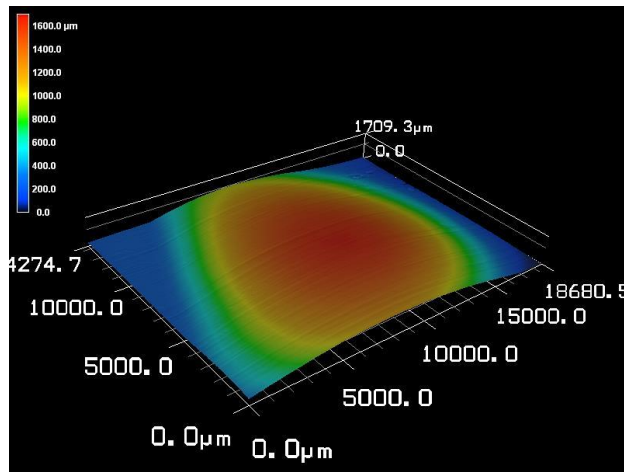
Figure 26. Relief Image of Blister on 5L9S-12

5.3 <u>Weight Loss Evaluation</u>

During the laboratory generation of blisters by incremental increases in temperature exposure, the weights of the samples were measured after each exposure. The resultant weight loss provides data that is representative of moisture retained in the sample. During the time in the fuel pool, water can enter the Boral® matrix from the exposed sides. The water appears to have been retained in the material; internal oxidation to cause corrosion products to block water egress may actually trap water by sealing some of the egress paths. The measured weight losses from the samples that were heated to generate blisters was

normalized to a sample weight loss percentage and plotted in Figure 27. The normalized weight loss also approximates a weight loss per unit surface area for the samples nominally the same thickness. The trend is consistent for the samples tested and shows a small weight loss rate up to 121 °C (250 °F) then a rise in the rate which probably is associated with a water – steam transformation. The weight loss can be associated with:

- Surface oxide de-hydration
- Surface artifact (epoxy paint) loss
- Moisture and/or hydrogen escape from core region

In looking at the results from the 10 minutes and one hour holds there is a time dependency on the weight loss. This would suggest a rate controlling mechanism that is postulated not to be a surface related effect but more of an internal transport through the core to the free surface sides. There is clearly internal moisture and hydrogen gas present as observed from the blister formations. The presence of internal moisture combined with the observations that a) the rate changes at the water-steam transformation temperature, b) there is no significant visual surface change and c) the surface oxide is very thin and not containing sufficient H_2O for the observed weight losses, supports the conclusion that the weight loss is primarily a loss of internal moisture and some hydrogen gas generated from corrosion. Further testing would be required to fully understand the mechanisms occurring, evolving species and rates at longer times and higher temperatures.
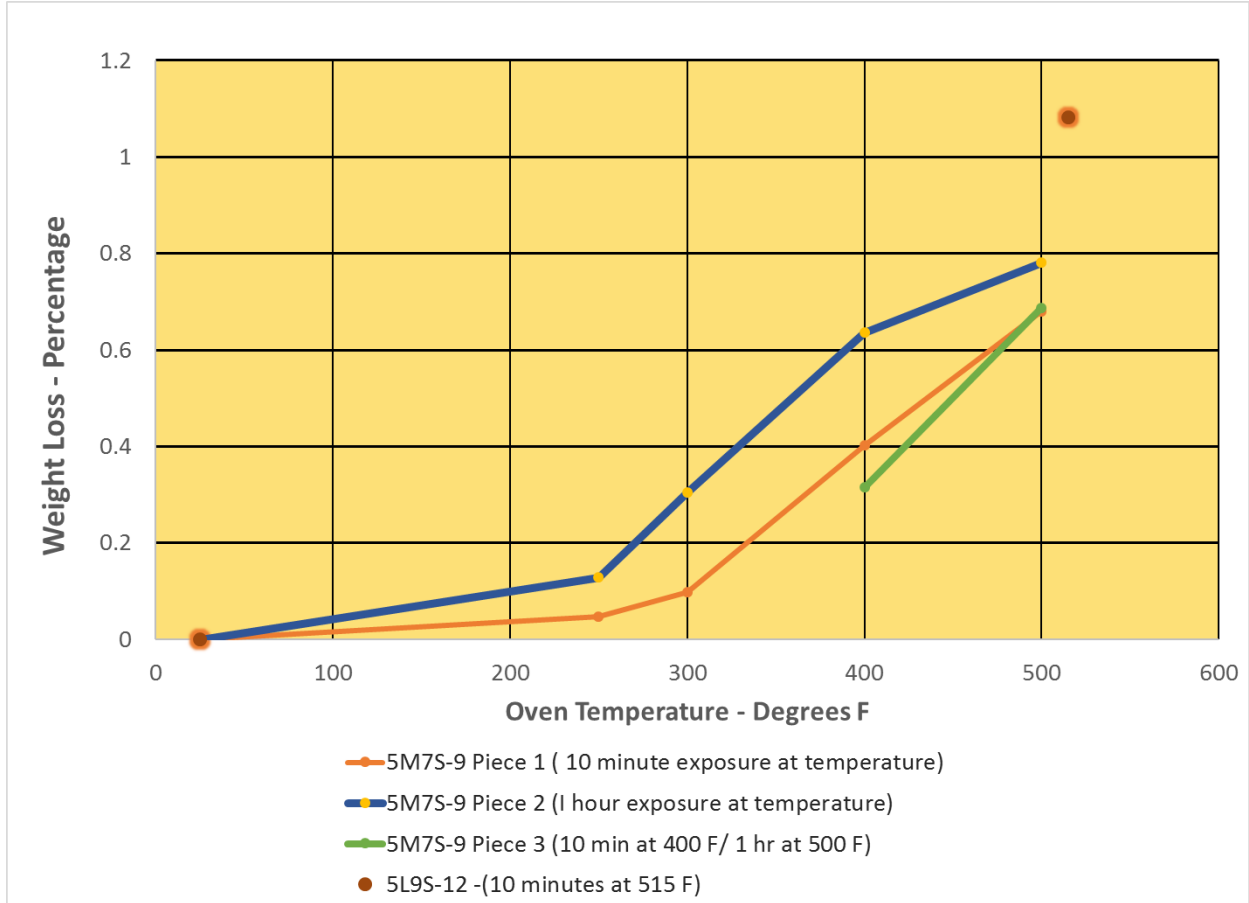
Figure 27. Incremental Weight Loss During Blister Formation Heating Cycle

5.4 <u>Areal Density</u>

5.4.1 Areal Density (AD) Measurement by Badger and PSU

The evaluation of the Boral® panels from Zion include the SRNL AD measurements and two sets of AD measurements taken using neutron attenuation with BADGER and by PSU.

5.4.1.1 BADGER Results

BADGER results for select Region 1 panels are shown in Figure 28 [12]. Panel 2K20S-10 was used for the SRNL dissolution areal density measurement procedure development. While the results for panel 2K20S-10 represent one specific axial section, they can be compared to these BADGER data on Region 1 sister panels.

The BADGER results for the Region 2 panels shown in Figure 29 range from about 0.0276 to 0.314 with error bars ranging from about 0.024 to 0.034 gm $B^{10}/$ cm^2 .
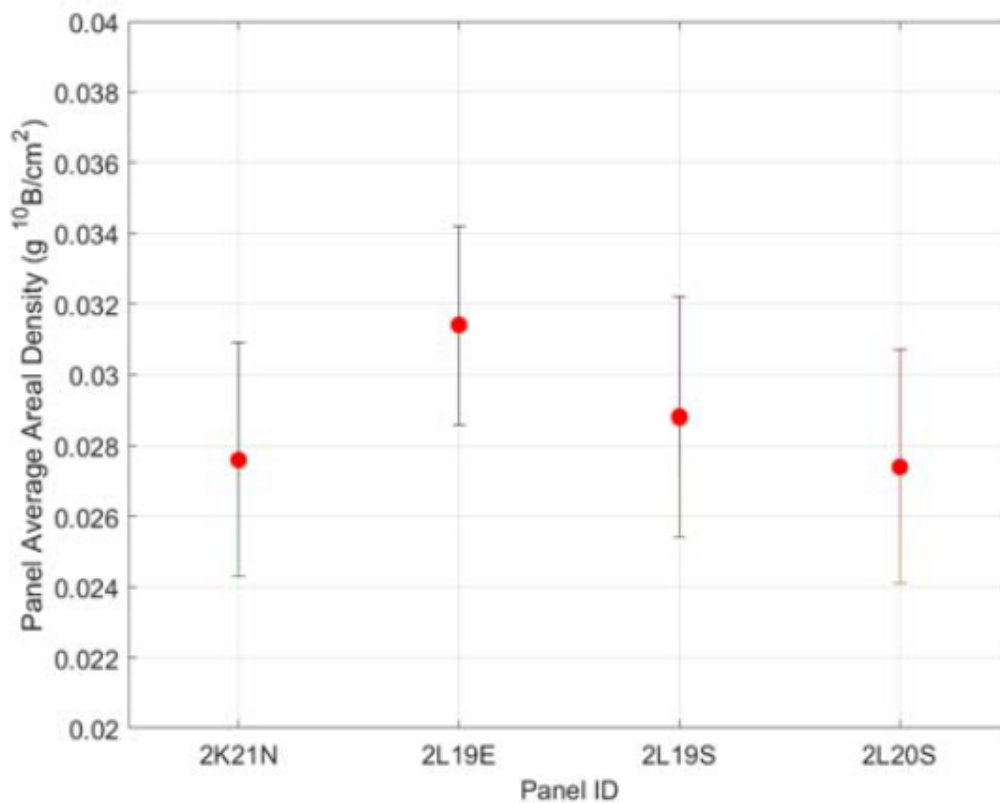
Figure 28. BADGER results for selected Region 1 Boral® panels. (preliminary data subject to change) (12)
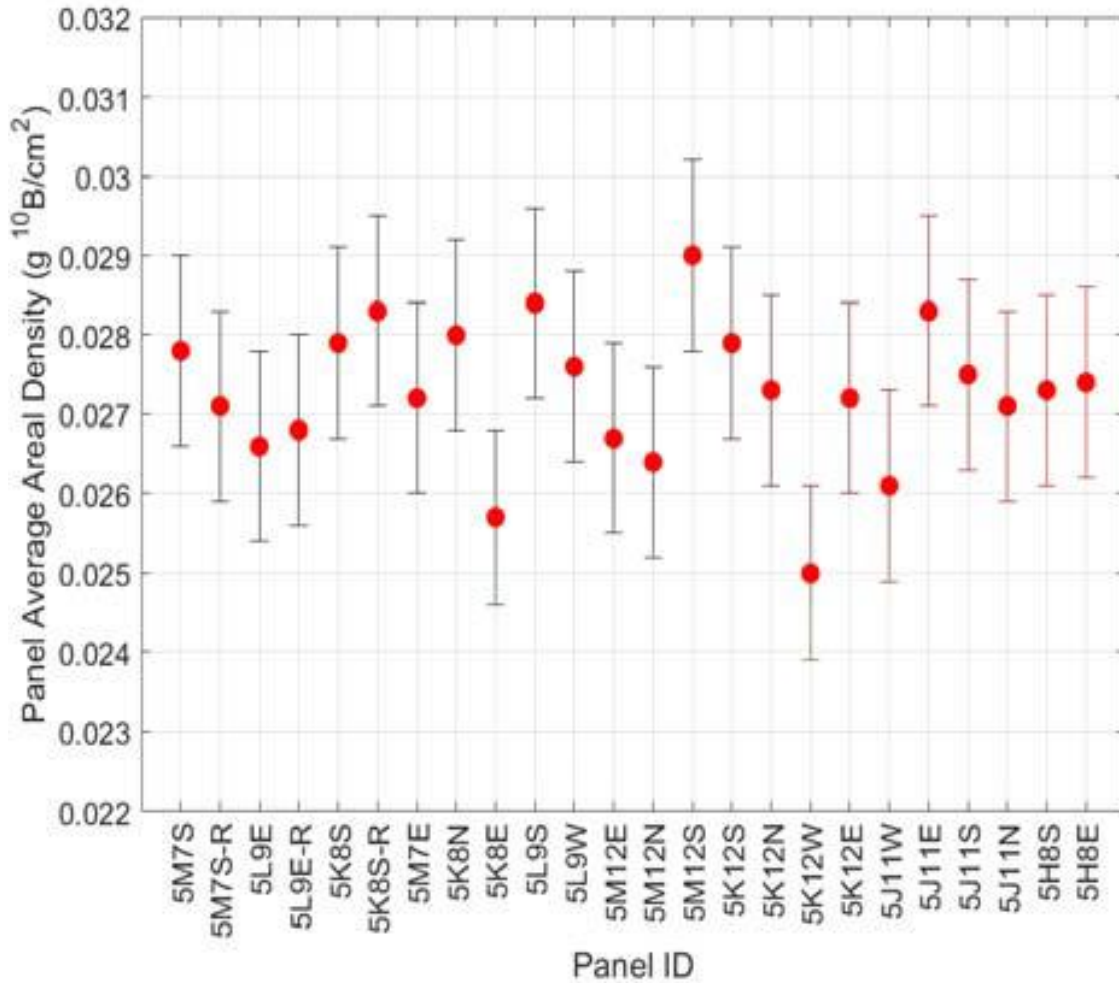
Figure 29. BADGER Results for the region-2 panels (preliminary data subject to change) (12)

5.4.1.2 Pennsylvania State University (PSU) Evaluation

A neutron attenuation technique was used at PSU to determine the AD values for all the panel sections provided to EPRI. AD values on the test panels were measured at six locations on the panels as shown in Figure 30. The results of the AD measurements are shown in Figure 31 for Region 1 panels and Figure 32 for Region 2 panels [13]

Following the AD measurements performed at Penn State, EPRI provided panels 2K21N-2 (Region 1) and 5M7S-6 (Region 2) to SRNL for analysis. Seven samples in total were analyzed: 1 sample for 2K21N-2 and 5 samples from 5M7S-6. Additional samples were received from 2K21N-2 but had significant surface contamination that prevented their transfer for testing. These panels were initially measured non-destructively for AD by NETCO using BADGER and PSU using the neutron attenuation technique described in [3]
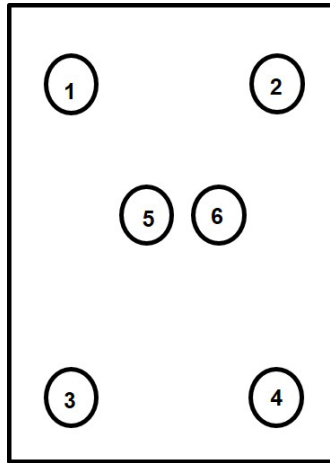
Figure 30. The B-10 areal density was measured at PSU using a n-attenuation method at six locations
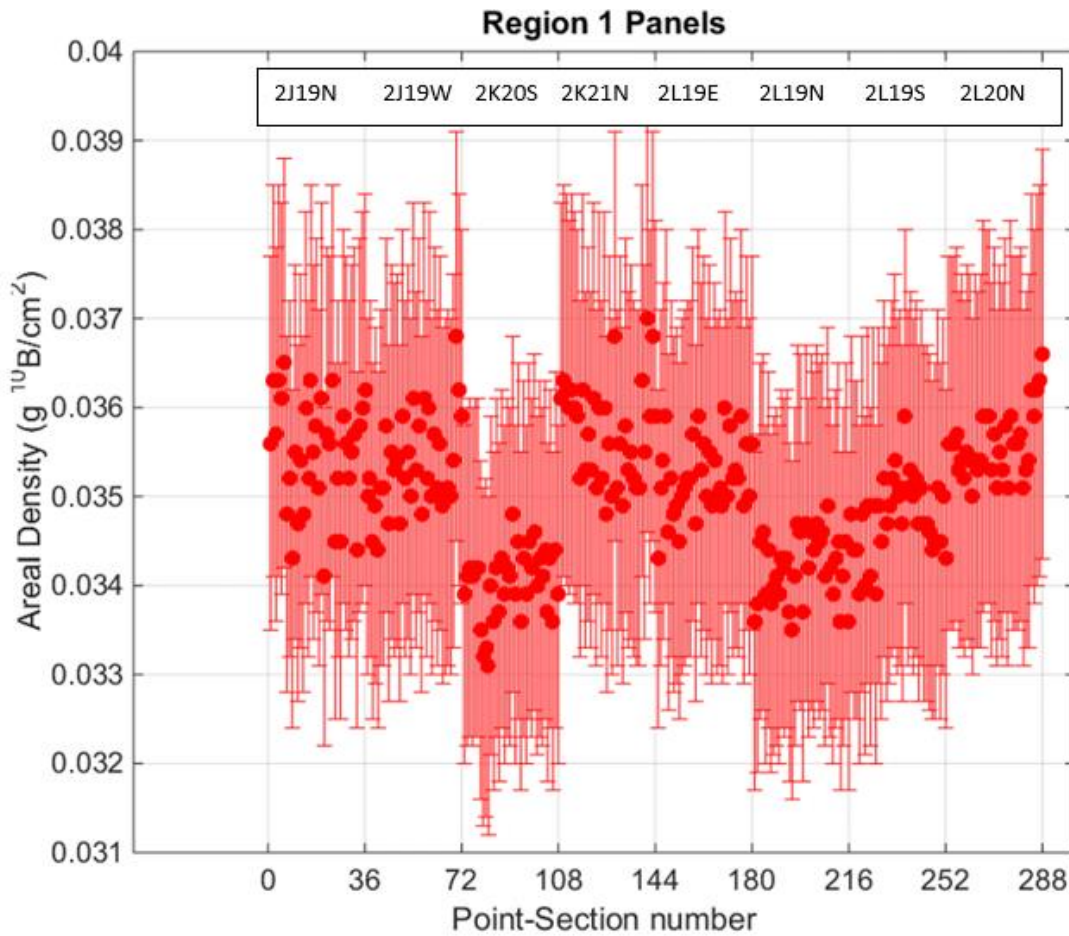
Figure 31. PSU AD Measurements on Region 1 Boral® (12) (courtesy of EPRI)
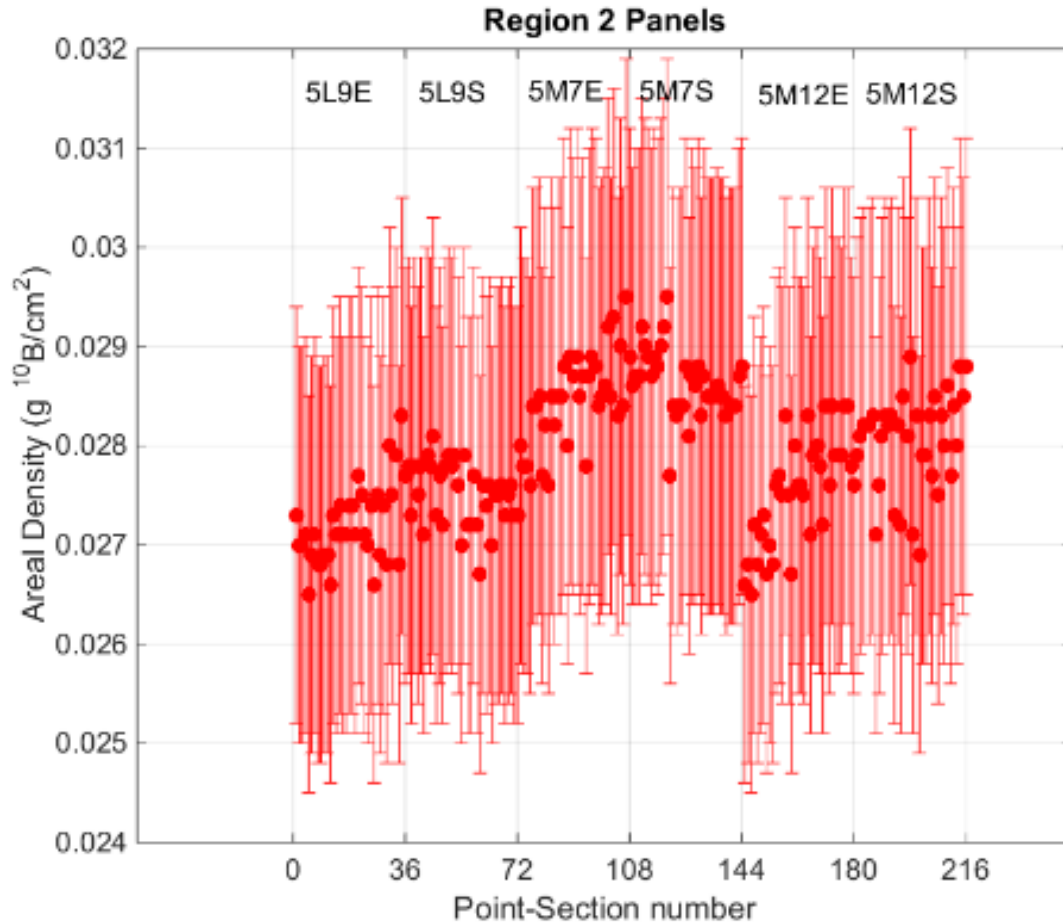
Figure 32. PSU AD measurements for Region 2 Panels (12) (courtesy of EPRI)

5.4.2 SRNL Chemical Digestion AD Measurements

5.4.2.1 Results from 2K21N-2 and 5M7S-6

Figure 31 shows the 2K21N panel has an average AD of about 0.0355 gm ^{10}B/ cm^2, with a +/- 3 sigma range from 0.0330 to 0.0385 gm ^{10}B /cm^2. The PSU results for the six scans on section 2K21N-2 are reported as averaging 0.0361 gm ^{10}B /cm^2. Figure 32 shows PSU results from Region 2 and includes panel 5M7S. The PSU results provided with the samples show for section 5M7S-6 an average AD of 0.0282 gm ^{10}B /cm^2.

The specimens analyzed by SRNL in relation to their location on the plate shown in Figure 30 are the following: 5M-A (location 1), 5M-B (location 2), 5M-C (location 5), 5M-D (location 6), 5M-E (location 3), 5M-F (location 4), 2K-C (location 5). The point-to-point comparison of the SRNL digestion results to the PSU neutron attenuation point IDs are shown in Table 8.

Table 8. Comparison of point identification between SRNL and PSU

Test ID	
SRNL	Penn State
5M7S-6	
5MA	5M07S-06:1
5MB	5M07S-06:2
5MC	5M07S-06:5
5MD	5M07S-06:6
5ME	5M07S-06:3
5MF	5M07S-06:4
2K21N-02	
2KA	2K21N-02:1
2KB	2K21N-02:2
2KC	2K21N-02:5
2KD	2K21N-02:6
2KE	2K21N-02:3
2KF	2K21N-02:4

The PSU results along with preliminary BADGER results and SRNL results are compared in Table 9 The preliminary BADGER, PSU and SRNL results for Region 2 (5M7S) are in general agreement; within 3% to 5%. For the Region 1 results (2K21N and 2K20S) the Badger AD results are lower than the PSU and SRNL AD results. The SRNL and PSU results for the region 1 samples range from 20% to 30% higher than the BADGER results. The determination of the basis for this difference is outside of the scope of this program.

It should be noted that the ^{10}B AD total measurement uncertainties for the SRNL chemical analysis AD method results are approximately 22%. This is due to an average total ^{10}B measurement uncertainty of 20.1% associated with the ^{10}B mass spectrometry results (see Appendix E for the treatment of uncertainties). The total ^{10}B measurement uncertainty is the combined method uncertainty and sampling uncertainties (i.e. the standard deviation of repeat measurements). The method uncertainty was 20% and the sampling uncertainty ranged from 1.15 % to 3.27 %, resulting in an average total measurement uncertainty of 20.1%. The mean ^{10}B concentration for the five Region 2 samples (panel 5M7S-6) was 18.4 wt. %, which is within the range of ^{10}B natural abundance (i.e. 17.5 wt % to 18.9 wt %).

Table 9. Comparison of AD results [g of ^{10}B/cm^2] from BADGER, PSU and SRNL Evaluations.

Panel	5M7S-6							2K21N-2	
	5MA	5MB	5MC	5MD	5ME	5MF	Ave	2KC	Ave
SRNL*	0.0277	0.0279	0.0270	0.0288	0.0273	0.0283	0.0278	0.0333	
PSU average	0.0283	0.0284	0.0284	0.0288	0.0277	0.0284	0.0283		0.0360
BADGER							0.0270		0.0277
% difference for SRNL data versus BADGER							3%		20%
% difference for PSU data versus BADGER							5%		30%
*Assume Al-B$_4$C and 1% impurity									

5.5 <u>EC Testing Results and Discussion</u>

5.5.1 Core Corrosion Electrochemical Experiments

Cladding was removed on one side of a previously blistered sample: 5L9S-12. The cladding was removed by peeling it off slowly using pincers. The specimen was mounted and electrochemical experiments were performed using Solutions 3 to 6 at three temperatures: 25, 75 and 98 °C (Solutions 1 and 2 were added to the scope after the core corrosion testing was completed). Corrosion rates were obtained by LPR and Tafel constants from Tafel plots.

Figure 33 shows the corrosion rates obtained for the four solutions at three temperatures. To determine the corrosion rate for the core, the LPR data was adjusted assuming that aluminum is the only component that it is corroding and that the surface area was composed of 60% aluminum and 40% boron carbide particles. (The Al: boron carbide surface area ratio was determined via metallography.) Thus, the surface area of the active sample was reduced to 60% of the sample size for the LPR-determined corrosion rate. Since the corrosion rate determined via LPR is inversely proportional to the sample surface area, the resulting corrosion rates are higher than if the whole sample surface area was used.
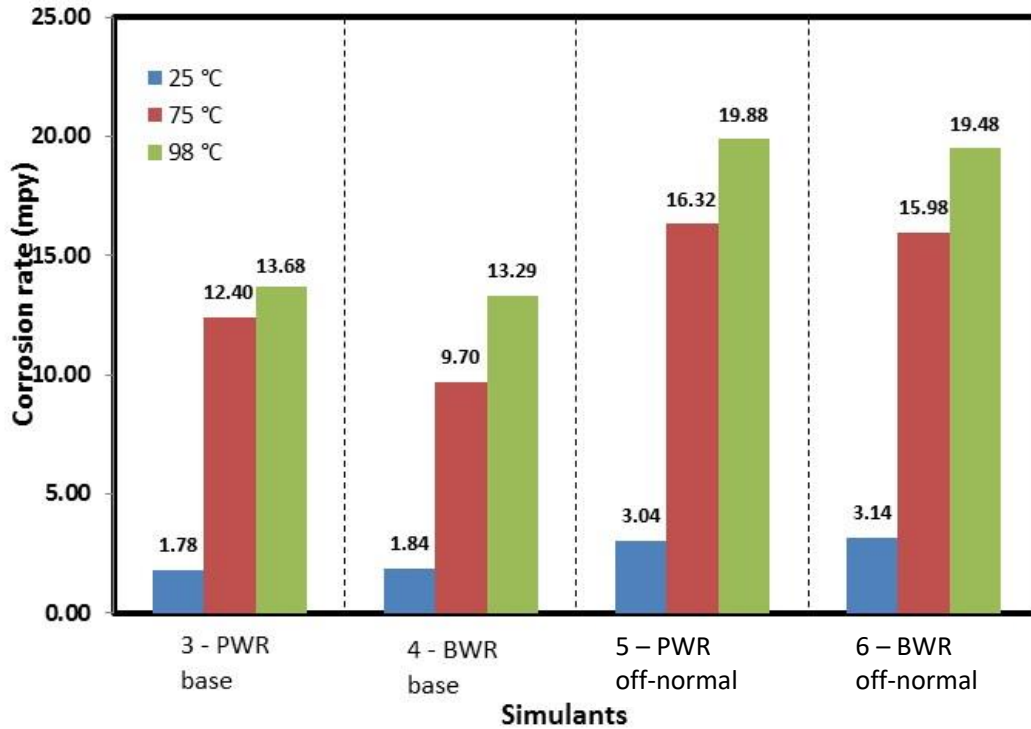
Figure 33. Corrosion rates of cermet core 5L9S-12 in four simulants at three temperatures

As expected, corrosion rates increased with increasing temperature and with the concentration of species in solutions. At room temperature, the corrosion rates are about 0.025 to 0.076 mm/yr (1 to 3 mils/yr) and increased to rates exceeding 0.254 mm/yr (10 mils/yr) at temperatures over 75 °C (167 °F). The corrosion seems to be exacerbated by galvanic effects of aluminum particles in the matrix with inert boron particles.

Arrhenius plots are shown in Figure 34 for the core exposed in Solutions 3 through 6 at three temperatures. Performing the electrochemical experiments at different temperatures allows the formation of an Arrhenius plot. An Arrhenius plot is often used to analyze the effect of temperature on the rates of electrochemical reactions (i.e., corrosion rates). The plot gives a straight line from which activation energies can be determined. The Arrhenius equation is shown below in linearized form,

$$\ln i_{corr} = \ln A - \frac{E_a}{RT}$$

where i_{corr} is the corrosion current density (µA/cm2); A is the pre-exponential factor which is an empirical relationship between temperature and corrosion rate; R is the gas constant with value 8.314 J/mol.K; T is temperature (K) and E_a is the activation energy, which is the minimum energy required to start the electrochemical reaction (J/mol). In an Arrhenius plot, the plot of $\ln i_{corr}$ vs. 1/T provides E_a/R as the slope of the line and $\ln A$ as the y-axis intercept.

It is noted that similar corrosion rates were measured for material in solutions 5 and 6 (off-normal) and, likewise, similar values were obtained from solutions 3 and 4 (nominal). The linear regression of the points showed similarities in slope denoting similar electrochemical reactions. Activation energies for the core were calculated from the slope and ranged from 24 to 27 kJ/mol. Table 10 lists the calculated activation energies.
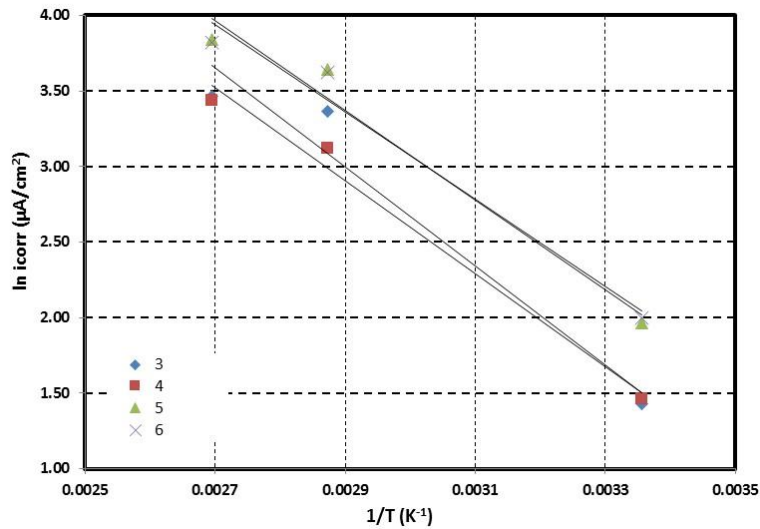
Figure 34. Arrhenius plot of 5L9S-12 core tested in four solutions

Table 10. Activation energies obtained from the Arrhenius plot for the core of 5L9S

Solutions	Activation Energy (Ea) (kJ/mol)
3-PWR base	27.3
4-BWR base	25.6
5-PWR off-normal	24.7
6-BWR off-normal	24

Using the calculated activation energies (Table 10) and the measured corrosion rates (Figure 33), an equation (model) can be developed for the corrosion occurring at the different conditions. For example, using the PWR base data, another form of equation 1 is:

Corrosion rate $= A \times e^{-E_a/RT}$ or Corrosion (distance) $= A \times$ time x $e^{-E_a/RT}$ (2)

$A =$ corrosion rate/ $e^{-E_a/RT}$ (3)

$A = 1.78$ mpy/ $e^{-(27,300/(8.317 \times (273 + 25))}$

$A = 108173$ (4)

Corrosion (mils) $= 108173 \times$ time (years) x $e^{-27,300/8.317/T(K)}$ (5)

Table 11 lists values of thickness loss due to corrosion calculated using equation 5 based on the core corrosion rate in PWR base water. The amount of corrosion at 40 °C represents what might be observed after a year of exposure of the core to the nominal test conditions while the amount of corrosion at 98 C represents the potential performance at an elevated temperature for shorter durations of 7 days and 30 days. These rates and values are listed for information only and reflect a more severe condition because, as will

42

be discussed in a later section, the corrosion rate is expected to decrease with exposure time and oxide build-up. To develop more accurate values for modeling the corrosion at this condition, further testing to develop a steady state corrosion rate is required.

Table 11. Calculated Corrosion Rate of the Cermet Core in PWR Base Water

Time [days]	Temperature [C]	Corrosion* [mils]	Corrosion* [μm]
365	40	3.03	77.03
7	98	0.30	7.60
30	98	1.28	32.58

*Based on an Al : boron carbide surface area ratio of 60:40

5.5.2 Cladding Corrosion Electrochemical Experiments

Two conditions were tested at various temperatures: fresh surface cladding and clad with an aged or oxidized surface generated by exposure over time while immersed in the test solution. The aging procedure produces a more representative oxidized surface condition for the samples rather than the as-received surface which has had handling and decontamination treatments. At the start of this program, corrosion measurements were performed on as-received sample surfaces. The results from these initial tests are included in Appendix B for information. The results obtained showed higher corrosion rates than expected based on the estimates obtained from the analysis of the panel cross-section. Thus, the surface oxide characteristics were analyzed via X-ray diffraction (XRD). The XRD measurements of the as-received panel specimens did not show an expected crystalline film. It is suspected that thermal de-watering of the oxyhydroxide film occurred during panel retrieval from the Zion SFP and subsequent handling and surface preparations. De-watering of the oxyhydroxide film would degrade the passivating capacity) of the as-received surface film making it less representative of panels in the SFP. It was decided to produce a representative surface oxide condition by immersing the samples in the solution and test the corrosion rate change with exposure time. However, due to programmatic constraints, the tests on the lab-grown oxide samples were only performed at 40 °C (104 °F).

5.5.2.1 Fresh Surface Corrosion

Fresh surface was obtained by grinding the surface of the sample with 600 grit SiC paper until a uniform surface was obtained. The grinding was done carefully to prevent the appearance of core particles since the cladding is very thin. The electrochemical experiments were performed for samples exposed at each of the six solutions at 25 °C (77 °F), 75 °C (167 °F) and 98 °C (208 °F). Figure 35 displays the corrosion rates derived from constants from Tafel and CPP plots.
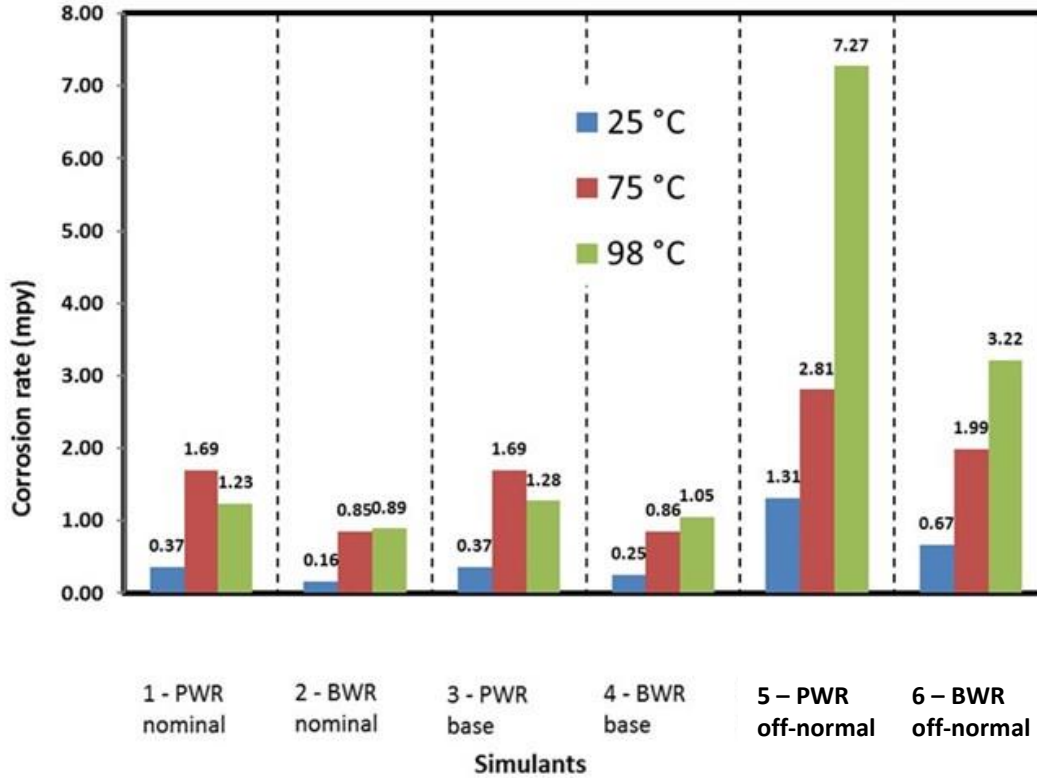
Figure 35. Corrosion rates of aluminum cladding 5L9S-4 in six simulants at three temperatures

The EC testing performed on freshly ground cladding surfaces resulted in generally higher corrosion rates for the specimens tested in the simulated PWR water than the specimens tested in the simulated BWR water at each testing temperature. The corrosion rates for the ground specimens represent possible upper bound rates for these testing conditions since protective oxides that form in the simulants have little time to develop during the EC testing. It will be shown later in this report that the corrosion rates of ground specimens decrease significantly with increasing testing time for both the PWR and BWR base simulants.

The Arrhenius plots for the fresh surface cladding are presented in Figure 36. For the cladding, the Arrhenius plots resulted in almost equally linear parallel slopes. There was also a slight change in slope for simulant 6 compared to simulant 2 and no change for simulant 5 and simulant 1. This further explains that the nominal and base conditions exhibit similar performance, especially when comparing to off-normal conditions. The activation energy values are given in Table 11. For the cladding, activation energies were obtained from 17.6 to 23 kJ/mol. Compared to core corrosion it is still relatively close to the activation energies obtained demonstrating that aluminum corrosion is the dominant electrochemical reaction occurring.
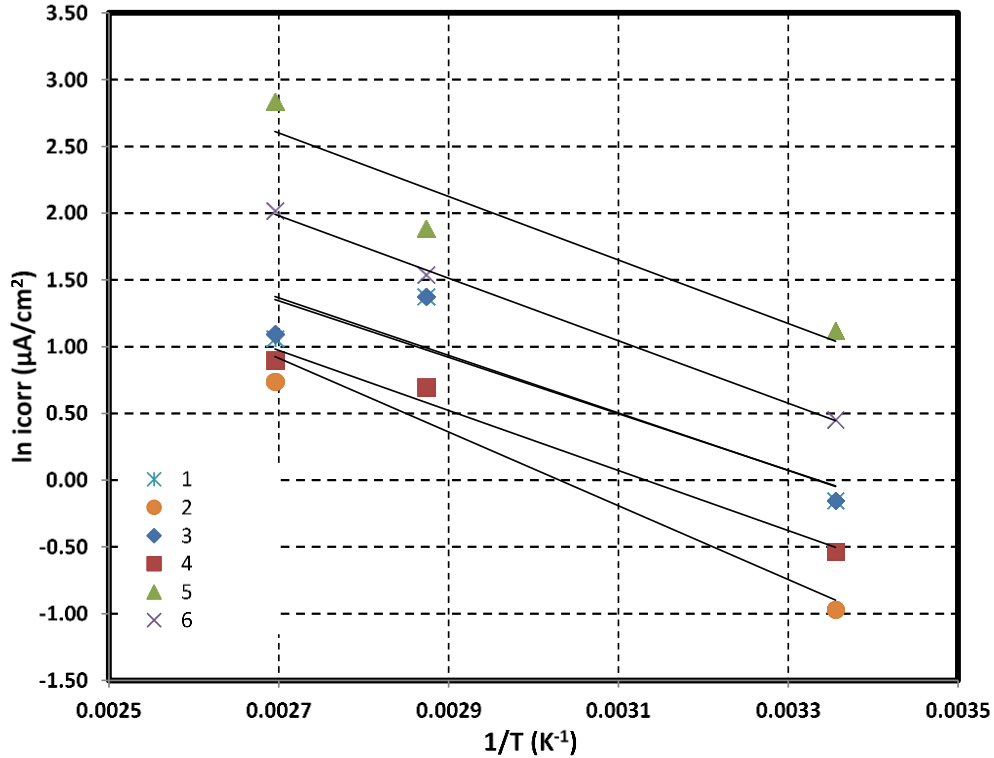
Figure 36. Arrhenius plot of aluminum cladding 5L9S-4 tested in six solutions

Table 12. Activation energies obtained from the Arrhenius plot for the aluminum cladding 5L9S-4

Solutions	Activation Energy (Ea) KJ/mol
1-PWR nominal	17.6
2-BWR nominal	23
3-PWR base	17.9
4-BWR base	18.7
5-PWR off-normal	19.8
6-BWR off-normal	19.5

CPP scans for the six solutions at 25 °C and for two solutions at 75 and 98 °C are shown in Figure 37 and Figure 38, respectively. Values for corrosion potential Ecorr, passivation current i_{pass}, passivation range and the repassivation potential E_{rp} from the CPP scans are listed in Table 13. Gray shaded areas indicate that experiments were not performed for those conditions. At 25 °C (Figure 37), a very active anodization behavior was observed for samples in all simulants with a small passive hump in the scan for the samples in solutions 1 and 4. The OCP obtained was from -0.317 to -0.446 V vs. SCE. The CPP curves reached the 2 V limit during the scans, except for the CPP curve of solution 5, which met the threshold current at approximately 1.06 V vs. SCE. The scans showed positive hysteresis, which indicates pitting susceptibility, and, as observed in the pictures below Figure 37, all samples showed differing degrees of pitting. As expected, the pitting is more prevalent with larger diameters and greater apparent depths for samples exposed to solutions 5 and 6 than for solutions 1-4. At 75 and 98 °C (Figure 38), experiments were only

performed for specimens exposed to solutions 1 and 2. OCP was consistent with respect to the OCP at 25 °C only for the sample in solution 1 at 75 °C. All other OCPs went to more negative values to a range of -0.842 to -0.900 V vs. SCE. The lower OCP potential resulted in an increment in passive region (i.e, voltage change in which current remained at the same value after E_{corr} determination). As indicated in Table 13, the passive regions were larger for solution 2 (BWR nominal) than solution 1 (PWR nominal), especially for temperatures at 75 and 98 °C. Positive hysteresis was observed and the 2 V limit was reached for all of the scans. The change in OCP to more active values is believed to be caused by the transition of oxide crystalline structure from gibbsite/bayerite to boehmite, although there is not conclusive evidence. Pictures presented in Figure 38 bottom, as expected, showed the appearance of localized corrosion which was more aggressive at 98 °C than at 75 °C.
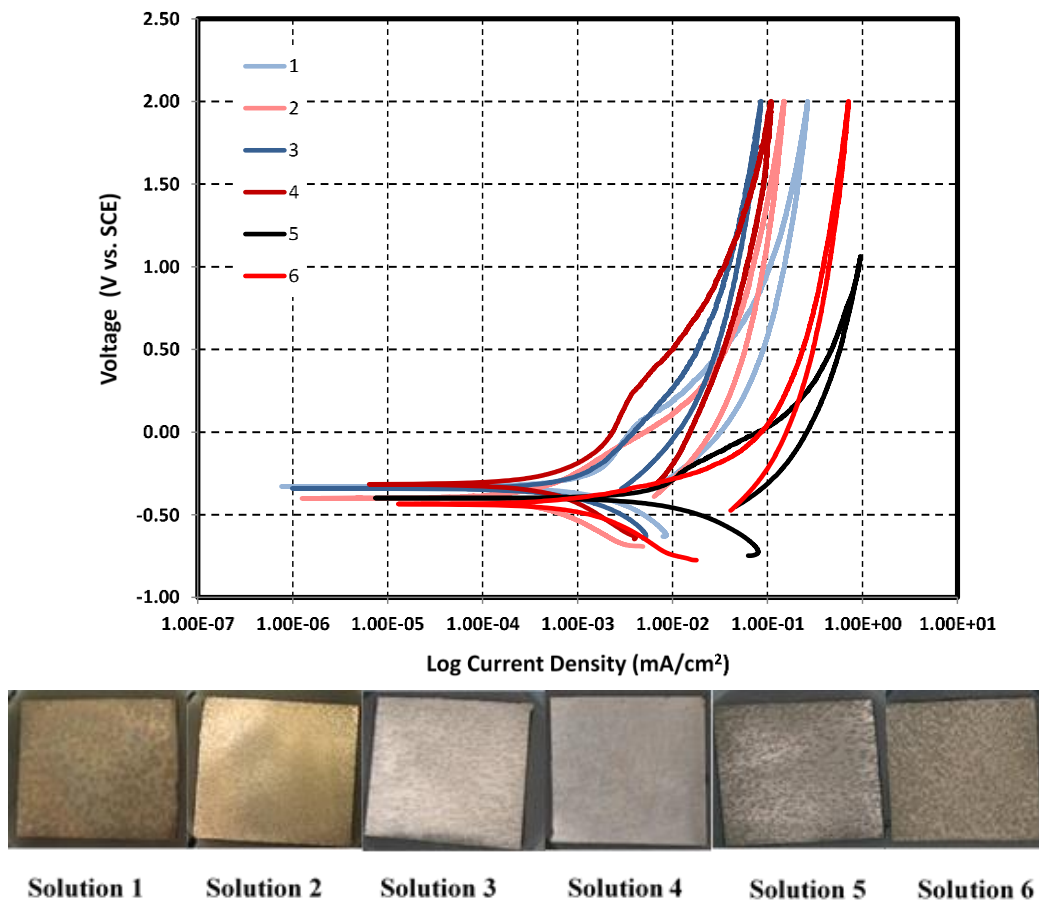
Figure 37. (top) CPP scans for fresh surface cladding 5L9S-4 exposed in solutions 1 to 6 at 25 °C and (bottom) after test pictures (The color difference in solutions 1 and 2 are just light changes)
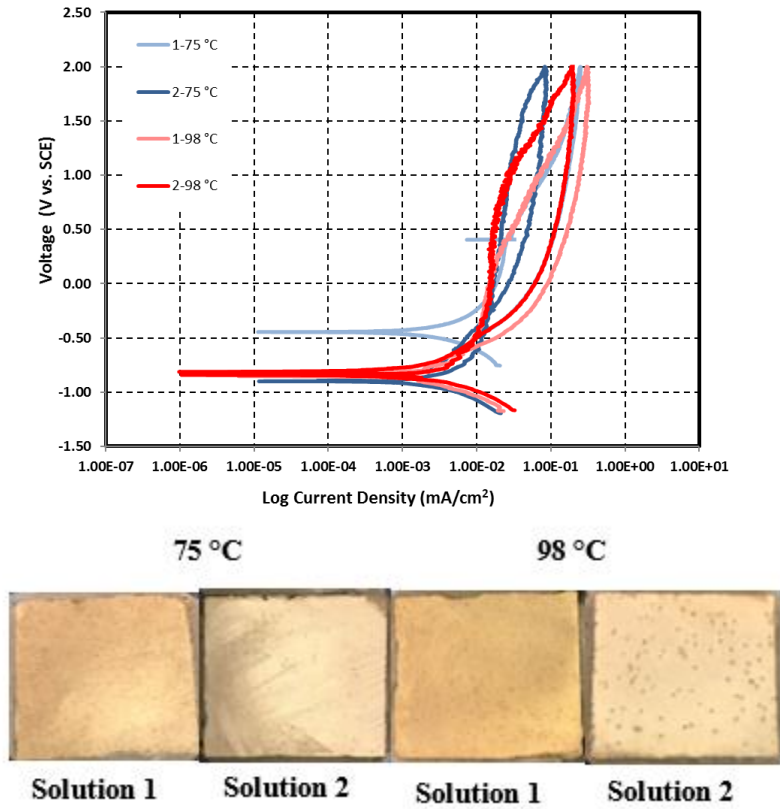
Figure 38. (top) CPP scans for fresh surface cladding 5L9S-4 exposed in solutions 1 and 2 at 75 and 98 °C and (bottom) after test pictures

Table 13. CPP parameters obtained from CPP scans of fresh surface 5L9S-4 experiments

Solution	Temperature (°C)	E_{corr} (V vs. SCE)	i_{pass} (µA/cm²)	Passive range (V)	E_{rp} (V vs. SCE)
1	25	-0.329	3.1	0.15	-
	75	-0.446	18.6	0.59	-
	98	-0.842	16.7	0.85	-0.632
2	25	-0.400	-	-	-
	75	-0.900	30.5	2.39	-0.300
	98	-0.842	10.3	1.55	-0.513
3	25	-0.34	-	-	-
	75				
	98				
4	25	-0.317	2.7	0.31	-
	75				
	98				
5	25	-0.399	11.0	0.06	-
	75				
	98				
6	25	-0.435	-	-	-
	75				
	98				

5.5.2.2 Corrosion Rates for Clad Surface with Surface Oxide grown During Exposure (Aged Oxide Surface)

Two sets of tests were carried out on cladded samples to evaluate the impact of a surface oxide grown under typical SFP water conditions on the resultant corrosion rates. The sample surfaces from panel 5L9S-4 were polished with 600 grit paper to produce a fresh aluminum alloy surface prior to exposure to the test solutions. Initially it was observed that corrosion rates over time were different regarding the solution condition depending on whether it was refreshed during the exposure time or allowed to degrade over time. Considering the large volume of the fuel pool water and the range of chemistries addressed in the test matrix, it was determined that a controlled solution refresh was representative of the pool exposure conditions. The two sets of test parameters adopted were:

- PWR Simulant 3 with a controlled solution refresh during the test at 40 °C.
- BWR Simulant 4 with a controlled solution refresh during the test at 40 °C.

- <u>Tests in 40 °C PWR Base Water Simulant 3 and BWR Base Water Simulant 4 (with solution refresh during test exposure)</u>

To understand the effect of maintaining a relatively constant immersion solution chemistry, corrosion tests were performed with solution monitoring and periodic solution changes when the chemistry exceeded a predetermined range. The EC experiments consisted on running LPR and EIS experiments initially and weekly in a solution with refreshment of the solution to maintain conductivity to less than 12 µS/cm. To maintain low conductivity, a solution change-out was performed before the solution reached 12 µS/cm and at the completion of each EC measurement interval. Table 14 records the solution changes and pertinent

chemistry values for the PWR simulant 3. Table 15 has the chemistry information for the BWR simulant 4.

Table 14. pH and Conductivity Measurements for Immersion Test Simulant 3 With Refreshed Chemistries During the Test Exposure

Condition	Simulant: 3-PWR base	
	pH	Conductivity (μS/cm)
Before at room temp.	5.01	9.2
Before at 40 °C	4.75	8.4
After test at 40 °C	5.06	20.5
New solution at 40 °C - 1st change	4.54	7.5
Day 3 at 40 °C	N/A	10.8
New solution at 40 °C - 2nd change	5.06	7.4
Week 1 before test at 40 °C	5.14	8.9
Week 1 after test at 40 °C	5.06	25.7
New solution at 40 °C - 3rd change	4.91	7.7
Week 2 before test at 40 °C	4.92	10.0
Week 2 after test at 40 °C	5.1	12.5
New solution at 40 °C - 4th change	4.8	7.2
Week 3 before test at 40 °C	4.76	9.6
Week 3 after test at 40 °C	4.95	12.2
New solution at 40 °C - 5th change	4.71	7.8
Week 4 before test at 40 °C	4.67	8.3
Week 4 after test at 40 °C	4.98	11.2
New solution at 40 °C - 6th change	4.78	7.7

Table 15. pH and Conductivity Measurements for Immersion Test Simulant 4 With Refreshed Chemistries During the Test Exposure

Condition	Simulant: 4-BWR base	
	pH	Conductivity (μS/cm)
Before at room temp.	7.62	2.35
Before at 40 °C	7.83	3.85
After test at 40 °C	7.95	7.12
New solution at 40 °C - 1st change	7.8	3.04
Day 3 at 40 °C	N/A	7.2
New solution at 40 °C - 2nd change	6.35	2.65
Week 1 before test at 40 °C	6.58	5.68
Week 1 after test at 40 °C	7.11	9.02
New solution at 40 °C - 3rd change	7.13	2.97
Week 2 before test at 40 °C	6.78	4.17
Week 2 after test at 40 °C	6.8	4.82
New solution at 40 °C - 4th change	6.6	2.42
Week 3 before test at 40 °C	5.7	4.4
Week 3 after test at 40 °C	5.7	5.29
New solution at 40 °C - 5th change	5.73	4.42
Week 4 before test at 40 °C	6.38	9.78
Week 4 after test at 40 °C	6.1	15.5
New solution at 40 °C - 6th change	6.02	6.74
Week 6 before test at 40 °C	6.78	10.78
Week 6 after test at 40 °C	6.81	13.43

Corrosion rate measurements were taken during the long-term exposure and are shown in Figure 39 and Figure 40. The PWR simulant 3 exposure shown in Figure 39 indicates that maintaining a consistent solution conductivity and pH results in a lower long-term corrosion rate. For example, at the end of the four week exposure the refreshed solution sample corrosion rate was 0.08 mpy compared to the non-refreshed rate of 0.39 mpy. The refreshed condition is considered more representative (compared to the non-refreshed) of the chemistry in a well maintained SFP and thus representative of the expected temperature dependent corrosion rates for the Boral® clad. The data also supports a general conclusion that for both the PWR and BWR base conditions (simulants 3 and 4) that the longer-term corrosion rates at 40 °C is about 0.1 mpy.
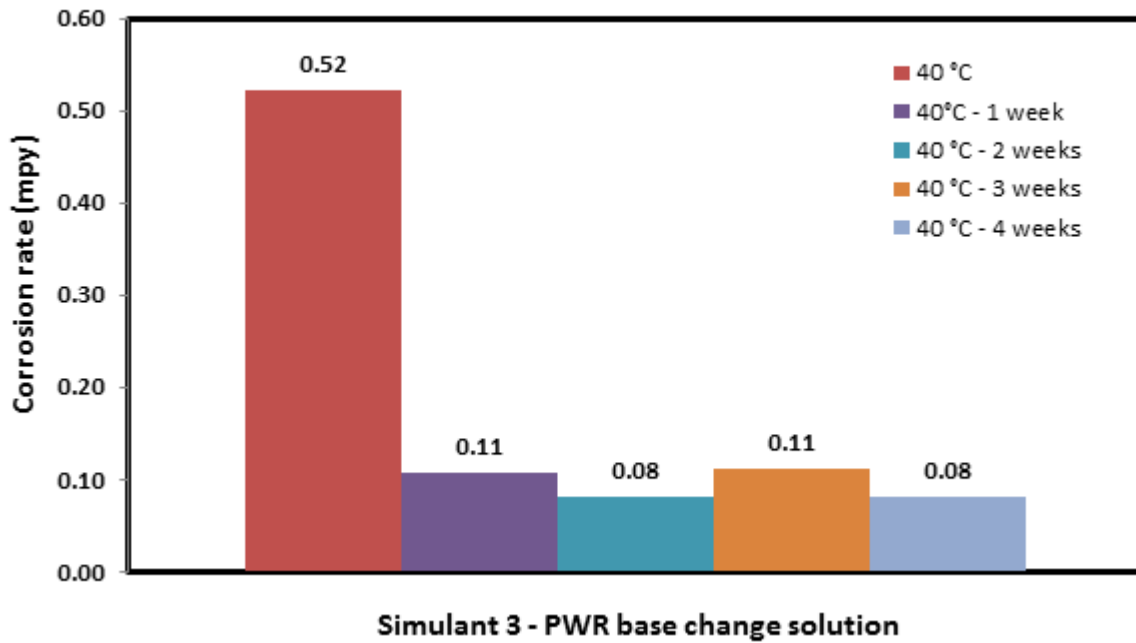
Figure 39. Weekly Corrosion Rates in PWR Simulant 3 at 40°C with periodic change of solution.
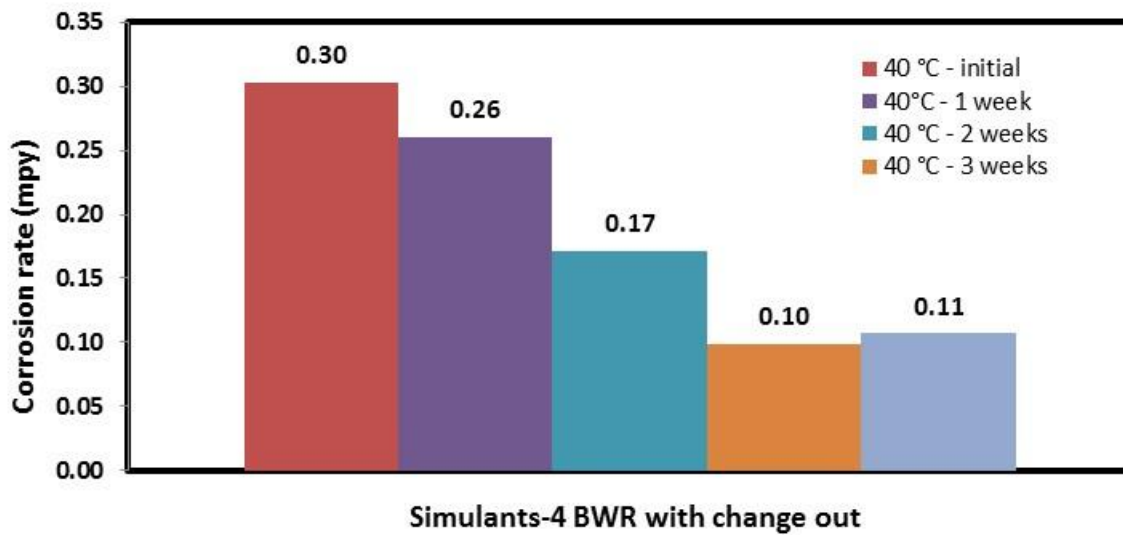
Figure 40. Weekly corrosion rates for fresh surface specimen in solution 4 at 40°C with periodic change of solution.

Using the data generated for the "aged" sample corrosion rates, an equation for predicting the metal loss of the cladding with exposure was derived using the following assumptions:

Activation energy = 17.9 KJ/mol based on the activation energy for the PWR fresh surface base simulant. Since the tests for the aged surface were limited to one temperature, the activation energy cannot be calculated from the data set. However, for this calculation it is assumed that the activation energy from the fresh surface tests apply. The nominal corrosion rate of 0.10 mpy as measured at the end of the exposures is adopted as the corrosion rate at 40 °C. Table 16 lists some results using equation 6 to predict the extent of clad corrosion for the PWR base condition.

$$A = \text{corrosion rate}/ e^{-E_a/RT} \tag{3}$$

For the aged clad surface a value for $A = 0.10 \text{ mpy}/e^{-17900/8.317/313} = 96.88$

$$\text{Corrosion (mil)} = 96.88 \times t \text{ (years)} \times e^{-17900/8.317/T(K)} \tag{6}$$

Table 16. Results of some sample calculations for long term corrosion of the Boral® clad in base PWR simulant

Time [days]	Temperature [C]	Corrosion [mils]	Corrosion [μm]
30	25	0.01	0.15
30	98	0.02	0.61
365	25	0.07	1.80
365	40	0.10	2.54
365	98	0.29	7.44

5.5.2.3 XRD Results on Oxide Films

The generation of a semi-protective oxide film on the cladding surface is an important characteristic affecting the general corrosion rate. The extended term (four to six weeks) exposure tests indicate that the corrosion rate changes with time. The change is attributed to the surface oxide formation and equilibrium reached between the oxide formation and dissolution rates in the different simulants and at the different temperatures.

To provide more data on the surface oxide film, x-ray Diffraction (XRD) spectra were obtained from samples exposed to BWR and PWR conditions. XRD was used to determine distinctive crystalline structures of the oxide/oxyhydroxide film developed.

XRD was performed on the sample with approximately 8 weeks exposure in solution PWR-base (Solution 3) with solution conductivity less than 12 μS/cm (Figure 41). The spectrum for this sample was compared with a spectrum from another sample that was polished to 600 grit prior to XRD measurement. Comparing the two spectra, the sample exposed to PWR-base solution does not show any oxide/oxyhydroxide distinctive peaks and, if there are peaks, they may be overshadowed by the aluminum peaks intensities. It is believed that the oxide layer formed has a very small thickness and undetectable by standard XRD. A picture of the specimen after LPR testing and before XRD analysis is shown in Figure 42.
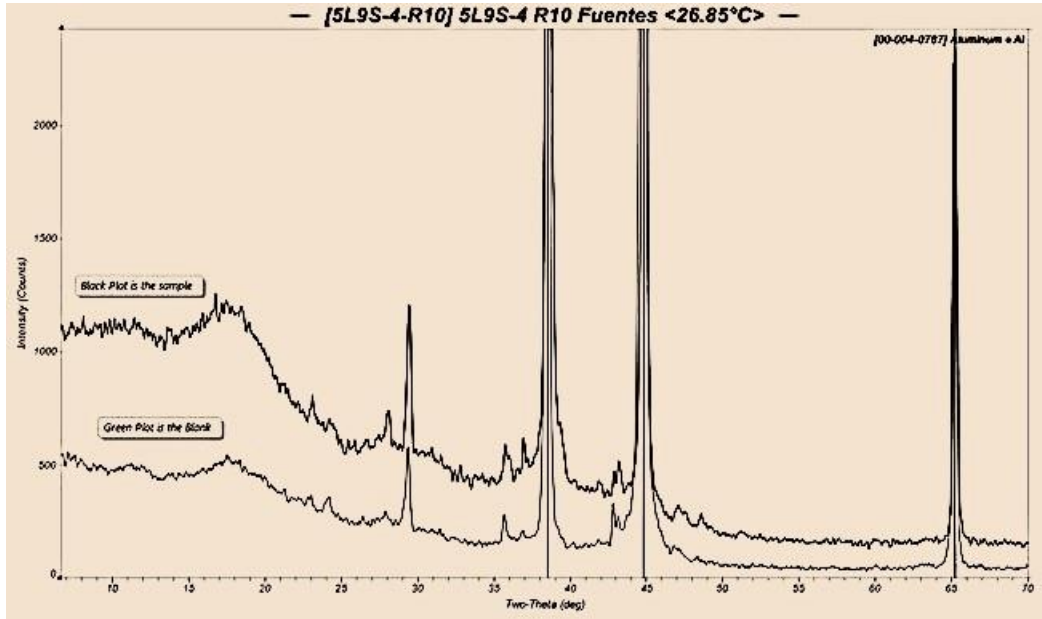
Figure 41. XRD spectra of sample exposed for 8 weeks in Solution 3 at 40 °C compared with freshly surfaced sample polished to 600 grit
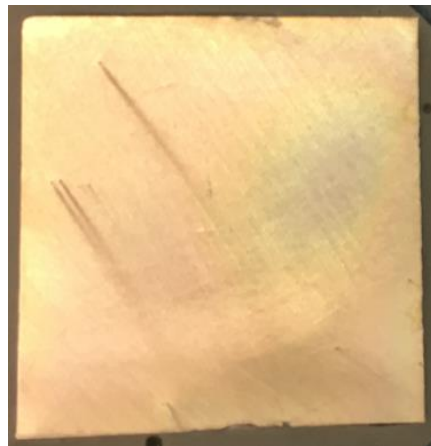
Figure 42. Picture of surface of specimen immersed in Solution 3 (PWR base) after 8 weeks before XRD analysis

Another XRD spectrum, Figure 43, was taken from a sample exposed to the BWR simulant 4. The XRD shows the presence of the bayerite oxide on the coupon following 6 weeks exposure. The peak at 29.5° was observed on the base metal spectra in Figure 41 so it is part of the structure of the aluminum cladding. A picture of the specimen is shown in Figure 43, showing a comparatively duller surface than the specimen immersed in solution 3 for 8 weeks (Figure 42).
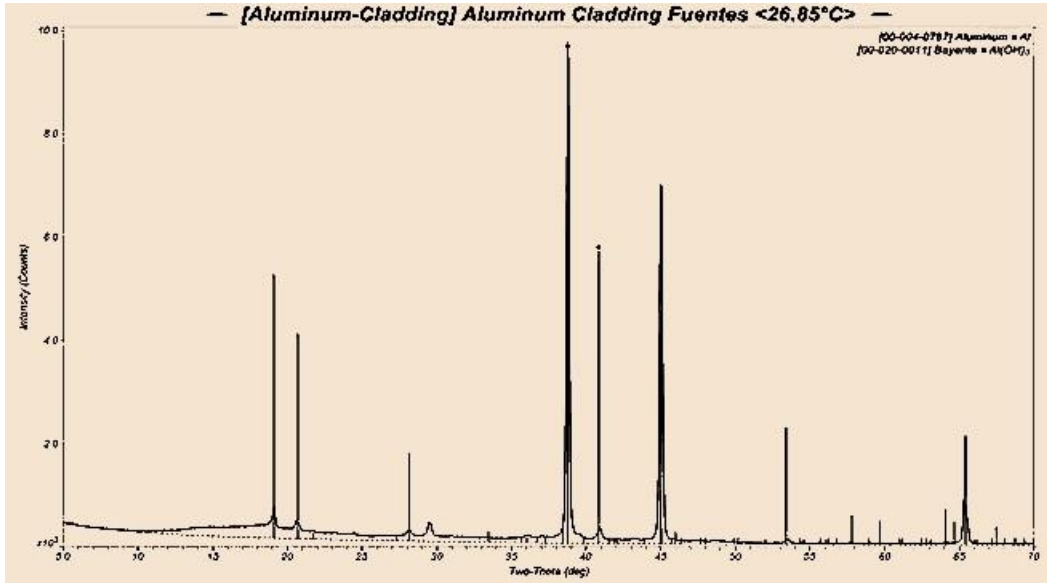
Figure 43 XRD spectra of surface of coupon after 6 weeks exposure in solution 4 at 40 °C with change of solution

Figure 44 Picture of surface of specimen immersed in Solution 4 (BWR base) after 6 weeks before XRD analysis

5.5.2.4   Extended Time in Simulant and Final Corrosion Rate Measurements

Final LPR and CPP experiments were performed on specimens after performing XRD to study the susceptibility of localized corrosion after long term immersion and see how it changes with the development of an oxide layer. The coupon exposed to solution 3 (PWR base) was immersed for 8 weeks at 40 °C and the final corrosion rate obtained was 0.06 mpy, which is similar to what is was obtained after 4 weeks. Similar outcomes were obtained for the coupon exposed to solution 4 (BWR base) with a final corrosion rate of 0.08 mpy after 6 weeks.

CPP results of coupons exposed for 8 weeks at solution 3 and 6 weeks at solution 4 are presented in Figure 45. As observed, the CPP results exhibit similar performance for both samples. The forward scan for both samples had the lowest current densities of any of the samples (i.e. samples starting with fresh surfaces and with as-received oxidized Region 1 cladding). This is indicative of the more protective nature of the oxide.

Both specimens also reached similar current densities at the 2 V vs. SCE limit indicating similar protective oxide characteristics even though the oxide produced by Solution 3 did not show high intensities for a particular oxyhydroxide structure in XRD.
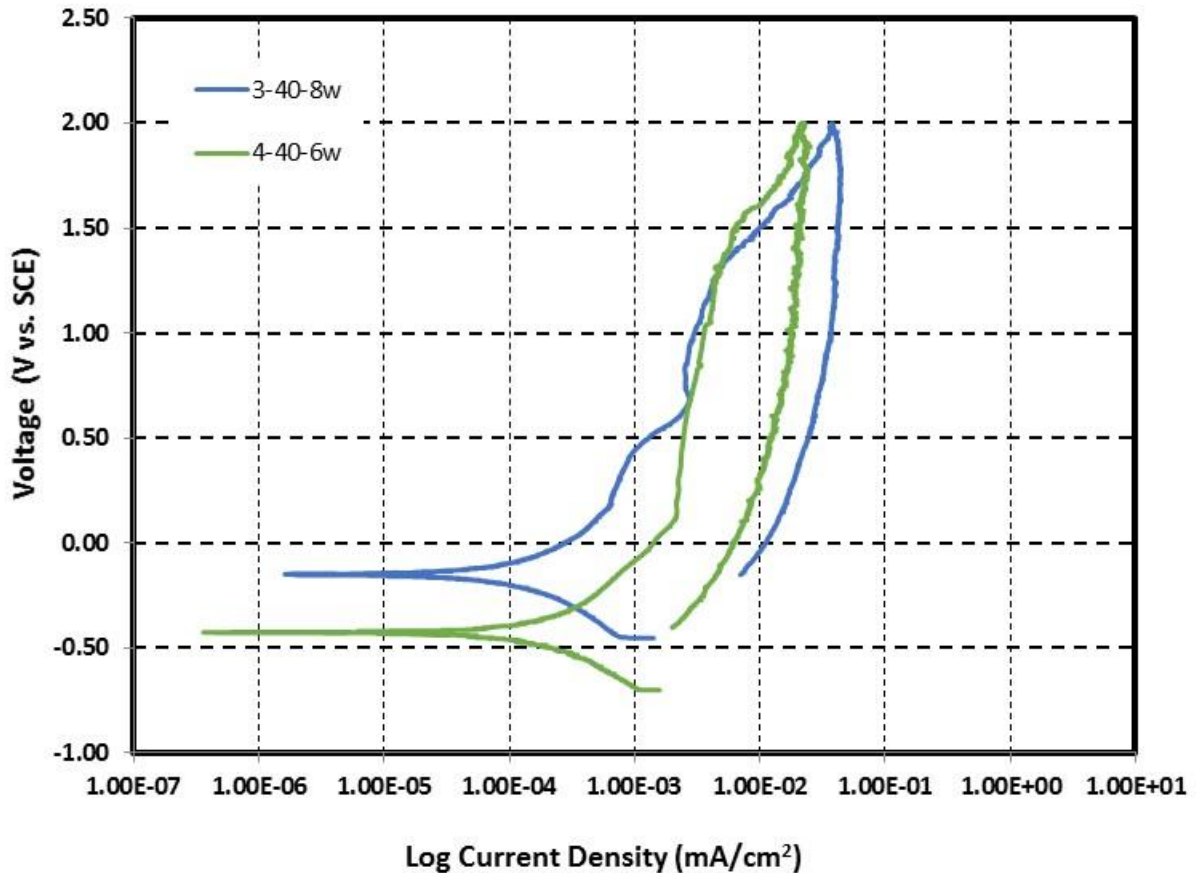
Figure 45. CPP results of coupons exposed in Solution 3 and 4 after 6 and 8 weeks of immersion, respectively at 40 °C. The experiments were performed after removing the samples for XRD analysis

5.6 Immersion Testing

5.6.1 Weight Measurements from the Immersion tests at 98°C at atmospheric pressure

Four specimens for immersion testing of approximate surface area of 4 cm^2 were cut from panel 5L9E-6 that was previously blistered. The blister was removed to provide a specimen with one-face de-cladded. The cladding side was polished to 600 grit to start with a fresh surface free of oxide, then it was rinsed in nitric acid and heating at a vacuum in oven at 230-240 °C. Figure 46 show pictures of the specimens prior to immersion.
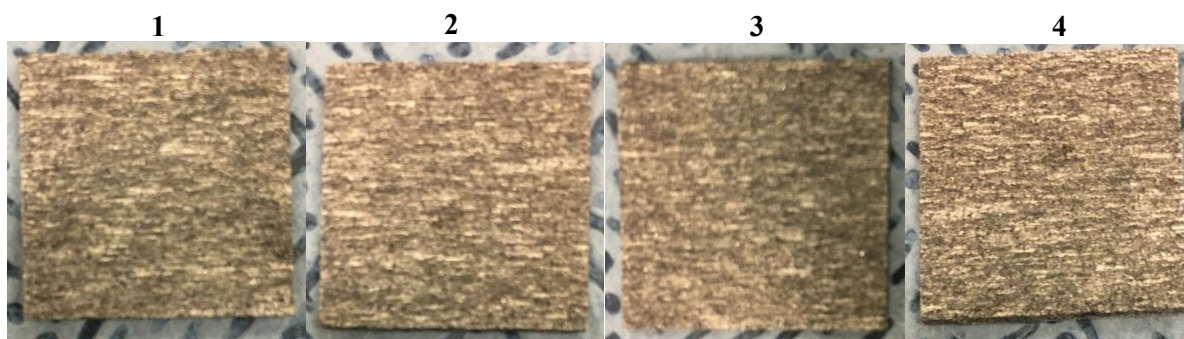
Figure 46. Pictures of Boral® coupons one-faced declad prior to immersion

The weight was recorded in triplicate after the sample was rinsed in nitric acid, vacuum dried and after the weight change was below 0.0006 g maximum. Table 17 lists the weights in triplicate prior to immersion.

Table 17. Weight of coupons initially and prior to immersion

Samples	Initial weight (g)	Prior to immersion weight in triplicate (g)			Average weight (g)	Standard deviation (g)
1	1.8748	1.8314	1.8315	1.8319	1.8316	0.0003
2	1.9644	1.9235	1.9238	1.9238	1.9237	0.0002
3	1.9663	1.9229	1.9235	1.9236	1.9233	0.0004
4	1.9673	1.91	1.9105	1.9106	1.9104	0.0003

Samples 1 to 3 were immersed in the solution while sample 4 acted as control and was left separated inside the hood.

The immersion test was conducted in 1.5 L of Solution 5 (Off-normal PWR chemistry) at 98 °C and it was stirred to approximately 200 rpm for 12 days. Figure 47 shows the setup in use inside the hood. The glass dish at the back of the setup contained sample 4, as observed in the picture. The glass baskets contained the sample that were exposed. A condenser was used with a chiller to prevent evaporation of the solution.
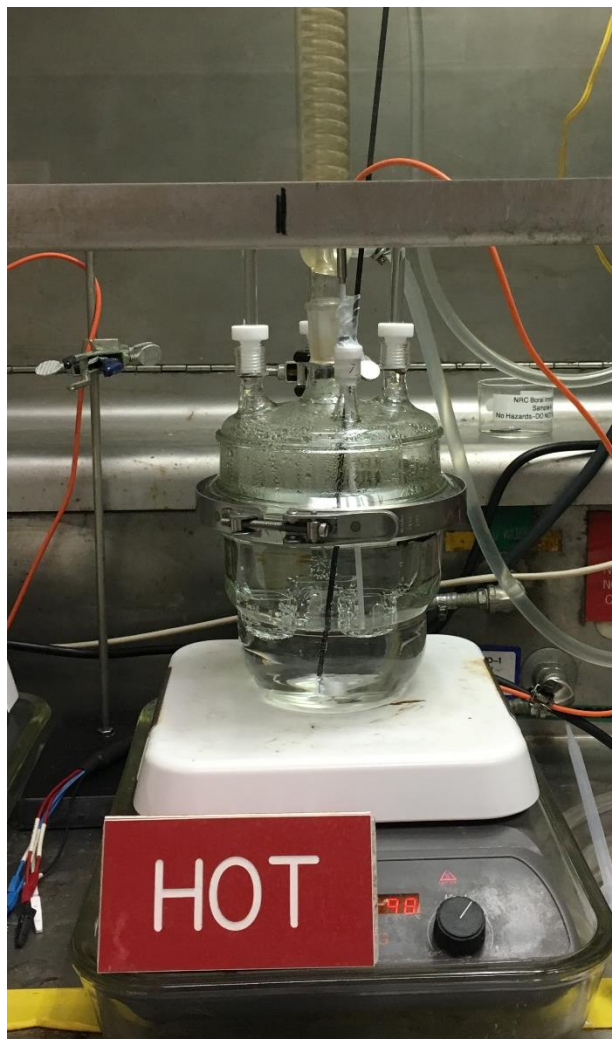
Figure 47. Picture of immersion test setup in operation

Initial and final measurements of pH and conductivity of the solution were taken at room temperature. Aliquots of the solution were taken at day 1, day 5 and day 9 to also measure the pH and conductivity at room temperature. Table 18 lists the pH and conductivities measured during the duration of the test.

Table 18 pH and conductivity measurements of Solution 5 during immersion test

| Measurements | Initial | Water samples (20 mL approx.) | | | Final |
		1st day	5th day	9th day	
pH	4.89	5.21	5.55	5.67	5.81
Conductivity (µS/cm)	97.0	94.1	99.7	102.3	105.2

Figure 48 shows specimens after the test. The three samples immersed showed rust spots and the samples became darker in appearance compared to initial pictures. The rust appears to be from iron impurities that were present in the cladding. Table 19 shows the weight obtained post immersion and after nitric acid rinsing and vacuum drying in triplicate to record weight change.

<table>
<tr><th>1</th><th>2</th><th>3</th><th>4</th></tr>
</table>
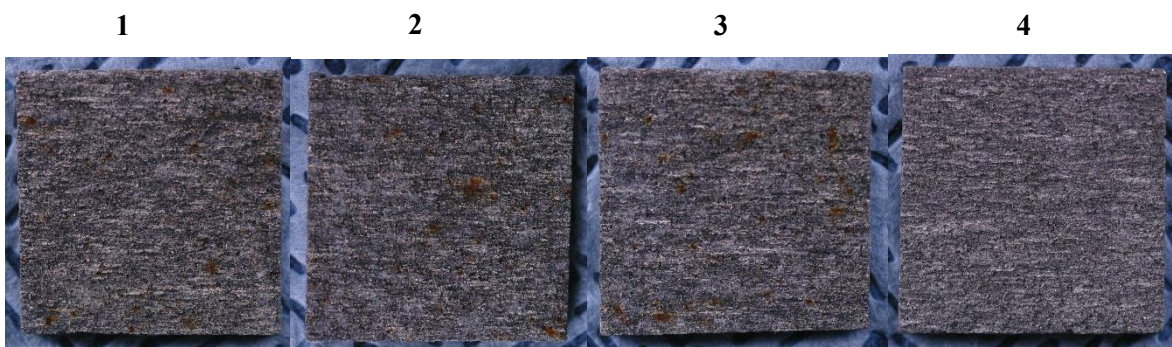
Figure 48. Pictures of Boral® coupons one-faced declad after immersion

Table 19. Weight of coupons post immersion and weight gain/loss results

Samples	Weight post immersion (g)	After treatment weight in triplicate (g)			Average weight (g)	Standard deviation (g)	Weight gain/loss (mg)
1	1.8748	1.8314	1.8315	1.8319	1.8316	0.0003	-3.4
2	1.9644	1.9235	1.9238	1.9238	1.9237	0.0002	-3.8
3	1.9663	1.9229	1.9235	1.9236	1.9233	0.0004	-4.5
4	1.9673	1.91	1.9105	1.9106	1.9104	0.0003	1.2

During the test, the coupons did not show signs of particle dislocation or loss. Even after rinsing several times in 5 minutes intervals with nitric acid, particles remained visually intact on core. As observed in Table 20 there was a small weight gain observed in the samples immersed while the sample unexposed show insignificant weight loss (reflected in table by a negative sign). Based on the small weight gains obtained, it can be concluded with confidence that there was no boron loss after exposure for 12 days at 98 °C in any of the samples.

5.6.2 Weight Gain Measurements from Parr tests at 125 °C

There was large variability in weight change data for the high temperature immersion test results. A generic polynomial fit of the data is shown in Figure 49. The results show a consistent increase in weight gain during the initial exposure of the samples and after about 100 hours the weight gain peaks and starts to decline indicating a loss of surface oxide with extended immersion exposure past 100 hours. The large variability in the weight change data is attributed to the lack of adhesion of the surface oxides formed during exposure.
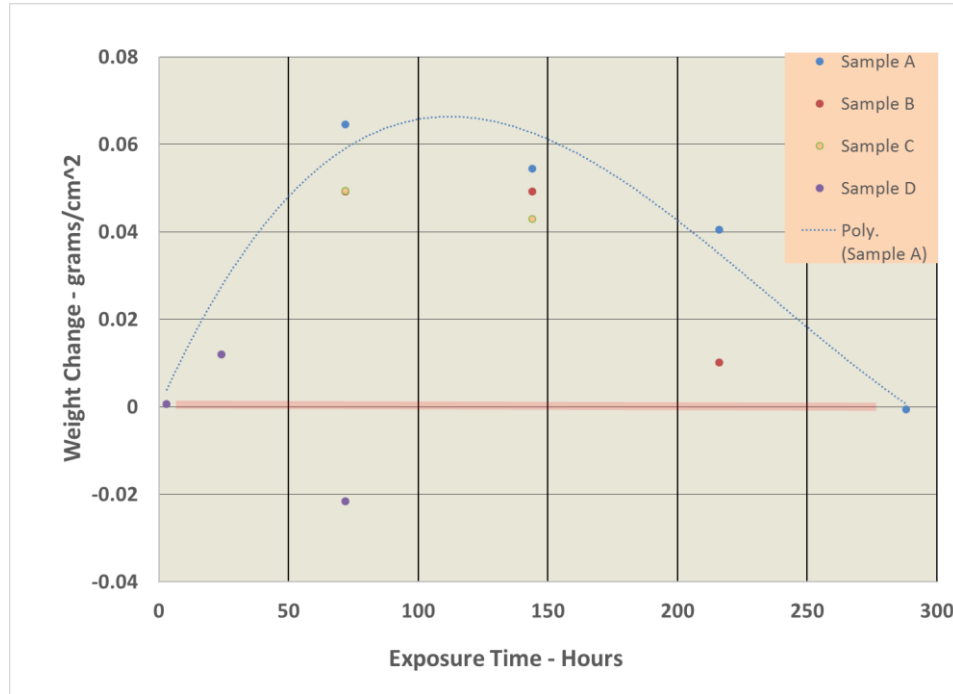
Figure 49. Weight Change Values for Core Exposure Samples from Panel 5L9S-4 at 125 °C in Solution 3. Note specimens A-D are specimens 1-4, respectively

5.6.3 Optical Observations

Figure 50 shows a sample immediately after opening a Parr vessel, then after cleaning. It is apparent that most surface oxides formed during exposure were not strongly adherent, and therefore weight gain data is of questionable quantitative value.
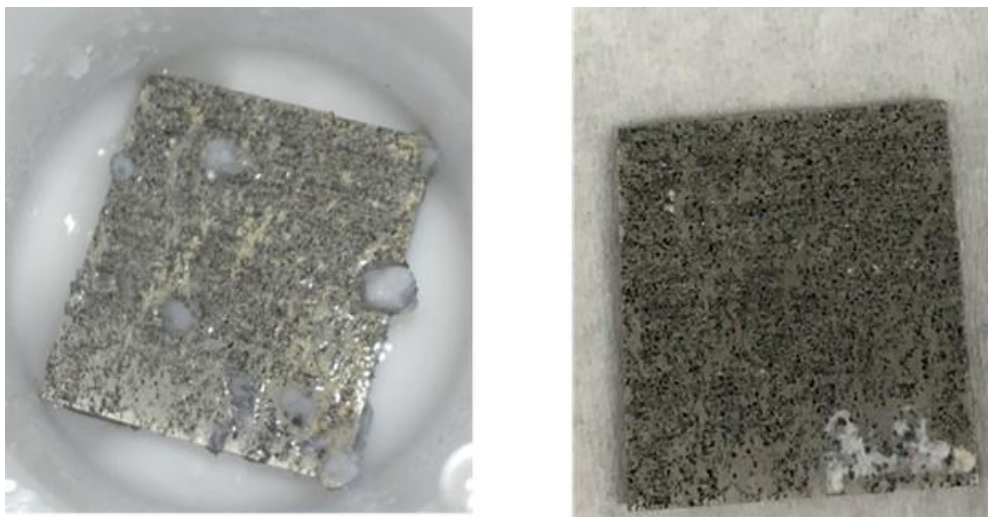
Figure 50. Left: sample 1 after 3 day exposure. Right, sample 1 after a gentle cleaning, showing removal of oxides

Supplemental to the weight-change data, microstructural examination of the samples and Parr vessel solution analysis were undertaken. The samples were examined via SEM, and laser confocal microscopy (LCM). The SEM analysis showed a thin oxide layer growing over the surface and beginning to partially cover carbides as documented in Figure 51. There was no significant B_4C particle loss observed for this sample.

LCM optical images and height relief data before and after exposure for one sample are shown in Figure 52 with the arithmetic mean roughness for the samples tabulated in Table 20. In general, the surface roughness increased slightly for all but one sample. The increased surface roughness may be the result of oxide build-up on formerly smooth carbide surface. The height relief data show a similar structure after exposure as before. The sporadic nature of the oxide adhesion complicated further analysis.

Table 20. Surface analysis data taken by LCM on samples from 5L9S-4

Arithmetic mean roughness (surface data)		
Coupon (exposure time)	Before	After
4 (3 day)	6.5 μm	6.9 μm
3 (6 day)	6.4 μm	6.4 μm
2 (9 day)	6.4 μm	7.3 μm
1 (12 day)	6.3 μm	8.5 μm
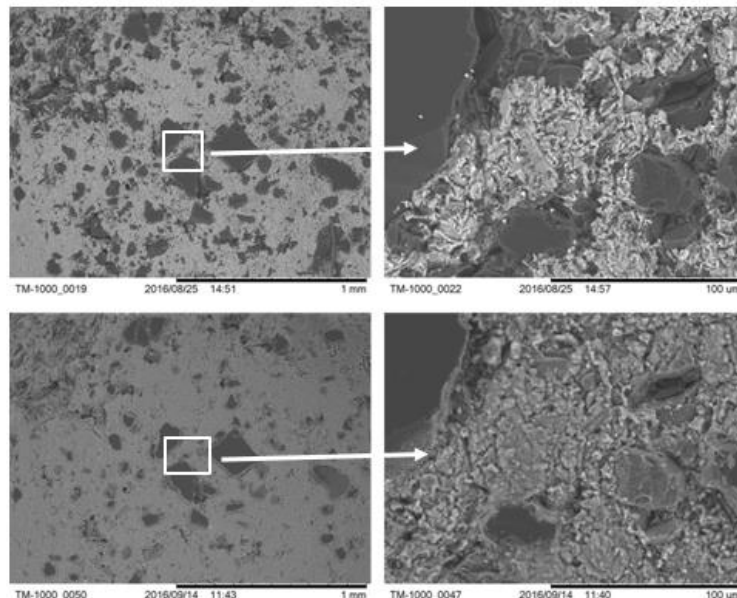
Figure 51. SEM of 5L9S-4 before exposure (Top two images) and after exposure (Two bottom images) taken at the same relative location. The images on the right are at a higher magnification, and from a point close to the center of the images on the left.
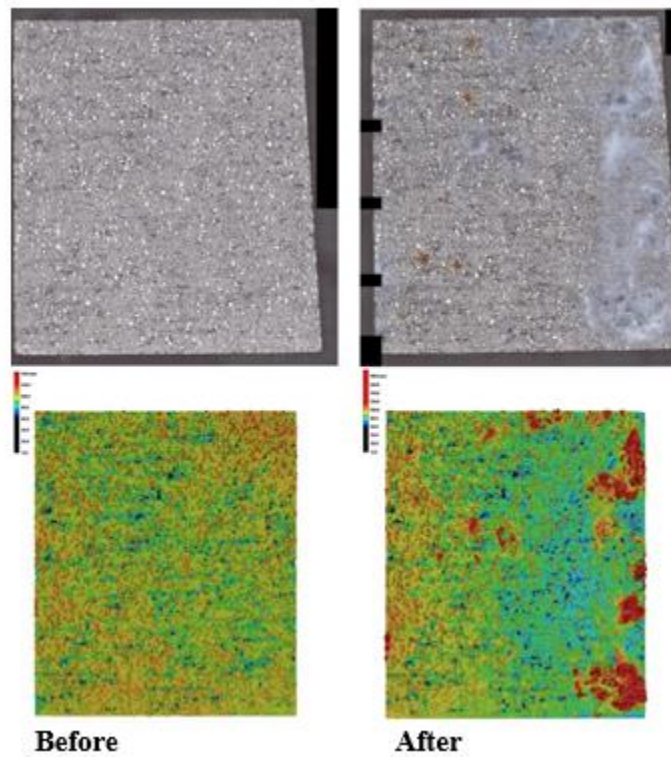
Figure 52. LCM optical and height relief data for 5L9S-4 coupons before exposure and after 12 days exposure. Height relief magnified 1000x in lower images.

A high magnification comparison of the B_4C surface distribution before and after the 12 day immersion test is shown in Figure 53. There is no significant change in the B_4C large particle distribution. There may have been loss of some of the very small particles associated with the surface corrosion but the relative impact on the B areal density is postulated not to be significant.

SRNL-TR-2018-00244
Revision 0

Figure 53. High Magnification Pictures of Sample 5L9S-4 (top left corner) before (left) and after (right) the 12 Days of Exposure

5.6.4 Evaluations of Test Solutions

The test solution was tested for pH and conductivity after a 3 day exposure from a sample that had been exposed for a total of 12 days (4th solution charge). The pH had gone from 4.6 to 6.05, and the conductivity from 88.2 µS/cm to 155.4 µS/cm. This change indicates that corrosion product is being accumulated into the test water.

The third solution charge was taken after the solution was gently agitated against the sample surface. This solution was shaken to ensure suspension of particulates and passed through a vacuum assisted filtration system using an eyedropper to keep most of product in the center of the filter. The filter was dried under partial vacuum prior to bifocal light microscopy. B$_4$C particles appeared to have been present in the oxide filter cake, refer to Figure 54, but EDS or another analysis technique is needed to qualify this assumption. SEM/EDS was not performed since the sample was in a fragile condition and was non- conducting which would require additional preparation and handling processes.

Figure 54. Filter cake resulting from filtration of the solution charge after 3 days exposure and agitation on the surface oxide of a declad Boral® coupon.

6.0 Discussion and Conclusions

6.1 Program Objective (1) Identify the degradation mechanisms affecting Boral® panels :

The two-primary degradation mechanisms observed were surface pitting and general corrosion of the cladding. The pitting was more prevalent in Region 2 compared to Region 1 but was not extensive in either region. A pit that was determined visually to be representative of a worse case condition was characterized and measured to be 0.25 to 0.30 mm deep. Based on subsequent clad thickness measurements this pit is assumed to have breached the clad. The pit foot-print is relatively small and there is no indication of any significant NAM loss due to pitting in general.

Another degradation mechanism observed was general surface (clad) corrosion. The dimensional and microstructural measurements have provided data that indicates the Boral® panels to have experienced general corrosion in the range 50 to 100 μm during the service in the Zion Fuel pool. Variations in corrosion were observed to be associated with axial locations along the panel, and for Region 1, the retaining straps had a localized effect on the corrosion rate.

6.2 Program Objective (2) Evaluate the performance of Boral® panels under normal and off-normal conditions:

The visual inspections concluded that the panel sections were not significantly degraded and are in good condition after the in-service exposure. There were no visible signs of significant B_4C loss or core exposure. The clad surface corrosion rate was modeled by a series of equations using activation energies obtained from the EC testing performed at different temperatures. For example, using the model the predicted corrosion rate for base PWR water at 40°C is less than 2.54 μm /year (0.10 mpy) and compares well to the observed rate of 2.3 to 4.3 μm per year (0.086 – 0.171 mpy) based on the dimensionally determined surface loss (50 to 100 μm) over an exposure time of 22+ years. These results also agree with corrosion testing results for Boral® performed as part of a qualification testing program by Brooks and Perkins as reported by EPRI in the NAM Handbook [14]. In the Boral® qualification testing, aqueous corrosion testing of Boral® specimens at 38 °C (100°F) for 1 year resulted in a maximum corrosion rate of approximately 0.14 mils/year.

Under off-normal conditions involving higher temperatures and more aggressive chemistry, the clad will oxidize at a faster rate than under normal conditions of pool chemistry and temperature. Different pool water chemistries were evaluated to estimate the impacts of a postulated off-normal condition on the corrosion rates, and, typically, three different temperatures were introduced as variables to determine a corrosion activation energy. Using the corrosion model developed for specimens with ground surfaces and assuming a temperature of 98°C in PWR base water, the corrosion after 1 year is predicted to be 7.44 μm (0.29 mils) which is significantly less than the existing clad thickness of about 0.235 mm (0.0092 inch). Since testing was not performed on "aged" cladding in PWR off-normal simulant, a direct prediction of the corrosion rate is not available, but it is likely to be less than the corrosion rate exhibited by the ground specimens based on the results obtained from EC testing on specimens with oxides grown *in situ*. The EC tests on the exposed core indicated that the core material is resistant to corrosion. For example, the model developed indicates that for a 30-day exposure[a] of the core in the most aggressive water chemistry (i.e. off-normal PWR at 98°C) only 41.5 microns of core material is lost to corrosion (19.88 mpy /365 days x 30 days = 1.6 mil or 41.5 μm or 0.0415 mm; single sided). Assuming that Region 2 is the worst case because the core region is thinner than for Region 1 panels (nominal core thickness of 1.64 mm) and two-sided corrosion loss (0.083 mm loss) occurs, the potential loss of core material for this condition is about 5%.

The saturation temperature of the water in the SFP at the base of the spent fuel bundle is estimated to be approximately 123 °C based on standard steam tables and is the maximum temperature expected during a loss of cooling accident. Corrosion testing of specimens with the cermet core exposed by finely grinding away the cladding were performed in Parr vessels in solution #5 (PWR off-normal) at 125 °C for various durations up to 12 days. The results showed that the specimens exhibited corrosion and non-adherent oxide formation. The oxide sluffed off the specimens making it difficult to obtain corrosion rates based on specimen weight changes. However, visual examinations of the specimens by high resolution optical microscopy, SEM and LCM showed that boron carbide loss was non-detectable after 12 days of exposure at 125 °C. An analysis of the post-test solutions for boron carbide loss supported the visual examination results. Thus, under postulated off-normal conditions where significant surface area of the core is exposed to degraded SFP water at elevated temperatures, the amount of corrosion does not appear to result in significant B_4C losses during the testing time frame.

Panel blistering has been observed in some fuel pools although not on the Zion panels received. To obtain some information on clad blisters some lab generated (thermally) blisters were evaluated. The artificial generation of blisters required relatively high temperatures (greater than 100°C) to produce a combination of increased pressure from steam generation and clad bond weakening from strength versus temperature. The high temperatures required for blister formation suggests that Boral®, while having water in the cermet core, is resistant to steam-generated blister formation during both normal conditions and off-normal, conditions for temperatures below boiling.

6.3   Program Objective (3) Determine the impact on acceptability during and after off-normal conditions

The condition of the Boral® panels after an off-normal event will directly depend on the off-normal conditions; however, the temperature is somewhat limited to the temperature of boiling water and the tests have shown that the Boral® clad and core are resistant to excessive corrosion over the limited times of an off-normal excursion For example, for an exposure in PWR off-normal water at 98°C for a month it is predicted that the corrosion will consume less than 16 μm (0.63 mils) (7.27 MPY/12 months/year X 25.4 μm per mil) per surface of the clad and that the core will remain encased in cladding and no significant loss of NAM will occur. Even if there are locally exposed core areas, the corrosion rate of the core material is

---

[a] 30-days was selected for illustrative purposes since it encompasses potential degraded conditions. Shorter durations at the same temperature result in less corrosion.

relatively slow, as discussed in the previous paragraph. While highly dependent on the specific environmental factors, due to the maximum temperature limits in the pool and the relatively slow corrosion rates, the testing conducted in this project indicated that the Boral® panels would continue to perform their safety function following off-normal conditions bounded by the testing conditions.

6.4 Program Objective (4) Develop long term predictions of the progression of Boral® degradation in the SFP environment

The surface condition of the received panels was determined to be good with no significant pitting, blistering, or other defects. Subsequent metallography evaluations indicated that the typical sample had a surface oxide with measured thickness of three μm or less. Since the macro measurements of clad surface loss to corrosion indicate a material loss of 50 to 100 μm, the bulk of the oxide apparently did not remain on the clad surface after formation.

The different measured thicknesses on Region 1 sections with residual hold down strap indications indicate that on a local basis the hold down strap isolated the original clad surface from the pool water. That is, corrosion of the aluminum alloy cladding directly underneath the strap did not occur or was significantly protected from general corrosion.

Axial panel thickness measurements showed what appeared to be a trend of decreasing thickness from top to bottom. If the panel thickness differences were not due to manufacturing processes, the epoxy paint or some unidentified influence not related to corrosion, then they can be conservatively assumed to be due to corrosion. Thus, the general corrosion rate for the panels was higher for the bottom sections than for the top sections. Region 2 had less of an axial variability in corrosion than Region 1, perhaps being associated with the sheathing of Region 2 panels. The higher apparent corrosion rate near the bottom of the panels suggests that there may be some axial water chemistry non-uniformity and/or temperature gradients in the SFP. From the corrosion tests the activation energy for corrosion was determined for the six environments. The activation energy used with an Arrhenius can be used to predict the corrosion performance while in the SPF environment. For example, in the PWR base solution and at 40° C (local temperatures adjacent to the fuel assemblies will be greater than bulk pool temperatures) the predicted corrosion is 2.54 μm /year which is in the same ball park as calculated from the dimensional measurements of 2.5 to 4 μm per year. Based on both the calculated rates and the observed rates, an estimation (which is dependent on the clad thickness and temperatures), it is extrapolated to take an additional 70 years for clad corrosion general penetration at 0.14 MPY for ~10 mil thick cladding observed on the as-received panels. There was some pitting observed in the Zion panels and that is expected to worsen with exposure.

6.5 B^{10} Areal Density Measurements

Panel samples were analyzed to determine the B^{10} areal density for the Boral®. The SRNL AD measurements are in close agreement with the values generated by PSU for the Region 1 and Region 2 panel samples tested. The SRNL, PSU and BADGER values for Region 2 are in general agreement (nominally within +/- 5%). For Region 1, the trend is for the SRNL values to be 20% higher than BADGER. The Region 1 PSU value is about 30% higher than BADGER. The determination of the basis for the Region 1 BADGER – SRNL difference in AD is not within the scope of this program.

7.0 List of Appendices

    A. EC Test Data
    B. Surface Pitting, Contour and Corrosion Evaluations
    C. Dimensional Measurements
    D. Blister Evaluation
    E. Results of Chemical Method Protocol for B-10 Areal Density
    F. SRNL Receipt Inspection Compendium

8.0 References

1 Witness Report: Removal and Sectioning of Boral® Fuel Rack Modules B and P from Zion Fuel Pool; Harris M. C.: NETCO (Curtiss-Wright); EPRI Contract MA 10002836; November 19, 2015

2 Procedure for Implementation of Traceability Verification for Boral® Extraction Utilizing Alaron Services; NETCO (Curtiss-Wright); SEP-300096-05, September 2015

3 *Evaluation of BORAL® Panels from Zion Spent Fuel Pool and Comparison to Zion Coupons*. EPRI, Palo Alto, CA: 2016. 3002008196

4 ASTM C791-12, "Standard Test Methods for Chemical, Mass Spectrometric, and Spectrochemical Analysis of Nuclear-Grade Boron Carbide," ASTM International, West Conshohocken, PA

5 *BWRVIP-130: BWR Vessel and Internals Project, BWR Water Chemistry Guidelines – 2004 Revision,* EPRI, Palo Alto, CA: 2004. 1008192

6 *PWR Primary Water Chemistry Guidelines: Volume 1, Revision 4*, EPRI, Palo Alto, CA: 1999. TR-105714-V1R4

7 ASTM G102–89(2015), "Standard Practice for Calculation of Corrosion Rates and Related Information from Electrochemical Measurements," ASTM International, West Conshohocken, PA

8 ASTM G106-89(2015), "Standard Practice for Verification of Algorithm and Equipment for Electrochemical Impedance Measurements," ASTM International, West Conshohocken, PA

9 ASTM G5–14, "Standard Reference Test Method for Making Potentiodynamic Anodic Polarization Measurements," ASTM International, West Conshohocken, PA

10 ASTM G59-97(2014), "Standard Test Method for Conducting Potentiodynamic Polarization Resistance Measurements," ASTM International, West Conshohocken, PA.

11 K. Waldrup, "Strategy for Managing the Long-Term Use of Boral® in Spent Fuel Storage Pools", EPRI, Palo Alto, CA:1025204, 2012

12 Akkurt, H. EPRI Neutron Absorber Projects-Zion & Accelerated Corrosion Tests; NRC Public Meeting August 10, 2016

13 AAR Cargo Systems letter to Stewart Brown NRC dated April 30,2004

14 *Handbook of Neutron Absorber Materials for Spent Nuclear Fuel Transportation and Storage Applications – 2006 Edition.* EPRI, Palo Alto, CA: 2006. 1013721

Appendix A – Electrochemical (EC) Testing Details

I - Technique

Open circuit potential (OCP) was measured until the potential of the sample equilibrated in the solution. The time to equilibrate varied from 2 to 7 hours. After the OCP was equilibrated to within +/- 10 mV in 1 hour, linear polarization resistance (LPR) testing was performed over a potential range of +/- 25 mV around the OCP at a rate of 0.167 mV/s. Figure A- 1 shows a voltage vs. current density plot obtained from an LPR experiment of fresh surface at 25 °C in solution 5 (PWR Degraded). The slope of the curve is used as the sum of the polarization resistance and solution resistance ($R_p + R_s$). The solution resistance is not typically considered; however, it was a factor in this case due to the low conductivity of the solutions used. To obtain the corrosion rate through electrochemical experiments ASTM G102 was used. The corrosion rate (CR) is calculated by using Faraday's Law shown below,

$$CR=K\ \frac{B}{R_p\ \rho\ SA}\ EW \tag{1}$$

where K is a constant with value depending of units used, B is the Stern-Geary constant which is related to the electrochemical behavior of the material in the environment; EW is the equivalent weight (g) of the material; ρ is the material density (g/cm^3) and SA is the surface area of the sample (cm^2). To calculate the CR in mpy, the value for K was 0.1288 mpy g/μA cm per ASTM G102. For aluminum 1100, ρ is 2.71 g/cm^2 and EW is 8.99.

The Stern-Geary constant is calculated from Tafel slopes from a distinct linear region near the corrosion potential on a potential vs. log current plot,

$$B=\frac{\beta_a\beta_c}{2.303(\beta_a+\beta_c)} \tag{2}$$

where β_a and β_c are the slope of the anodic and cathodic Tafel reactions, respectively. To obtain the solution resistance and the anodic and cathodic Tafel reactions, an EIS routine and CPP experiment were performed.
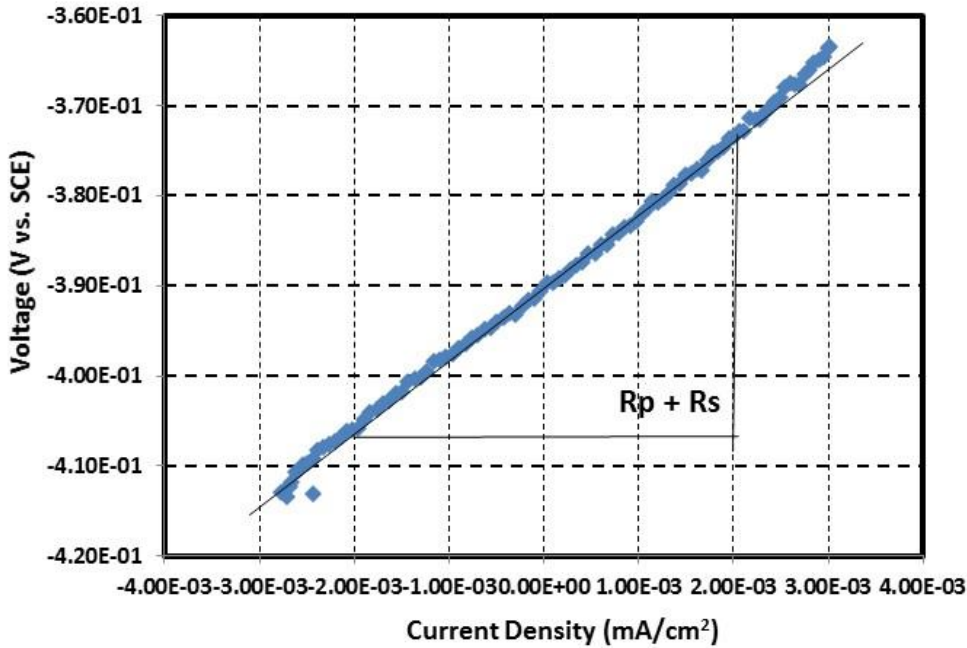
Figure A- 1 Voltage vs. current density plot of 5L9S-4 fresh surface cladding at 25°C in solution 5 PWR Degraded

After performing the LPR, EIS was performed by changing the frequency from 50 kHz to 5 mHz at 10 points per decade and from 50 mHz to 1.670 mHz at 4 points per decade. The resulting plot of imaginary resistance vs. real resistance, known as a Nyquist plot, provides data to determine the solution resistance and can provide a confirmation of the polarization resistance. An example of the Nyquist plot is shown in Figure A-2 for fresh surface at 25 °C in solution 5 PWR Degraded.
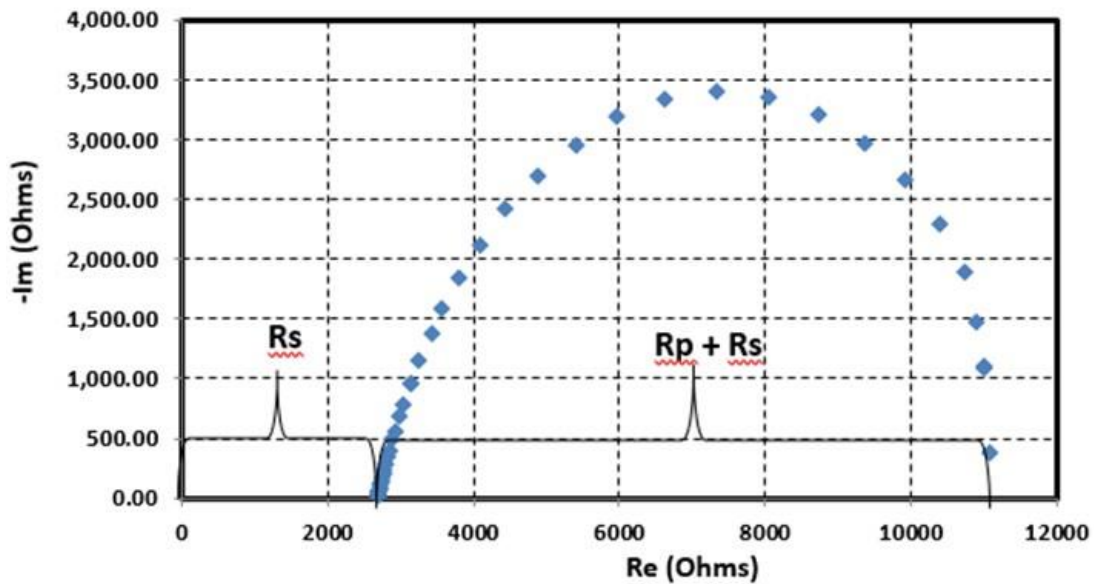
Figure A-2 Nyquist plot of 5L9S-4 fresh surface cladding at 25°C in solution 5 PWR Degraded

In Figure A-2, the Nyquist plot does not show the applied frequency, but rather, the resulting impedances where each point on the plot is the impedance at one frequency. The data obtained at high frequencies are on the left side of the plot and data obtained at low frequencies are on the right. . The intersection of the plot with the real resistance axis (x-axis) is known as the solution resistance (Rs). As the frequencies continued to decrease, a semicircle will form and the extrapolation of the point completing the semicircle with the real resistance axis is the sum of the polarization resistance and solution resistance. By subtracting the solution resistance, polarization resistance can be obtained. The solution resistance was subtracted from the LPR slope to obtain the polarization resistance.

When EIS was complete, the OCP was again recorded for 10 minutes and then a CPP experiment was performed. The CPP test was conducted by applying a cyclic potential ramp from -300 mV vs. OCP up to either a potential of 2 V vs. SCE or a threshold current of 1 mA/cm^2 at a scan rate of 0.167 mV/s. The potential was returned to the OCP to complete the test. CPP can assess the susceptibility of the sample to localized corrosion by the change in current densities of the forward and reverse scans. Additionally, it can be used to obtain the anodic and cathodic Tafel slopes at potentials 50 to 100 mV from the OCP [2]. To explain the CPP experiment and the information that can be obtained, important aspects of this approach are summarized as a reference here since they will be utilized in the discussion of the results. Figure A- 3 shows a schematic of an idealized CPP curve along with experimental parameters that are measured from the curve.
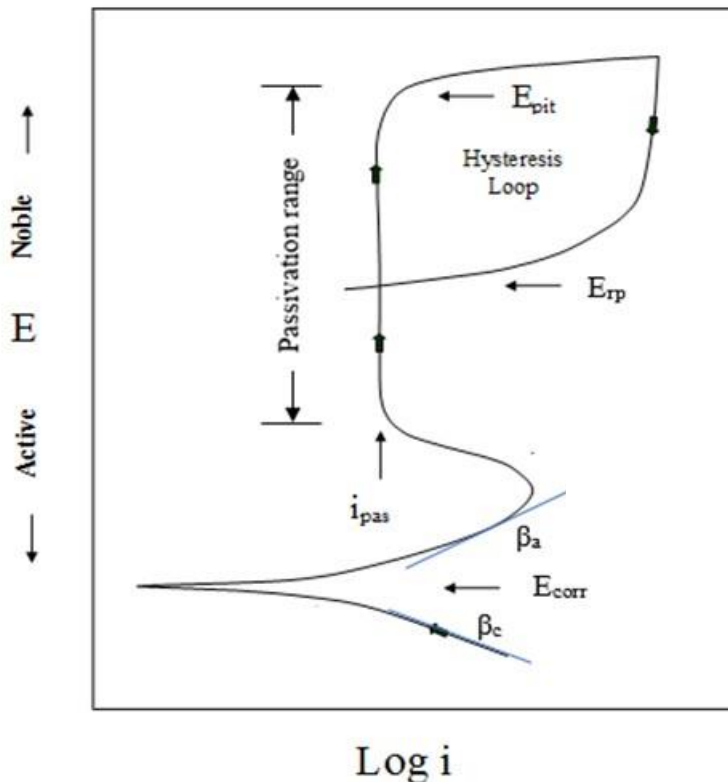
Figure A- 3 Schematic of an idealized CPP curve with parameters with backward scan reaching forward scan

Definitions for the parameters shown in Figure A-3:

- E_{corr} is the corrosion potential. It is the potential at zero current, measured on the forward scan. It is a value analog to OCP stabilization.
- E_{pit} is the pitting potential. It is the potential at which stable pits initiate on the forward scan. The increase in current at this potential may not be associated with pitting. The potential may be the result of other anodic reactions (e.g., oxygen evolution). In that case the potential may be referred to as the transpassive potential (E_{trans}). A transpassive potential is often observed for samples that have negative hysteresis.
- E_{rp} is the repassivation potential. It is the potential at which pits (if they occur) passivate and stop growing on the reverse scan.
- i_{pass} is the passive current density. It is the current density in the passive range.

At the start of the scan, the voltage continues to sweep until the current approaches to zero instantly and then continues until reaching the vertex current density or maximum potential. If there is a passive region, there is a current density that is almost constant with little dependence of potential known as the passive current density i_{pass}. At the reverse scan, the scan can go to a negative hysteresis or positive hysteresis. A negative hysteresis, where the current on the reverse is lower than during forward scan, is usually characterized by a condition free of localized corrosion. On the contrary, a positive hysteresis, when the current on the reverse scan is higher than during forward scan, is usually indicative of the occurrence of localized corrosion such as pitting or crevice corrosion. A diagram for positive hysteresis is shown in Figure A- 4. When the current in the reverse scan crosses the forward scan (as observed in Figure A- 3), the potential when this occurs is known as the repassivation potential E_{rp}. A repassivation potential is indicative of a case in which localized corrosion reaches a potential of passivation.
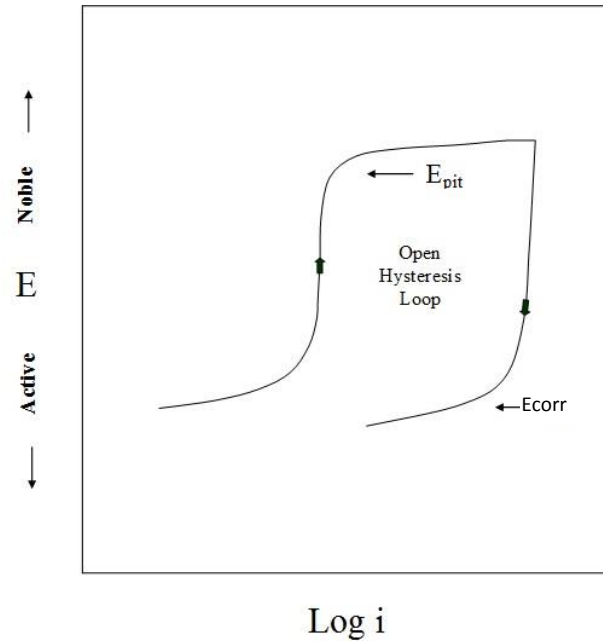
Figure A- 4 Schematic of idealized CPP curve showing positive hysteresis

Performing the electrochemical experiments at different temperatures allow the formation of an Arrhenius plot. An Arrhenius plot is often used to analyze the effect on temperature on the rates on electrochemical reactions (i.e., corrosion rates). The plot gives a straight line from which activation energies can be determined. The Arrhenius equation is shown below in linearized form,

$$\ln i_{corr} = \ln A - \frac{E_a}{R\,T} \qquad\qquad (3)$$

where i_{corr} is the corrosion current density ($\mu A/cm^{2)}$ obtained by dividing B with the surface area SA; A is the pre-exponential factor which is an empirical relationship between temperature and corrosion rate; R is the gas constant with value 8.314 J/mol.K; T is temperature (K) and E_a is the activation energy which is the minimum energy required to start the electrochemical reaction (J/mol). In an Arrhenius plot, the plot of $\ln i_{corr}$ vs. $1/T$ provides E_a/R as the slope of the line and $\ln A$ as the y-axis intercept.

References
G102 – 89, "Standard Practice for Calculation of Corrosion Rates and Related Information from Electrochemical Measurements," ASTM International, West Conshohocken, PA 2015
R. G. Kelly, J. R. Scully, D. W. Shoesmith, R. G. Buchheit, "Electrochemical Techniques in Corrosion Science and Engineering", page 44 CRC Press, Boca Raton, FL, 2003

II - As received service oxidized cladding corrosion tests.
Electrochemical corrosion in nominal, base and degraded chemistries on samples with the as-received surface condition were also performed. However, since the surface also had decontamination processing, drying and other handling procedures it is postulated that surface condition may no longer represent the

actual condition when in the fuel pool. Panel 2K20S-10 was chosen as the source for samples to be used in this set of tests because it is from Region 1 and was directly exposed to the pool water during operation.

Corrosion rates using LPR were calculated for each of the six simulants and at three temperatures; 25 °C, 75 °C and 98 °C. The results are displayed in Figure A- 5. At 98 °C for Solutions 3 and 5 there was an unstable OCP during the 8 hours exposure that affected the LPR results and the determination of corrosion rates for those solutions. Therefore, no values for corrosion rates for those two conditions were reported. It is postulated that at temperatures around 80 °C and above, a transformation of the crystalline structure of the oxyhydroxide from bayerite/gibbsite to boehmite may be occurring that can affect equilibrium potential. Observed corrosion rates are similar for the nominal, base and degraded conditions except for solution 5 in which the corrosion rate increases over 17 times the corrosion rate at 25 °C. Since the reason for the increase in corrosion rate at 75 °C was not clear, two more experiments in solution 5 were performed at 45 and 60 °C, which are below the gibbsite/boehmite transformation temperature. . At 45 and 60 °C the corrosion rates obtained were 1.49 and 5.63 mpy, respectively.
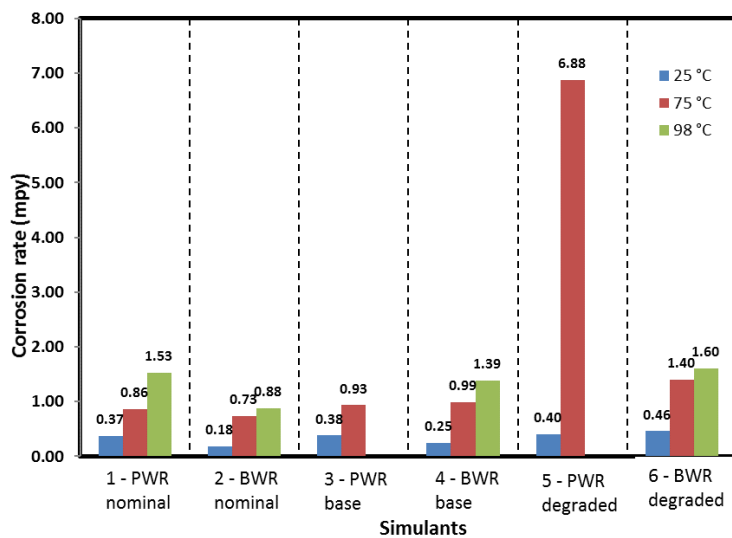
Figure A- 5 Corrosion rates of aluminum cladding 2K20S-10 in six simulants at three temperatures

The Arrhenius plot presented in Figure A- 6 shows the results of the solutions and temperatures from Figure A- 5 plus the two-additional tests at 45 and 60 °C for solution 5. As observed, the slopes of the linear regressions and the values are close for solutions 1, 2, 3, 4 and 6. For Solution 5, i_{corr} is similar to other solutions at 25 °C but increases exponentially at higher temperatures. This increases the slope of the linear regression. The values for activation energy were calculated based on those slopes and using the below equation and are listed in Table A - 1.

The activation energies have similar values to those reported before except for solution 5 which has an activation energy of 52 kJ/mol. This difference in activation energy potentially corresponds to a different

mechanism that is occurring for PWR degraded conditions and may have to do with the delay in transformation of the structure of the oxide plus an increase in the corrosion response due to the higher concentration of aggressive species.
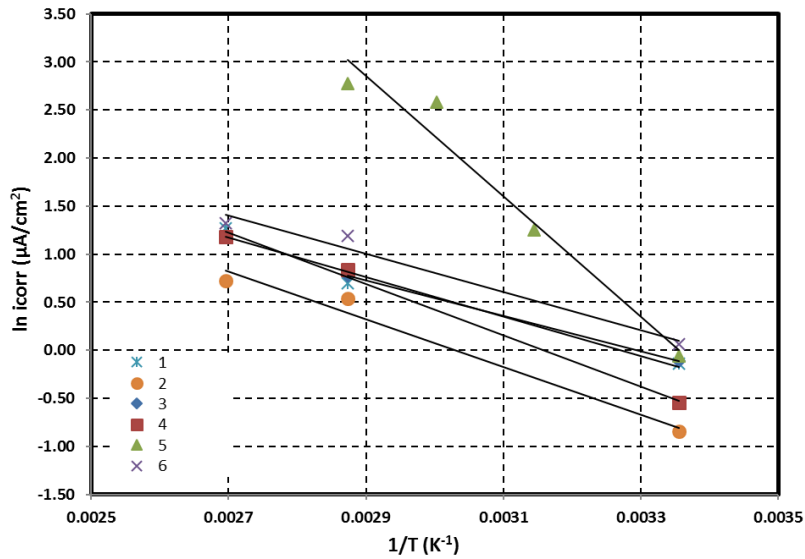
Figure A- 6 Arrhenius plot of aluminum cladding as serviced oxidized 2K20S-10 tested in six solutions.

Table A - 1 Activation energies obtained from the Arrhenius plot for the aluminum cladding 2K20S-1

Solutions	Activation Energy (Ea) KJ/mol
1-PWR nominal	17.1
2-BWR nominal	20.6
3-PWR base	15.4
4-BWR base	22.1
5-PWR degraded	52
6-BWR degraded	16.5

The CPP experiments were performed for the six solutions at three temperatures: 25 °C, 75 °C and 98 °C. Figure A- 7,Figure A- 8, and Figure A- 9 show the results of the specimens for each temperature studied. The corrosion potential E_{corr}, passivation current i_{pass}, passivation range, and the repassivation potential E_{rp} from the CPP scans are listed in Table A - 2. For all cases, there was active anodization present and, in some cases, a passivation regime, similar to what it was observed for a fresh surface. At room temperature or 25 °C (Figure A- 7, top), the CPP scan shows that all six scans reached the potential limit of 2 V vs. SCE and have similar OCP potential of a range of -0.314 to -0.497 V vs. SCE.

A blown up insert in Figure A- 7 for the CPP scans showed different hysteresis were obtained. The hysteresis can be an indication of the corrosion processes taking place during the reverse scan. If the forward and reverse scans retrace each other, there is likely no change in the corrosion process. Positive hysteresis is characterized by higher current densities on the reverse scan compared to the forward scan

and vice versa for negative hysteresis. Positive hysteresis is usually an indication that pitting is occurring while negative hysteresis is an indication that the surface is in the passive state (no pitting). In the case of positive hysteresis, or pitting, it is possible for the surface to experience re-passivation while the potential is decreasing and is indicated by the potential at which the reverse scan crosses the forward scan (i.e., the re-passivation potential, E_{rp}). It was observed that for the Region 1 as-serviced oxidized surface exposed to solution 4, the results exhibited mixed hysteresis up until about 0.4 V vs. SCE while the other specimens tested in the other solutions show positive hysteresis. Specimens tested in solution 3 exhibited positive hysteresis but had a E_{rp} of 0.133 V vs. SCE, which is noticeably higher than the E_{rp} for the other solutions but the specific reason is not known.. It was noted that similar behavior was not observed for solutions 1 and 2, even though these solutions were more representative of the Zion SFP than solutions 3 and 4. One explanation may be that the characteristics of the oxide or oxyhydroxide may have changed with time between when the experiments were performed in solutions 3 and 4 (i.e, February 2017) and the time when the experiments were performed in solutions 1 and 2 (i.e., November 2017). Changes in the characteristics of the oxide or oxyhydroxide may alter the corrosion protection mechanism. Additionally, the surface oxide may have changed during sample preparation due to the necessarily harsh procedures that were used for decontamination and dehydration after they were removed from the Zion SFP.

At temperatures of 75 °C and 98 °C (Figure A- 8 and Figure A- 9 respectively), the OCP potentials for solution 2 and 4 and 6 (BWR based solutions) changed to more negative potential ranges (i.e., -0.9 to -1.2 v vs. SCE) which can indicate a change in the corrosion mechanism to a more active surface dependent on temperature. This is similar to what was observed for specimens with freshly ground surfaces tested in solutions 1 and 2.

During the forward scan for solutions 1 through 4, the potential reached the potential limit of 2 V vs. SCE, whereas solutions 5 and 6 reached the threshold current density of 1 mA/cm^2 at lower potentials. This indicates higher susceptibility of pitting corrosion even with the formation of an initial oxide/oxyhydroxide surface. During the reverse scans, the re-passivation potentials where closer to OCP, except for solution 3. The absence of a re-passivation potential indicates that at this temperature, the sample is more susceptible to localized corrosion and less likely to re-passivate once pits are initiated. The before and after pictures are different for each case and show a higher oxide disappearance for solutions with no boric acid (BWR-based) than solutions with boric acid (PWR-based). The more aggressive solutions show the appearance of higher diameter/depth pits on the surface. Based on the CPP results, as expected, solutions 5 and 6 have a higher susceptibility of pitting corrosion than solutions 1 to 4 and the effect is more deleterious at higher temperatures. However, the presence of an oxide/oxyhydroxide is beneficial and can minimize pit density where the susceptibility of localized corrosion is present.
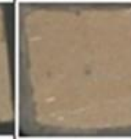
Figure A- 7 (top) Cyclic Potentiodynamic Polarization results for cladding 2K20S-10 in all simulants at 25 °C with insert showing the mixed hysteresis in more detail, and (bottom) before and after pictures
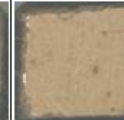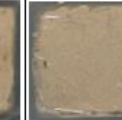
Figure A- 8 (top) Cyclic Potentiodynamic Polarization results for cladding 2K20S-10 in all simulants at 75 °C, and (bottom) before and after pictures

Figure A- 9 (top) Cyclic Potentiodynamic Polarization results for cladding 2K20S-10 in all simulants at 98 °C, and (bottom) before and after pictures

Table A - 2 CPP parameters obtained from CPP scans of Region 1 2K20S-10 experiments

Solution	Temperature (°C)	E_{corr} (V vs. SCE)	i_{pass} ($\mu A/cm^2$)	Passive range (V)	E_{rp} (V vs. SCE)
1	25	-0.314	1.6	0.17	-
	75	-0.32	19.8	0.57	-
	98	-0.786	11.4	0.71	-0.661
2	25	-0.409	N/A	N/A	-
	75	-0.873	7.5	0.45	-0.508
	98	-1.030	23.4	1.74	-0.383
3	25	-0.377	-	N/A	0.133
	75	-0.402	5.8	0.52	-0.244
	98	-0.701	6.6	0.53	-
4	25	-0.497	-	-	-*
	75	-1.03	27.2	0.88	-0.546
	98	-0.947	15.4	1.15	-0.767
5	25	-0.433	-	-	-
	75	-0.549	64.8	0.79	-
	98	-0.382	1.3	0.34	-
6	25	-0.462	2.4	0.08	-
	75	-1.140	16.6	0.74	-0.828
	98	-1.020	13.0	0.65	-0.861

*Mixed hysteresis was observed in the CPP.

Appendix B -Surface Pitting, Contour and Corrosion Evaluations

Surface Pitting

Two sections from panel section 5L9S-4 were chosen to characterize a worst-case pitting condition. Figure B - 1 shows the pitting and surface contour sample locations from the section. Figure B - 2 is a magnified view of the pitted area and the depth profile from the LCM. The pit surface morphology is oval with dimensions of 1.5 x 0.8 mm. The depth of the pit is measured to range from 250-300 microns depth relative to the current surface plane. Subsequent evaluations of cross-section views indicate that this is the thickness range of the cladding in Region 2 from which this sample originates. This depth does not include corrections for lost surface from corrosion. The pit bottom is flat and suggests that the pitting has exposed the core in this area. Figure B - 3 is an LCM view of the pit and visually shows the relative elevations via the color-depth range. As a measure of approximate pit density, the visual examination classified segment 4 of panel section 5L9S with between 5 and 10 pits with apparent depths greater than 100 microns. Region 2 appears to have more extensive pitting than Region 1. Some of the surface indications are related to possible local paint accumulations and the pitting density is judged to be relatively low and does not appear to be a significant issue with the panel conditions.
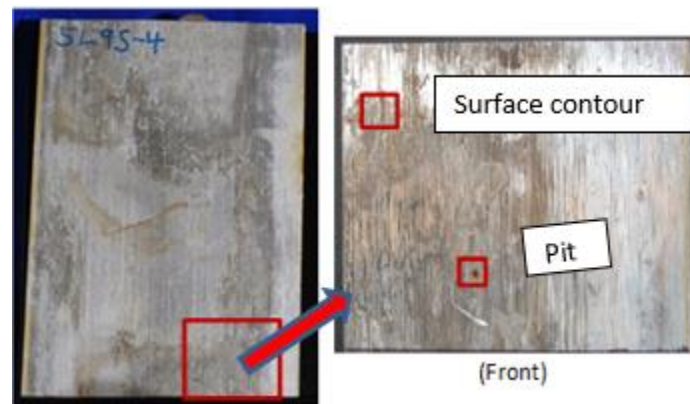
Figure B - 1 Sample Locations
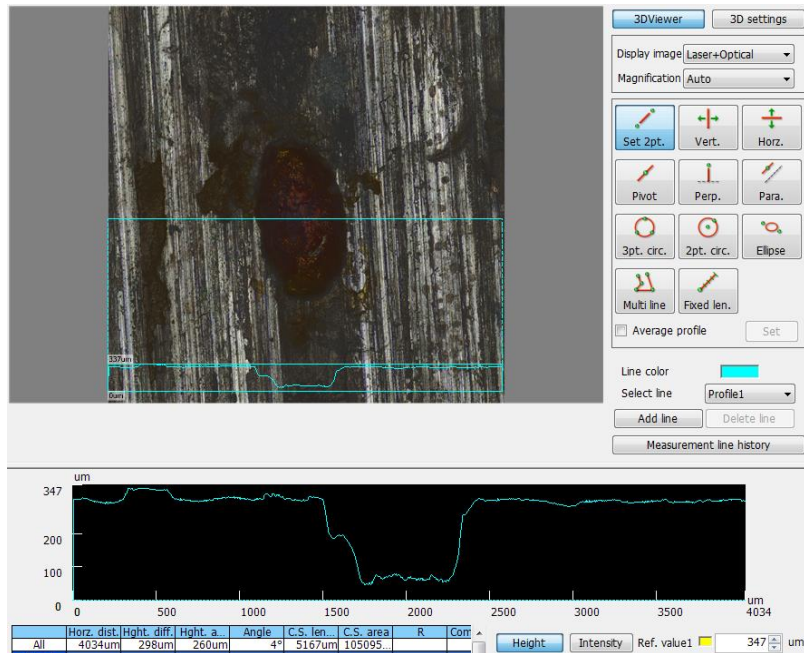
Figure B - 2 View of Pit Surface and Depth Profile
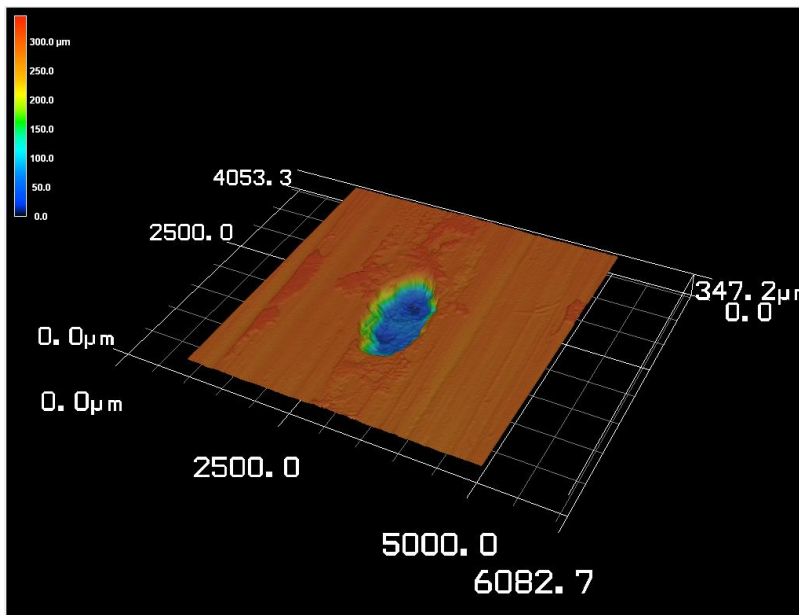
Figure B - 3- LCM Macro View of Pit

Surface Contour

A sample from panel section 5L9S-4 was examined to obtain a representative measure of the surface contour profiles observed on some of the sections. From a qualitative view, the surfaces of Region 1 were "smoother" with less irregularities than those observed from Region 2. A surface contour sample was also

taken from 5L9S-4 as shown in Figure B - 1. A magnified view of the surface as in Figure B - 4 shows a range in surface peaks and valleys of from 25 to 60 microns in relative height differences. There is a distinct axial flow orientation to the surface contour patterns.
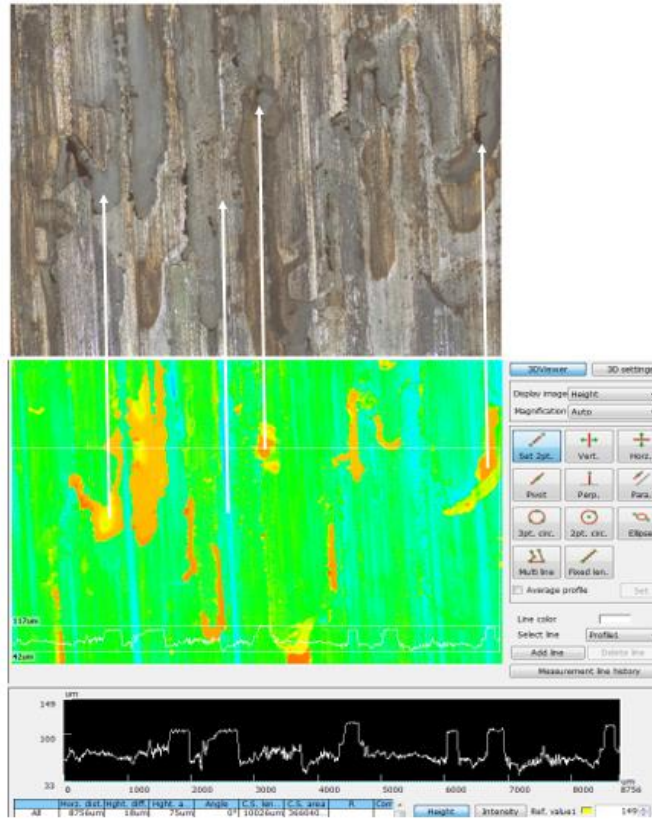
Figure B - 4 Example of Surface Contour Morphology from panel section 5L9S-4

Hold Down Strap and Tab Indications on Region 1 Panels
Most of Region 1 panels were not enclosed in a sheath but were directly exposed to the pool water and were held to the cell walls by stainless steel straps at intervals along the length of the panel. At the locations where the straps were in direct and sustained contact with the BORAL panels there is a significantly different surface texture as shown in Figure B - 5.
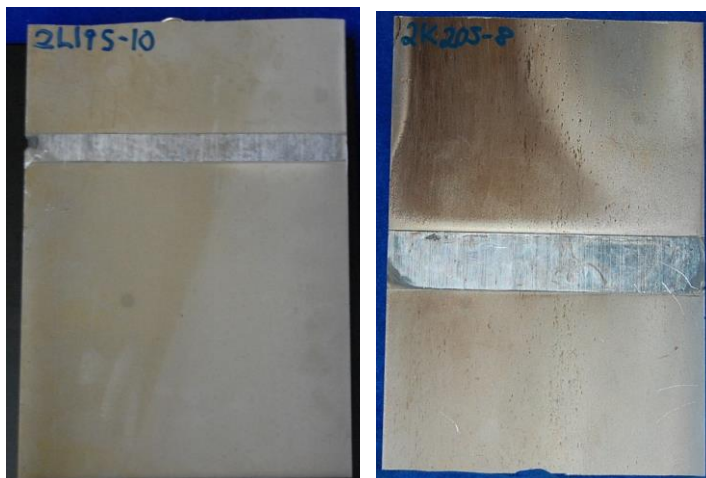
Figure B - 5 Example of Hold-down Strap Surface Indications

At these locations under the strap, the surface appears to be near as-manufactured condition and the area under the strap has an obvious raised surface above the plane of the adjacent section surface. Cross-sectional metallography samples were taken from this type of area and the results are shown in Figure B - 6. From the cross-sections the average thickness for a section under the strap is about 315 microns and the thickness away from the strap averages about 235 microns for a difference of 80 microns for panel 2K20S-10. If it is assumed the strap surface approximates the beginning surface height, then about 80 microns or 3.15 mils of surface removal via corrosion has occurred while in service.
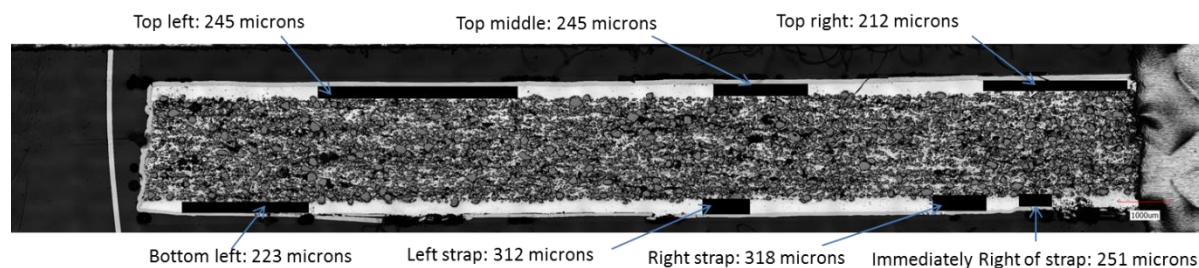
Figure B - 6 Panel 2K20S-10 Thickness Measurements Around Strap Coverage Area.

Surface Corrosion
There was no significant oxide thickness alluded to from the visual inspections. To characterize the surface condition for oxide, a sample was electro-less nickel coated to retain thin surface features and covered with a glass slide prior to cross-sectional mounting for the microscopic examination. Figure B - 7 and Figure B - 8 are pictures showing the interface structures observed on a Region 1 sample from panel section 2K20S-10. There is no large oxide thickness observed on the surface of the sample. A layer that is about 14 microns thick is observed between the Ni plating and the clad structure (possibly sealant coating). There is not an interaction area between the unknown material and the Al cladding and the

bonding does not appear to be very strong. There is no similar area observed on the back side of the sample as shown in Figure B - 9; however, there is an interaction zone at the surface of the backside that suggests a possible oxide film of about 1 micron in thickness. Like the backside observation from 2K20S-10, the surface of 5M7S-7 has an oxide film indication that ranges from 1 to 3 microns as shown in Figure B - 10.
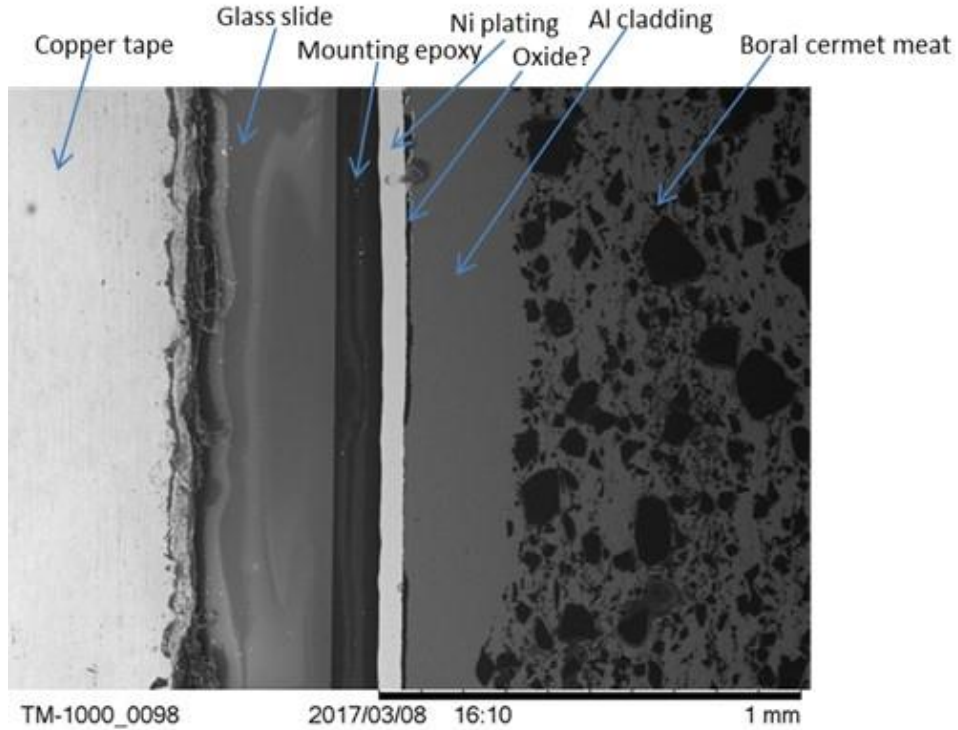
Figure B - 7 Low magnification BSE SEM micrograph highlighting the Boral cross-section and specimen mount to facilitate edge retention -2K20S-10
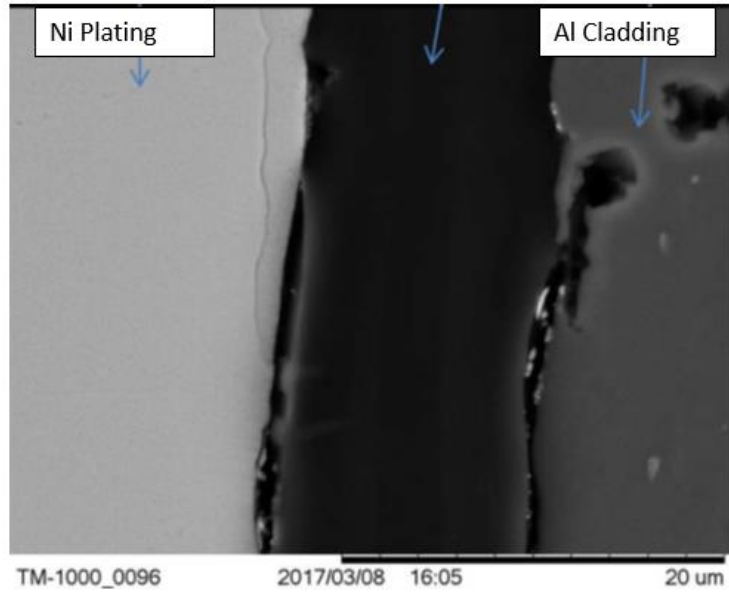
Figure B - 8 Higher Magnification of Interface Area -2K20S-10
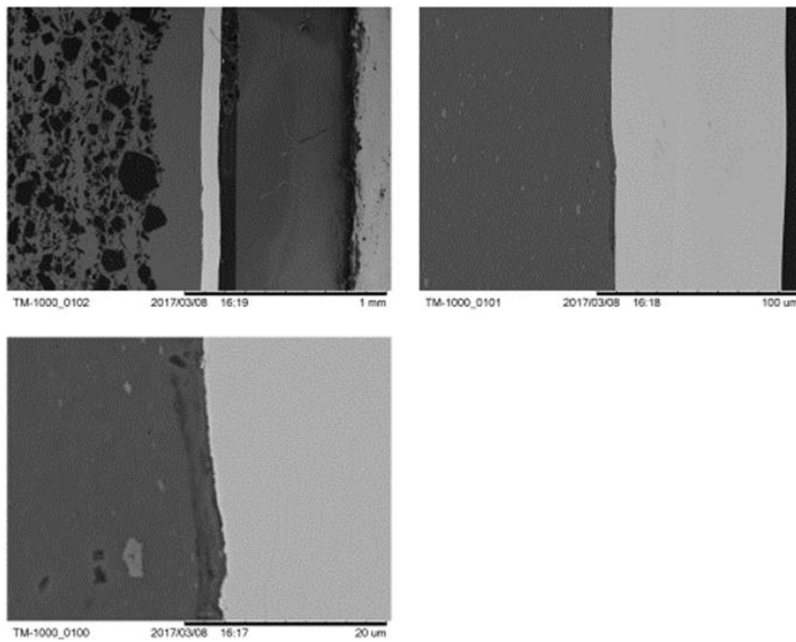
Figure B - 9 Back Side Area of Mounted Sample -2K20S-10
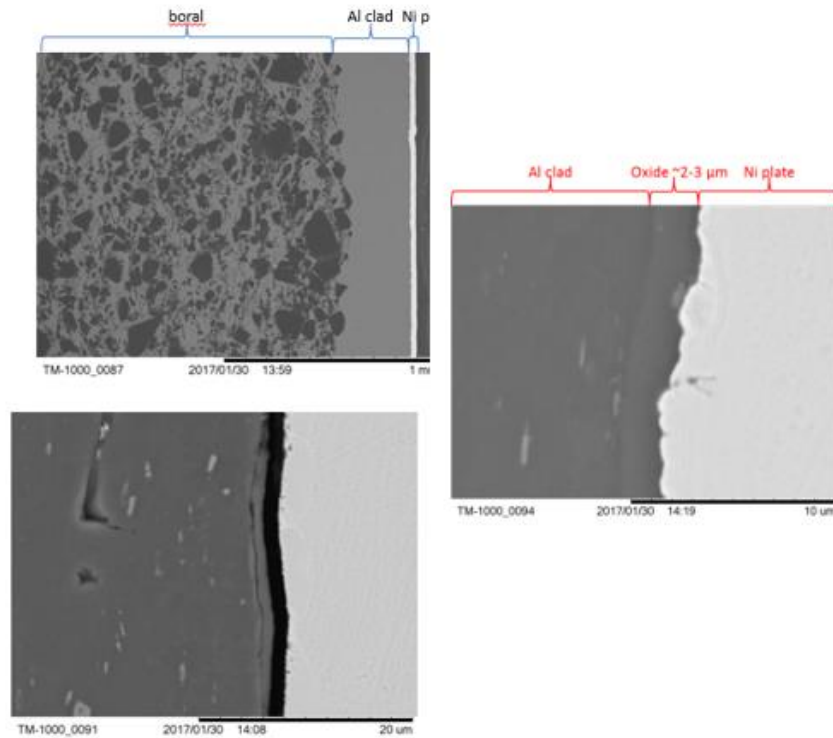
Figure B - 10 SEM Micrographs of 5M7S-7 showing oxide film ranging from 1 to 3 microns.

A further evaluation of the surface of 2K20S-10 was performed. An area from 2K20S-10 was scraped off and analyzed by XRD. The spectrum was compared to spectra from various Al oxides and elemental Al. The different aluminum and aluminum oxide spectra are shown in Figure B - 11 and the spectra obtained from the surface scrapings of the Zion BORAL sample is shown in Figure B - 12. The spectra from a similar section surface (with as-received film present) is shown in Figure B - 13 for comparison. The conclusion reached is that there is no significant oxide peak observed from the scraped surface material or the direct surface XRD and that only aluminum metal is seen in the spectra. This XRD data along with the prior morphology evaluations lead to the conclusion that the 14-micron zone observed on sample 2K20S-10 in not an oxide but is probably the epoxy paint that was applied to some of the panel sections and that there is a small oxide film present on the samples that is in the range of 1 to 3 microns in thickness.
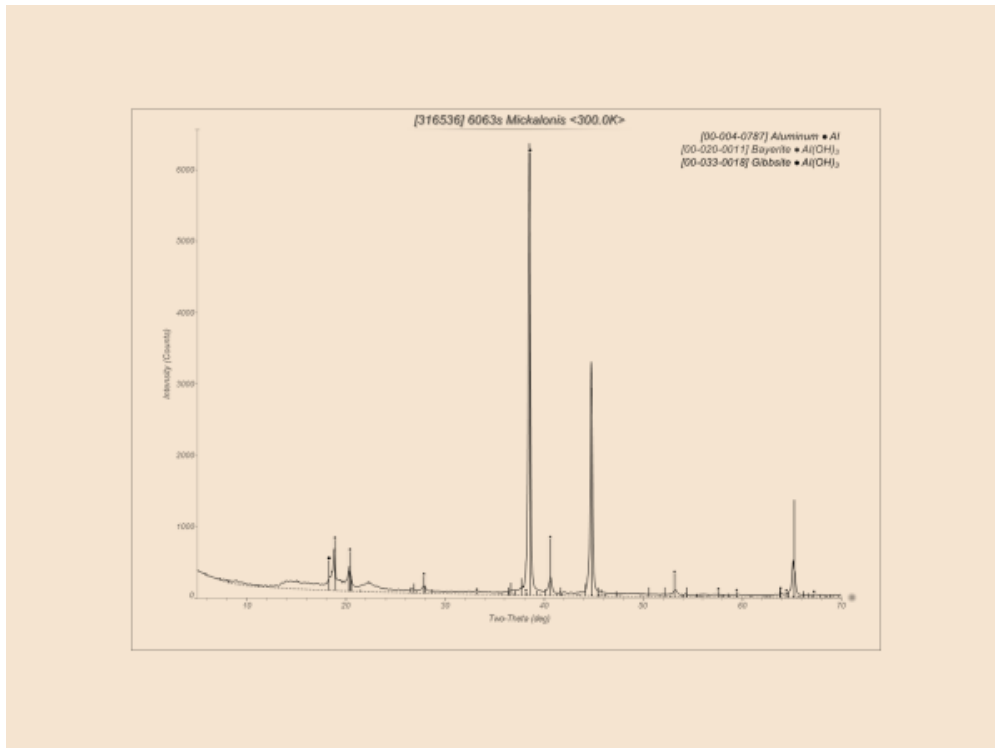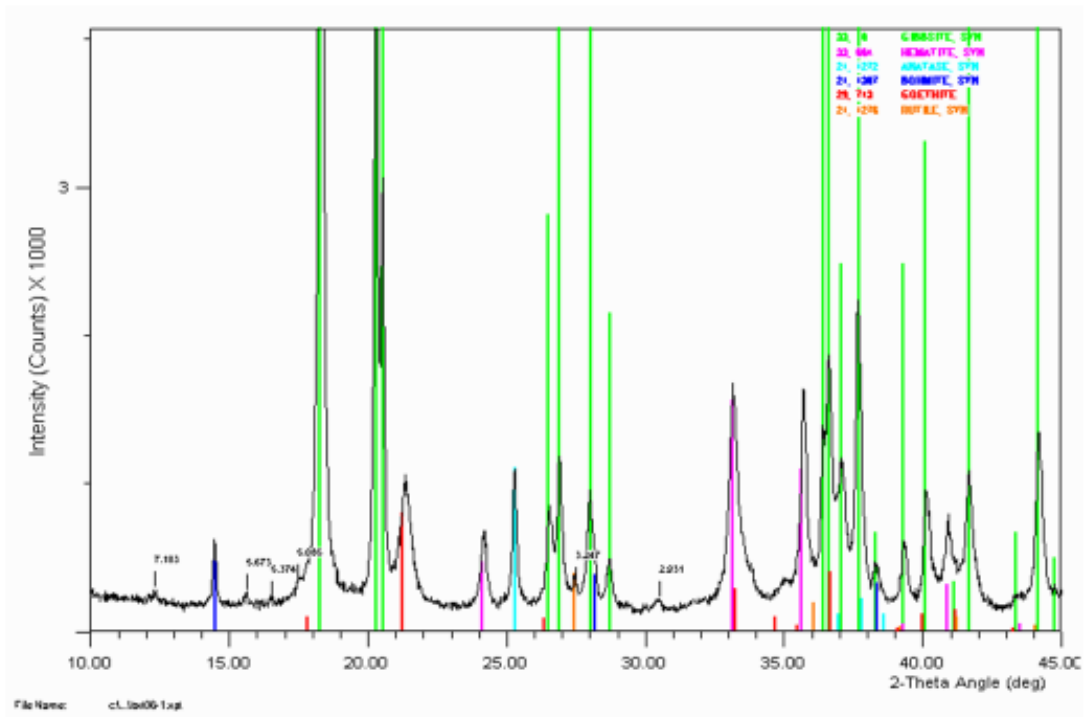
Figure B - 11   Spectra for Aluminum Various Aluminum oxides and hydroxides
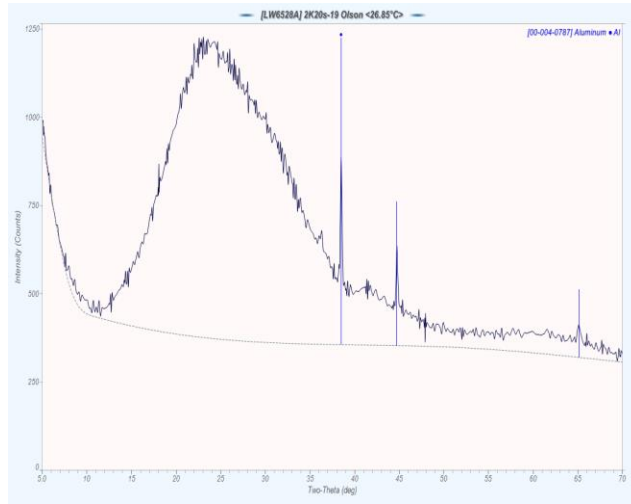
Figure B - 12 Measured Spectra from scrapped material from sample surface, characteristic of an amorphous material and aluminum
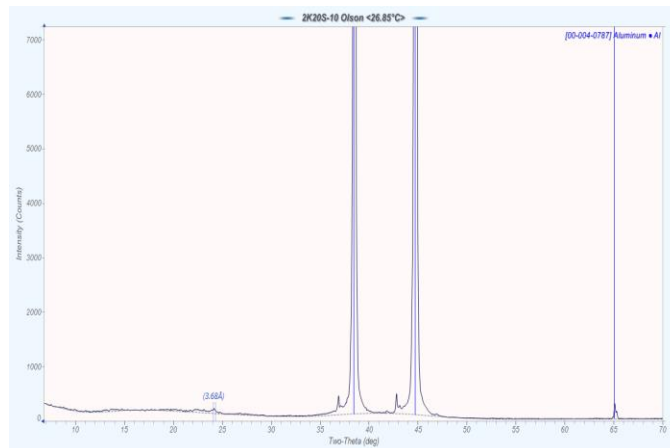
Figure B - 13 Spectra from XRD Examination of Front Surface of a Sample in As-received Condition – The only significant signal is aluminum metal.

Microstructural Cross-section characterizations

Some samples were removed from the panel sections, mounted and polished for examination of the BORAL cross-section. Figure B - 14 shows examples of the microstructures observed. The clad thickness and core thicknesses can be estimated from the pictures; however, for most pictures the scale is not accurate for dimensions 90 ^{0} off the scale axis due to possible picture distortion with handling. Some samples had total thickness measured at the time of viewing and are accurate.
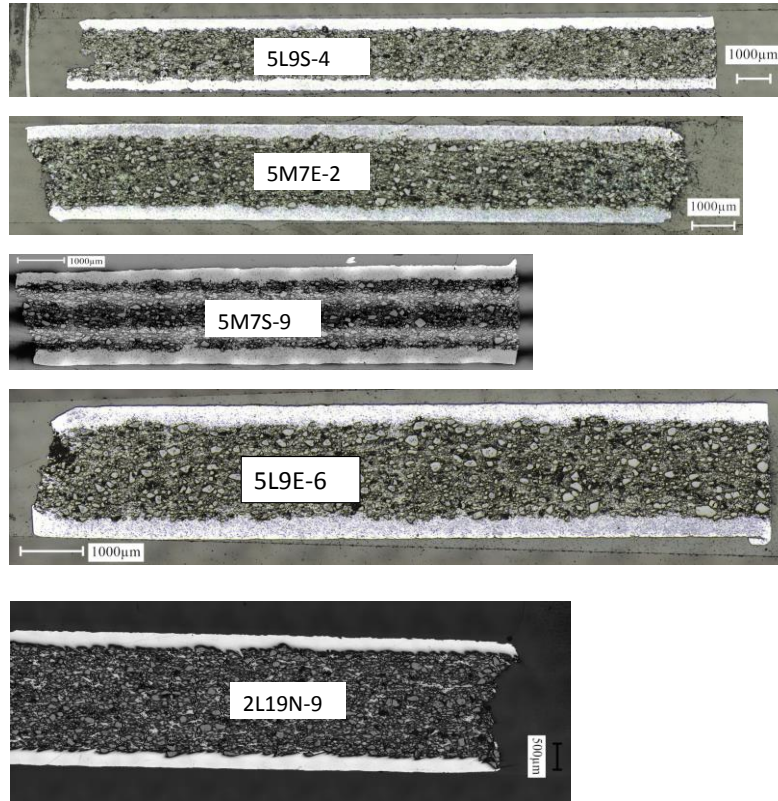
Figure B - 14 Examples of Cross section views

Some of the polished samples were viewed with the confocal microscope at an enhanced magnification to evaluate the B_4C-Al matrix morphology. Figure B - 15 includes typical examples of the BORAL cross-sections. Because of the nature of the hard B_4C particles in the softer Al matrix there is a very small amount of area where the B_4C particles have been removed by the polish and pits are remaining. There was no unexpected microstructure or non-random B_4C distributions observed in the micrographs (except for some minor clustering of some large particles as shown in the figure).

TM-1000_0004   2L19-9   1 mm   TM-1000_0009   5M7E-2   1 mm
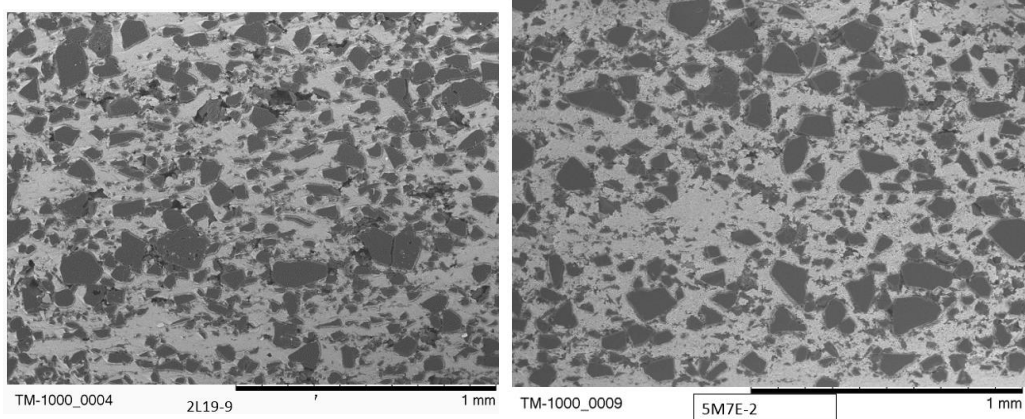
Figure B - 15 Examples of BORAL Microstructure

Some samples were examined using the confocal microscope to characterize the as-polished surface morphology. Examples of observed conditions are shown in Figure B - 16. The polishing technique resulted in a smooth B₄C particle polish. The micrographs also show that there is a five to eight microns difference in height between the B₄C and the Al matrix polished surfaces, with the Al being shallower due to the softer characteristic of Al and easier removal with polish.
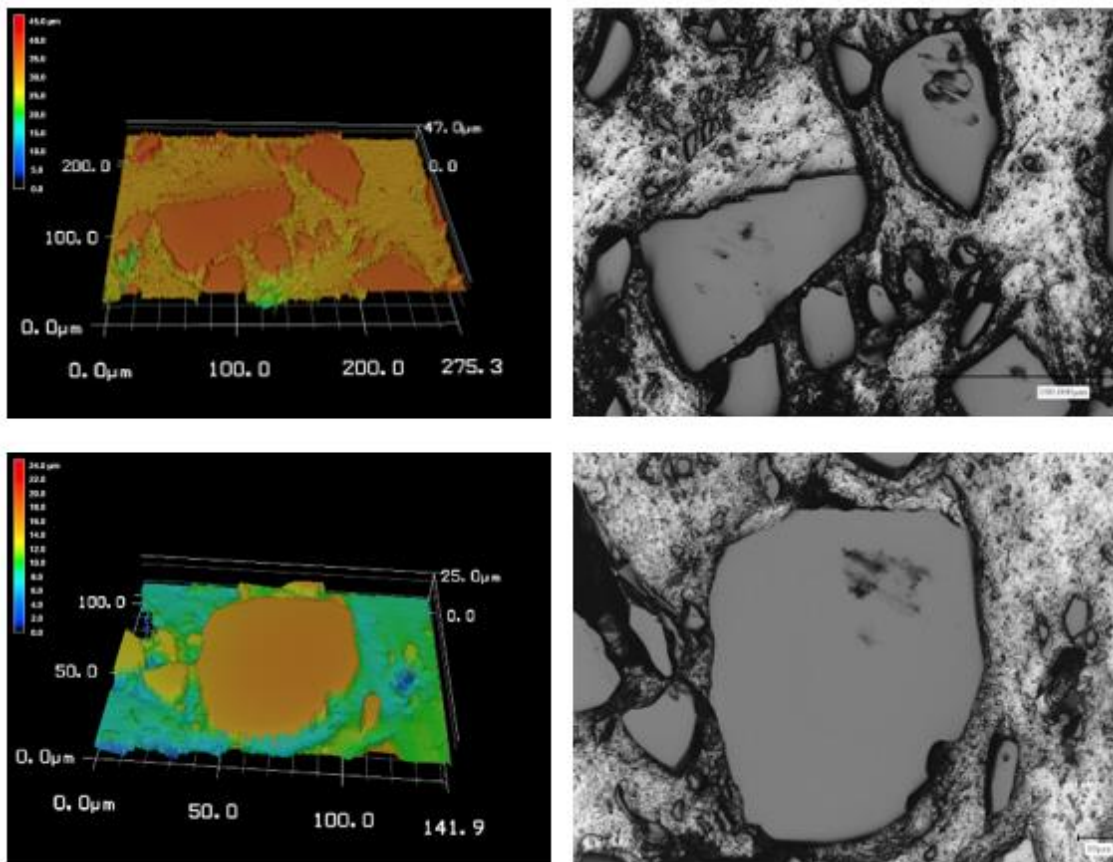
Figure B - 16 Examples of Relative Surface Contours in Polished Samples

For characterization, the flow hole indication on one of the Region 2 panels was examined and a photomicrograph of the indication is shown in Figure B - 17. Based on an estimate from the calibration bar, the indication appears to penetrate all the way through the cladding for a distance of 3000 microns or more. The photograph angles preclude an accurate depth measurement. The wall is relatively straight and uniform which suggests that the clad penetration was probably a result of a machining operation rather that corrosion attack.
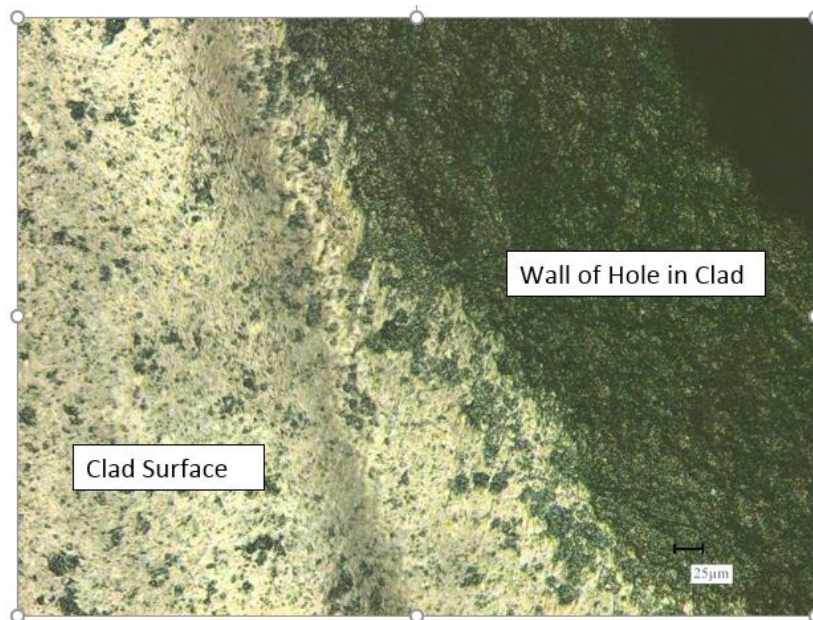
Figure B - 17 Photomicrograph of Wall of Flow Hole Artifact on a Region 2 Top Segment

Appendix C – Dimensional Measurements

Two panels from Region 1 and three from Region 2 were selected for detailed dimensional measurements. The panel identifications are listed in Table C - 1. They are in sets of three sections from each of the five full length panels. The sections were chosen to represent the top, middle and bottom areas of each panel. Section #1 is the bottom section and #12 is the top. Plate thicknesses (using a micrometer) and widths (using a caliper) were measured at specific positions to determine relative dimensional changes between and along the different panels. The measurements were taken at equivalent locations on the selected panels per the template shown in Figure C - 1. Section length measurements were not taken since they varied with the cutting procedure and, thus, have no direct reference to the panel characteristics. In addition to the standard dimensional measurements, for the Region 1 sections that had artifacts from the hold down straps, a set of thickness measurements were taken at the locations of strap contact with the BORAL panel as shown in Figure C - 1. Figure C - 2 summarizes the measurement values.

Table C - 1 List of Dimension Samples

Panel	Sections
2L19S	**2, 8, 12**
2K20S	**2,6, 12**
519E	**2, 8, 12**
5M7E	**2, 6, 12**
5M12E	**1, 7, 11**
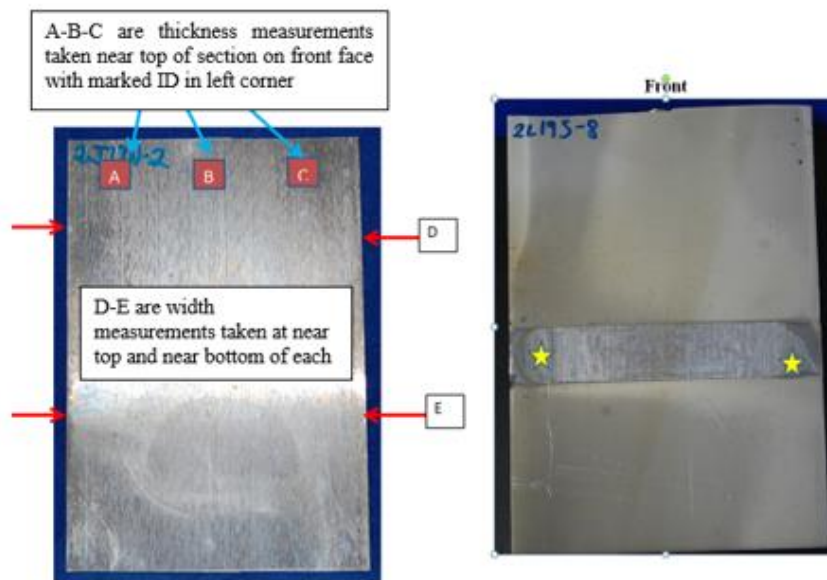
Figure C - 1 Thickness and Width Measurement Template and Example of Thickness Measurement Location at Strap Contact Location

C-1

The thickness and width measurements are listed in Table C - 2. The average thickness for the six Region 1 sections is 0.0995 inches (2.53 mm) with values ranging from 0.0963 to 0.1021 inches (2.44 to 2.59 mm). The nine measurements from the Region 2 sections had an average thickness of 0.0887 inches (2.25 mm) with values ranging from 0.0852 to 0.0938 inches (2.16 to 2.38 mm). Region 1 is thicker than Region 2 panels by nominally 0.11 inches (2.79 mm). Some of the range in values can be attributed to the presence of the epoxy sealant and manufacturing tolerances but some of the variation is related to axial position.

Table C - 2 Summary of Dimensional Measurments

Panel #		THICKNESS-inches			Avg Thickness	WIDTH-inches		AVG WIDTH
		A	B	C		D	E	
2L19S-2		0.0992	0.0978	0.0972	0.09807	8.269	8.275	8.272
2L19S-8		0.101	0.0979	0.1	0.09963	8.267	8.27	8.269
2L19S-12		0.1019	0.1018	0.1012	0.10163	8.275	8.275	8.275
	avg	0.1007	0.0992	0.0995	0.09978	8.2703	8.2733	8.272
2K20S-2		0.1021	0.0963	0.0948	0.09773	8.275	8.267	8.271
2K20S-6		0.1021	0.0993	0.0968	0.0994	8.264	8.266	8.265
2K20S-12			0.101	0.0982	0.0996	8.271	8.276	8.274
	avg	0.1021	0.0989	0.0966	0.09919	8.27	8.2697	8.270
5L9E-2		0.089	0.0871	0.0858	0.0873	7.531	7.525	7.528
5L9E-8		0.0929	0.0868	0.0852	0.0883	7.54	7.532	7.536
5L9E-12		0.0871	0.0883	0.0854	0.08693	7.537	7.536	7.537
	avg	0.0897	0.0874	0.0855	0.08751	7.536	7.531	7.534
5M7E-2		0.0895	0.0894	0.0895	0.08947	7.523	7.526	7.525
5M7E-6		0.0902	0.0908	0.089	0.09	7.528	7.525	7.527
5M7E-12		0.0938	0.0895	0.0909	0.0914	7.535	7.54	7.538
	avg	0.0912	0.0899	0.0898	0.09029	7.5287	7.5303	7.530
5M12E-1		0.0888	0.0882	0.0861	0.0877	7.549	7.551	7.550
5M12E-7		0.0892	0.0882	0.0871	0.08817	7.53	7.534	7.532
5M12E-11		0.0895	0.0891	0.0881	0.0889	7.538	7.528	7.533
	avg	0.0892	0.0885	0.0871	0.08826	7.539	7.5377	7.538

Figure C - 2 Panel Width Measurements

The panel sections width measurements are relatively consistent and show that the Region 1 panels are nominally 8.27 inches wide and the Region 2 panels are 7.53 inches wide. The widths are consistent within the region and do not show any significant variation regarding axial position as shown in Figure C-2.

Panel Thickness

The average panel thicknesses for the samples measured are 0.0995 inches (0.253 cm) for Region 1 and 0.0887 inches (0.225 cm) for Region 2 in the areas where the panel has been directly exposed to the spent fuel pool water. There were additional thickness measurements taken in specific areas on Region 1 panels which had thicker values. The thickness measurements are documented in Figure C - 3 and show a trend for thicker measurements near the top axial position, suggesting a possible differing surface corrosion rate depending on axial location with the highest near the panel bottom. The -1 location is the bottom axial section and -12 is the top section from the panels.
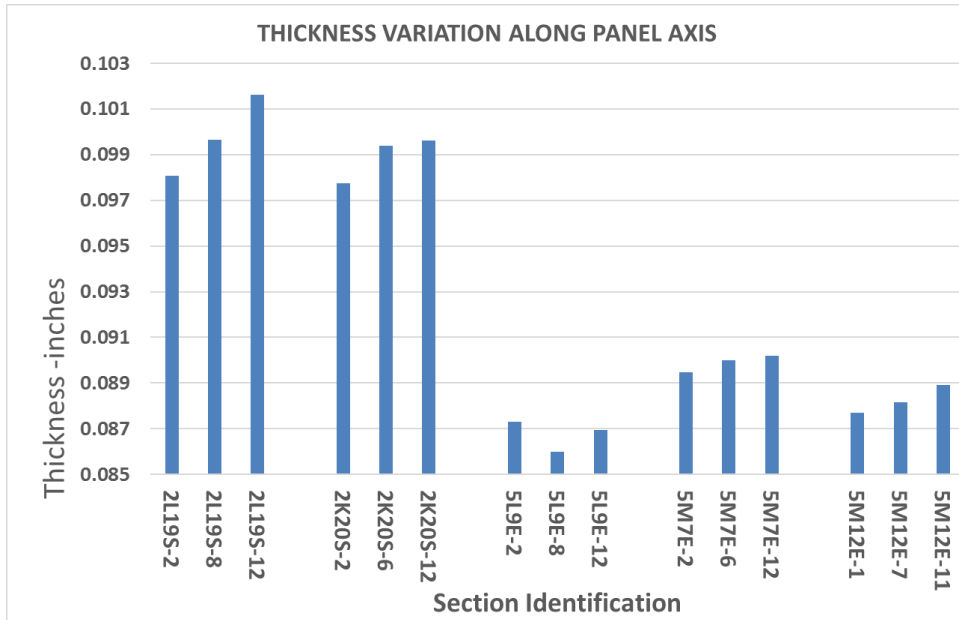
Figure C - 3 Showing the trend for Increasing Thickness at the Higher Axial Locations

The dimensional measurements were not a primary focus of the Zion BORAL evaluation and; thus, the measurement population was limited. However, based on the available data it is postulated that for Region 1 the surface corrosion was about 1 to 1.5 mils (25 to 38 microns)/surface greater at the bottom than at the top. For Region 2 panels which were enclosed in the sheath the amount of corrosion appears to be closer to 0.5 mil (13 micron)/surface or less delta between the top and bottom locations. This difference in the amount of corrosion is in addition to the general surface corrosion that was also present.

Region 1 Strap Effects

Upon the initial visual inspection of the segments, it was observed that the Region 1 sections that were in contact with the steel hold down straps had a raised surface at the locations under the strap. Specific thickness measurements were taken at these strap locations for comparison with adjacent non-strap locations. The panel surfaces at the strap location look similar to what would be expected as the as-built surface condition. It is postulated that the straps protected the clad area in contact with the steel strip from significant surface corrosion either by a galvanic mechanism and/or a shielding from excess oxide buildup. The difference in thickness between these two locations is assumed to be a function of the surface corrosion occurring on one side of the panel section. The measurements are shown in Table C - 3 and shown graphically in Figure C - 4.

Table C - 3 Measurements from Strap location for Region 1*

Panel #	THICKNESS AWAY FROM STRAP -inches	THICKNESS AT STRAP		AVG THICKNESS AT STRAP	DELTA THICKNESS FOR STRAP AREA MINUS NON-STRAP AREA-in
		F	G		
2L19S-2	0.0981		0.1013	0.1013	0.0032
2L19S-8	0.0996	0.1030	0.1010	0.1020	0.0024
2L19S-12	0.1016	0.105	0.1025	0.10375	0.0021
2K20S-2	0.0977	0.1012	0.099	0.1001	0.0024
2K20S-12	0.0996	0.1029	0.1002	0.10155	0.0020

 *(a value of 0.1055 inches (2.68 mm) for 2L19S-2 F was removed from the calculation since it represented an excessive variation of over 4 mils (102 micron) at one axial location and could be an artifact from surface contamination)
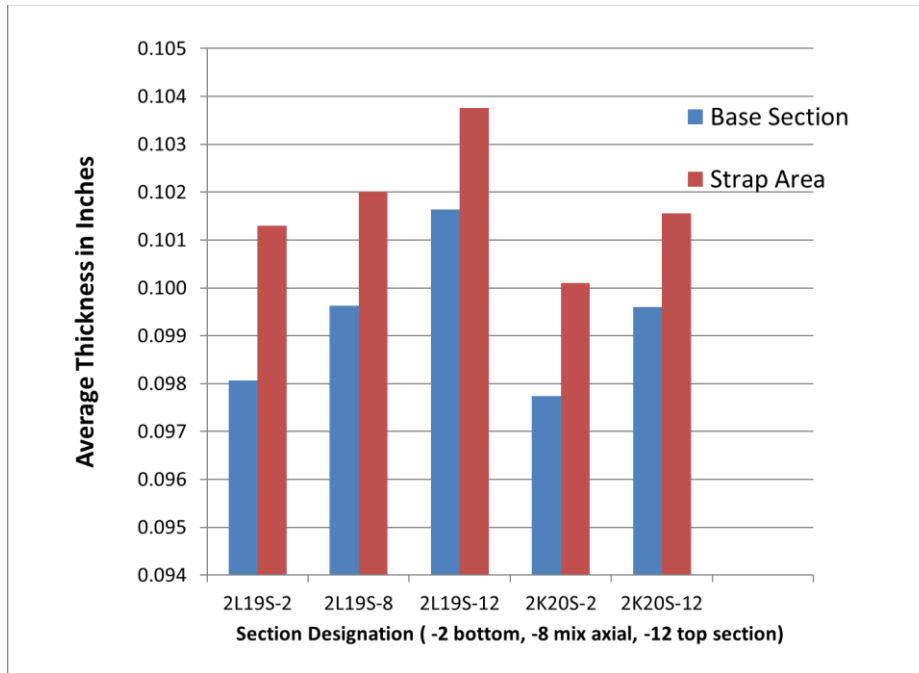
Figure C - 4 Comparison of Thickness at Strap and Non-Strap Locations

Comparing the strap area thicknesses to the non-strap area thicknesses, and using the step-height change between the protected clad (strap) and the non-protected clad (non-strap) thicknesses, it is estimated that:

- There is a difference in thickness of approximately 0.05 mm (0.002 inch) for both 2L19S-12 and 2K20S-12 sections between strap and non-strap area. It is assumed that no corrosion occurs directly under the strap. That is, the strap is 100% protective to the original clad underneath it.

- There are slight differences in the step height (thickness) of the strap to adjacent non-strap region going from top to bottom. This suggests a difference in corrosion of about 0.05 to 0.08 mm (2 to 3 mils) with the bottom being greater. Specifically, the difference in thickness between the strap and non-strap regions from bottom to top are as follows:
  - Panel section 2L19S-2: 0.081 mm (0.0032 inch) (bottom), 0.058 mm (0.0023 inch) (mid-panel) and 0.053 mm (0.0021 inch) (top)
    Panel section 2K20S: 0.061 mm (0.0024 inch) (bottom) and 0.048 (0.0019 inch) (top)

- The 24.9 mm (0.098 inch) thicknesses in the non-strap area compared to the starting thickness estimates indicate a single sided corrosion in the range of 0.05 to 0.08 mm (2 to 3 mils) in the bottom locations for Region 1 or about 0.0025 to 0.004 mm/yr (0.1 to 0.15 mils/year) for a 20-year life.

In Appendix B the cross-section measurement of sample 2K20S-10 reports a difference in clad thickness (corrosion) as 80 microns or 3.15 mils; whereas, the data from the macro measurement comparisons suggest a difference of about 2 mils (51 microns) in the clad (corrosion). The different values may be attributed to inherent variables in each measurement procedure even without additional data to resolve the differences there is sufficient consistency to support a general corrosion of about 2 to 3 mils (51 to 76 microns) of surface corrosion.

Appendix D – Blister Evaluation

Blister Formation Mechanisms

For the Zion panels involved in this study there were no observed blisters from the fuel pool operation. Some blisters were formed during the panel removals for this study and are discussed below. There are two primary postulated mechanisms associated with blister formation observed on in-service BORAL panels. Both mechanisms involve the ingress of water into the Boral core and a subsequent oxidation reaction with the aluminum matrix forming an aluminum oxide. This oxide formation releases hydrogen which is retained in the matrix because the oxide formation also effectively seals the ingress/egress matrix pathways. Along with the hydrogen there is also some moisture retention as hydroxides and perhaps free water depending on the exposure timing. Upon heating, the hydrogen may migrate to a void area at the clad/core interface and eventually produce enough pressure to cause a interface failure and a subsequent blister in the clad. Likewise, the residual moisture upon heating might be converted to steam and produce a blister.

Blisters Formed During Panel Removal

Three sections (1, 9 and 11) from panel 2K21N had blisters that were generated by excess heating from a torch during panel removal from the cell. An example from panel 1 is shown in Figure D - 1. An observation from this panel is that some blisters showed indications of center collapse. This may be an indication that the blisters were formed by steam generated from residual water in the matrix during cutting. The blisters likely collapsed due to the pressure differential following condensation of the steam.
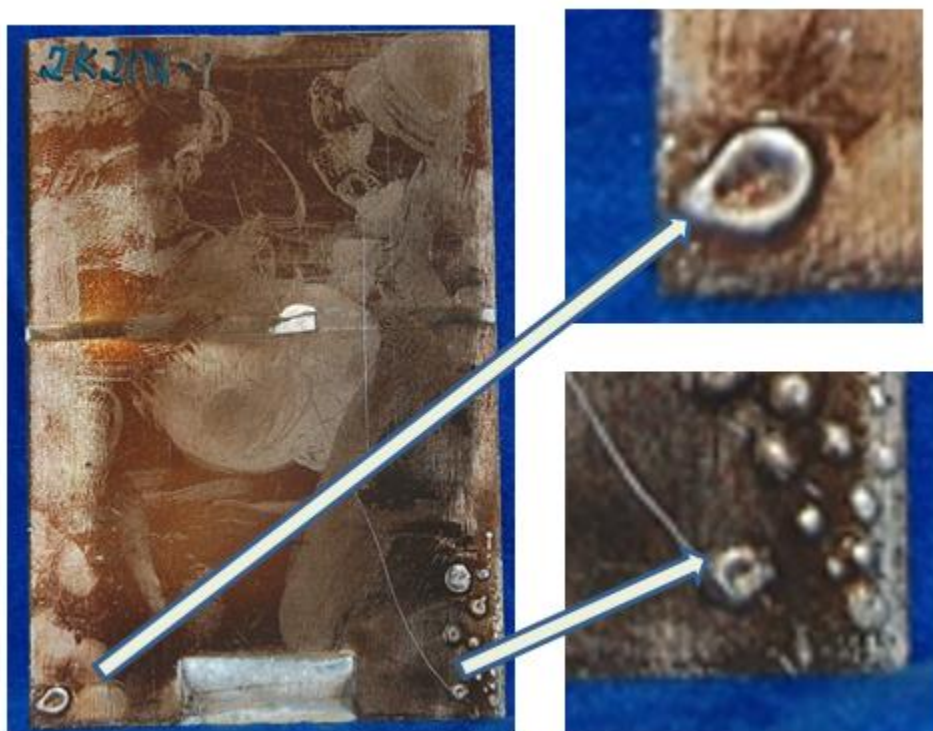
Figure D - 1 Blisters Formed on Section 2K21N-1 Due to Excessive Heating During Panel Removal

<u>Lab Generated Blisters</u>

Since there were no naturally formed blister to evaluate, a procedure was implemented to artificially generate blisters on panel samples. The initial procedure was to heat a panel sample in an oven to 515^0F (268^0C) for ten minutes. This procedure was not successful in generating a blister on the panel surface of a sample from 2L19N-9. Two additional panels were selected for the blister formation procedure, 5M7S-9 and 5L9S-12. The Region 1 panels, 2xxx, were more contaminated requiring more resources to clean for testing than the Region 2 panels and thus, were not chosen in this limited effort for blister generation. There is not enough data available to ascertain if there exists a difference in blister generation between Region 1 and Region 2.

<u>5L9S-12 Blisters</u>

Blisters were produced in panel specimen 5L9S-12 as shown in Figure D - 2. The panel was placed in air in an oven at 515°F (268^0C) for a total time of one hour. A popping sound was heard within minutes of the exposure start. The blisters were observed after the few minutes of exposure and no significant growth occurred with the remaining exposure. The blistered panel sample had a measured weight loss of 2.33 grams from the initial weight of 215.39 grams which is assumed to be moisture loss. There were seven blisters observed on the front face with diameters of 2.55, 1.20. 1.61. 0.9, 2.50. 2.24, and 0.70 inches (6.48, 3.05, 4.09, 2.29, 5.69. and 1.78 cm). There were 3 blisters on the back with diameters of 3.35, 0.9 and 0.60 inches (8.51, 2.29 and 1.52 cm). One of the mid-size (~1-inch diameter) blister area was sectioned and mounted for viewing as shown in Figure D - 3. Some of the B_4C particles are retained/embedded in the aluminum cladding. It is estimated from the visual exam that $\leq$ 5% of the B_4C is embedded in the aluminum. The blister lift-off gap at the peak distance is equal to or grater than the core thickness. Figure D - 4 is a confocal view of the blister prior to sectioning and shows the relative height to be 1709 microns or 67 mils.
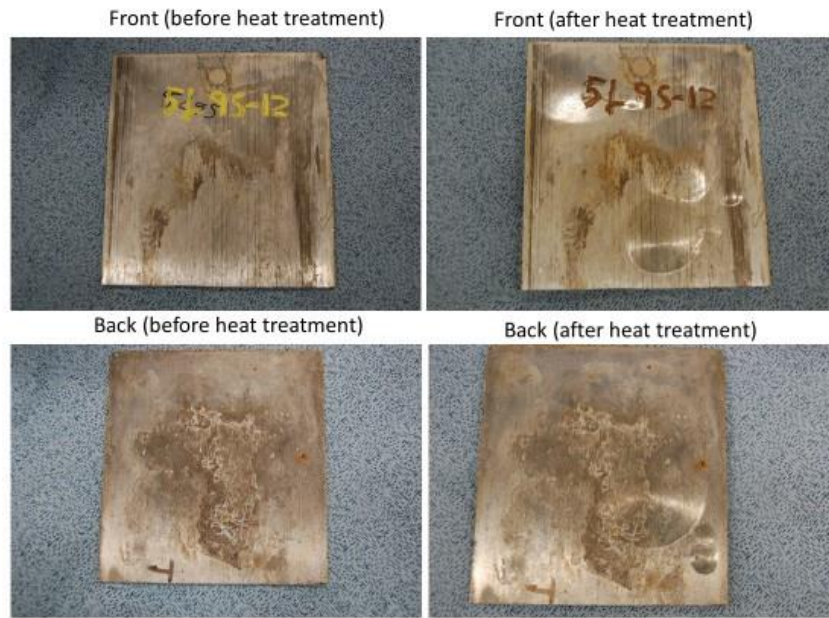
Figure D - 2 Blister formation on Sample from 5L9S-12
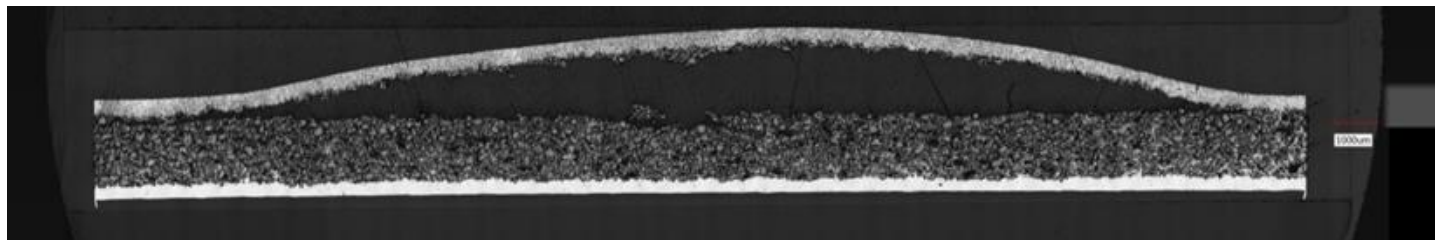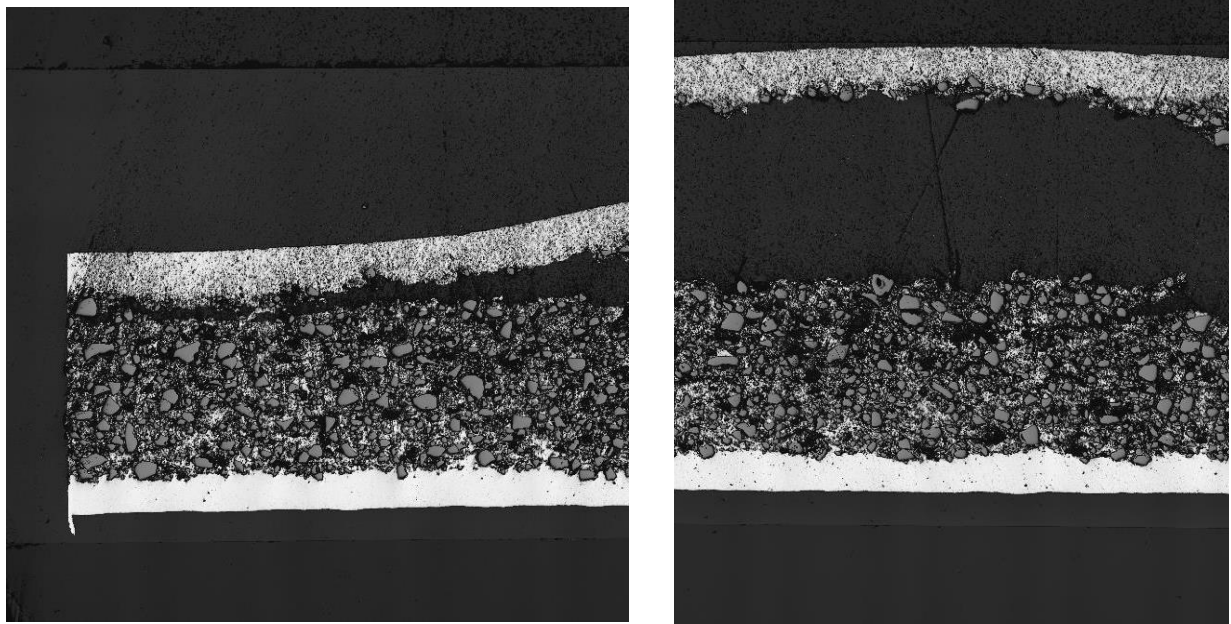
Figure D - 3 Sample 5L9S-12 Blister Morphology
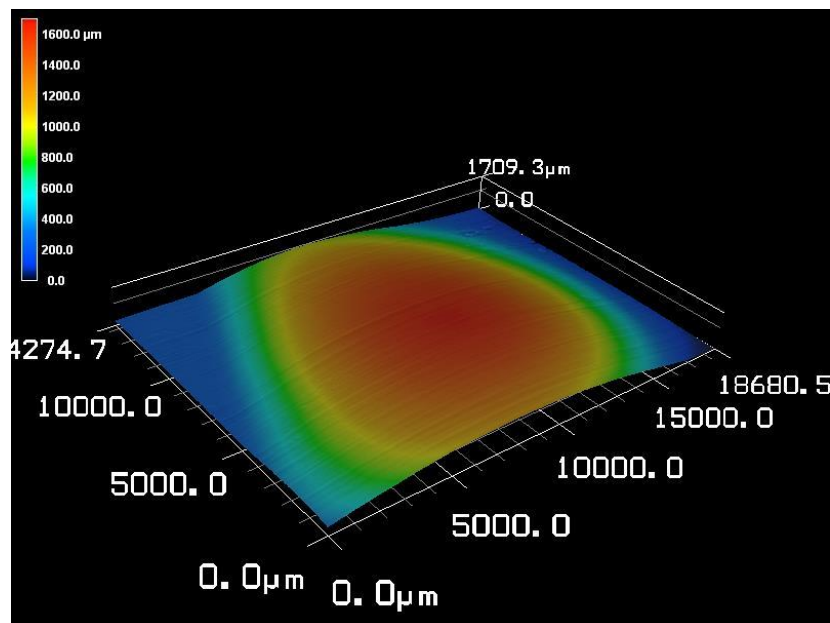
Figure D - 4 Confocal Image of Blister on 5L9S-12

5M7S-9 Blisters

Using a sample from 5M7S-9 (piece 1), blister formation was explored through rapid (10 min) successive heating at specified temperatures. Photographs were taken, and weight loss was recorded following each exposure. The results are detailed below:

- Initial weight: 111.2629g
- Heat to 250 °F (121 °C), expose for 10 minutes. After 10 minutes at 121 °C: 111.2108g
- Heat to 300 °F (149 °C), expose for 10 minutes. After 10 minutes at 300 °C: 111.1537g
- Heat to 400 °F (204 °C), expose for 10 minutes. After 10 minutes at 204°C: 110.8152g
- Heat to 500 °F (260 °C), expose for 10 minutes. After 10 minutes at 204°C: 110.5062

When heating at 400 °F (204 °C), for 10 minutes, there was a weight loss of 0.34g and one blister was formed. After heating to 500°F (260 °C) for 10 minutes, the blister did not change in size and no other blisters were formed. Figure D - 5 shows pictures of front and back 5M7S-9 initially and after 400°F (204 °C). The blister appeared after 6.5 minutes in the oven and it was characterized by a popping sound.
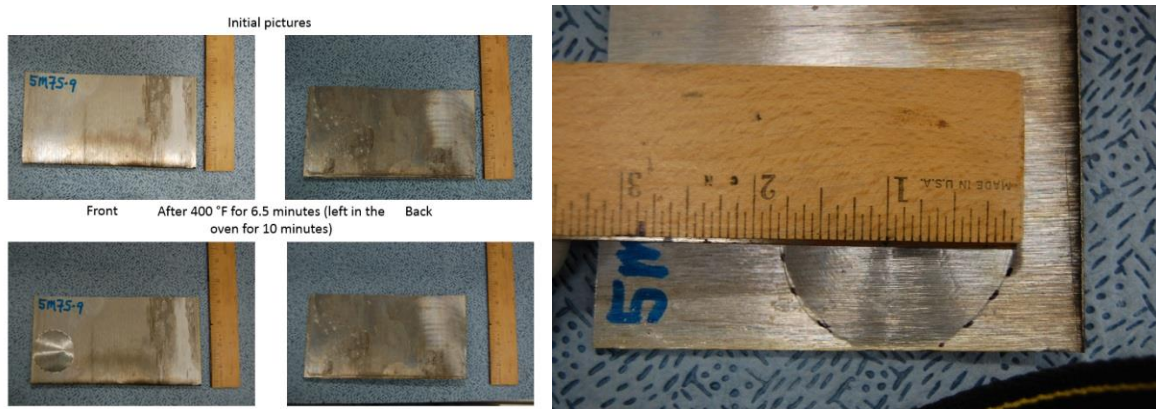
Figure D - 5 Blister Formation on Sample 5M7S-9 Piece 1

A second attempt was performed (5M7S-9 piece 2) to induce blister formation following longer exposure at each successive temperature. The objective was to determine if blisters may form at lower temperatures given a longer time at temperature. During the heating at 250 and 300 °F (121 °C and 149 °C) the weight loss was considerable. There was a weight loss of approximately of 0.14 g and 0.19 g, respectively. However, there were no changes on the surface of the coupon (i.e., no blisters formed). After heating piece 2 for 1 hour at each temperature, there were still no blisters on the surface of the panel. Even after an additional 30 minutes at 527 °F (275⁰C), there were no blisters formed on the surface. The results are detailed below:

- Piece 2 - Initial weight: 107.9134g
- Heat to 250 °F (121 °C), expose for 1 hour. After 1 hour at 121 °C: 107.7749g
- Heat to 300 °F (149 °C), expose for 1 hour. After 1 hour at 300 °C: 107.5853g
- Heat to 400 °F (204 °C), expose for 1 hour. After 1 hour at 204°C: 107.2277g
- Heat to 500 °F (260 °C), expose for 1 hour. After 1 hour at 204°C: 107.0706g

Likewise, piece 3 from 5M7S-9 was heated at 400 and 500 °F for 10 minutes to 1 hour to see if blisters would form but none were observed. The weight losses associated with the heating were recorded as:

- Initial weight: 108.923g
- Heat to 400 °F (204 °C), expose for 10 minutes. After 10 minutes at 204°C: 108.579g
- Heat to 500 °F (260 °C), expose for 1 hour. After 1 hour at 260°C: 108.174g

The weight loss is attributed to de-hydration of free water trapped in the specimen. This means that water (if present) was assumed to escape the specimen and did not pressurize the cladding. The relatively fresh cut edges of the samples may have contributed to any water/steam release. Some of the weight loss may also be attributable to surface moisture loss.

To obtain some exposed core areas for corrosion testing, sample 5L9E-6 was heated in an oven at 500^0 F (260 °C) for ten minutes. The blisters formed are shown in Figure D - 6. One of the blisters has a rupture crack and the line of blisters on the back and near the edge support the mechanism of water ingress at the edges as a source for the internal pressure generation. For corrosion samples, the blister domes were removed to expose the core NAM to evaluate corrosion rates on the core versus rates for the cladding.
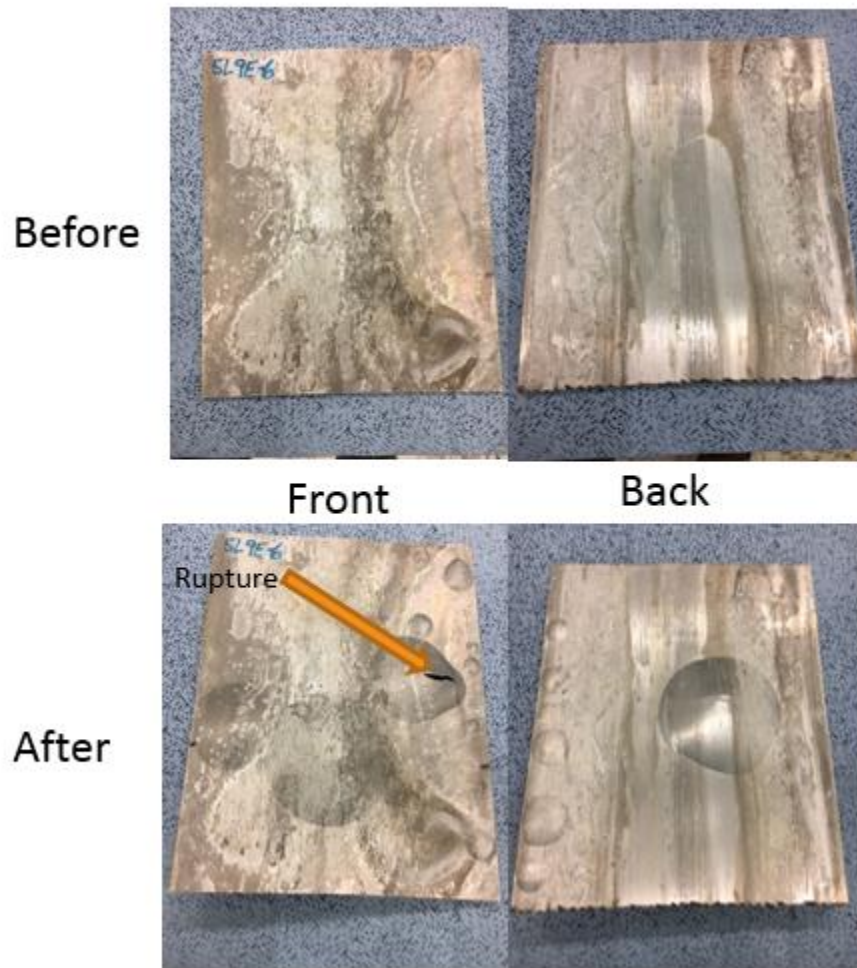
Figure D - 6 Blisters Formed on 5L9E-6 at 500^0 F (260 °C),

Weight Loss Evaluation

The measured weight losses from the samples heated to generate blisters were normalized to a sample weight loss percentage and plotted in Figure D - 7. The normalized weight loss also approximates a weight loss per unit surface area for the samples nominally the same thickness. The trend is consistent for the samples tested and shows a small weight loss rate up to 250 °F (121 °C), then a rise in the rate which is probably associated with a water – steam transformation. The weight loss can be associated with a combination of one of the following: surface oxide de-hydration, surface artifact (epoxy paint) loss and/or moisture and/or hydrogen escape from core region

In looking at the results from the 10 minutes and one hour holds, there is a time dependency on the weight loss. This would suggest a rate controlling mechanism that is postulated to be related to internal transport through the core to the free surface sides rather than to a surface related mechanism. There is clearly internal moisture and/or hydrogen gas present as observed from the blister formations. The presence of internal moisture combined with the observations that a) the rate changes at the water-steam

transformation temperature, b) there is no significant visual surface change and c) the surface oxide, as discussed previously, is very thin and not containing sufficient H_2O for the observed weight losses, supports the conclusion that the weight loss is primarily a loss of internal moisture and possibly some hydrogen gas generated from corrosion. Further testing would be required to fully understand the mechanisms occurring, evolving species and rates at longer times and higher temperatures.
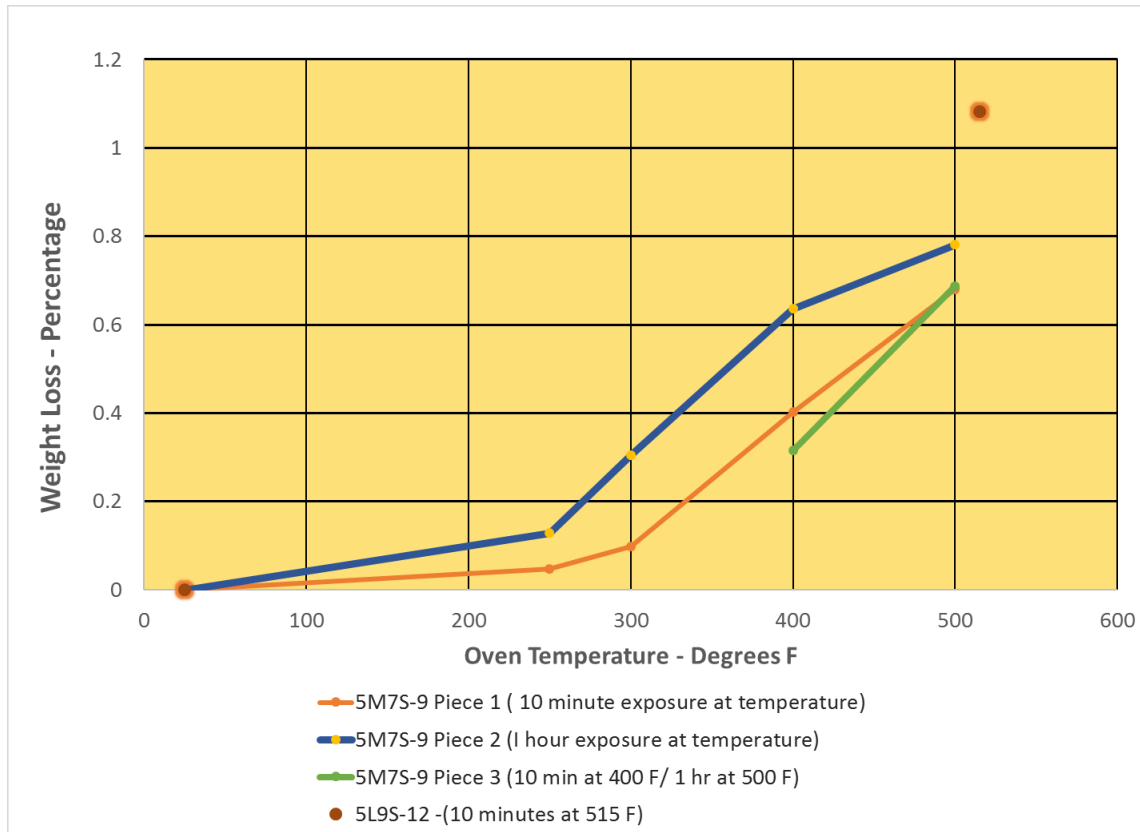
Figure D - 7 Incremental Weight Loss During Blister Formation Heating Cycle

Appendix E – Results of Chemical Method Protocol for B-10 Areal Density

I.   Calculation to Determine ^{10}B Areal Density (AD) Results for Panel 2K20S-10 Samples

Five adjacent coupon specimens were cut from the 2K20S-10 panel section and used to measure the ^{10}B Areal Density (AD) by chemical digestion and isotopic analysis. The five adjacent coupons are likely to have similar ^{10}B AD values; the results of the testing would thus provide an indication of reproducibility.

The testing and analysis of these materials established a chemical method protocol for radiologically-contaminated materials that was applied to the common material (see part II below) measured for ^{10}B AD by neutron attenuation at PSU and BADGER for comparison.

The total uncertainty for the ^{10}B AD by the chemical method is described in part III.

There is no consensus protocol for a chemical method for ^{10}B AD in Boral®. An ASTM International standard ASTM C791 deals with the analysis of boron carbide particles and does not provide specific guidance for calculating the boron level in compounds such as Boral®. The following describes the steps used in the protocol applied in this work.

Options for the calculation of the Boral® ^{10}B AD were evaluated and the following methods were adopted:

- The relative mass of B in a sample of the Boral® is measured by the ICP-OES and has variables of relatively high detection limits for some elements, and the carbon is lost from the B_4C during the sample fusion for the ICP-OES measurement.   The ^{10}B/B ratio for each specimen is used with the normalized ICP-OES levels for B with the assumption of 1% impurity levels. The 1% impurity level assumption is based on (1) the ICP-OES measurements which indicate about 0.5% impurity levels for Fe and Ca and while other elements are below detection levels, they are assumed to add another 0.5%; and (2) the aluminum in the Boral® typically contains about 1% impurities (AAR Cargo Systems letter to Stewart Brown NRC dated April 30, 2004).
- The ^{10}B to B isotopic ratio varies slightly between sample measurements. This is probably due more to the measurement uncertainty than the actual ratio variations. Thus, the average ^{10}B:B ratio for the sample set was used for the subsequent AD calculations.
- The AD samples were sheared from the BORAL panels. Subsequently it was observed that the sheared edges had an angle such that there is a bias towards a higher calculated frontal area. The samples were consumed in the test, so a re-measurement was not possible. The examination of a replicate sample indicated that the area bias is about 5% (higher than actual). The frontal areas used in the AD determinations include the 5% bias applied (deducted) from the area result.

Table E-1 Weight and Dimension Characteristics of 2K20S-10 Samples

2K20S-10 panel samples	1	2	3	4	5
mass -gram	0.9852	1.0195	1.0008	1.0412	1.0344
length -mm	13.32	13.42	13.41	13.44	13.6
width mm	12.88	13.18	13.1	13.59	13.48
thickness- mm	2.51	2.51	2.52	2.51	2.52
area with 5% bias deducted – cm^2	1.630	1.680	1.669	1.735	1.742

Table E-2 Summary of ICP Measurements and ^{10}B ratios for 2K20-10 AD Samples

ICP-OES Results from 2K20S-10 Samples					
	ug/g	ug/g	ug/g	ug/g	ug/g
	Sample 1	Sample 2	Sample 3	Sample 4	Sample 5
Element					
Al	607000	597000	628000	630000	629000
B	272000	275000	274000	292000	297000
C	75486	76318	76041	81036	82424
TOTAL	954486	948318	978041	1003036	1008424
Total plus 1% estimated impurities	964031	957801	987821	1013066	1018508
Carbon Content is calculated as = B ppm/ Number of B atoms in B$_4$C/mw B x mw of C (example : 272000/4/10.8 X12 =75556)					
^{10}B	49400	50700	50800	54000	56200
^{11}B	223000	224000	225000	238000	243000
^{10}B fraction	0.181	0.185	0.184	0.185	0.188
^{10}B fraction averages are within the normal range of natural B -^{10}B levels. An average ^{10}B level of 18.45 % is assumed in subsequent calculations.					
Sample mass [grams]	0.9852	1.0195	1.0008	1.0412	1.0344
Sample surface area [cm^2]	1.630	1.680	1.669	1.735	1.742
^{10}B grams in Sample =B wt / Total wt x ^{10}B wt fraction x mass (incl. adjustment for 1% impurities)	0.0513	0.0540	0.0512	0.0554	0.0557
^{10}B Areal Density: AD = grams ^{10}B / sample area [g/cm^2]	0.0315	0.0321	0.0307	0.0319	0.0320
Std Dev of the five 2K20S-10 samples AD values	0.00058		Average AD of the five samples =		0.0316

The measured sample weight and dimension characteristics for the five adjacent coupon specimens were cut from the 2K20S-10 panel section are listed in Table E-1. The ^{10}B to B ratio (wt. ratio) is calculated from a set of values measured by ICP-MS. An average value of 0.1846 for the ^{10}B/B ratio (wt. ratio) is indicated by the measurements for this data set. The measurements and calculations for the 2K20S-10 panel samples are shown in Table E-2. The standard deviation of the five values is 0.00058 gm ^{10}B/ cm^2. The absolute standard deviation value of 0.00058 is a relative standard deviation of 0.00058/0.0316 or 0.018.

II.   AD Results for Panels 5M7S-6 and 2K21N-2 Samples

Six samples from Region 2 panel 5M7S-6 and one from 2K21N-2 were tested using the chemical digestion and mass spec analysis. The sample characteristics are listed in Table E-3. Table E-4 presents the data and calculations for samples from the Region 2 5M7S-6 panel and the Region 1 2K21N-2 panel. Comparing the limited number of samples available, it strongly indicates that there is a difference in AD values for Region 1 and Region 2. However, this difference is fully expected since Region 1 panels have a thick cermet core. The relative standard deviation (std dev /average) for the six Region 2 samples is 0.0237 (0.00066/0.0278).

Table E-3 Characteristics for the 5M7S and 2K21N samples

	5M07S-06						2K21N-02
	5M-A	5M-B	5M-C	5M-D	5M-E	5M-F	2K-C
mass (g)	1.1064	0.9346	1.0349	0.8216	1.1416	1.0687	0.8792
A (mm)	15.4	12.5	13.9	12.6	15.0	12.9	13.5
B (mm)	14.4	13.94	14.4	12.0	14.8	15.2	11.6
C (mm)	14.9	13.26	13.7	13.04	14.8	13.3	12.6
D (mm)	14.2	14.2	14.2	12.3	14.5	15.4	11.4
thickness (mm)	2.31	2.36	2.34	2.36	2.34	2.39	2.64
area in cm^2 (with 5% bias correction)	2.053	1.717	1.875	1.478	2.069	1.905	1.438

Table E-4 Summary of AD Results for 5M7S-6 and 2K21N-2 Panels

AD calculations for samples from 5M7S-6 and 2K21N-2 Panels							
	ug/g	ug/g	ug/g	ug/g	ug/g	ug/g	ug/g
	5MA	5MB	5MC	5MD	5ME	5MF	2K21N-2
Element							
Al	614000	603000	579000	608000	565000	600000	574000
B	271000	265000	236000	271000	235000	257000	278000
C	75208	73543	65495	75208	65217	71323	77151
TOTAL	960208	941543	880495	954208	865217	928323	929151
Total plus 1% estimated impurities	969810	950958	889300	963750	873870	937606	938442
Carbon Content is calculated as = B ppm/ Number of B atoms in B_4C/mw B x mw of C (example : 271000/4/10.81 X12 =75208)							
^{10}B	50600	502000	452000	519000	448000	503000	522000
^{11}B	224000	2220000	1990000	2310000	1990000	2230000	2310000
^{10}B fraction	0.1843	0.1844	0.1851	0.1835	0.1838	0.184	0.1843
^{10}B fraction averages are within the normal range of natural B -^{10}B levels. An average ^{10}B level of 18.41 % is assumed in subsequent calculations.							
Sample mass [grams]	1.1064	0.9346	1.0349	0.8216	1.1416	1.0687	0.8792
Sample surface areawith bias [cm^2]	2.053	1.717	1.875	1.478	2.069	1.905	1.438
^{10}B grams in Sample =B wt / Total wt x ^{10}B wt fraction x mass (incl. adjustment for 1% impurities)	0.0569	0.0479	0.0506	0.0425	0.0565	0.0539	0.0479
^{10}B Areal Density : AD = grams B10 /sample area [g/cm^2]	0.0277	0.0279	0.027	0.0288	0.0273	0.0283	0.0333
^{10}B AD uncertainty [g/cm^2]	0.0062	0.0063	0.0061	0.0065	0.0061	0.0064	0.0075
Std dev of AD the five 5M7S-6 samples[g/cm^2]	0.0007		Average AD of the five 5M7S-6 samples[g/cm^2]			0.0278	

III. Areal Density Measurement Uncertainty

The uncertainties associated with the AD measurements using the chemical digestion technique are described. The uncertainties of the equipment used in the weight and dimensions measurements are;

Unit identifier	measurement device	uncertainty	unit
MT-CL15	Sartorius Lab Analytical CPA324S	0.0002	g
MT-CL16	Starrett model 721 caliper	0.01	mm

The steps in the chemical method measurements, and the associated uncertainties are identified below:

Step Number	Measurement	Absolute Uncertainty; Relative Uncertainty
1	Specimen cut to measured square approximately 1 cm x 1 cm (measuring with calibration-controlled calipers at each side, and average to get one length and one width)	Caliper uncertainty of 0.01 mm, and caliper relative uncertainty for the ~10 mm dimension is about 0.01 mm/ 10 mm or 0.001. A bias is assumed based on the sample non-uniform sample shape due to rough shearing during sectioning from the panel (resultant of radioactive material handling constraints). Since the samples have been consumed it is not possible to directly quantify the morphology uncertainty for this sample set. However, as an estimate for this characterization taken from a replicate sample a value of 5% bias high for the area or a factor on area of 0.05 is subtracted from the measured area. The uncertainty on the bias is estimated to be high and on the order of about 0.01 or $0.01/0.05 = 20\%$ relative uncertainty. Since the bias is not a direct factor in the AD calculation, the uncertainty needs to be appropriately weighted; i.e. since the 0.2 relative uncertainty only applies to the 5% factor it is weighted by .05 or $0.2 \times 0.05 = 0.01$ Summary: Caliper calibration uncertainty ($\sigma_{l1,l2}$): 0.01 mm Area bias correction factor (β): 0.95 Area bias uncertainty (σ_β) = 0.01
2	Weigh specimen on analytical balance	Specimen weight to ±200 μgm; weight uncertainty (σ_m) =0.0002 g
3	ICP-OES for normalized B	The ICP-OES reports for the B measurement; Relative Standard Deviation (RSD) (σ_B/B) = 0.10
4	ICP-MS for normalized ^{10}B	The ICP-MS reports for the ^{10}B measurement; Relative Standard Deviation (RSD) ($\sigma_{10_B}/^{10}B$) = 0.20

The equation used to calculate ^{10}B AD is:

$$AD = \left(\frac{m}{A}\right) \times B \ (wt.\%) \times {}^{10}B \ (wt.\%)$$

$AD = {}^{10}B \ areal \ density$

$A = Area = l_1 \times l_2 \times \beta$

$\beta = area \ estimate \ bias \ factor = 0.95$

$l_1 \ and \ l_2 = the \ sample \ mean \ length \ and \ width$

$m = mass$

$B(wt.\%) = Total \ B \ weight \ fraction \ (relative \ B \ with \ 1\% \ impurities)$

$^{10}B \ (wt.\%) = {}^{10}B \ abundance \ as \ weight \ fraction \ of \ B$

AD uncertainty is determined using the following equation:

$$\sigma_{AD} = AD \sqrt{\left(\frac{\sigma_m}{m}\right)^2 + \left(\frac{\sigma_A}{A}\right)^2 + \left(\frac{\sigma_B}{B}\right)^2 + \left(\frac{\sigma_{{}^{10}B}}{{}^{10}B}\right)^2}$$

where $\sigma_{(x)}$ is the uncertainty for each respective measurement. The relative uncertainty for the area is:

$$\frac{\sigma_A}{A} = \sqrt{\left(\frac{\sigma_{l_1}}{l_1}\right)^2 + \left(\frac{\sigma_{l_2}}{l_2}\right)^2 + \left(\frac{\sigma_\beta}{\beta}\right)^2}$$

The ^{10}B AD measurement uncertainties for 5M7S-6 and 2K21N-2 samples are given in Table E-4 above.

Appendix F

SRNL Receipt Inspection Compendium

1.0   Panels Received at SRNL

The panel identification and sectioning information is provided in the main report and Reference 1. The specific panels received at SRNL are listed in Table 1. A detailed compendium of the surface pictures taken of the panels and the radiation smear data is provided at the end of this attachment.

Table 1: List of Panel Sections Received at SRNL

Region/Module	Panel ID		Sections
1 / B	2K19W		1,3,5,7,9.11
1 / B	2J19N		2,4,6,8,10,12
1 / B	2K21N		1,3,5,7,9.11
1 / B	2K20S		2,4,6,8,10,12
1 / B	2L19N		1,3,5,7,9.11
1 / B	2L19S		2,4,6,8,10,12
1 / B	2L20N		1,3,5,7,9.11
1 / B	2L19E		2,4,6,8,10,12
2 / P	5M12S		1,3,5,7,9.11
2 / P	5L9S		2,4,6,8,10,12
2 / P	5M7S		1,3,5,7,9.11
2 / P	5M7E		2,4,6,8,10,12
2 / P	5M12E		1,3,5,7,9.11
2 / P	5L9E		2,4,6,8,10,12

2.0   Initial General Observations of Panel Conditions

From the receiving visual inspections, the following observations of surface conditions were made:

2.1. Paint

The surfaces of some panels appear to be masked by the encapsulation paint to varying degrees. The exposed region 1 surfaces are most affected. An example of the paint condition is shown in Figure 1. Note that the overspray stopped running when the hold down strip was encountered. It appears that Region 1 has more general paint coverage than region 2 which would be expected since region 2 panels were in a steel sheath.

Figure 1 Front Panel 2L19E-6, and example of worst-case condition of encapsulation paint coverage.
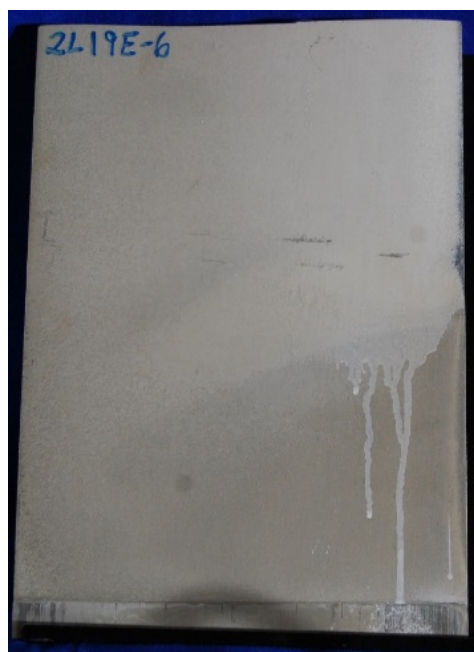
2.2. Flow Holes

For Region 2 (Module P) panels the BORAL core was sheathed in stainless steel which was attached to the cell wall. To allow circulation within the sheath a flow hole was drilled through the sheath outer wall at the top of the panel. Some of the Region 1 cells also had sheathes and flow holes. Panels sections from 2J19N and 2L19N do not have surface indications of strap contact and 2J19N has a flow hole indication. Panel 12 from 2L19N was not included in the shipment so the verification of a flow hole cannot be made for that panel; however, the panels with the XX19N designation are from the outer module wall and as shown in Figure 8 have the stainless-steel sheath. An example of the flow hole indication is shown in Figure 2. The visual observation is that there is clad penetration at the flow hole. Options for this condition include that the clad penetration occurred during the machining of the flow hole if done post core sheathing and/or that there is some electrochemical assisted corrosion that occurred in service.

Figure 2 Example of Flow hole indication on Panels 2J19L and 5L19E

2.3. **Metal Retaining Straps Indications**

On Region 1 /module B panels, the exposed BORAL was attached to the cell walls by metal bands and end tabs, refer to Figure 6. The area under the straps visually appears to have less corrosion than the adjacent areas. This condition will be addressed in detailed dimensional measurements. Subsequent thickness measurements indicated that the surface adjacent to the straps is about 0.002 inches below the strap contacted surface. Examples of the strap indications are found in Figure 3
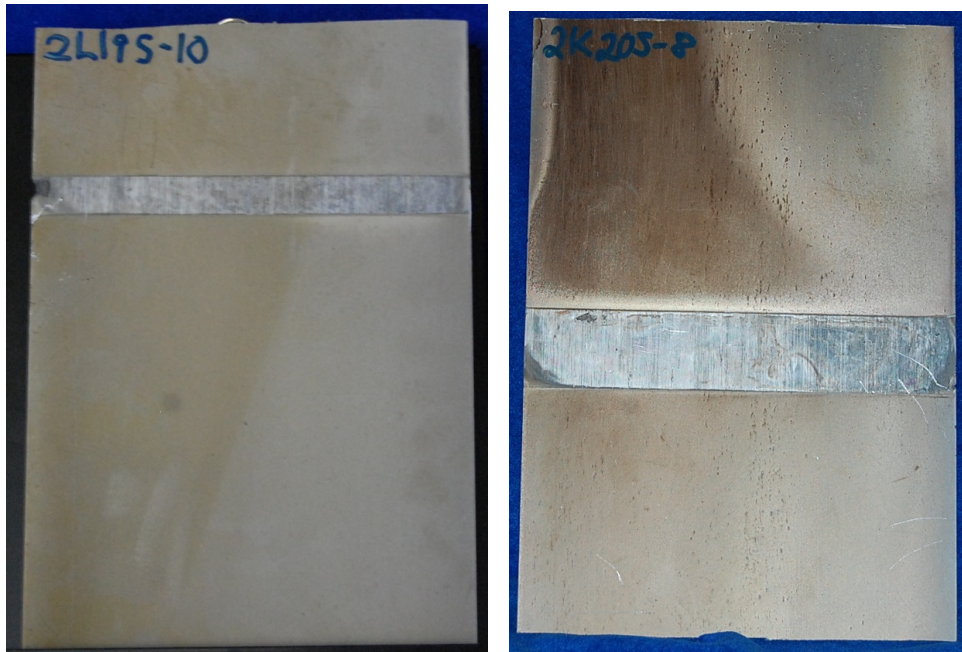
Figure 3 Example of residual indications from straps.

2.4. **Pitting**

Surface pitting was observed but for most of the panels it was not very severe. For a few panels, the pitting appeared to have penetrated the clad. The surface condition with the paint and some other residual materials did not support a quantitative pitting characterization. Figure 4 shows an example of a potentially severe pitting condition that will be further evaluated.
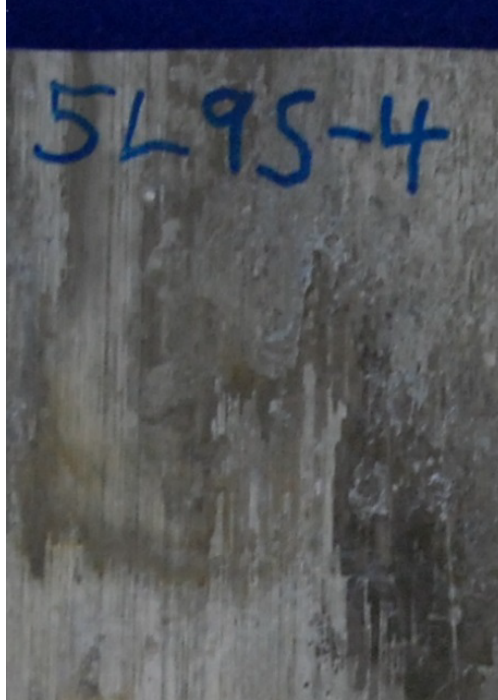
Figure 2 Possible worst-case pitting condition.

2.5. **Blisters**

The panel sections were inspected for any surface blistering. There were four sections that had blister s that are attributed to excessive heat during panel removal and are not suspected of formation during normal operation. The panels were 2K21N 1, 3, 9 and 11. Examples of the condition is shown in Figure 5. There were no observed blisters on any of the panel sections except for the heat related handling blisters noted on 2K21N.
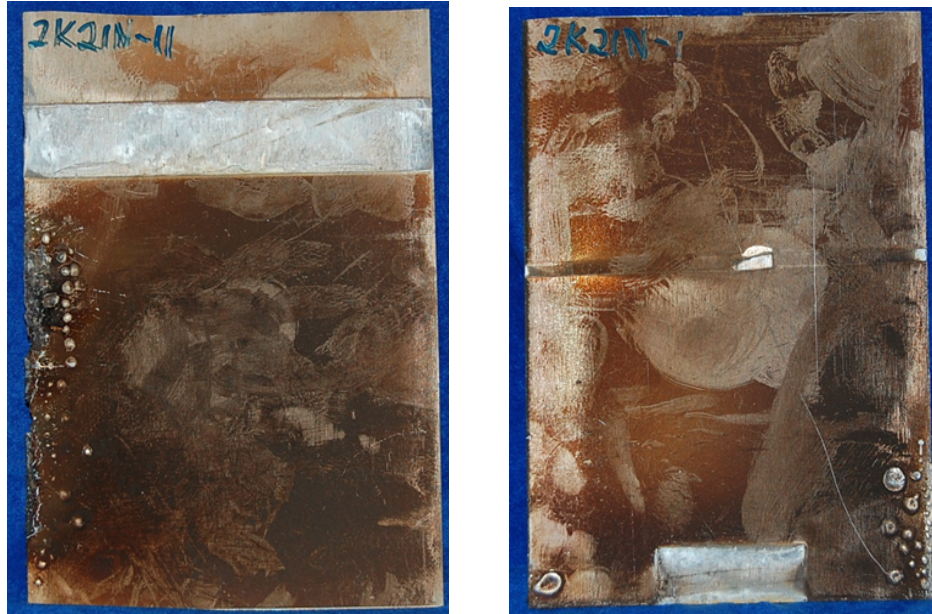
Figure 5 Observed blisters due to excessive heat during panel removal.

2.6. **General Corrosion and Flow Patterns**

There are no obvious areas of heavy localized corrosion on the panels. The surface depression relative to the area under the steel straps in Region 1 (Figure 3 suggests that there has been measurable surface corrosion and that most of the resultant oxide is no longer adherent to the plate surface.

Taking into account the more direct application of the sealant to the exposed Region 1 panels relative to the Region 2 panels, the Region 1 panels still have a more uniform surface with less mottling and less irregular surface depths compared to Region 2. Refer to Figures 6 and 7 for comparison examples. While not easily observed there does appear to be a series of flow patterns on the plates. These flow patterns are best seen on the back of the plates and show an axial (bottom to top) flow. Region 2 has more prominent axial flow indications compared to region 1. This may be a result of a mild convection flow with in the sheath associated with axial temperature gradients and the "open" sides of the panel in Region 1. Figure 8 has examples of flow patterns.
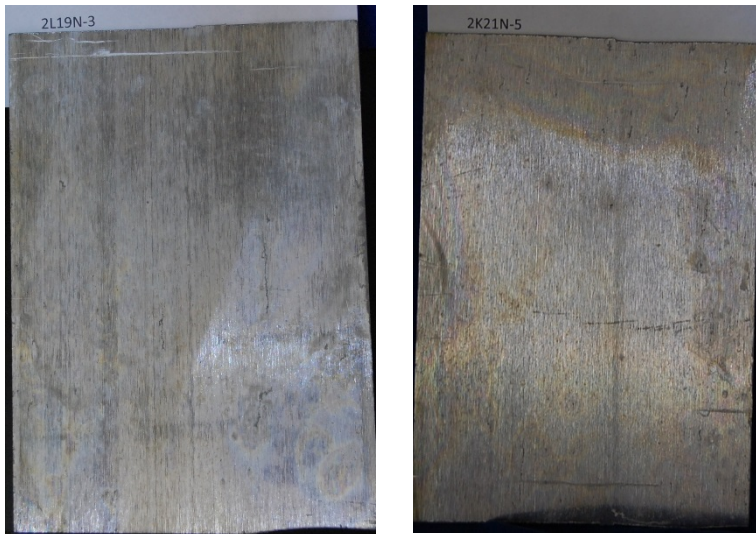
Figure 3 Typical surfaces from region 1 panels - back sides with no heavy sealant present.
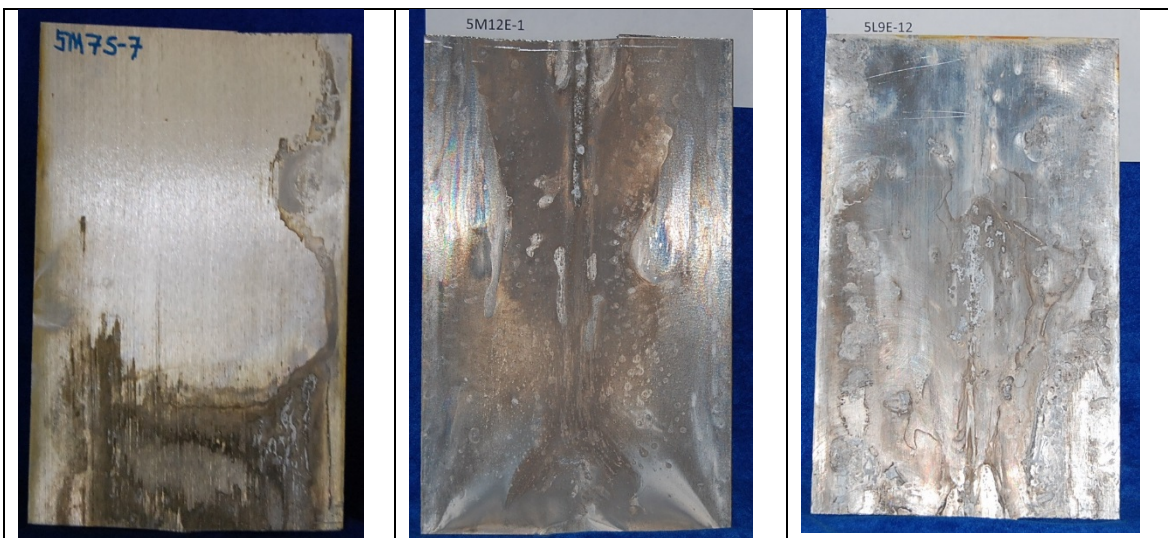
Figure 7 Back surfaces of Region 2 panels with mottled and irregular surface conditions.
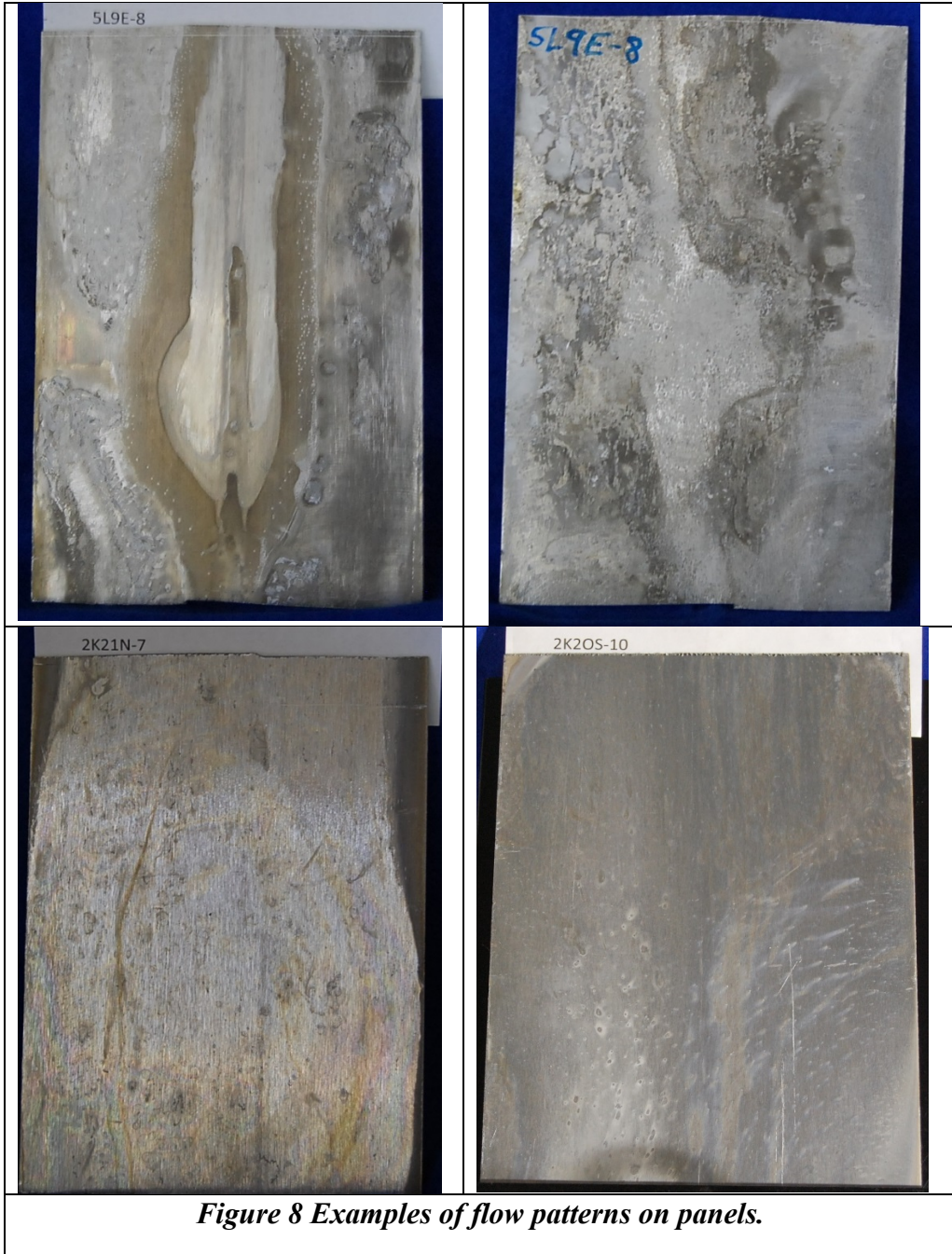
Figure 8 Examples of flow patterns on panels.

3.0 Reference

1. Harris, M.C. "Witness Report: Removal and Sectioning of BORAL Fuel Rack Modules B and P from Zion Fuel Pool", Curtiss-Wright / NETCO, November 2015

4.0 Documentation of the surface condition of the panels that were received at SRNL

In the pictures note that "front" represents the side away from the cell wall and "back" is the side that faces the cell wall.

PANEL: **2K19W**

Region: 1   **Module:** B

FRONT   BACK

(TOP)

**Highest Radiological Conditions
Occur in Section:** ___1___

Maximum Dose: 1 [mrem/hr]

Maximum Probe
  (α) : 400 [cpm/100cm²]
  (β/γ) : 220,000[cpm/100cm²]

Maximum Smear
  (α) : ND [cpm/100cm²]
  (β/γ) : 40,000 [cpm/100cm²]

(Bottom)
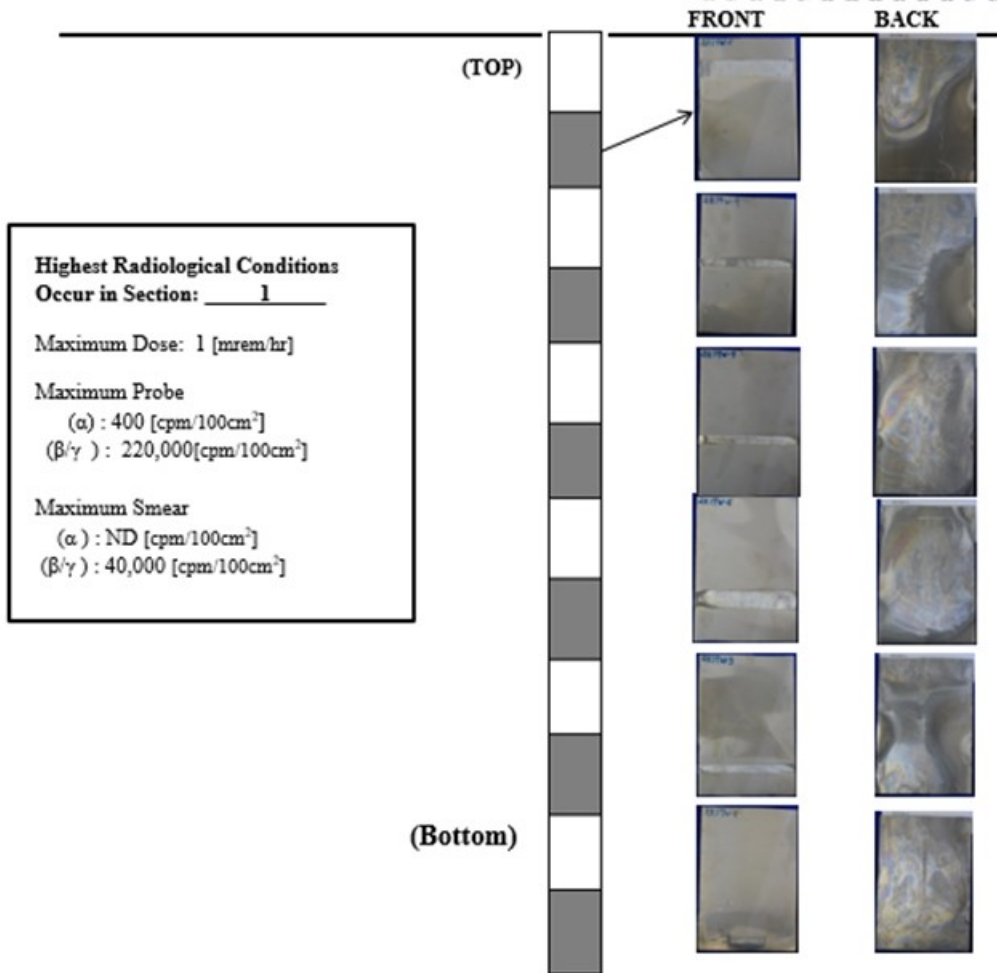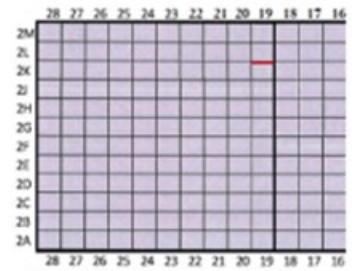
Sample ID: __2K19W__ - __1__
   (Panel #) *(Section #)*

Region: __1__ **Module:** __B__

	28	27	26	25	24	23	22	21	20	19	18	17	16
2M													
2L													
2K													
2J													
2H													
2G													
2F													
2E													
2D													
2C													
2B													
2A													
	28	27	26	25	24	23	22	21	20	19	18	17	16
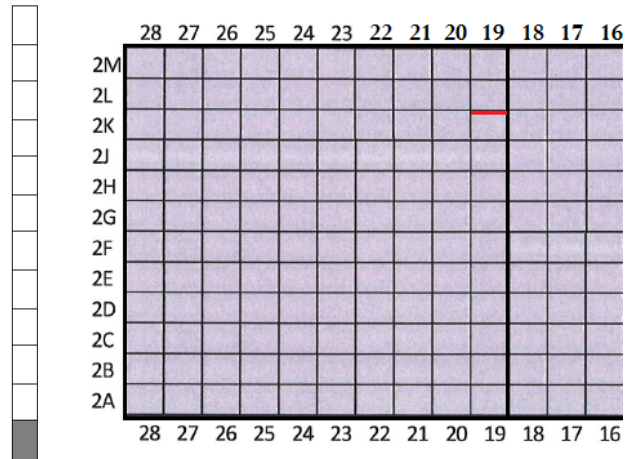
Front

Back

Sample ID: __2K19W__ - __5__
(Panel #)   *(Section #)*

Region: __1__   **Module:** __B__

	28	27	26	25	24	23	22	21	20	19	18	17	16
2M													
2L													
2K													
2J													
2H													
2G													
2F													
2E													
2D													
2C													
2B													
2A													
	28	27	26	25	24	23	22	21	20	19	18	17	16
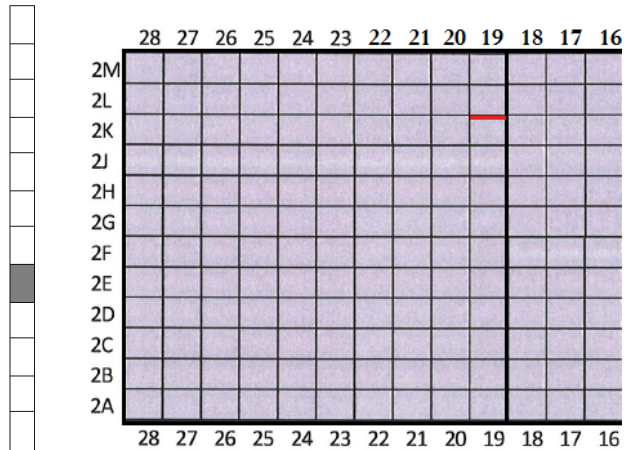
Front

Back

2K19W-5

Sample ID: __2K19W__ - __7__
(Panel #)   (Section #)

Region: __1__   **Module:** __B__

	28	27	26	25	24	23	22	21	20	19	18	17	16
2M													
2L													
2K													
2J													
2H													
2G													
2F													
2E													
2D													
2C													
2B													
2A													
	28	27	26	25	24	23	22	21	20	19	18	17	16
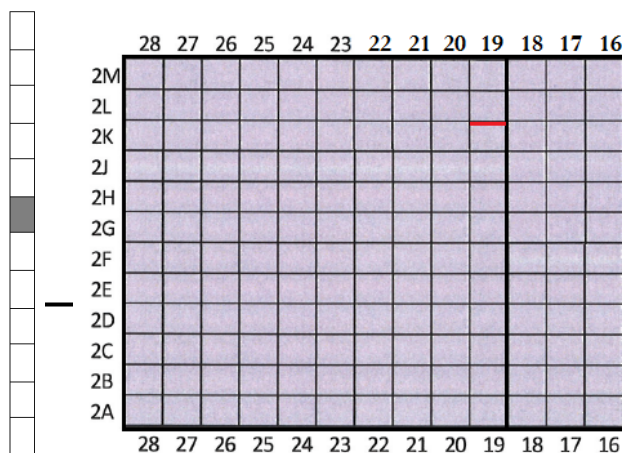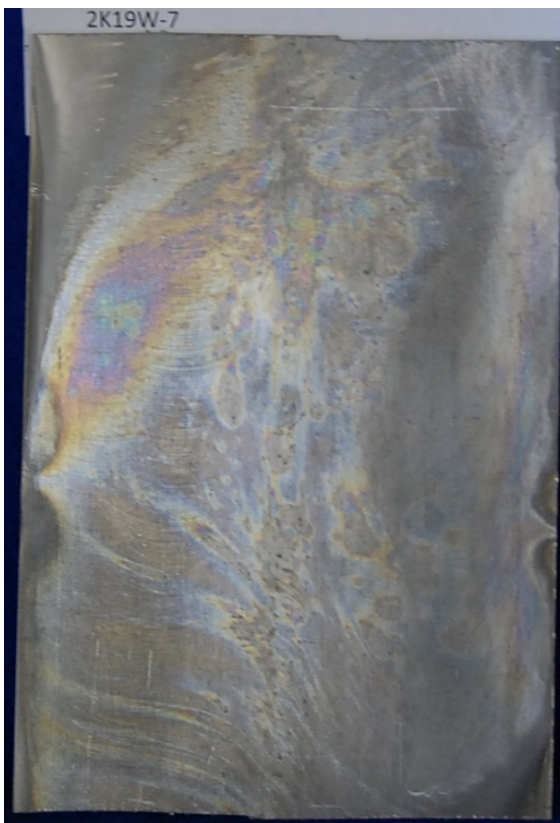
Front   Back

Sample ID: __2K19W__ - __11__
                 (Panel #)   *(Section #)*

Region: __1__   **Module:** __B__

_____

	28	27	26	25	24	23	22	21	20	19	18	17	16
2M													
2L													
2K													
2J													
2H													
2G													
2F													
2E													
2D													
2C													
2B													
2A													
	28	27	26	25	24	23	22	21	20	19	18	17	16
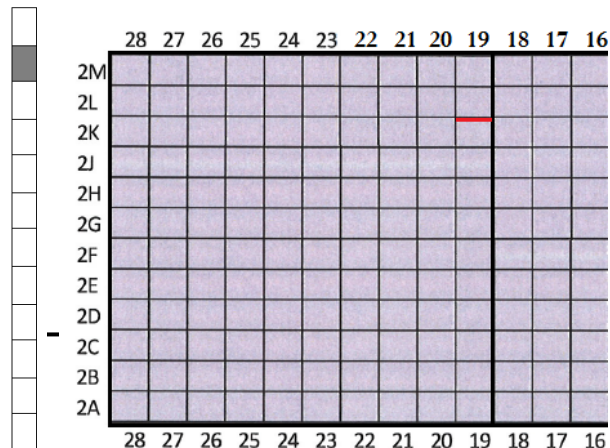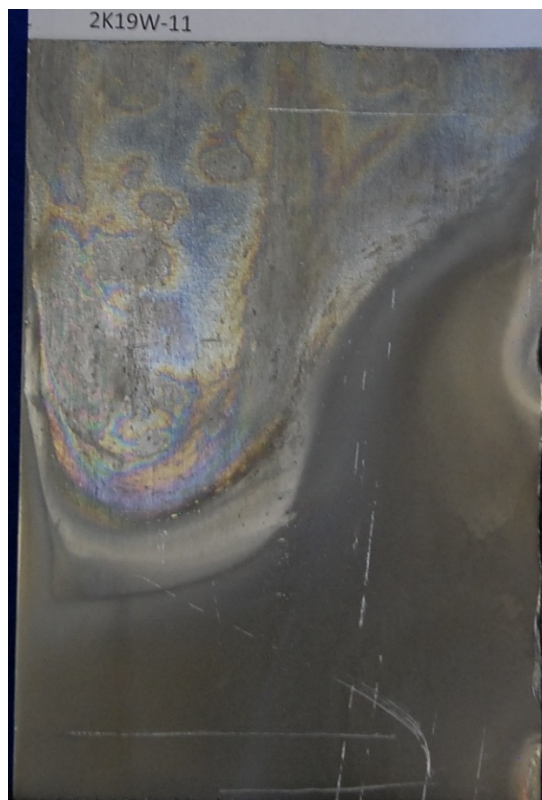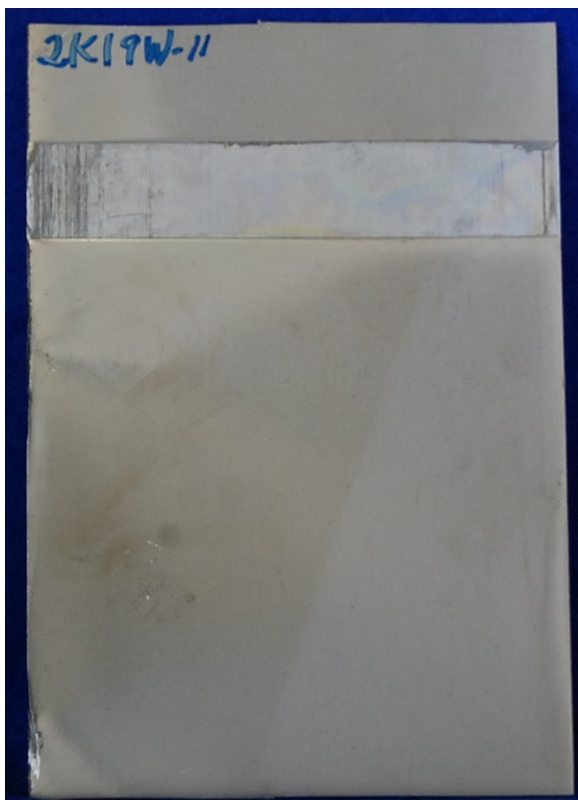
Front   Back

PANEL: **2J19N**

Region: 1   **Module: B**

FRONT   BACK

(TOP)

Highest Radiological Conditions
Occur in Section: 12
Maximum Dose: 1 [mrem/hr]
Maximum Probe
  (α) : ND [cpm/100cm^2]
  (β/γ) : 7,000 [cpm/100cm^2]

Maximum Smear
  (α) : ND [cpm/100cm^2]
  (β/γ) : 5,000 [cpm/100cm^2]

(Bottom)
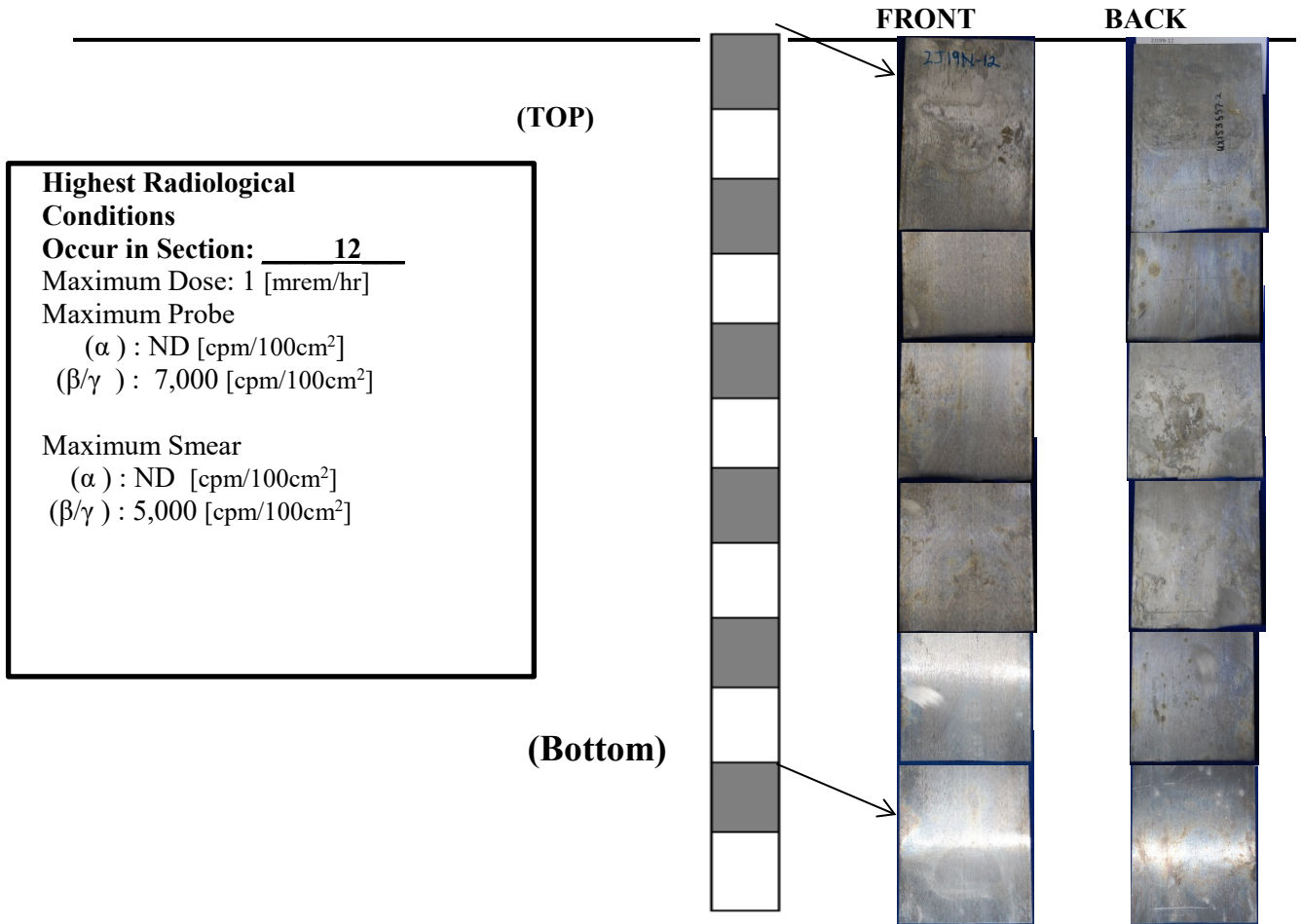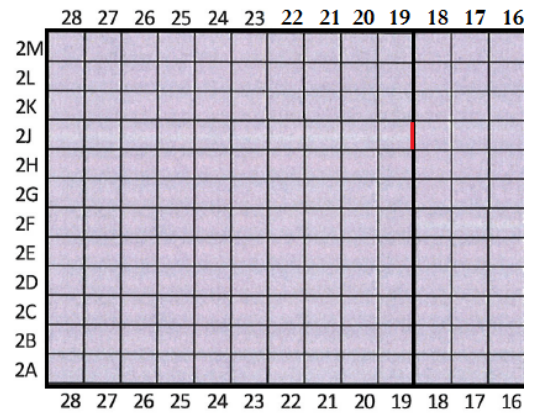
Sample ID: **2J19N** - **2**

(Panel #)   (Section #)

Region: **1**   **Module:** **B**

	28	27	26	25	24	23	22	21	20	19	18	17	16
2M													
2L													
2K													
2J													
2H													
2G													
2F													
2E													
2D													
2C													
2B													
2A													
	28	27	26	25	24	23	22	21	20	19	18	17	16
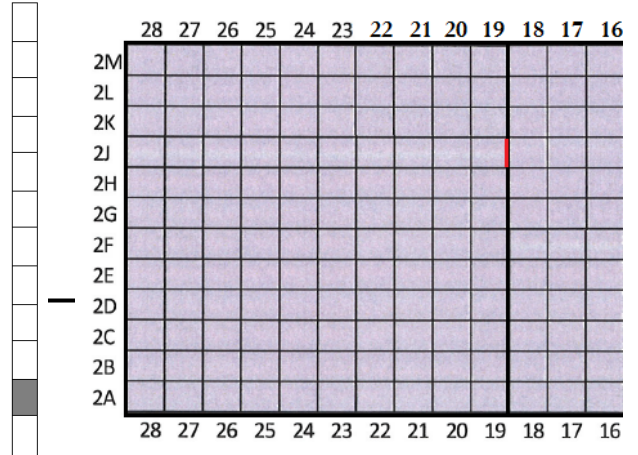
Front

Back

Sample ID: __2J19N__ - __4__
(Panel #)   (Section #)

Region: __1__   **Module:** __B__

	28	27	26	25	24	23	22	21	20	19	18	17	16
2M													
2L													
2K													
2J													
2H													
2G													
2F													
2E													
2D													
2C													
2B													
2A													
	28	27	26	25	24	23	22	21	20	19	18	17	16
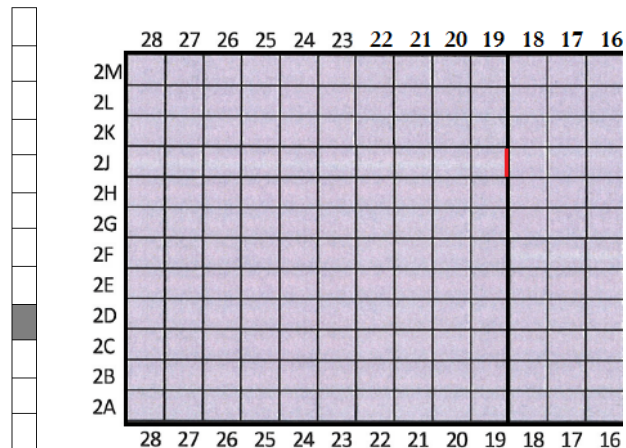
Front

Back

Sample ID: __2J19N__ - __6__
(Panel #)   *(Section #)*

Region: __1__   **Module:** __B__
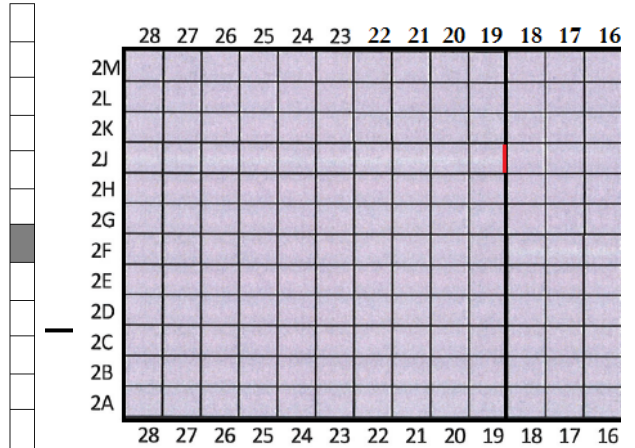
Front

Back

Sample ID: __2J19N__ - __8__

(Panel #)   *(Section #)*

Region: __1__   **Module:** __B__

	28	27	26	25	24	23	22	21	20	19	18	17	16
2M													
2L													
2K													
2J													
2H													
2G													
2F													
2E													
2D													
2C													
2B													
2A													
	28	27	26	25	24	23	22	21	20	19	18	17	16
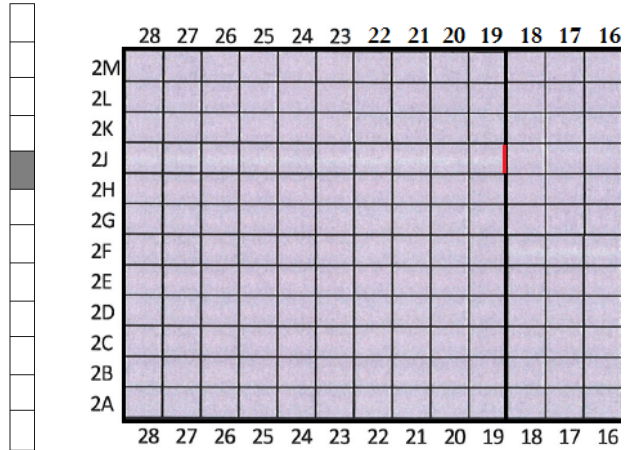
Front

Back

Sample ID: ___2J19N___ - ___10___
(Panel #)   *(Section #)*

Region: _1_   **Module:** _B_

	28	27	26	25	24	23	22	21	20	19	18	17	16
2M													
2L													
2K													
2J													
2H													
2G													
2F													
2E													
2D													
2C													
2B													
2A													
	28	27	26	25	24	23	22	21	20	19	18	17	16
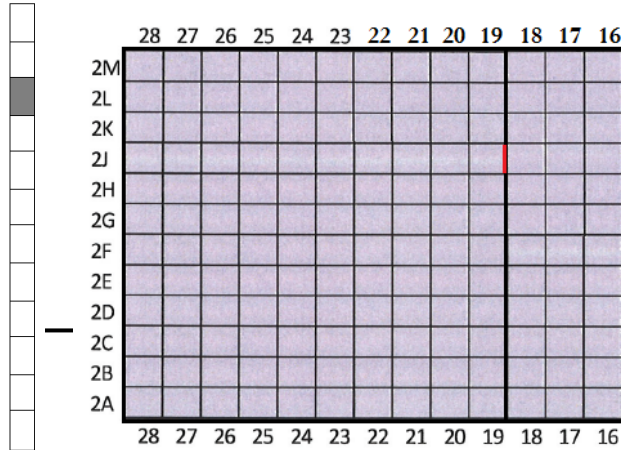
Front

Back

Sample ID: __2J19N__ - __12__
(Panel #) *(Section #)*

Region: __1__   **Module:** __B__

	28	27	26	25	24	23	22	21	20	19	18	17	16
2M													
2L													
2K													
2J													
2H													
2G													
2F													
2E													
2D													
2C													
2B													
2A													
	28	27	26	25	24	23	22	21	20	19	18	17	16
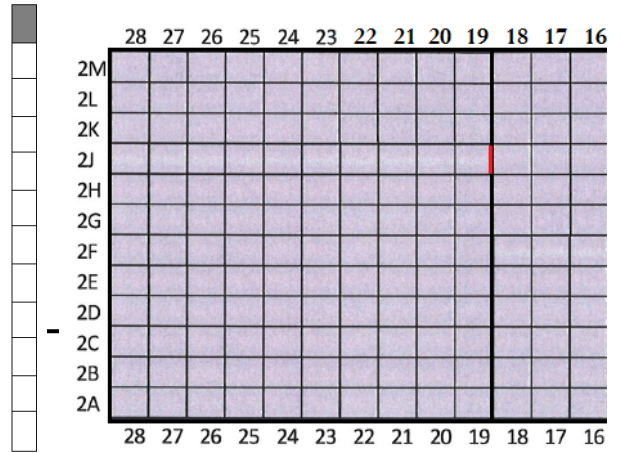
Front   Back

PANEL: <u>**2K21N**</u>

Region: <u>1</u>   **Module:** <u>B</u>
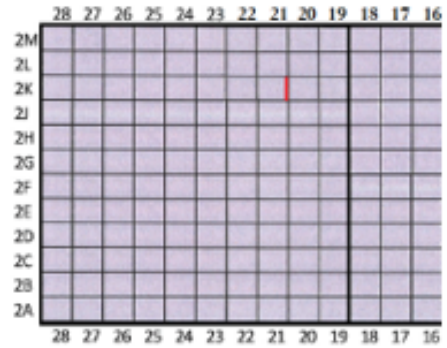
(TOP)

**Highest Radiological Conditions
Occur in Section:** _____11_____

Maximum Dose: 1.5 [mrem/hr]

Maximum Probe
  (α) : 1000 [cpm/100cm^2]
  (β/γ) : 300,000 [cpm/100cm^2]

Maximum Smear
  (α) : ND [cpm/100cm^2]
  (β/γ) : 40,000 [cpm/100cm^2]

FRONT   BACK

(Bottom)
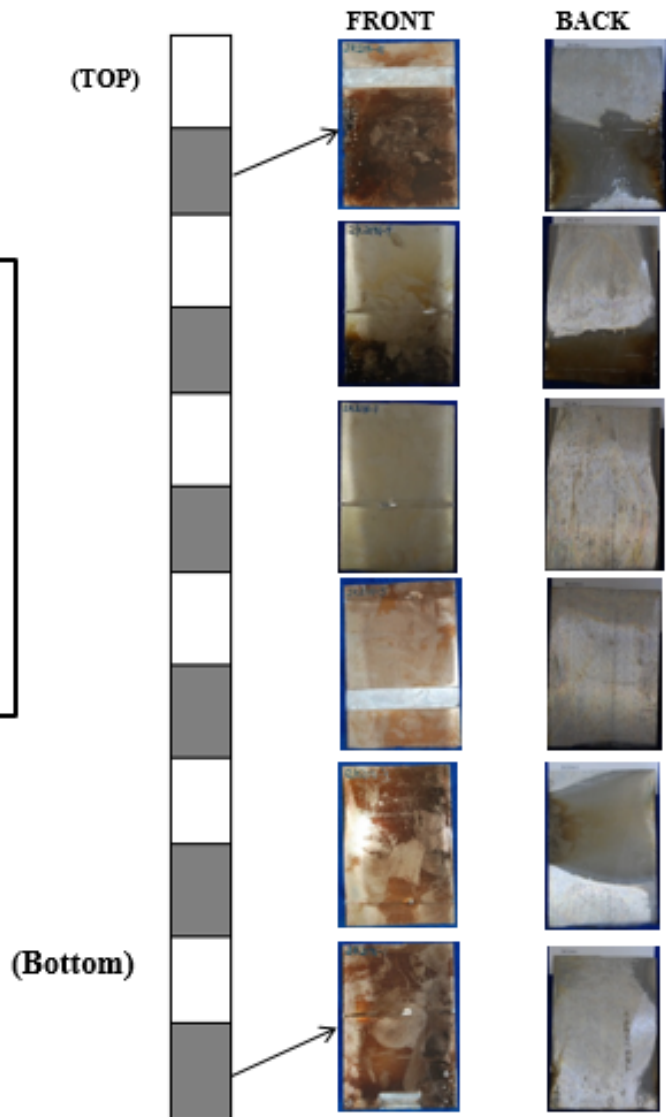
Sample ID: __2K21N__ - __1__
    (Panel #)   *(Section #)*

Region: __1__   **Module:** __B__

	28	27	26	25	24	23	22	21	20	19	18	17	16
2M													
2L													
2K													
2J													
2H													
2G													
2F													
2E													
2D													
2C													
2B													
2A													
	28	27	26	25	24	23	22	21	20	19	18	17	16

Front

Back

Sample ID: __2K21N__ - __3__

(Panel #)   *(Section #)*

Region: __1__   **Module:** __B__

	28	27	26	25	24	23	22	21	20	19	18	17	16
2M													
2L													
2K													
2J													
2H													
2G													
2F													
2E													
2D													
2C													
2B													
2A													
	28	27	26	25	24	23	22	21	20	19	18	17	16
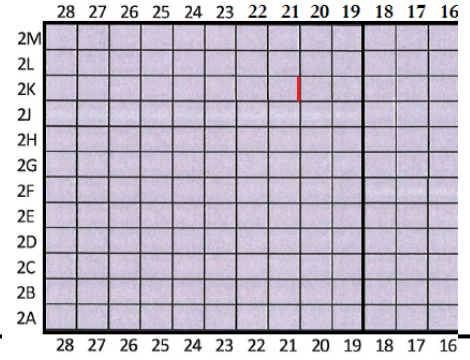
Front

Back

Sample ID: __2K21N__ - __5__
(Panel #)   *(Section #)*

Region: __1__   **Module:** __B__
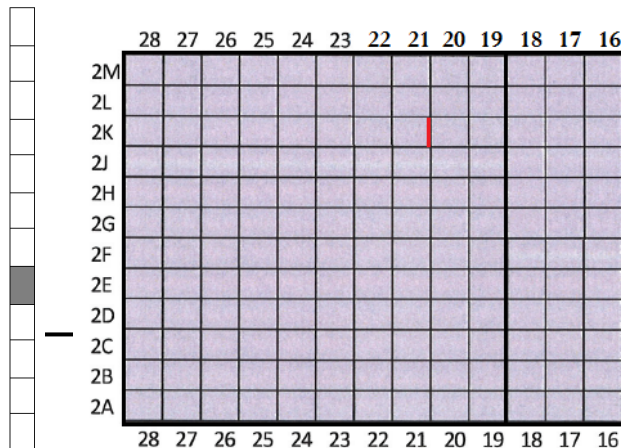
Front
Back

Sample ID: __2K21N__ - __7__
(Panel #)   *(Section #)*

Region: __1__   **Module:** __B__

	28	27	26	25	24	23	22	21	20	19	18	17	16
2M													
2L													
2K													
2J													
2H													
2G													
2F													
2E													
2D													
2C													
2B													
2A													
	28	27	26	25	24	23	22	21	20	19	18	17	16
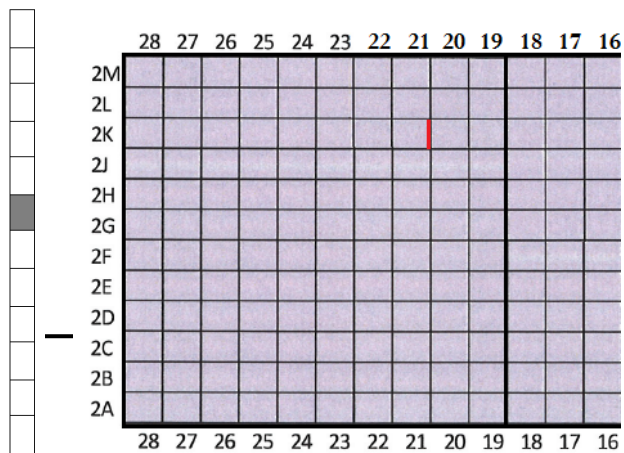
Front

Back

Sample ID: <u>**2K21N**</u> - <u>**9**</u>
(Panel #)   *(Section #)*

Region: <u>1</u>   **Module:** <u>B</u>

	28	27	26	25	24	23	22	21	20	19	18	17	16
2M													
2L													
2K													
2J													
2H													
2G													
2F													
2E													
2D													
2C													
2B													
2A													
	28	27	26	25	24	23	22	21	20	19	18	17	16
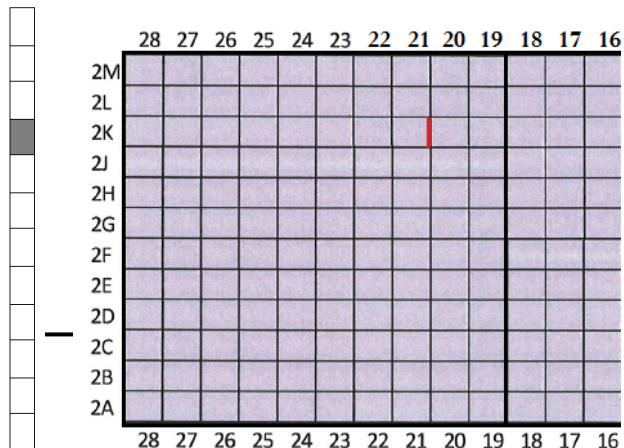
Front

Back

2K21N-9

Sample ID: __2K21N__ - __11__
(Panel #)   *(Section #)*

Region: __1__   **Module:** __B__

	28	27	26	25	24	23	22	21	20	19	18	17	16
2M													
2L													
2K													
2J													
2H													
2G													
2F													
2E													
2D													
2C													
2B													
2A													
	28	27	26	25	24	23	22	21	20	19	18	17	16
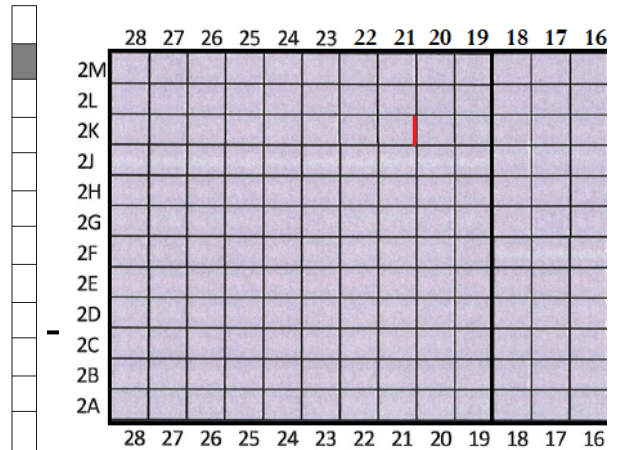
Front

Back

PANEL: __2K20S__

Region: __1__   **Module:** __B__

FRONT   BACK

(TOP)

Highest Radiological Conditions Occur in Section: ___10___

Maximum Dose: 1.5 [mrem/hr]

Maximum Probe
   (α) : 200 [cpm/100cm^2]
   (β/γ) : 180,000 [cpm/100cm^2]

Maximum Smear
   (α) : ND [cpm/100cm^2]
   (β/γ) : 10,000 [cpm/100cm^2]

(Bottom)
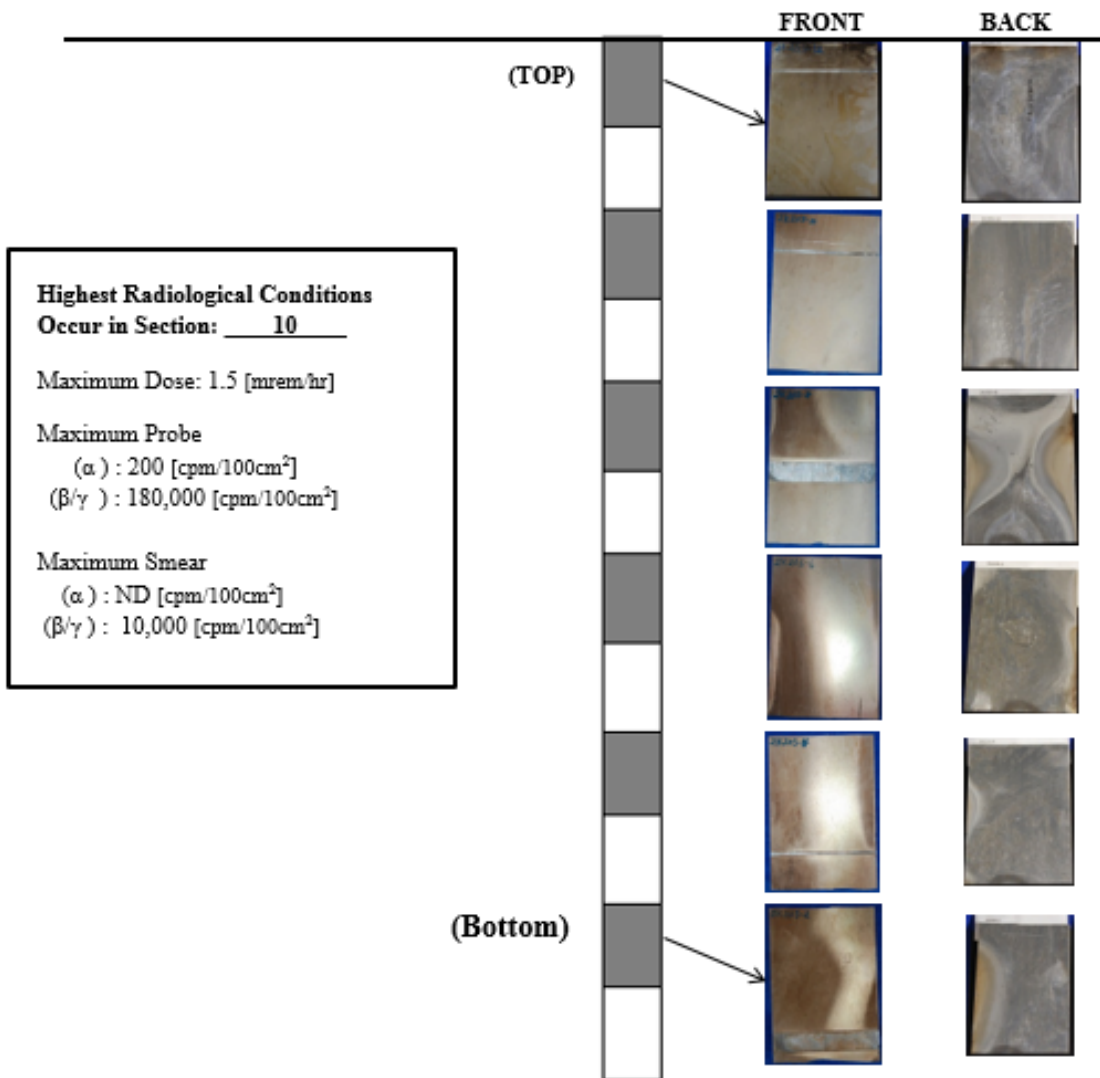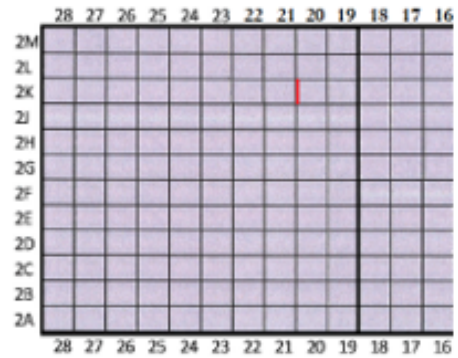
Sample ID: __2K20S__ - __2__
　　　　　　　(Panel #) 　　*(Section #)*

Region: __1__ 　　**Module:** __B__
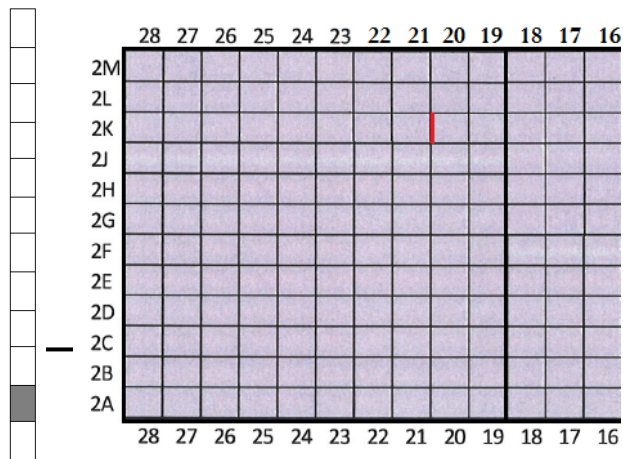
Front　　　　　　**Back**

Sample ID: __2K20S__ - __4__
(Panel #)   (Section #)

Region: __1__   **Module:** __B__

	28	27	26	25	24	23	22	21	20	19	18	17	16
2M													
2L													
2K													
2J													
2H													
2G													
2F													
2E													
2D													
2C													
2B													
2A													
	28	27	26	25	24	23	22	21	20	19	18	17	16
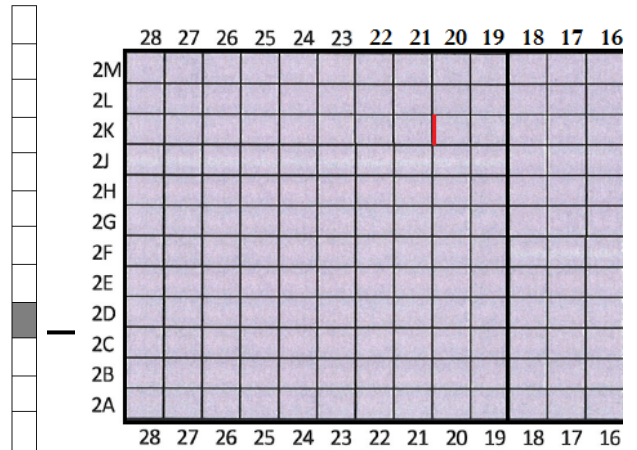
Front

Back

Sample ID: __2K20S__ - __6__
(Panel #)   (Section #)

Region: __1__   **Module:** __B__
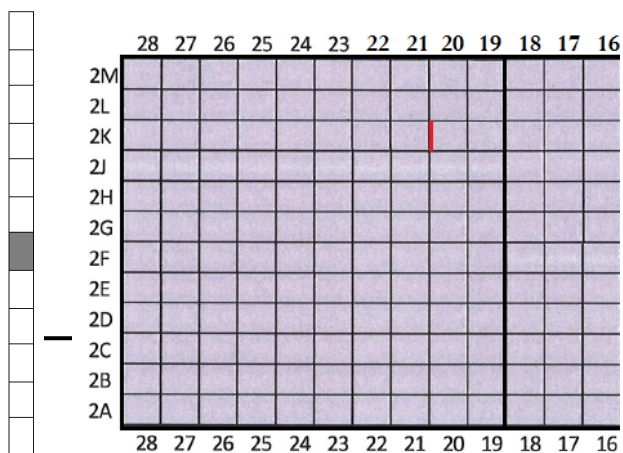
Front

Back

Sample ID: __2K20S__ - __8__

(Panel #)   (Section #)

Region: __1__   **Module:** __B__

	28	27	26	25	24	23	22	21	20	19	18	17	16
2M													
2L													
2K													
2J													
2H													
2G													
2F													
2E													
2D													
2C													
2B													
2A													
	28	27	26	25	24	23	22	21	20	19	18	17	16
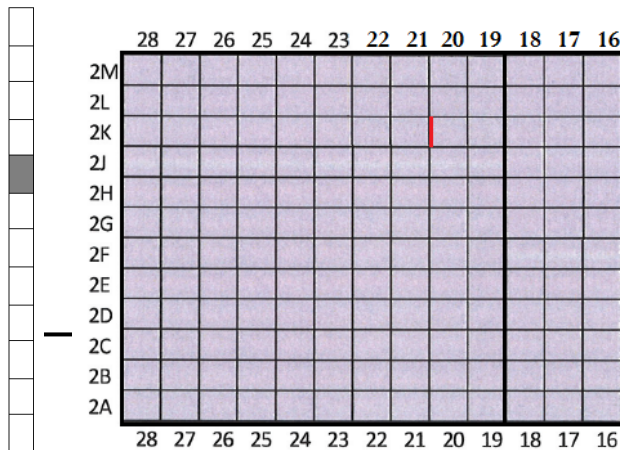
Front

Back

Sample ID: __2K20S__ - __10__
(Panel #)   *(Section #)*

Region: __1__   **Module:** __B__

	28	27	26	25	24	23	22	21	20	19	18	17	16
2M													
2L													
2K													
2J													
2H													
2G													
2F													
2E													
2D													
2C													
2B													
2A													

28 27 26 25 24 23 22 21 20 19 18 17 16
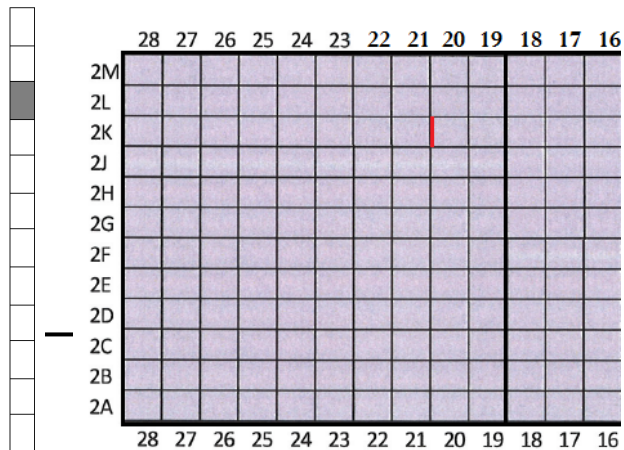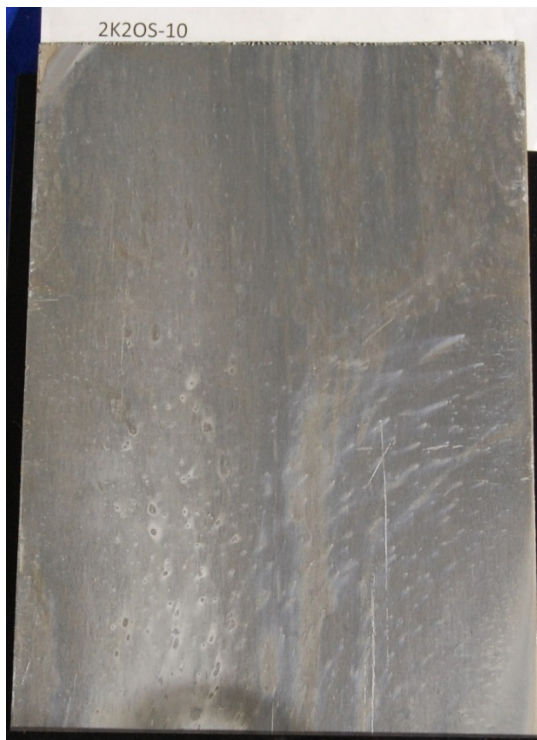
Front

Back

Sample ID: __2K20S__ - __12__
(Panel #)   *(Section #)*

Region: __1__   **Module:** __B__

Front

Back

	28	27	26	25	24	23	22	21	20	19	18	17	16
2M													
2L													
2K													
2J													
2H													
2G													
2F													
2E													
2D													
2C													
2B													
2A													
	28	27	26	25	24	23	22	21	20	19	18	17	16
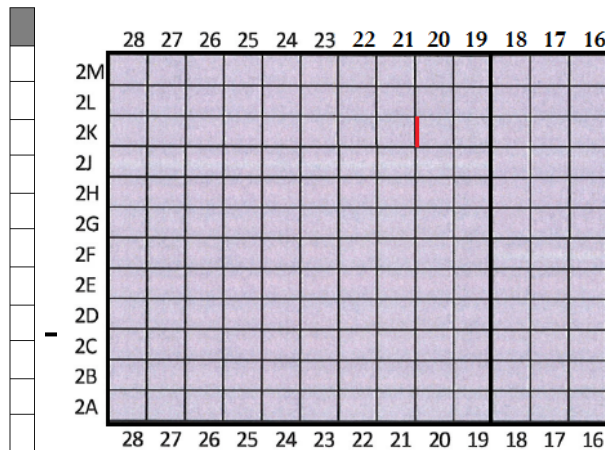
PANEL: __2L19S__

Region: __1__   **Module:** __B__

FRONT **BACK**

(TOP)
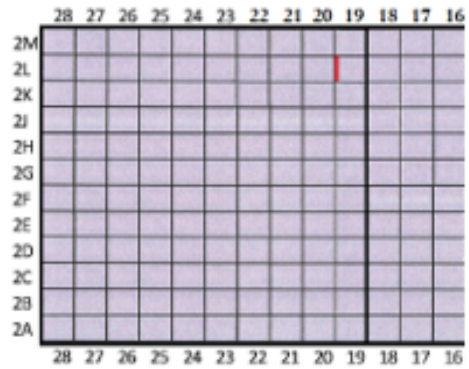
**Highest Radiological Conditions
Occur in Section:** _____10_____

Maximum Dose: 1 [mrem/hr]

Maximum Probe
   (α) : 250 [cpm/100cm^2]
 (β/γ) : 150,000 [cpm/100cm^2]

Maximum Smear
   (α) : ND [cpm/100cm^2]
 (β/γ) : 40,000 [cpm/100cm^2]

(Bottom)
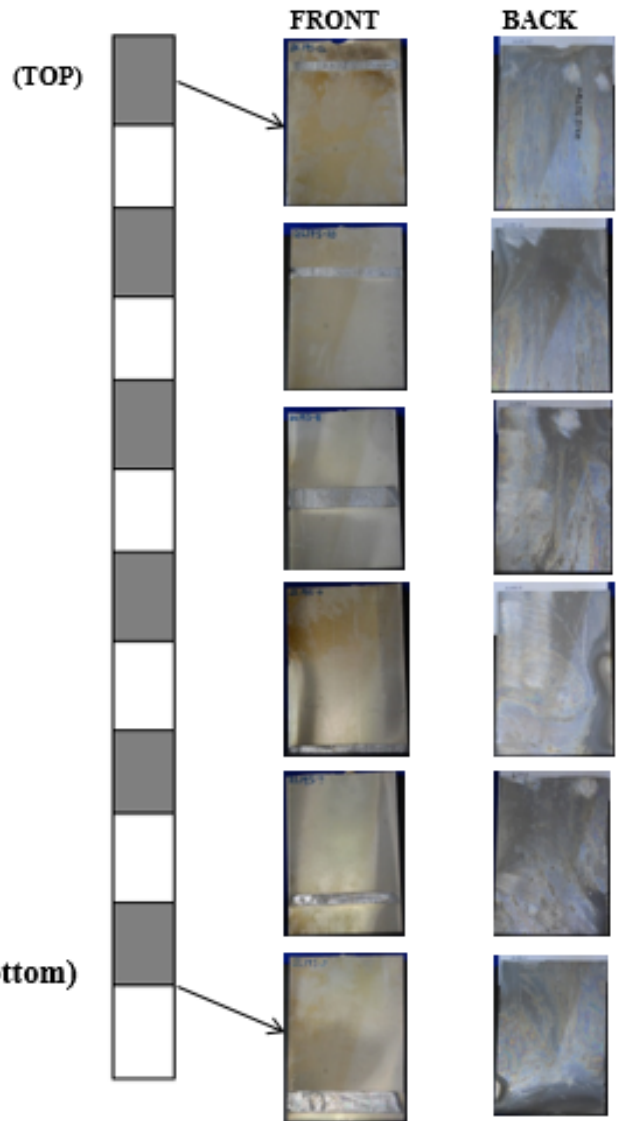
S

ample ID: ___**2L19S**___ - __**2**__

(Panel #)   (Section #)

Region: __1__   **Module:** __B__

_____

	28	27	26	25	24	23	22	21	20	19	18	17	16
2M													
2L													
2K													
2J													
2H													
2G													
2F													
2E													
2D													
2C													
2B													
2A													
	28	27	26	25	24	23	22	21	20	19	18	17	16
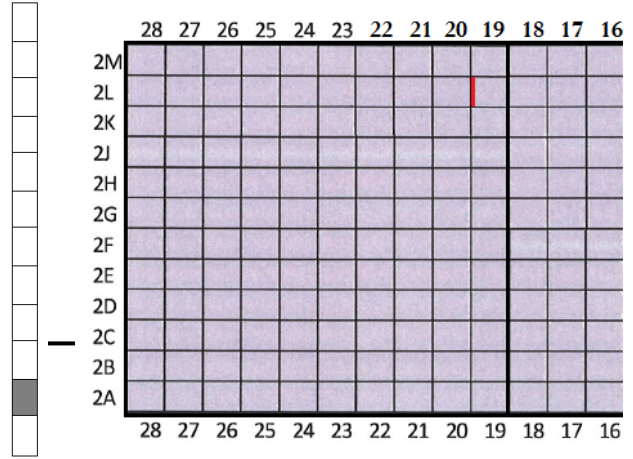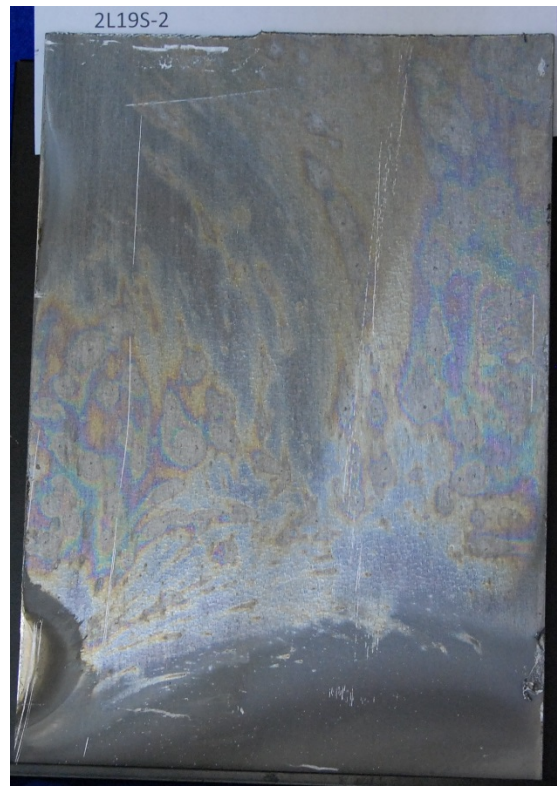
Front   # Back

Sample ID: ___2L19S___ - __4__

(Panel #)   (Section #)
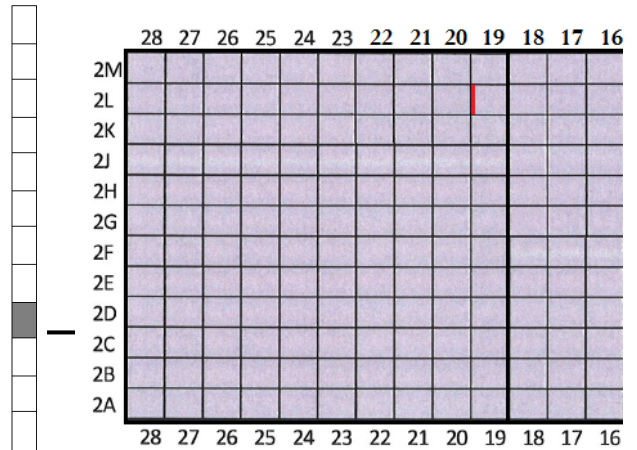
Region: _1_   **Module:** _B_
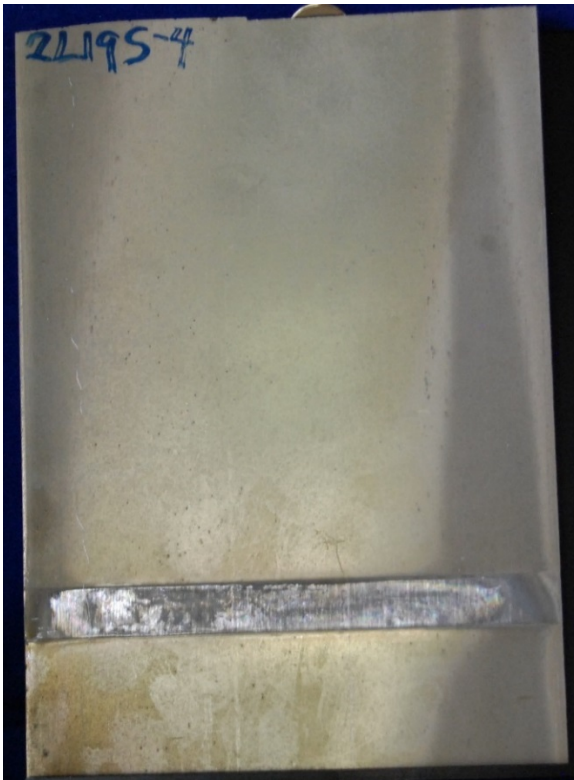
Front

Back

Sample ID: __2L19S__ - __6__
(Panel #)   *(Section #)*
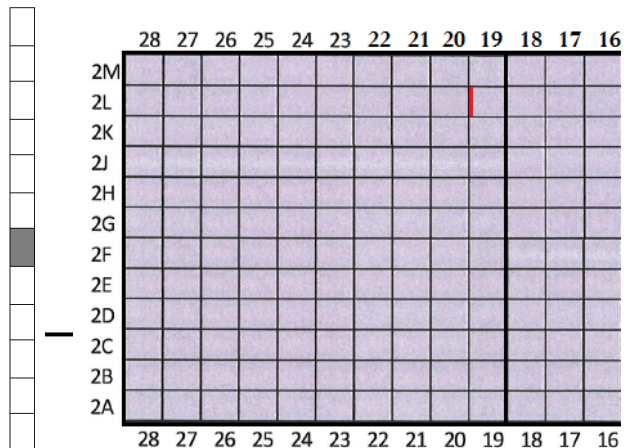
Region: __1__   **Module:** __B__
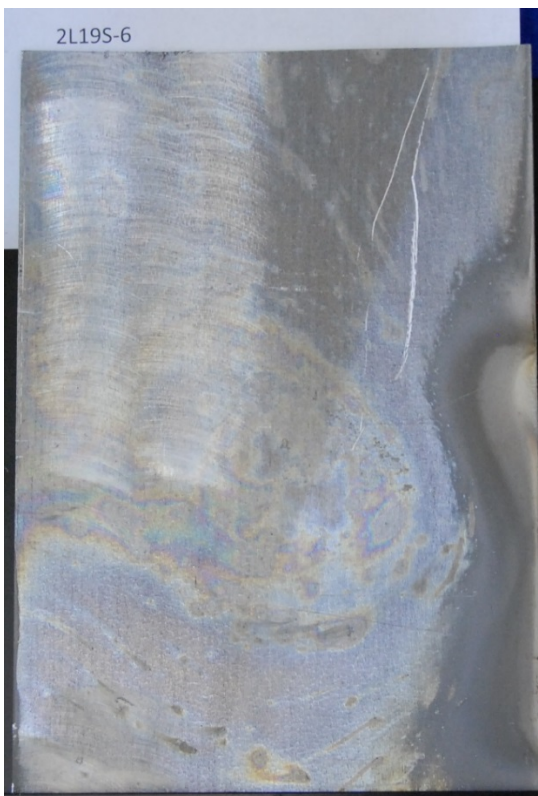
Front

Back

Sample ID: __2L19S__ - __8__

(Panel #) (Section #)
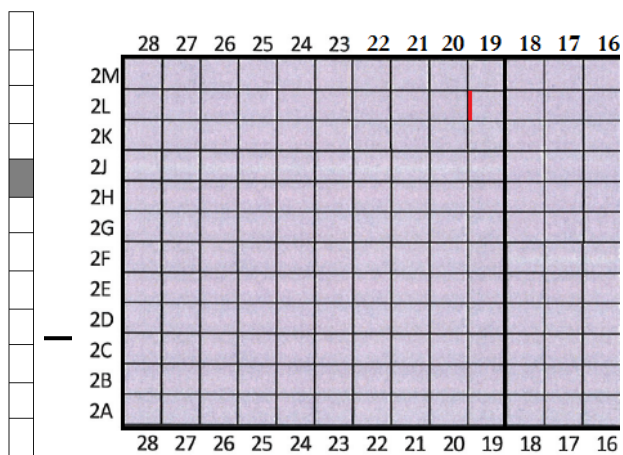
Region: __1__   **Module:** __B__
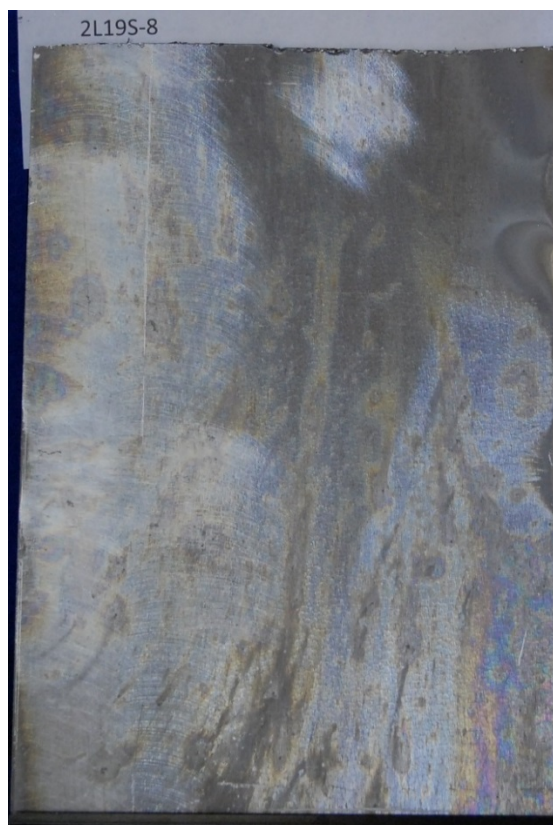
Front   Back

Sample ID: __2L19S__ - __10__
(Panel #)   (Section #)

Region: __1__   **Module:** __B__

	28	27	26	25	24	23	22	21	20	19	18	17	16
2M													
2L													
2K													
2J													
2H													
2G													
2F													
2E													
2D													
2C													
2B													
2A													
	28	27	26	25	24	23	22	21	20	19	18	17	16
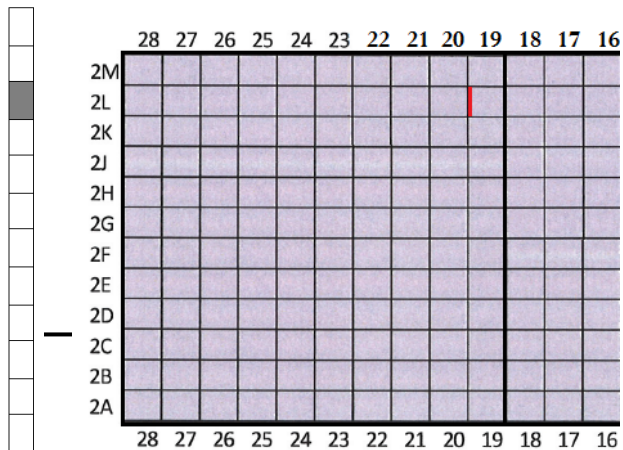
Front

Back

Back

Sample ID: <u>**2L19S**</u> - <u>**12**</u>
              (Panel #)   *(Section #)*
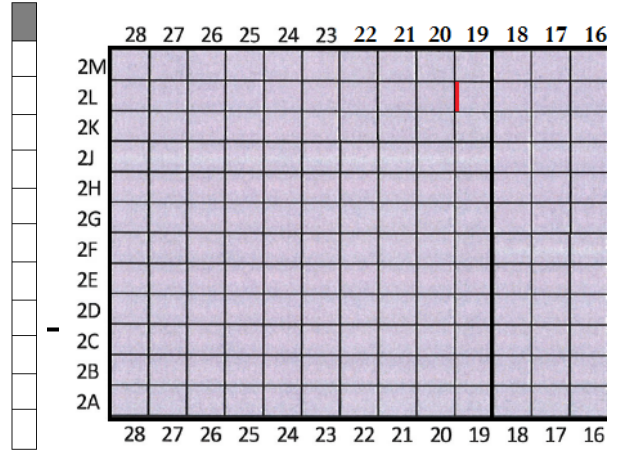
Region: <u>1</u>   **Module:** <u>B</u>

Front   Back

PANEL: **2L20N**

Region: 1   **Module:** B
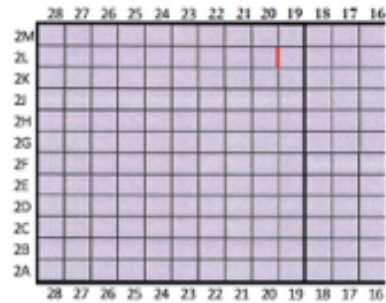
Highest Radiological Conditions Occur in Section: _____11_____

Maximum Dose: 1.5 [mrem/hr]

Maximum Probe
   (α) : 250 [cpm/100cm^2]
 (β/γ) : 100,000 [cpm/100cm^2]

Maximum Smear
   (α) : ND [cpm/100cm^2]
 (β/γ) : 12,000 [cpm/100cm^2]

(TOP)

FRONT   BACK

(Bottom)

Sample ID: __2L20N__ - __1__
(Panel #)   *(Section #)*

Region: __1__   **Module:** __B__

	28	27	26	25	24	23	22	21	20	19	18	17	16
2M													
2L													
2K													
2J													
2H													
2G													
2F													
2E													
2D													
2C													
2B													
2A													
	28	27	26	25	24	23	22	21	20	19	18	17	16
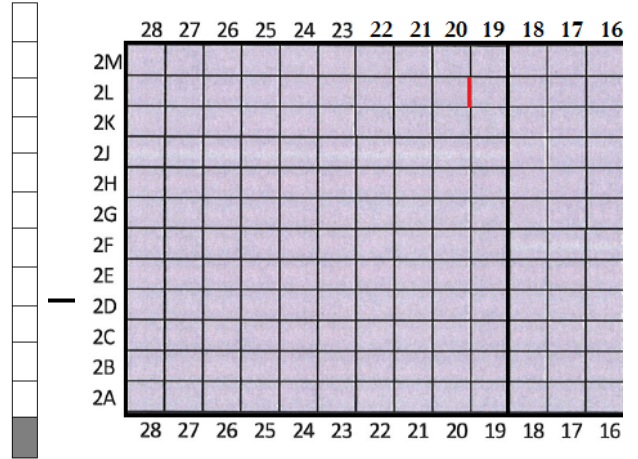
Front

Back

Sample ID: __2L20N__ - __3__
(Panel #)   *(Section #)*

Region: __1__   **Module:** __B__

	28	27	26	25	24	23	22	21	20	19	18	17	16
2M													
2L													
2K													
2J													
2H													
2G													
2F													
2E													
2D													
2C													
2B													
2A													
	28	27	26	25	24	23	22	21	20	19	18	17	16
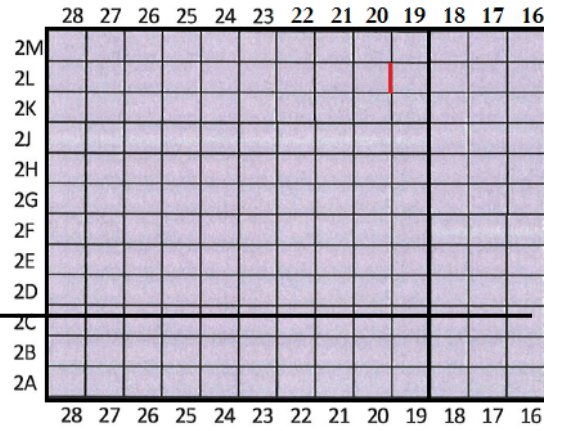
Front

Back

Sample ID: __2L20N__ - _5_

(Panel #)   (Section #)

Region: _1_   **Module:** _B_

	28	27	26	25	24	23	22	21	20	19	18	17	16
2M													
2L													
2K													
2J													
2H													
2G													
2F													
2E													
2D													
2C													
2B													
2A													
	28	27	26	25	24	23	22	21	20	19	18	17	16
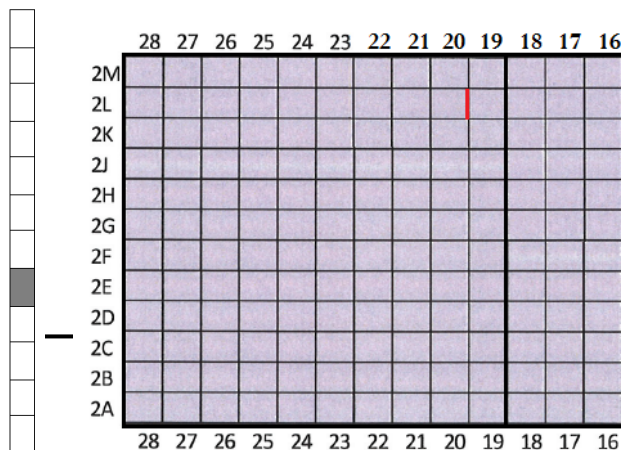
Front

Back

Sample ID: __2L20N__ - __7__
(Panel #)   *(Section #)*

Region: __1__   **Module:** __B__

	28	27	26	25	24	23	22	21	20	19	18	17	16
2M													
2L													
2K													
2J													
2H													
2G													
2F													
2E													
2D													
2C													
2B													
2A													
	28	27	26	25	24	23	22	21	20	19	18	17	16
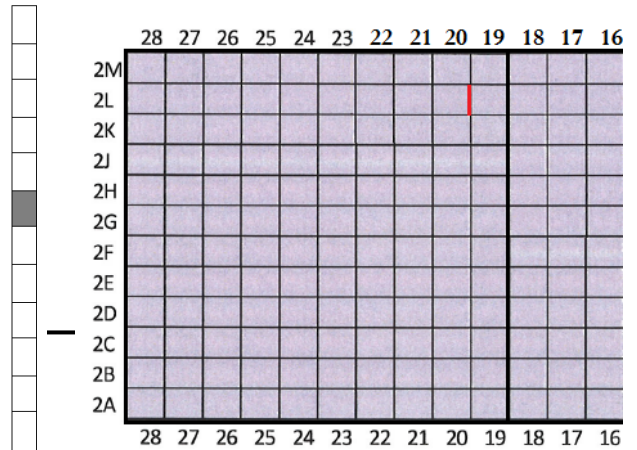
Front
Back

Sample ID: __2L20N__ - __9__
(Panel #)   (Section #)

Region: __1__   **Module:** __B__

	28	27	26	25	24	23	22	21	20	19	18	17	16
2M													
2L													
2K													
2J													
2H													
2G													
2F													
2E													
2D													
2C													
2B													
2A													
	28	27	26	25	24	23	22	21	20	19	18	17	16
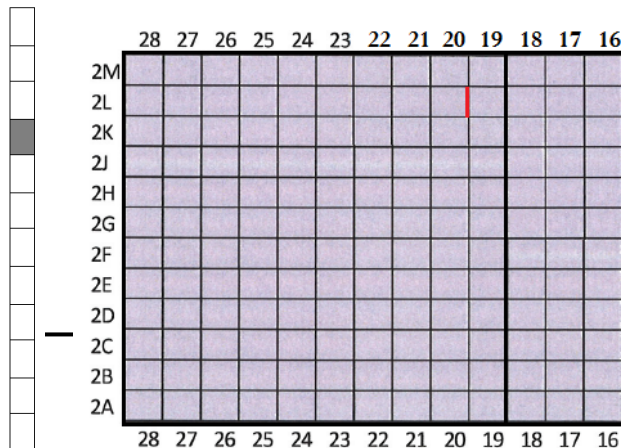
Front

Back

Sample ID: __2L20N__ - __11__
(Panel #)   *(Section #)*
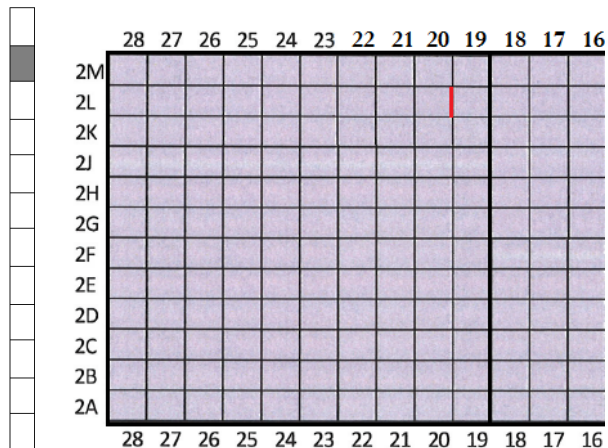
Region: __1__   **Module:** __B__
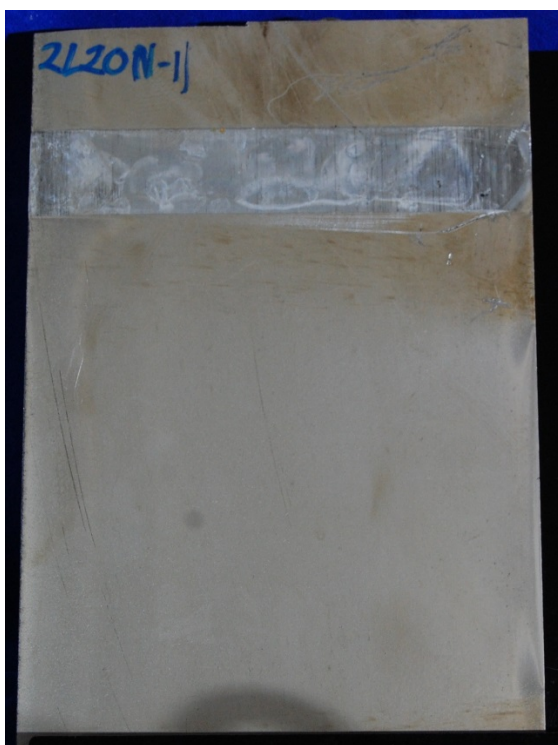
Front   Back

PANEL: **2L19E**

Region: __1__   Module: __B__
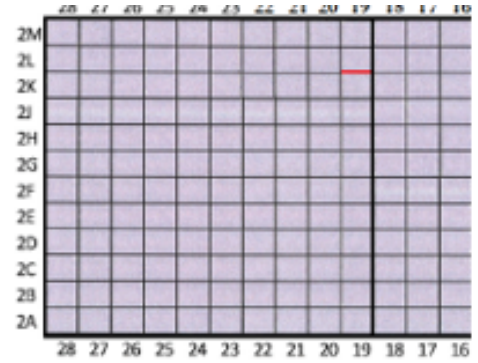
**Highest Radiological Conditions
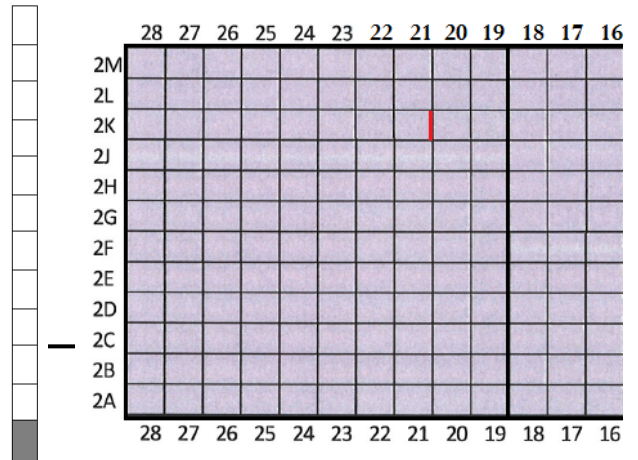Occur in Section:** _____12_____

Maximum Dose: 1 [mrem/hr]

Maximum Probe
 (α) : 200 [cpm/100cm²]
 (β/γ) : 200,000 [cpm/100cm²]

Maximum Smear
 (α) : ND [cpm/100cm²]
 (β/γ) : 30,000 [cpm/100cm²]

FRONT   BACK

(TOP)

(Bottom)

Sample ID: ___2L19E___ - __2__
(Panel #)   (Section #)

Region: __1__   **Module:** __B__

	28	27	26	25	24	23	22	21	20	19	18	17	16
2M													
2L													
2K													
2J													
2H													
2G													
2F													
2E													
2D													
2C													
2B													
2A													
	28	27	26	25	24	23	22	21	20	19	18	17	16
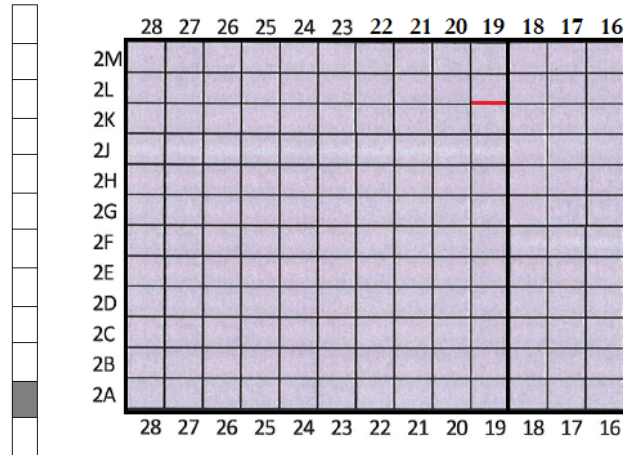
Front
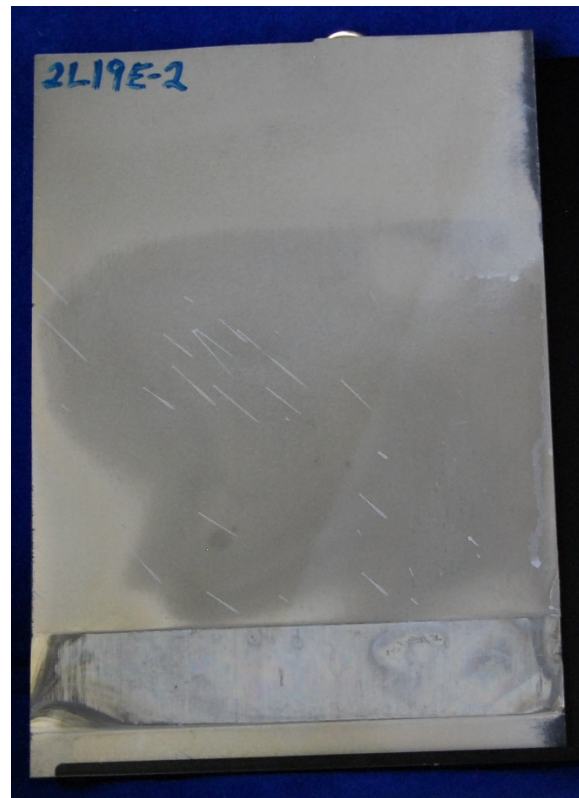
2L19E-2

Back

2L19E-2

Sample ID: __2L19E__ - __4__

(Panel #)　　　(Section #)
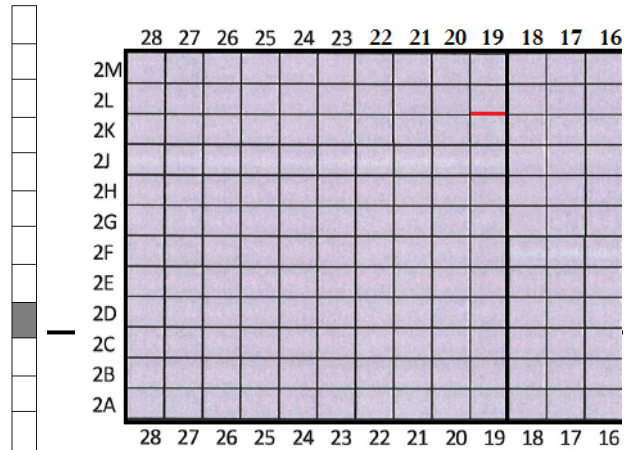
Region: __1__　　**Module:** __B__

Front

Back

Sample ID: __2L19E__ - __6__
(Panel #)   *(Section #)*
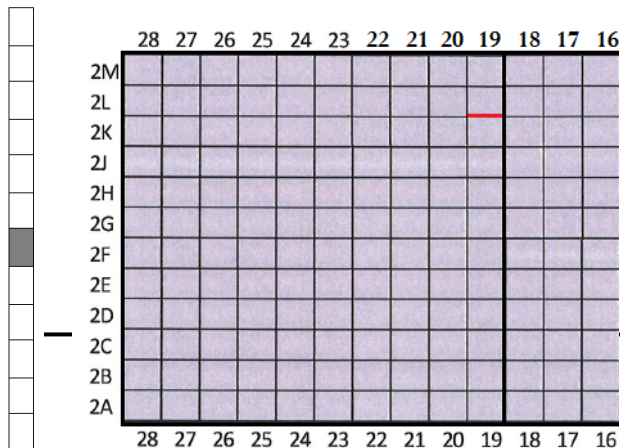
Region: __1__   **Module:** __B__

Front

Back

Sample ID: __2L19E__ - __8__
(Panel #)   *(Section #)*

Region: __1__   **Module:** __B__

	28	27	26	25	24	23	22	21	20	19	18	17	16
2M													
2L													
2K													
2J													
2H													
2G													
2F													
2E													
2D													
2C													
2B													
2A													
	28	27	26	25	24	23	22	21	20	19	18	17	16
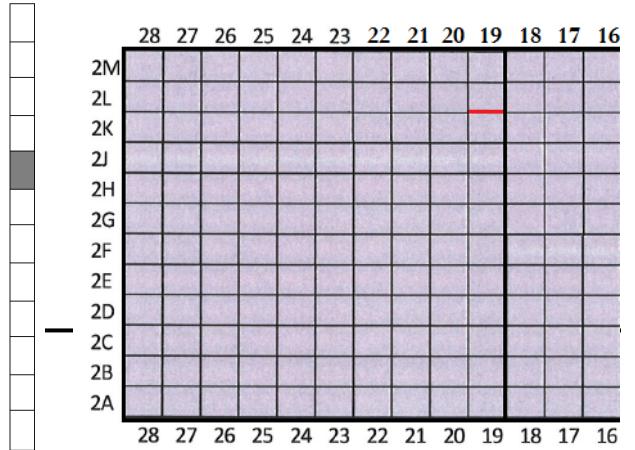
Front

Back

Sample ID: __2L19E__ - __10__
     (Panel #)   *(Section #)*

Region: __1__   **Module:** __B__

	28	27	26	25	24	23	22	21	20	19	18	17	16
2M													
2L													
2K													
2J													
2H													
2G													
2F													
2E													
2D													
2C													
2B													
2A													
	28	27	26	25	24	23	22	21	20	19	18	17	16
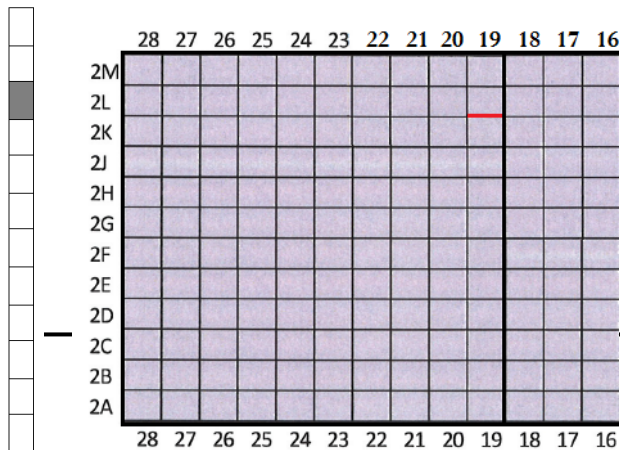
Front   Back

Sample ID: __2L19E__ - __12__
   (Panel #)   *(Section #)*
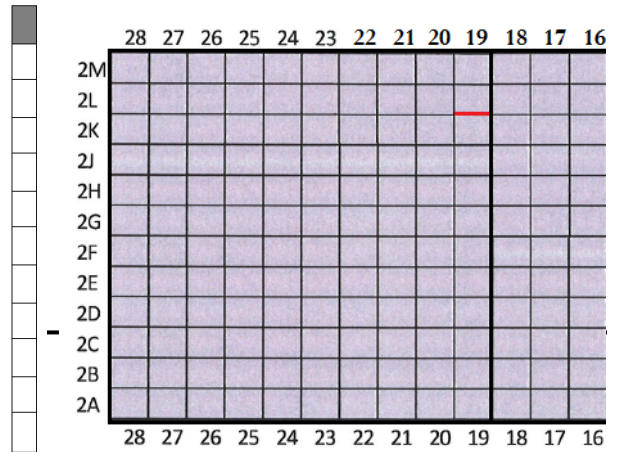
Region: __1__   **Module:** __B__

Front
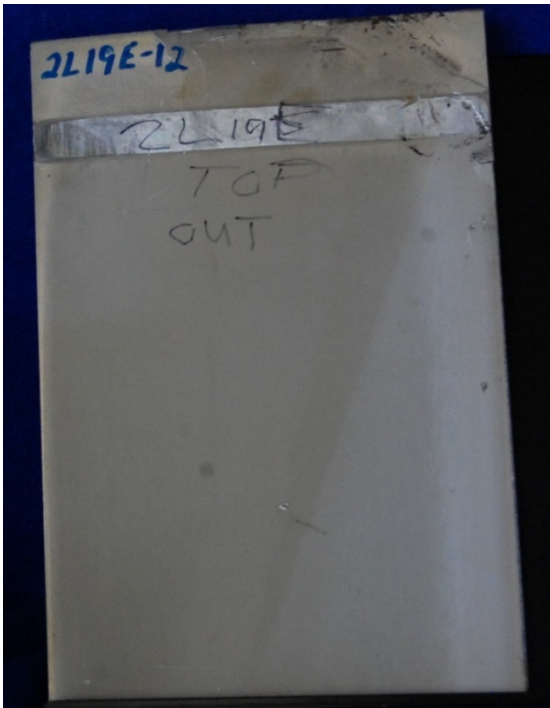
Back

PANEL: __5M12S__

Region: __2__ **Module:** __P__

(TOP)
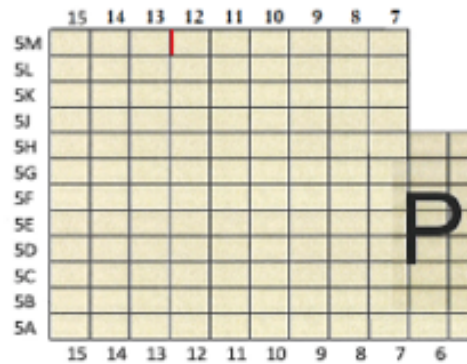
FRONT   BACK

Highest Radiological Conditions Occur in Section: ____11____

Maximum Dose: 1 [mrem/hr]

Maximum Probe
   (α) : ND [cpm/100cm^2]
   (β/γ) : 6,000 [cpm/100cm^2]

Maximum Smear
   (α) : ND [cpm/100cm^2]
   (β/γ) : 1,000 [cpm/100cm^2]

(Bottom)
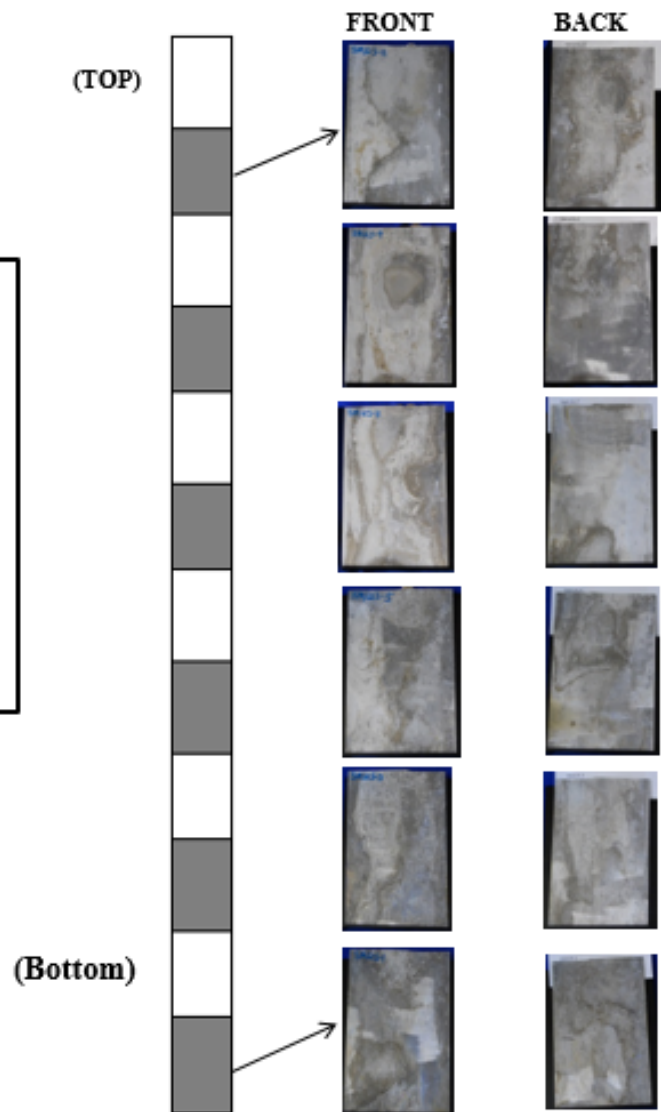
Sample ID: __5M12S__ - __1__

        (Panel #)   *(Section #)*

Region: __2__   **Module:** __P__
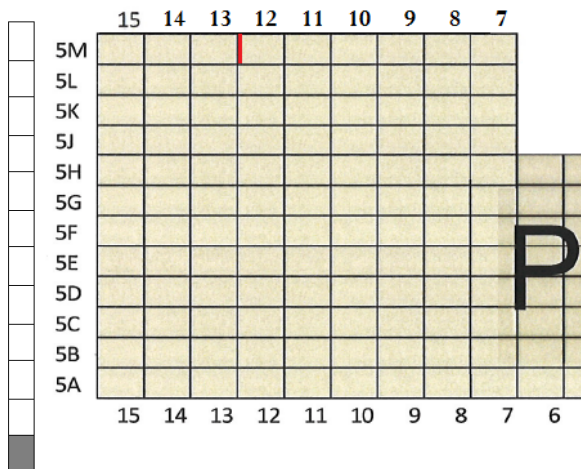
Front

Back

Sample ID: __5M12S__ - __3__

(Panel #)   *(Section #)*

Region: __2__   **Module:** __P__

	15	14	13	12	11	10	9	8	7	
5M										
5L										
5K										
5J										
5H										
5G										
5F										
5E										P
5D										
5C										
5B										
5A										
	15	14	13	12	11	10	9	8	7	6
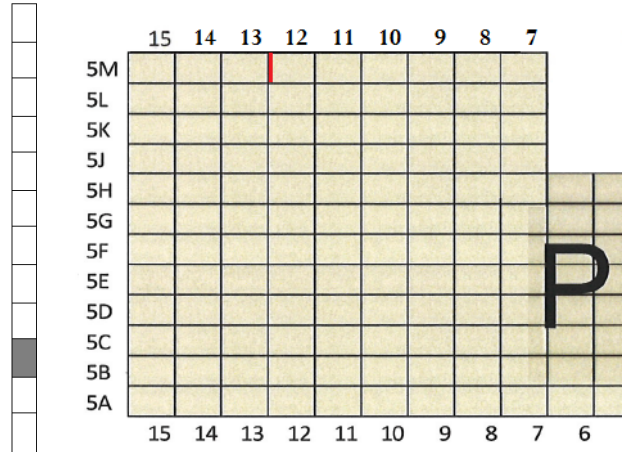
Front   Back

Sample ID: __5M12S__ - __5__

(Panel #)   *(Section #)*

Region: __2__   **Module:** __P__

	15	14	13	12	11	10	9	8	7	
5M										
5L										
5K										
5J										
5H										
5G										
5F										
5E										P
5D										
5C										
5B										
5A										
	15	14	13	12	11	10	9	8	7	6
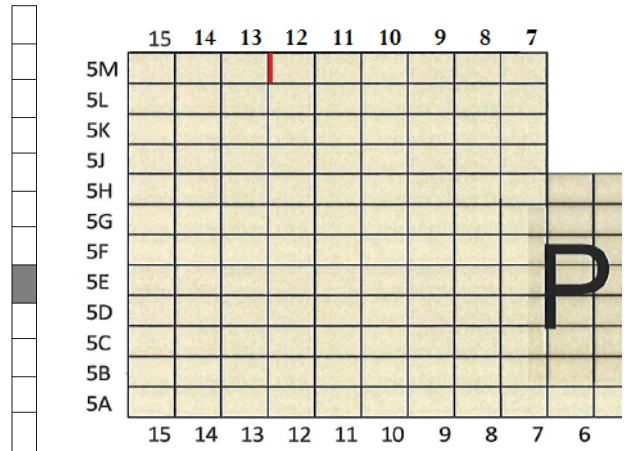
Front

Back

Sample ID: __5M12S__ - __7__

(Panel #)   *(Section #)*

Region: __2__   **Module:** __P__
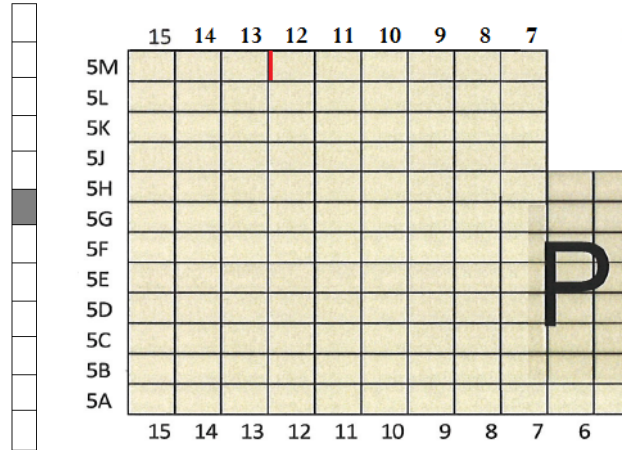
Front

Back

Sample ID: __5M12S__ - __9__
(Panel #) *(Section #)*

Region: __2__   **Module:** __P__
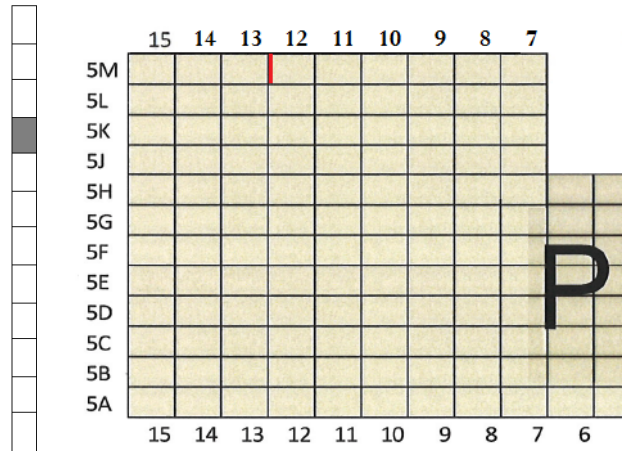
Front

Back

Sample ID: __5M12S__ - __11__
(Panel #)   (Section #)
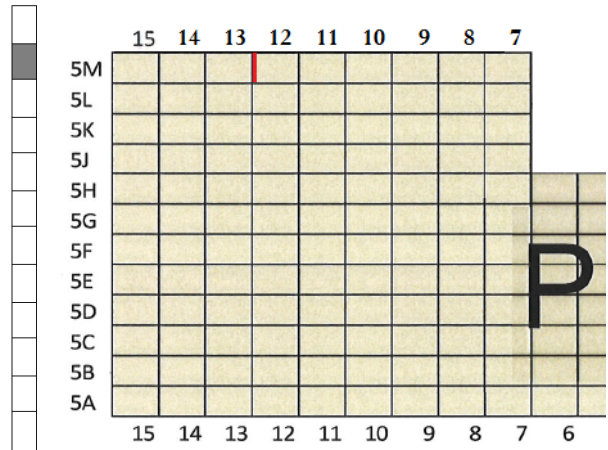
Region: __2__   **Module:** __P__

Front

Back

PANEL: **5L9S**

Region: **2**   **Module:** **P**

FRONT   BACK

(TOP)

**Highest Radiological Conditions
Occur in Section:** _____2_____

Maximum Dose: 1 [mrem/hr]

Maximum Probe
  (α) : ND [cpm/100cm²]
  (β/γ) : ND [cpm/100cm²]

Maximum Smear
  (α) : ND [cpm/100cm²]
  (β/γ) : ND [cpm/100cm²]

(Bottom)
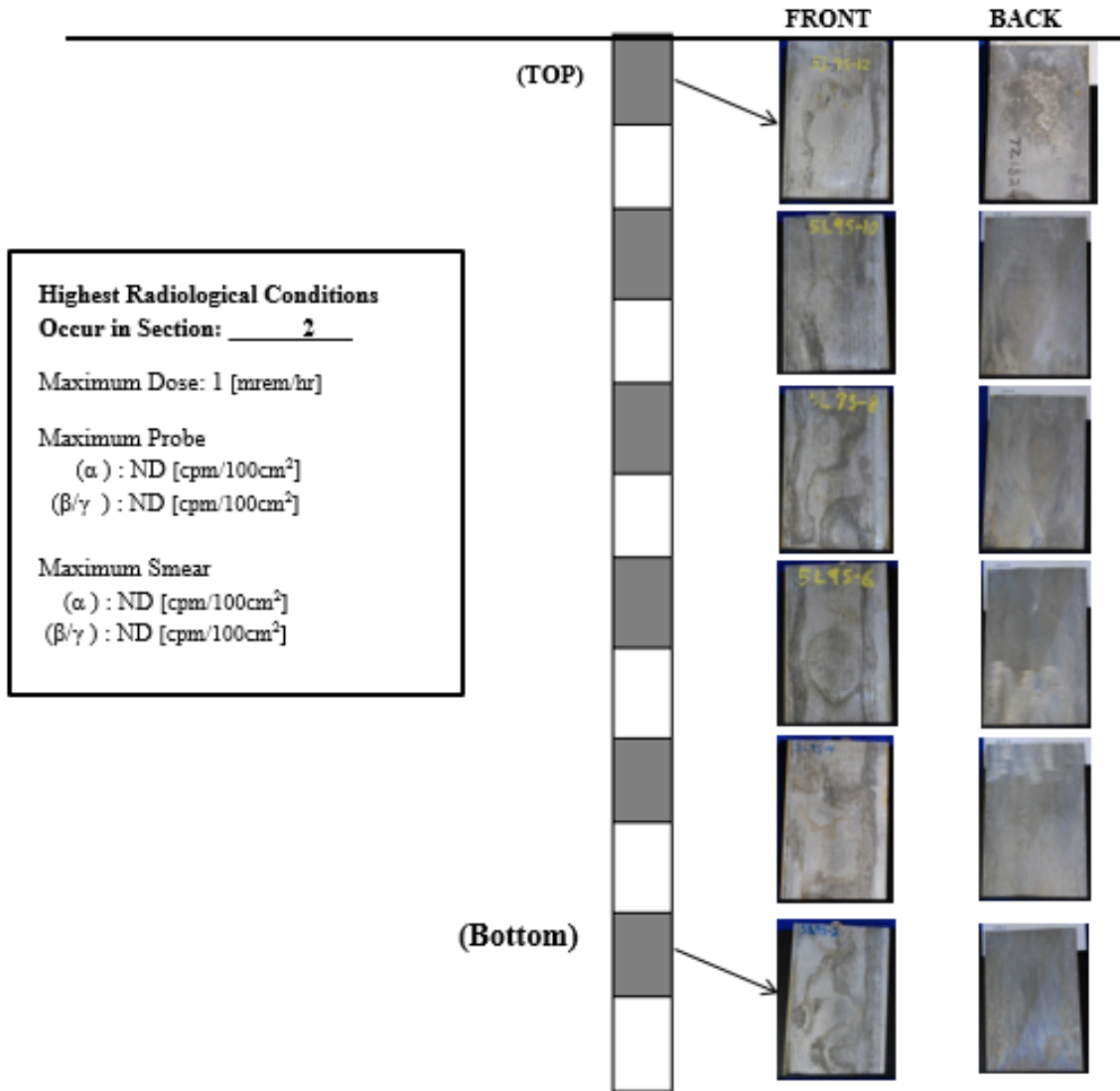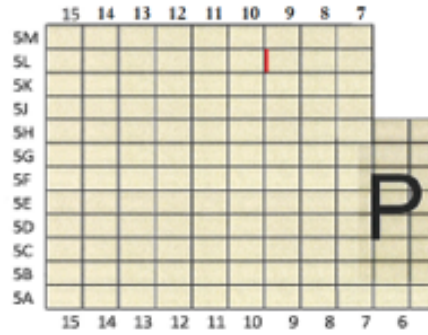
Sample ID: ___5L9S___ - _2_
(Panel #)   (Section #)
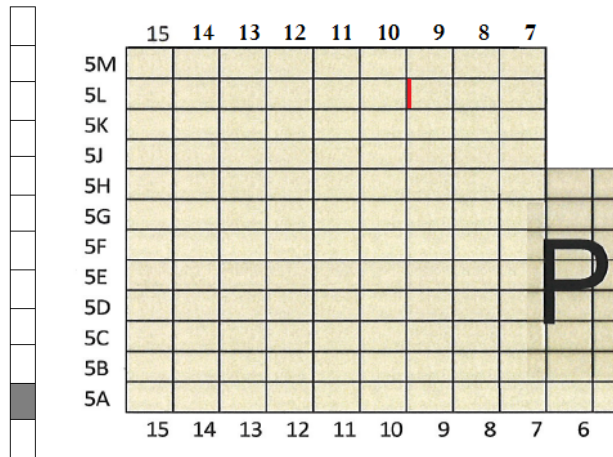
Region: _2_   **Module:** _P_

Front

Back

Sample ID: __5L9S__ - __4__
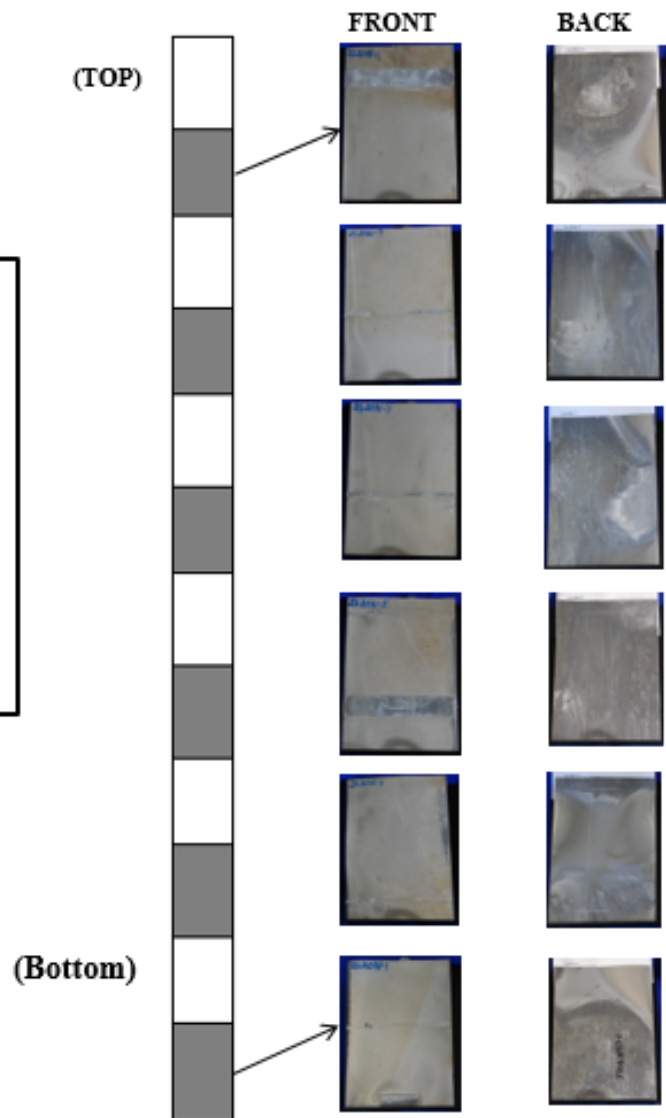(Panel #)　　(Section #)

Region: _2_　　**Module:** _P_

	15	14	13	12	11	10	9	8	7
5M									
5L									
5K									
5J									
5H									
5G									
5F									
5E									
5D									
5C									
5B									
5A									

P

Front

5L9S-4

Back

5L9S-4
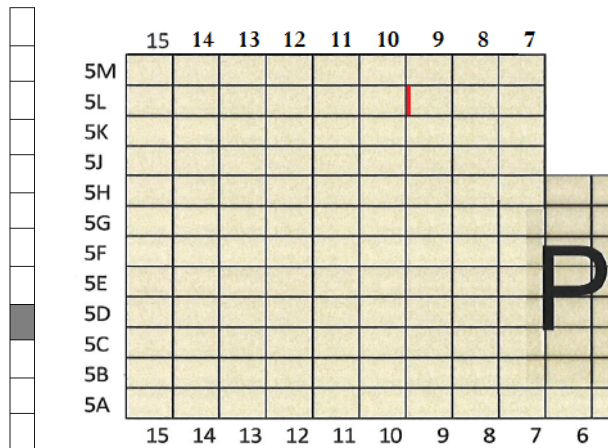
Sample ID: __5L9S__ - __6__
(Panel #)   (Section #)

Region: __2__   **Module:** __P__

	15	14	13	12	11	10	9	8	7	
5M										
5L										
5K										
5J										
5H										
5G										
5F										
5E										
5D										
5C										
5B										
5A										
	15	14	13	12	11	10	9	8	7	6

P

Front

Back

5L9S-6
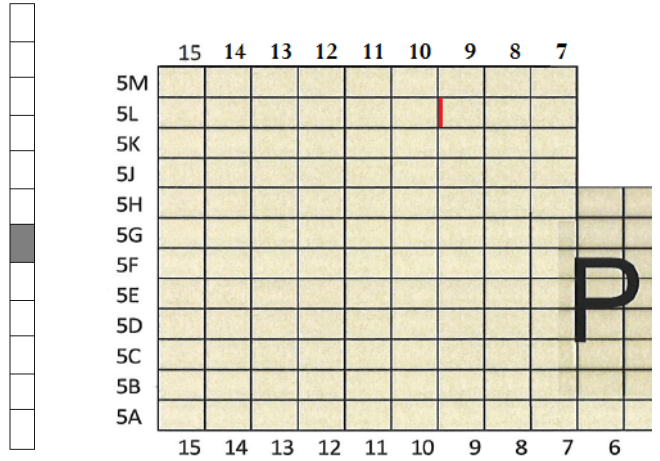
Sample ID: __5L9S__ - __8__
(Panel #)   *(Section #)*

Region: __2__   **Module:** __P__

	15	14	13	12	11	10	9	8	7
5M									
5L							I		
5K									
5J									
5H									
5G									
5F									
5E									
5D									
5C									
5B									
5A									

P
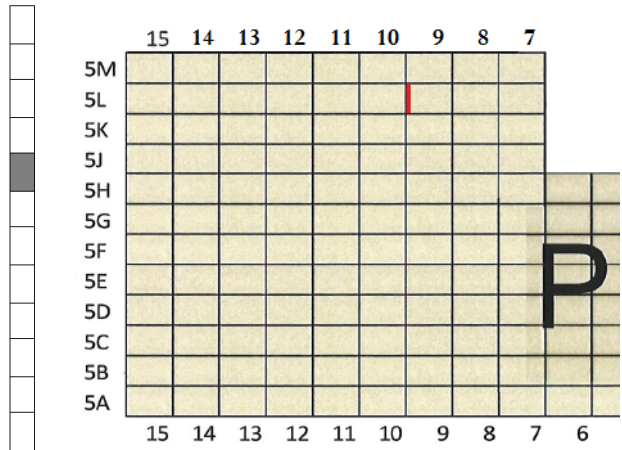
Front

Back

Sample ID: **5L9S** - **10**
(Panel #)   *(Section #)*
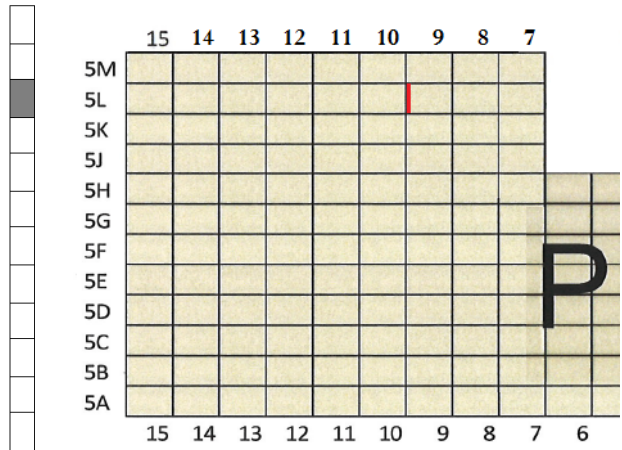
Region: **2**   **Module:** **P**

Front

Back

Sample ID: __5L9S__ - __12__
(Panel #)   (Section #)
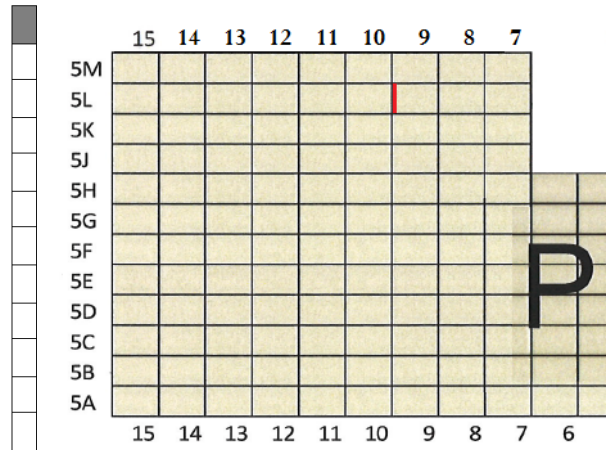
Region: _2_   **Module:** _P_

Front

Back

PANEL: **5M7S**

Region: **2**   **Module:** **P**

Highest Radiological Conditions Occur in Section: _____7_____

Maximum Dose: 1 [mrem/hr]

Maximum Probe
   (α) : ND [cpm/100cm^2]
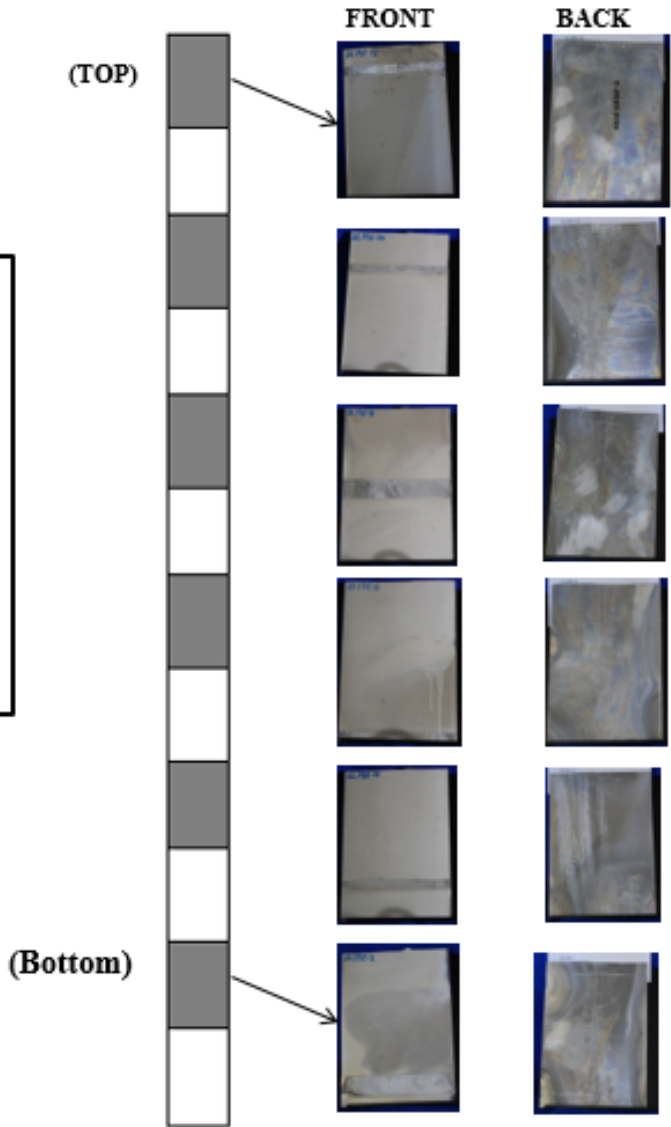   (β/γ) : ND [cpm/100cm^2]

Maximum Smear
   (α) : ND [cpm/100cm^2]
   (β/γ) : ND [cpm/100cm^2]

(TOP)

(Bottom)
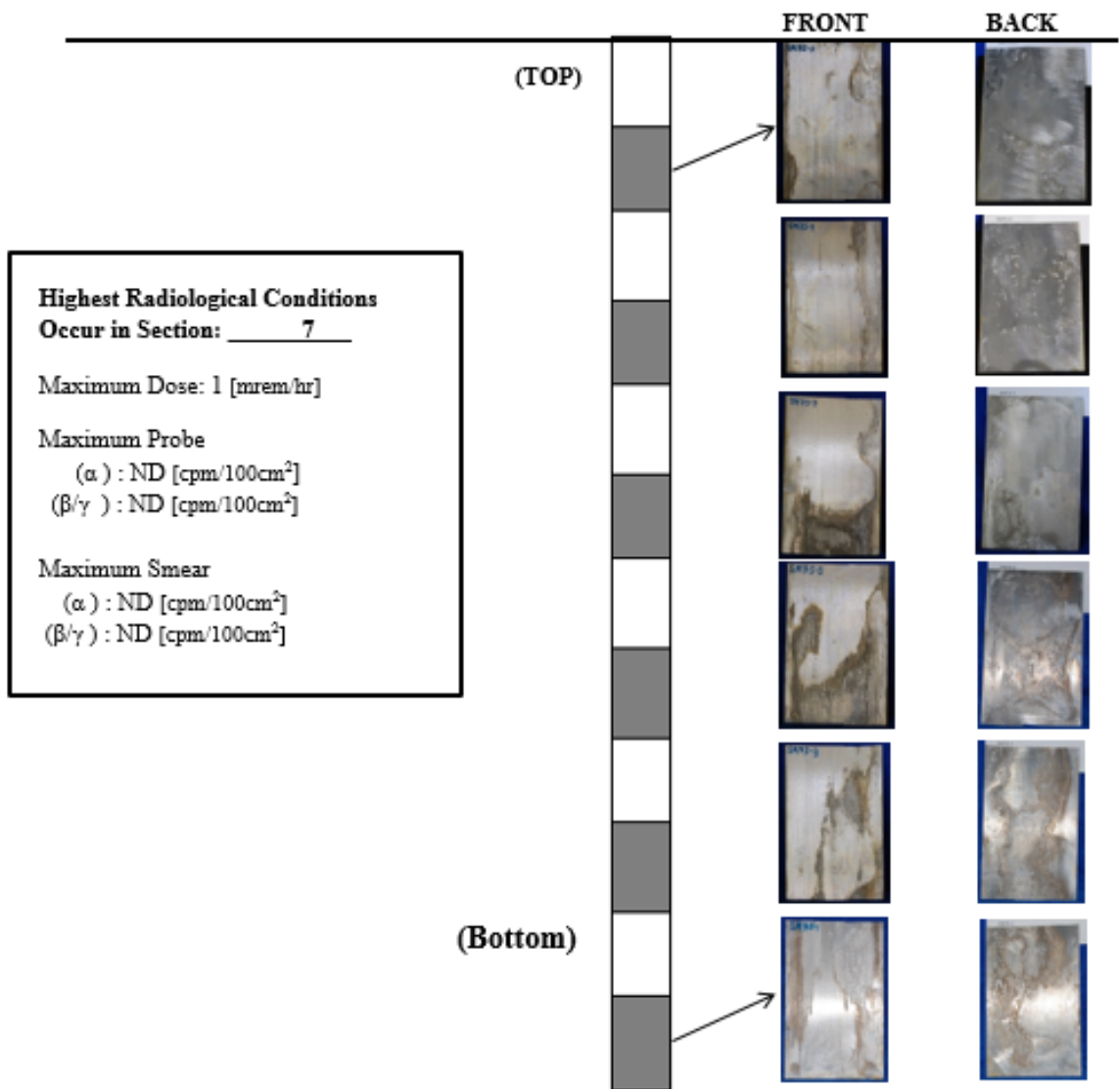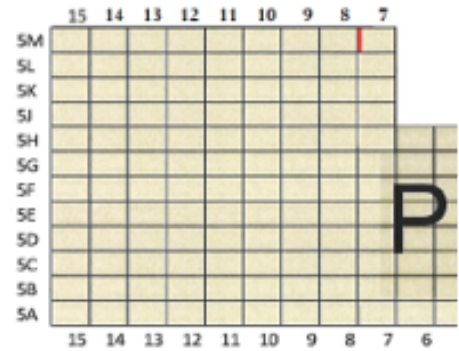
FRONT   BACK

Sample ID: ___5M7S___ - _1_

(Panel #)   (Section #)

Region: _2_   **Module:** _P_
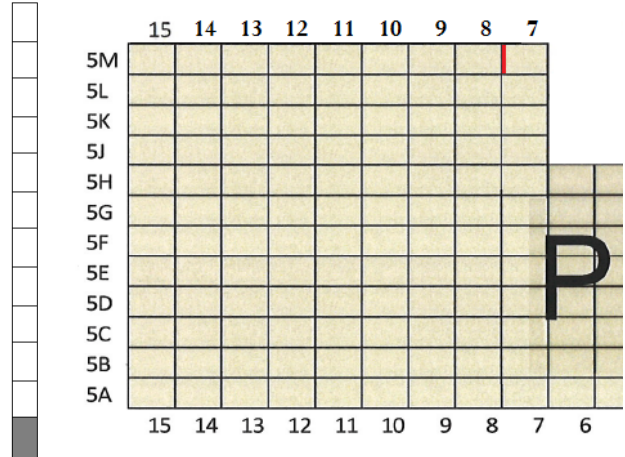
Front

Back

Sample ID: __5M7S__ - __3__
             (Panel #)   *(Section #)*

Region: __2__   **Module:** __P__

	15	14	13	12	11	10	9	8	7
5M									
5L									
5K									
5J									
5H									
5G									
5F									
5E									
5D									
5C									
5B									
5A									

P

Front

5M7S-3

Back

5M7S-3
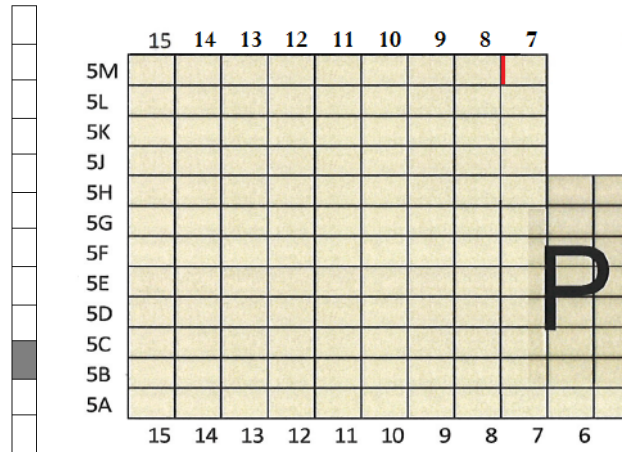
Sample ID: __5M7S__ - __5__
(Panel #)   (Section #)

Region: __2__   **Module:** __P__

	15	14	13	12	11	10	9	8	7
5M									
5L									
5K									
5J									
5H									
5G									
5F									
5E									
5D									
5C									
5B									
5A									
	15	14	13	12	11	10	9	8	7	6

P

Front

5M7S-5

Back

5M7S-5
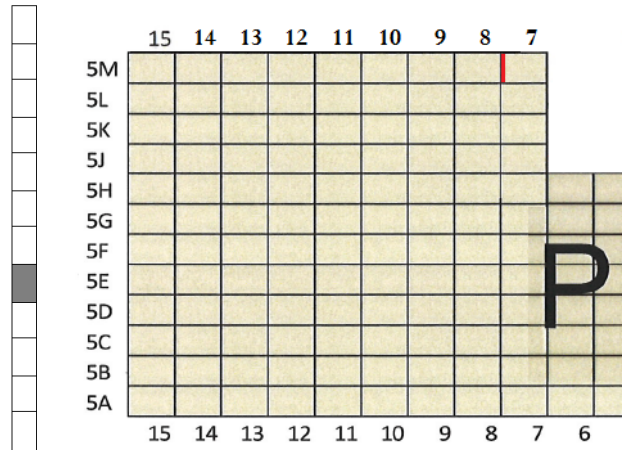
Sample ID: __5M7S__ - __7__
(Panel #)   *(Section #)*

Region: __2__   **Module:** __P__

	15	14	13	12	11	10	9	8	7
5M									
5L									
5K									
5J									
5H									
5G									
5F									
5E									
5D									
5C									
5B									
5A	15	14	13	12	11	10	9	8	7	6

P

Front

5M7S-7

Back

5M7S-7
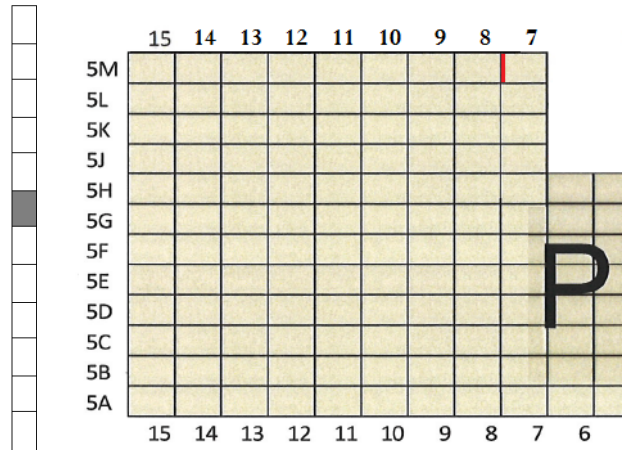
Sample ID: __5M7S__ - __9__
(Panel #)　　(Section #)

Region: _2_　　**Module:** _P_

	15	14	13	12	11	10	9	8	7
5M									
5L									
5K									
5J									
5H									
5G									
5F									
5E									
5D									
5C									
5B									
5A									

15　14　13　12　11　10　9　8　7　6

P

Front

5M7S-9

Back

5M7S-9

Sample ID: __5M7S__ - __11__
(Panel #)   *(Section #)*

Region: __2__   **Module:** __P__

	15	14	13	12	11	10	9	8	7
5M									
5L									
5K									
5J									
5H									
5G									
5F									
5E									
5D									
5C									
5B									
5A									
	15	14	13	12	11	10	9	8	7	6

P
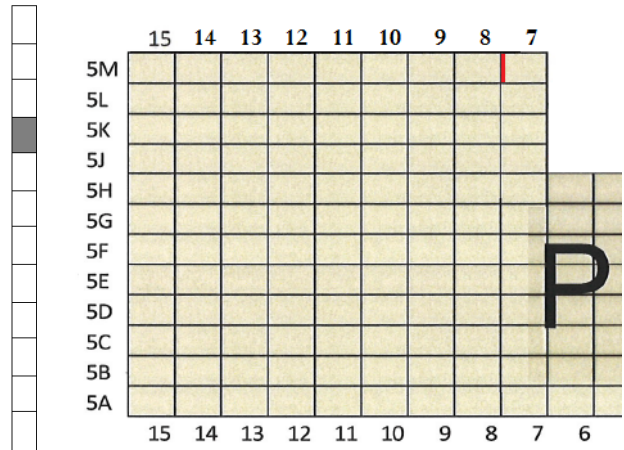
Front

Back

PANEL: __5M7E__

Region: _2_ Module: _P_

Highest Radiological Conditions Occur in Section: _____12_____

Maximum Dose: 1 [mrem/hr]

Maximum Probe
 (α) : ND [cpm/100cm^2]
 (β/γ) : 7,000 [cpm/100cm^2]

Maximum Smear
 (α) : ND [cpm/100cm^2]
 (β/γ) : _____ [cpm/100cm^2]

FRONT   BACK

(TOP)

(Bottom)
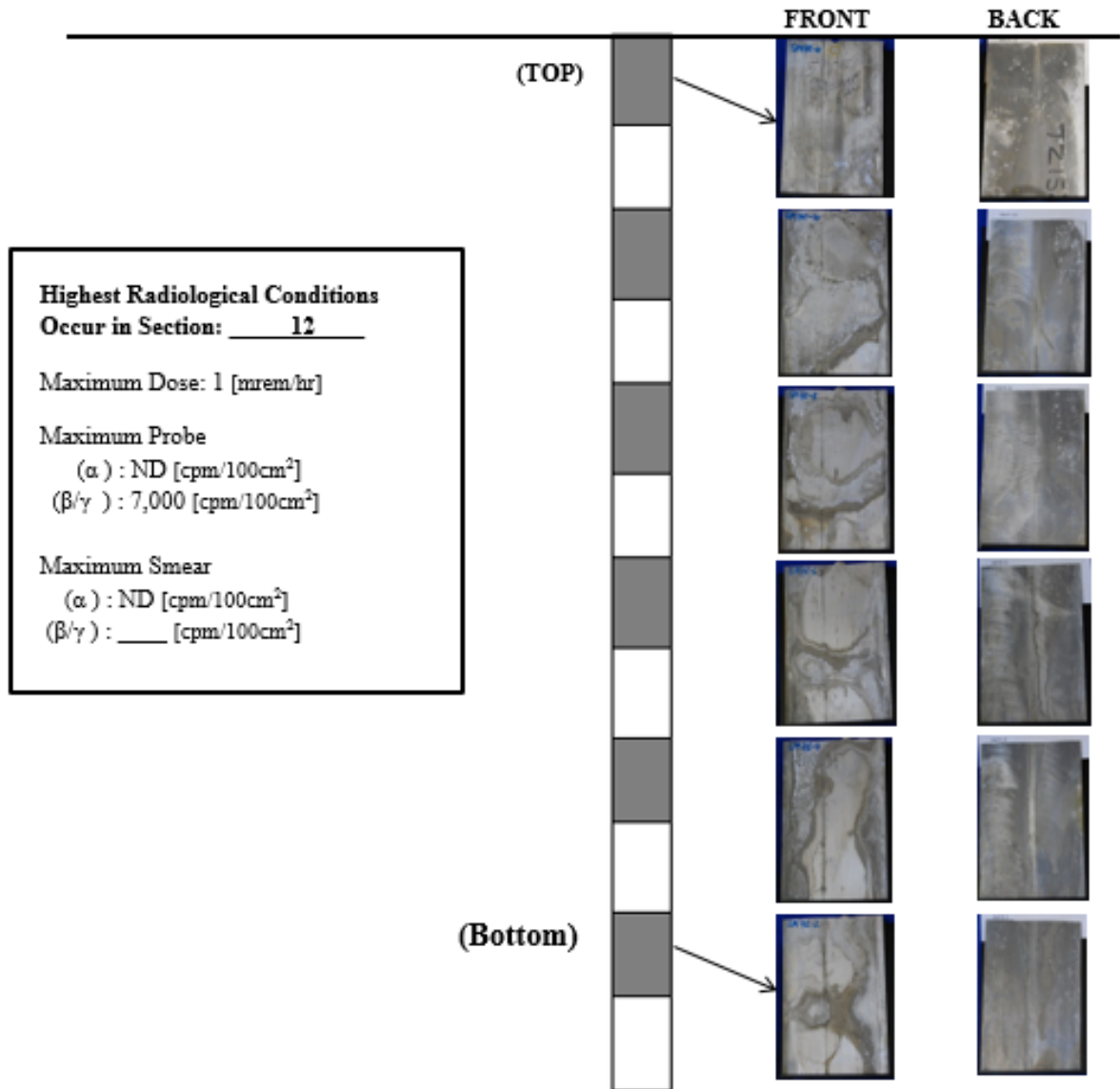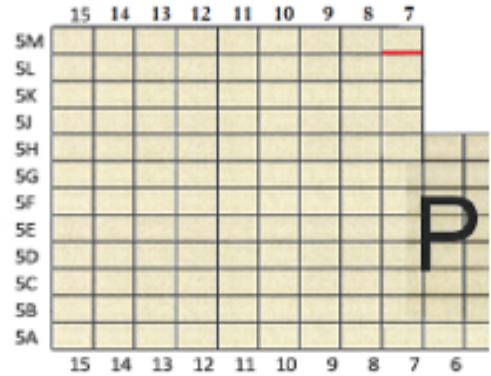
Sample ID: ___5M7E___ - _2_
(Panel #)   *(Section #)*

Region: _2_   **Module:** _P_

	15	14	13	12	11	10	9	8	7
5M									
5L									
5K									
5J									
5H									
5G									
5F									
5E									
5D									
5C									
5B									
5A									

15 14 13 12 11 10 9 8 7 6

P
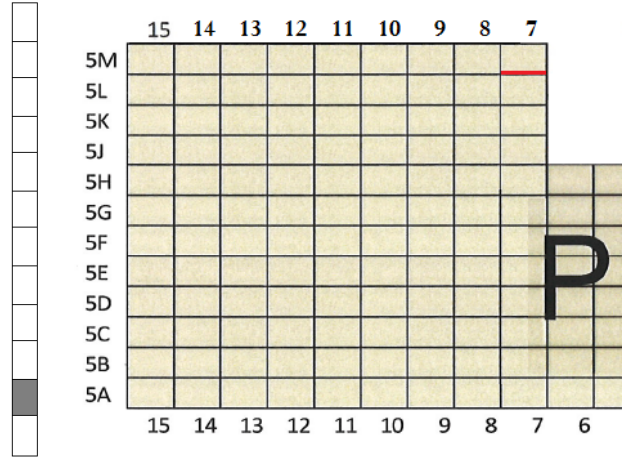
Front   # Back

Sample ID: __5M7E__ - __4__
(Panel #)   *(Section #)*

Region: __2__   **Module:** __P__

	15	14	13	12	11	10	9	8	7
5M									
5L									
5K									
5J									
5H									
5G									
5F									
5E									
5D									
5C									
5B									
5A									

P
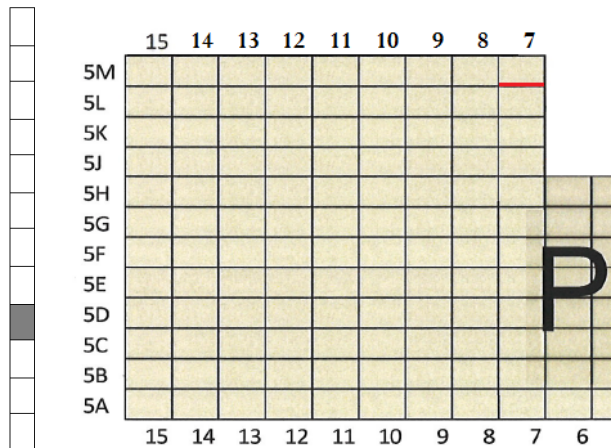
Front

Back

Sample ID: __5M7E__ - __6__
  (Panel #)   (Section #)

Region: __2__   **Module:** __P__
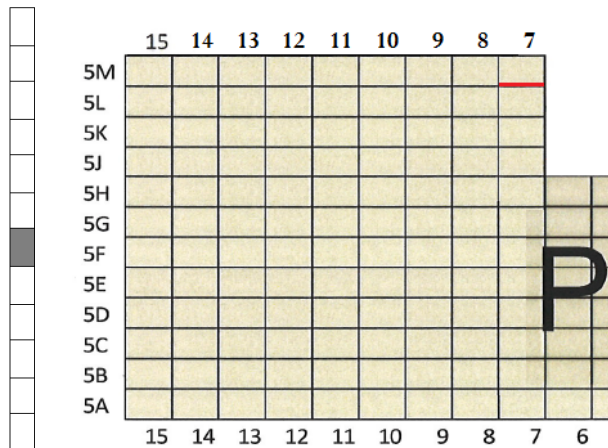
Front

Back

Sample ID: __5M7E__ - __8__
(Panel #) *(Section #)*

Region: __2__ **Module:** __P__

	15	14	13	12	11	10	9	8	7
5M									
5L									
5K									
5J									
5H									
5G									
5F									
5E									
5D									
5C									
5B									
5A									
	15	14	13	12	11	10	9	8	7	6

P
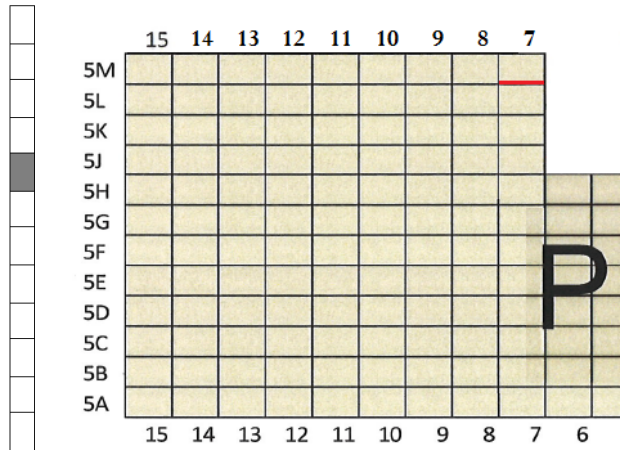
Front

Back

Sample ID: **5M7E** - **10**

           (Panel #)   *(Section #)*

Region: **2**   **Module:** **P**

	15	14	13	12	11	10	9	8	7
5M									
5L									
5K									
5J									
5H									
5G									
5F									
5E									
5D									
5C									
5B									
5A									

15 14 13 12 11 10 9 8 7 6

P
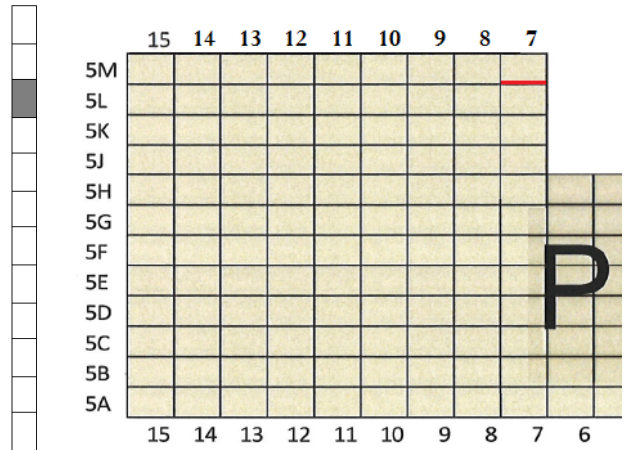
Front

Back

Sample ID: __5M7E__ - __12__
(Panel #)   *(Section #)*
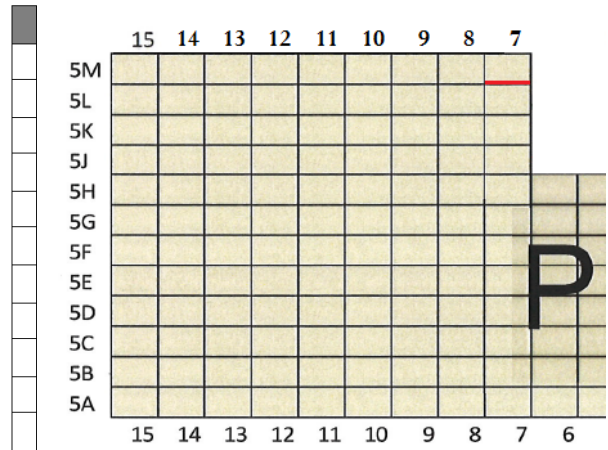
Region: __2__   **Module:** __P__
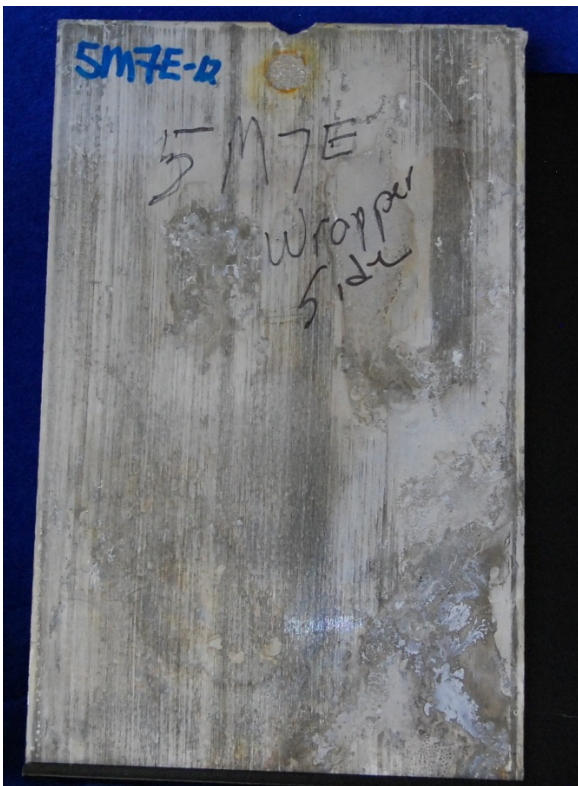
Front   Back

PANEL: **5M12E**

Region: 2   **Module:** P

FRONT   BACK

(TOP)

**Highest Radiological Conditions
Occur in Section:** 1

Maximum Dose: 1 [mrem/hr]

Maximum Probe
   (α) : ND [cpm/100cm^2]
 (β/γ) : 10,000 [cpm/100cm^2]

Maximum Smear
   (α) : ND [cpm/100cm^2]
 (β/γ) : ND [cpm/100cm^2]

(Bottom)
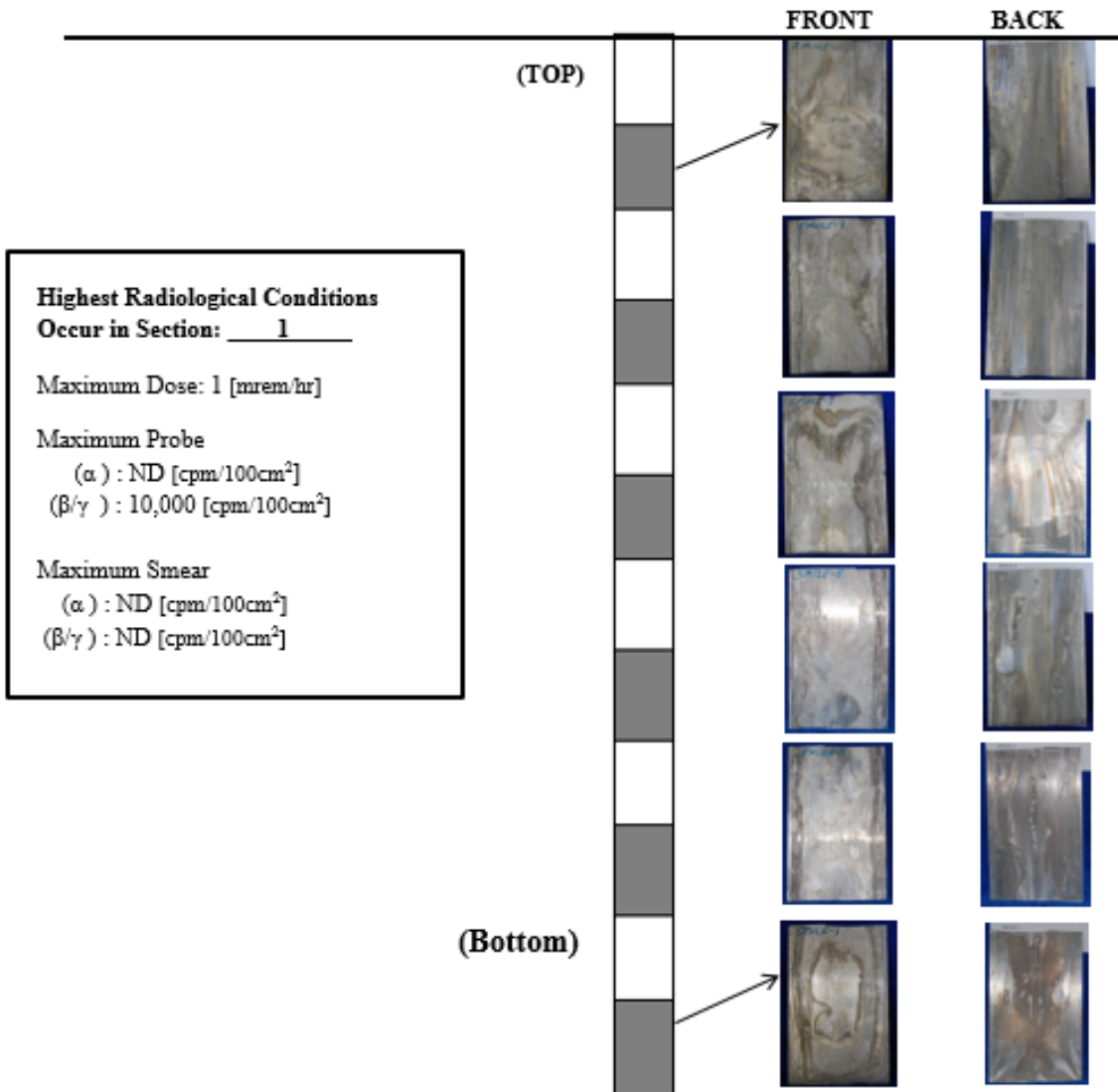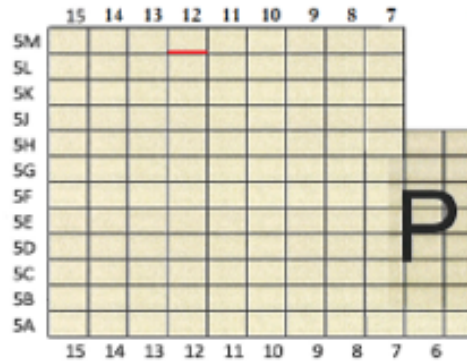
Sample ID: __5M12E__ - __1__
(Panel #)   (Section #)

Region: __2__   **Module:** __P__

	15	14	13	12	11	10	9	8	7	
5M										
5L										
5K										
5J										
5H										
5G										P
5F										
5E										
5D										
5C										
5B										
5A										
	15	14	13	12	11	10	9	8	7	6
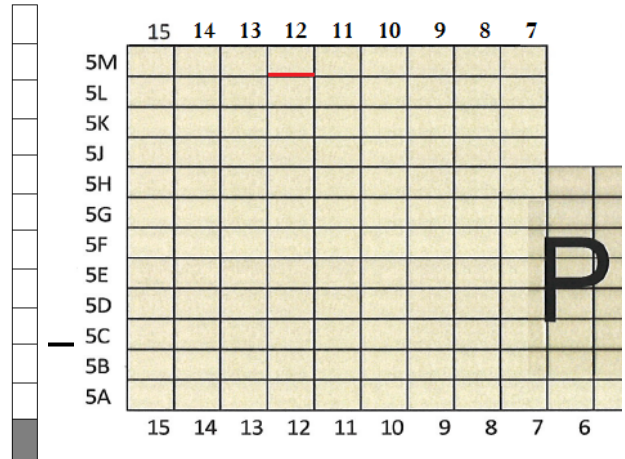
Front

5M12E-1

Back

5M12E-1

Sample ID: __5M12E__ - __3__
(Panel #)   (Section #)

Region: __2__   **Module:** __P__

	15	14	13	12	11	10	9	8	7
5M									
5L									
5K									
5J									
5H									
5G									
5F									
5E									
5D									
5C									
5B									
5A									

15 14 13 12 11 10 9 8 7 6

P
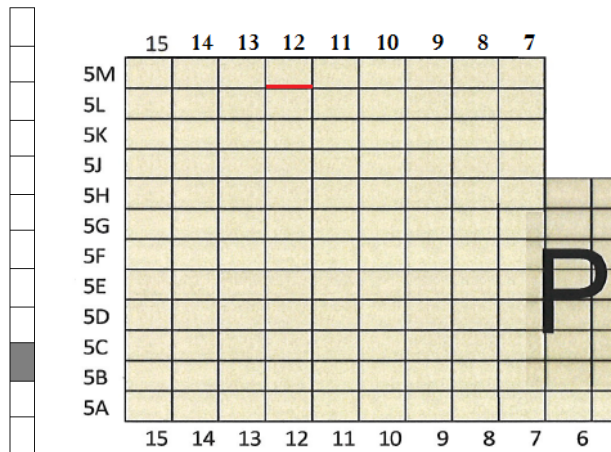
Front

Back

Sample ID: __5M12E__ - __5__
           (Panel #)   *(Section #)*

Region: __2__   **Module:** __P__

Front

Back

Sample ID: __5M12E__ - __7__

Region: __2__   **Module:** __P__

	15	14	13	12	11	10	9	8	7	
5M										
5L										
5K										
5J										
5H										
5G										
5F										
5E										
5D										
5C										
5B										
5A										

P
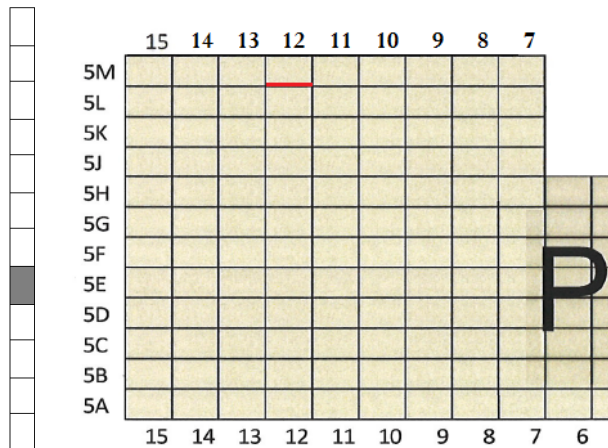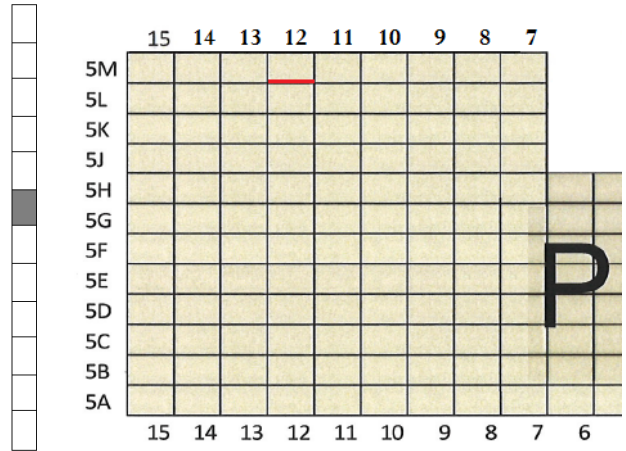
Front

Back

Sample ID: __5M12E__ - __9__
(Panel #)   *(Section #)*

Region: __2__   **Module:** __P_

	15	14	13	12	11	10	9	8	7		
5M											
5L											
5K											
5J											
5H											
5G											
5F											
5E											
5D											
5C											
5B											
5A											
	15	14	13	12	11	10	9	8	7	6	

P
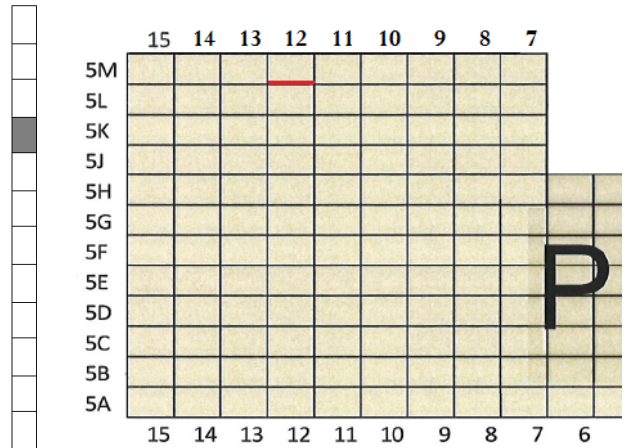
Front

Back

Sample ID: __5M12E__ - __11__

(Panel #)　　　(Section #)

Region: __2__　　　**Module:** __P__

	15	14	13	12	11	10	9	8	7
5M									
5L									
5K									
5J									
5H									
5G									
5F									
5E									
5D									
5C									
5B									
5A									
	15	14	13	12	11	10	9	8	7	6

P
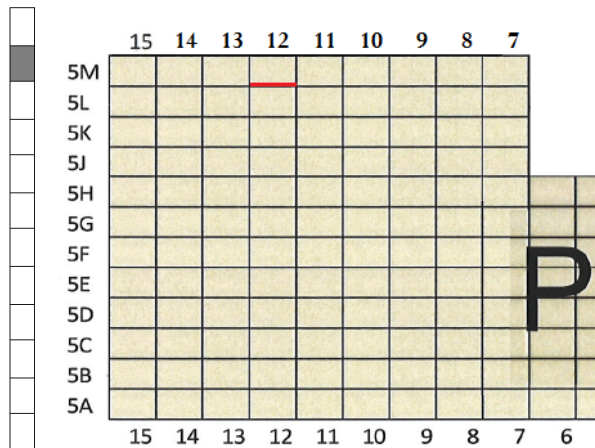
Front

Back

PANEL: **5L9E**

Region: **2** **Module:** **P**

Highest Radiological Conditions Occur in Section: _____6_____

Maximum Dose: 1 [mrem/hr]

Maximum Probe
   (α) : ND [cpm/100cm^2]
   (β/γ) : 5,000 [cpm/100cm^2]

Maximum Smear
   (α) : ND [cpm/100cm^2]
   (β/γ) : _____ [cpm/100cm^2]

(TOP)

(Bottom)
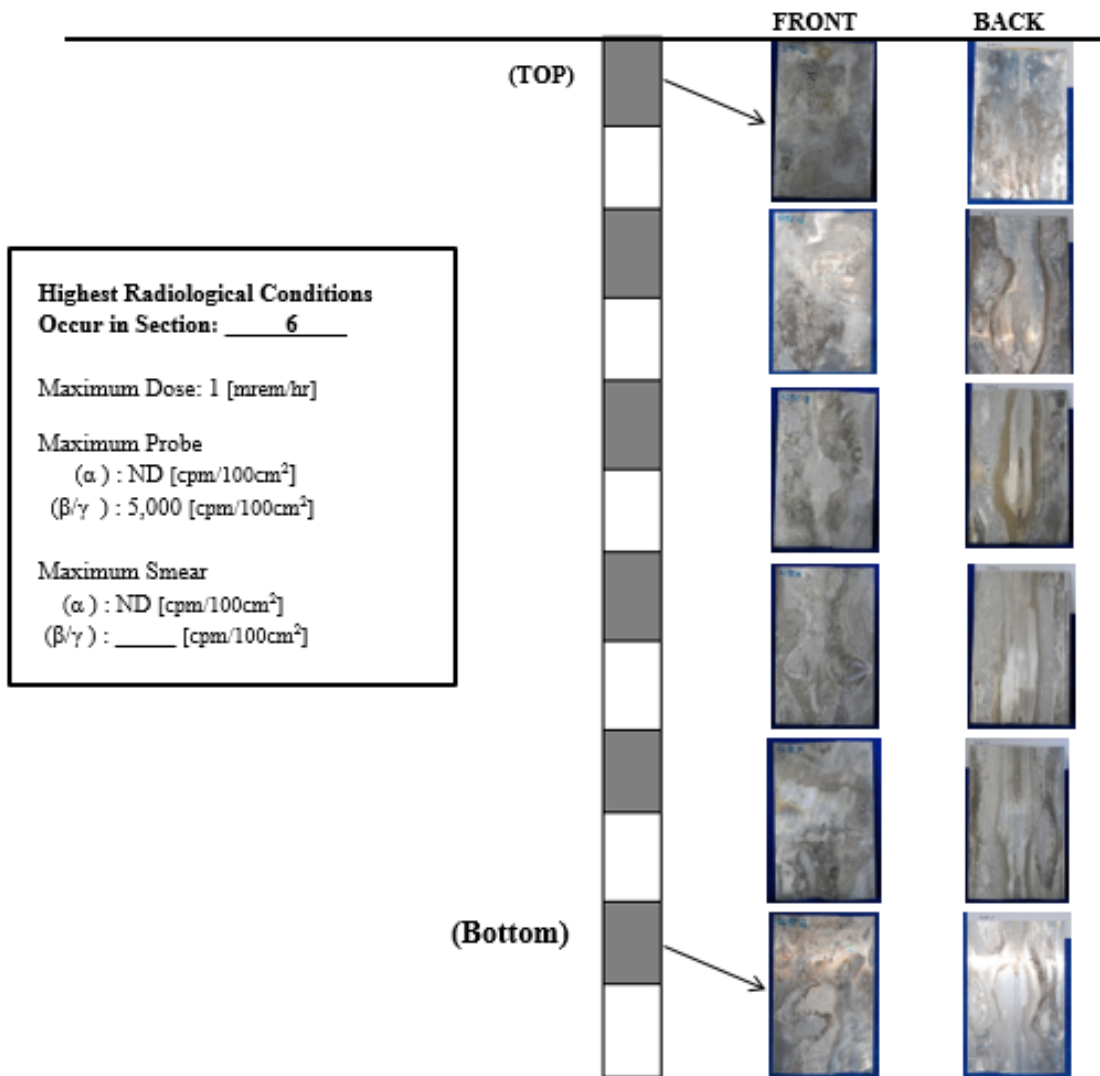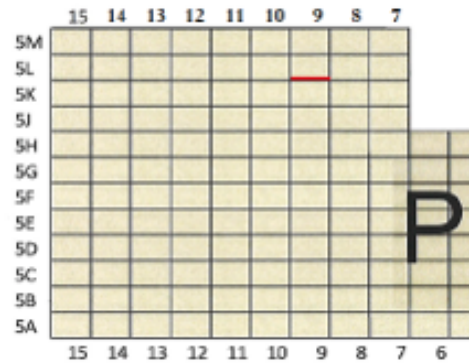
FRONT   BACK

Sample ID: ___5L9E___ - _2_

(Panel #)   (Section #)

Region: _2_   **Module:** _P_

	15	14	13	12	11	10	9	8	7	
5M										
5L										
5K										
5J										
5H										
5G										
5F										
5E										
5D										
5C										
5B										
5A										
	15	14	13	12	11	10	9	8	7	6

Front

Back

F-92
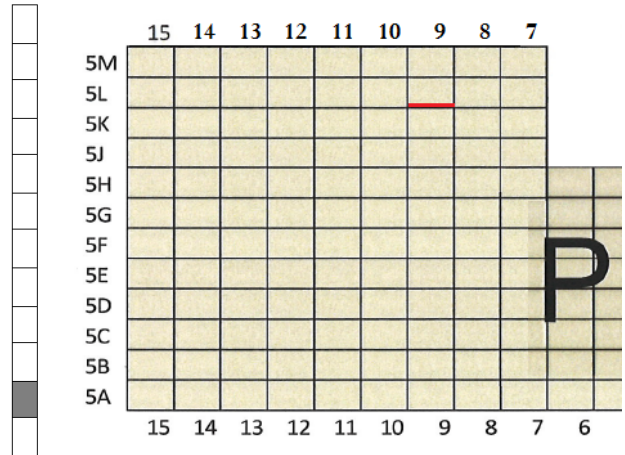
Sample ID: __5L9E__ - __4__
(Panel #)   (Section #)

Region: __2__   **Module:** __P__

	15	14	13	12	11	10	9	8	7
5M									
5L									
5K									
5J									
5H									
5G									
5F									
5E									
5D									
5C									
5B									
5A									

P

15 14 13 12 11 10 9 8 7 6
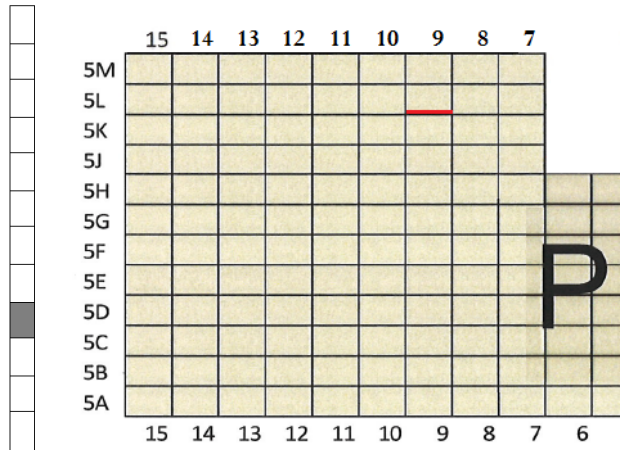
Front

Back

Sample ID: __5L9E__ - _6_
(Panel #) *(Section #)*

Region: _2_   **Module:** _P_

	15	14	13	12	11	10	9	8	7
5M									
5L									
5K									
5J									
5H									
5G									
5F									
5E									
5D									
5C									
5B									
5A									

P

15 14 13 12 11 10 9 8 7 6

Front

5L9E6

Back

5L9E-6
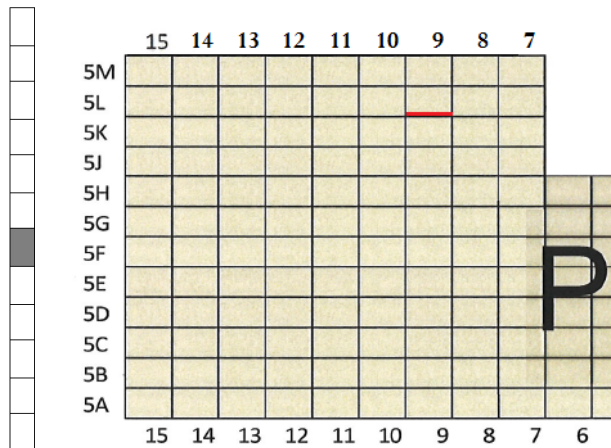
Sample ID: __5L9E__ - __8__
        (Panel #)   *(Section #)*

Region: __2__   **Module:** __P__

	15	14	13	12	11	10	9	8	7
5M									
5L									
5K									
5J									
5H									
5G									
5F									
5E									
5D									
5C									
5B									
5A									
	15	14	13	12	11	10	9	8	7	6

P

Front   ## Back

5L9E-8

5L9E-8
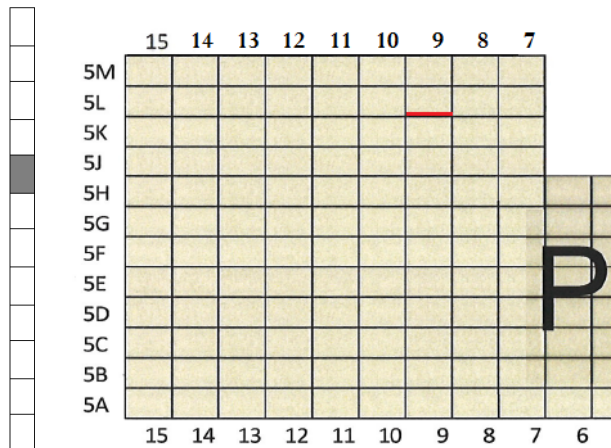
Sample ID: __5L9E__ - __10__

(Panel #)   (Section #)

Region: __2__   Module: __P__

	15	14	13	12	11	10	9	8	7
5M									
5L									
5K									
5J									
5H									
5G									
5F									
5E									
5D									
5C									
5B									
5A									
	15	14	13	12	11	10	9	8	7	6

P
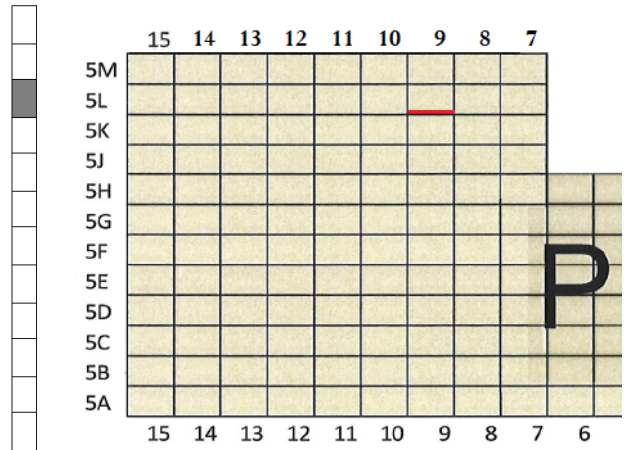
Front

Back

5L9E-10

Sample ID: **5L9E** - **12**
(Panel #)   _(Section #)_

Region: **2**   **Module:** **P**

	15	14	13	12	11	10	9	8	7	
5M										
5L										
5K										
5J										
5H										
5G										
5F										P
5E										
5D										
5C										
5B										
5A										
	15	14	13	12	11	10	9	8	7	6

Front

Back